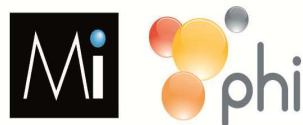


# **Evaluation of new meshes, a cell-based therapy, and animal model for Pelvic Organ Prolapse Repair**

**Daniela Ulrich, MD**

Submitted on 07.03.2014

The Ritchie Centre  
MIMR-PHI Institute of Medical Research  
Monash University  
Melbourne, Victoria, Australia



mimr-phi institute

27-31 Wright Street, Clayton, VIC 3168, Australia

Director Professor Bryan Williams

## Supervisors

Assoc. Prof. Dr Caroline Gargett, The Ritchie Centre, MIMR-PHI Institute of Medical Research and Monash University Department of Obstetrics and Gynaecology, Melbourne, VIC, Australia

Dr. Jerome Werkmeister, CSIRO Materials Science and Engineering, Clayton, VIC, Australia

Assoc. Prof. Dr. Anna Rosamilia, Monash University Department of Obstetrics and Gynaecology, Melbourne, VIC, Australia

Dr. Sharon Edwards, CSIRO Materials Science and Engineering, Geelong, VIC, Australia

**Notice 1**

Under the Copyright Act 1968, this thesis must be used only under the normal conditions of scholarly fair dealing. In particular no results or conclusions should be extracted from it, nor should it be copied or closely paraphrased in whole or in part without the written consent of the author. Proper written acknowledgement should be made for any assistance obtained from this thesis.

**Notice 2**

I certify that I have made all reasonable efforts to secure copyright permissions for third-party content included in this thesis and have not knowingly added copyright content to my work without the owner's permission.

## Table of Contents

<b>Acknowledgements</b> .....	<b>v</b>
<b>Summary</b> .....	<b>viii</b>
<b>List of Tables</b> .....	<b>x</b>
<b>List of Figures</b> .....	<b>x</b>
<b>Publications and abstracts arising from this thesis</b> .....	<b>xii</b>
Published Journal Articles .....	xii
Submitted Journal Articles .....	xii
Publications arising from collaborations related to my project.....	xii
Oral presentations .....	xiii
Poster presentations .....	xiv
<b>CHAPTER 1</b> .....	<b>1</b>
<b>INTRODUCTION</b> .....	<b>1</b>
1.1 Pelvic Organ Prolapse .....	1
1.1.1 Anatomy of the pelvis .....	2
1.1.2 Causes of Pelvic Organ Prolapse.....	4
1.1.3 Treatment options for Pelvic Organ Prolapse .....	6
1.1.3.1 Surgical treatment of Pelvic Organ Prolapse.....	7
1.1.3.2 Anterior vaginal wall repair.....	8
1.1.3.3 Posterior vaginal wall repair.....	8
1.1.3.4 Surgical treatment options with synthetic meshes.....	9
1.1.3.6 Posterior vaginal wall repair with mesh .....	10
1.1.3.7 Apical compartment repair with mesh.....	11
1.1.3.8 Mesh classification .....	11
1.1.4 The mesh dilemma- The knowledge gap.....	12
1.2 Stem Cells.....	14
1.2.1 Stem cell properties .....	15
1.2.1.1 Colony-forming unit activity .....	15
1.2.1.2 Self renewal .....	15
1.2.1.3 High proliferative potential .....	16
1.2.1.4 Stem cell differentiation .....	17

1.2.1.5 Tissue reconstitution in vivo.....	17
1.2.1.6 Stem Cell Niche.....	17
1.2.2 Mesenchymal Stem Cells .....	17
1.2.2.1 Properties and phenotype of MSC.....	17
1.2.2.2 Sources of MSC.....	18
1.2.2.3 Anti-inflammatory properties of MSC .....	19
1.2.2.4 Immunomodulatory properties of MSC .....	19
1.2.2.5 Identification of MSC in human tissues.....	20
1.2.2.6 Survival of transplanted of MSC .....	20
1.2.3 Endometrial MSC .....	21
1.2.3.1 EMSC Differentiation .....	23
1.2.3.2 Origin of eMSC .....	23
1.2.3.3 Prospective isolation and scale up culture of eMSC .....	24
1.2.3.4 Ex vivo culture of eMSC for cell-based therapies.....	24
1.2.3.5 W5C5+ eMSC Regenerate Stromal Tissue in vivo.....	25
1.2.4 Endometrial Regenerative Cells from menstrual blood .....	25
1.2.4.1 ERC and bmMSC have similar properties .....	26
1.3 Tissue Engineering .....	27
1.3.1 The potential of TE in the field of regenerative medicine.....	27
1.3.1.1 Cell based and tissue engineering approaches.....	27
1.3.2 TE used in reproductive tract disorders.....	29
1.3.3 TE for POP repair surgery- The gap.....	30
1.4 Experimental approaches for investigating a TE approach for POP repair.....	30
1.4.1 Animal Models for investigating POP repair surgery .....	30
1.4.2 Connective tissues of the pelvic floor structures .....	32
1.5 Biomechanical properties of pelvic floor tissue .....	34
1.5.1 Biomechanical properties of mesh following vaginal implantation.....	36
1.5.2 The gap in knowledge on biomechanical analyses of vaginal tissues.....	37
<b>RATIONALE .....</b>	<b>37</b>
<b>Aims and Hypotheses of this Thesis.....</b>	<b>38</b>
<b>CHAPTER 2.....</b>	<b>40</b>
Alternative materials for POP repair .....	40
<b>CHAPTER 3.....</b>	<b>59</b>
Endometrial MSC in Postmenopausal Endometrium.....	59

<b>CHAPTER 4.....</b>	<b>90</b>
A Tissue Engineering Construct for POP repair .....	90
<b>CHAPTER 5.....</b>	<b>110</b>
Ovine Vaginal Tissue Analysis .....	110
<b>CHAPTER 6.....</b>	<b>136</b>
Comparison of ovine and human vaginal tissue composition and properties .....	136
<b>CHAPTER 7.....</b>	<b>156</b>
<b>DISCUSSION.....</b>	<b>156</b>
<b>REFERENCES .....</b>	<b>161</b>
<b>APPENDICES.....</b>	<b>180</b>
Appendix 1 .....	181
Appendix 2 .....	195
Appendix 3 .....	208

## Acknowledgements

Foremost, I would like to express my sincere gratitude to my primary supervisor Assoc. Prof. Caroline Gargett for the continuous support of my PhD study and research. I thank her deeply for her kindness, patience, time, motivation, enthusiasm, and immense knowledge and expertise. Her guidance helped me at all the time of research and writing of this thesis. I could not have imagined having a better supervisor and mentor for my PhD study. I thank her immensely for her encouragement and understanding over these past three years and for inviting me to family dinners on special occasions.

My sincere thanks also goes to all my other supervisors. Dr. Jerome Werkmeister for offering his exceptional support and knowledge in many parts of my PhD and for the stimulating discussions during our meetings. I also thank Dr. Sharon Edwards who taught me to perform mechanical testing on biological tissue and its analysis with immense patience and expertise. My gratitude also goes to Dr. Anna Rosamilia for acquiring numerous tissue samples and providing excellent advice for my PhD projects. I thank her for integrating me into her clinical team and teaching me clinical skills in the pelvic floor clinic.

I also thank other CSIRO members who gave advice and supported me during this PhD like Dr Keith Mc Lean, Jacinta F. White and Dr. John AM. Ramshaw who were always available when I needed professional advice in the field of tissues and matrices. Dr. Christopher Su taught me how to perform biochemical analysis with great patience and friendliness and performed a lot of the tests when I was occupied with other duties.

Thanks to the Ritchie Centre and Prof. Euan Wallace who provided the facility, travel funds for an exciting conference and regular seminars or journal clubs. I thank him for offering me the clinical part time position that helped me to afford my beautiful apartment.

I also want to acknowledge the Evans family who supported my project financially and facilitated another international conference where I was chosen for the President's Presenter Award.

Also I thank Dr. Yen Pham deeply who was my first friend in Australia. I am so grateful for her friendship, advice in all belongings and the wonderful time we spent together both in the lab and outside.

A very special thank you also goes to Dr. Ina Rudloff who assisted with any research queries and also became a wonderful friend. I could share my European thoughts with her at every time of the week and day and am so grateful for having her in my life and enriching my experiences in Melbourne.

I also thank Ker Sin Tan for her professional help with my cells and the fact that I could always count on her. Also I want to thank Dr. Claudia and Marcel Nold who encouraged me with immense enthusiasm towards research and spent their spare free time with me when possible.

Another big thanks goes to Dr. Camden Lo, the most patient person I have ever met. He provided me with advice in numerous research activities and always had a solution for my problems. He invested a huge amount of work to facilitate the sophisticated image analysis on my thousands of images.

Appreciation also goes to Dr. Vincent Letouzey who designed my last PhD chapter and assisted with his time; advice both in research and in personal issues and also became a good friend.

In my daily work I have been blessed with a friendly and cheerful group at MIMR. Dr. James Dean, taught me to perform PCR. Tommy Supit taught me how to perform rat studies and surgery at MIMR. Dr. Gayathri Rajaraman showed me how to handle the eMSC. My thank goes to everybody who helped and is not mentioned here. Dr. Rosa Gualano assisted with administration duties and proof read some of my chapters.

Last but not the least, I would like to thank my family: my parents Gerhard and Elfriede Ulrich for the support they provided me through my entire life and in particular together with my brother Daniel Ulrich when they spent hours on Skype with me and encouraged me when I ran out of ambition.

In conclusion, I recognize that this research would not have been possible without the financial assistance of Monash University, the Australian Stem Cell Centre and the Southeast Melbourne Alliance for Regenerative Therapies who provided me with scholarships, and I express my gratitude to those agencies.

## List of Abbreviations

ATFP	arcus tendineous fasciae pelvis
bmMSC	bone marrow mesenchymal stem cells
CFU	colony forming unit activity
eMSC	endometrial mesenchymal stem cells
ECM	extracellular matrix
ERC	endometrial regenerative cells
Fbln	Fibulin
IDO	Indoleamine 2,3-dioxygenase
IFN	Interferon
MSC	mesenchymal stem cells
PA	polyamide
PA+G	polyamide coated with gelatin
PEEK	poly-ether-ether-ketone
PGE <sub>2</sub>	prostaglandin E <sub>2</sub>
POP	pelvic organ prolapse
PP	polypropylene
TE	tissue engineering
TNF- $\alpha$	tumor necrosis factor alpha

## Summary

Pelvic Organ Prolapse (POP) is defined as the descent of one or more of the pelvic structures and includes uterine prolapse, vaginal vault prolapse, and anterior or posterior vaginal wall prolapse. The resultant symptoms are urinary and bowel dysfunction, incontinence, and sexual dysfunction. POP is primarily caused by childbirth injury, but ageing, obesity and other factors also contribute. Common treatment of POP is surgery and includes native tissue surgical reconstruction alone or with implantation of either synthetic or biological mesh with the former having a higher success rate. However, the long-term outcome of synthetic mesh augmented surgery is unsatisfactory due to post-surgical complications. The most common problems are mesh exposure and pain possibly due to scarring, folding and/or contraction of synthetic meshes. Polypropylene (PP) was rapidly adopted for POP surgery and was not carefully reassessed to determine whether PP met the criteria for treating the damaged pelvic floor tissues.

Mesenchymal Stem Cells (MSC) have been discovered in almost every adult tissue and are highly proliferative, self-renew and differentiate into mesodermal lineages *in vitro*. MSC also have immunomodulatory and angiogenic properties making them ideal candidates for cell-based therapies. Recently MSC have been discovered in the regenerative endometrial lining of the uterus and specific markers (W5C5/SUSD2) have been identified for their prospective isolation. These endometrial MSC (eMSC) fulfil the classical criteria of adult MSC and can be obtained under minimally invasive procedures without anaesthesia or scarring from premenopausal women.

Tissue engineering is defined as a combination of cells and materials and is widely used in the field of regenerative medicine. Many cell types from the same or a different individual can be used in combination with a synthetic, biological or composite material. Of the urogenital organs, to date, researchers have only been able to reconstruct the human bladder and urethra using tissue engineering approaches.

In this thesis, new meshes designed specifically for POP repair surgery were evaluated in an abdominal wall fascial defect model to evaluate the extent of host tissue response, tissue integration and subsequent mechanical properties. Polyamide (PA), Polyamide plus Gelatin (PA+G) and Polyether-etherketone (PEEK) showed temporal inflammatory

responses that were different to that seen with PP meshes with enhanced neovascularisation, collagen production, and decreased inflammation. PA and PA+G could be a future treatment option for POP repair surgery.

Most women who suffer from POP are postmenopausal and we therefore characterised eMSC from postmenopausal women treated with or without exogenous estrogen. Similar to premenopausal women, eMSC can be obtained by a curettage procedure following short-term estrogen treatment. Postmenopausal eMSC are similar to premenopausal eMSC in terms of cloning efficiency and phenotype but are available in lower numbers and differentiate to a lesser degree.

The next step was to test the PA+G meshes and eMSC in a nude rat fascial wound model as a small preclinical proof of principle animal model. Meshes seeded with eMSC improved the tissue integration compared to meshes alone by increasing the neovascularisation, altering macrophages from an inflammatory to wound healing phenotype, decreasing the foreign body reaction, and improving the biomechanical properties in the long term, without engraftment.

This thesis also provides a comprehensive analysis of sheep vaginal tissue to generate baseline data in this large animal preclinical model, including biochemical, biomechanical and histological analyses. Sheep that have not delivered lambs have similar biomechanical and biochemical properties to parous sheep whereas pregnancy significantly changes both the tissue composition and mechanical properties. We also determined regional differences in postmenopausal sheep vagina and correlated the biochemical and histological results with postmenopausal women. The ovine vagina showed differences between the upper and lower region whereas human vagina did to a lesser degree but with similar tissue composition. These results can help to understand the biochemical tissue composition and passive biomechanical properties of ovine vagina and relate this to the histo-architecture at different reproductive stages as part of the establishment of a large animal preclinical model for evaluating regenerative medicine approaches for surgical treatment of pelvic organ prolapse. The next step would be to test the above mentioned TE construct in a large animal model; however this was not feasible within the time frame of this thesis.

In conclusion eMSC are a promising source of MSC independent of a women's stage of life and could be used for TE purposes. A Tissue Engineering construct might be the future treatment for POP but has yet to be evaluated in a large animal preclinical model.

## List of Tables

<b>Table 1.</b> Pelvic Organ Prolapse staging. ....	2
<b>Table 2.</b> The classification of synthetic biomaterials. ....	12

## List of Figures

<b>Figure 1.</b> Schematic drawings of a female pelvis showing different forms of POP.....	1
<b>Figure 2.</b> Schematic of the POP- Q system, showing the points of reference and their explanation. ....	2
<b>Figure 3.</b> Normal Female lower urogenital tract. ....	3
<b>Figure 4.</b> Schematic of the three levels of pelvic organ support. ....	4
<b>Figure 5.</b> Different pessaries.....	7
<b>Figure 6.</b> Sacrospinous fixation. Reproduced with permission from BARD Medical. ....	8
<b>Figure 7.</b> Schematic of anterior and posterior vaginal wall repair using mesh. ....	10
<b>Figure 8.</b> Optical micrographs of meshes. ....	12
<b>Figure 9.</b> The origin and specialisation of stem cells. ....	14
<b>Figure 10.</b> Stromal colony forming units from human endometrium.....	15
<b>Figure 11.</b> Hierarchy of tissue stem cell differentiation. ....	16
<b>Figure 12.</b> Schematic showing isolation procedures for obtaining endometrial stem/progenitor cells from human uterus and menstrual blood. ....	22
<b>Figure 13.</b> Stress strain curves showing variability between different human vaginal samples. ....	35

# General Declaration

## Monash University

### Declaration for thesis based or partially based on conjointly published or unpublished work

In accordance with Monash University Doctorate Regulation 17.2 Doctor of Philosophy and Research Master's regulations the following declarations are made:

I hereby declare that this thesis contains no material which has been accepted for the award of any other degree or diploma at any university or equivalent institution and that, to the best of my knowledge and belief, this thesis contains no material previously published or written by another person, except where due reference is made in the text of the thesis.

This thesis includes 4 original papers published in peer reviewed journals and 2 unpublished publications. The core theme of the thesis is pelvic organ prolapse. The ideas, development and writing up of all the papers in the thesis were the principal responsibility of myself, the candidate, working within the MMI-PHI Institute of Medical Research, under the supervision of Associate Professor Dr. Caroline Gargett.

The inclusion of co-authors reflects the fact that the work came from active collaboration between researchers and acknowledges input into team-based research.

In the case of the 6 chapters my contribution to the work involved the following:

Thesis chapter	Publication title	Publication status	Nature and extent of candidate's contribution
1	Toward the use of endometrial and menstrual blood mesenchymal stem cells for cell based therapies	Published (Appendix 1)	90%
2	A preclinical evaluation of alternative synthetic materials for fascial defect repair using a rat abdominal hernia model	Published	65%
3	Mesenchymal stem/stromal cells in Postmenopausal Endometrium	Under review in Human Reproduction	85%
4	Human endometrial mesenchymal stem cells modulate the tissue response and mechanical behaviour of polyamide mesh implants for pelvic organ prolapse repair	Published	75%
5	Influence of reproductive status on tissue composition and biomechanical properties of ovine vagina	In press in Plos One	70%
6	Regional variation in tissue composition and biomechanical properties of postmenopausal ovine and human vagina	Under review in the American Journal of Obstetrics and Gynecology	70%

I have not renumbered sections of submitted or published papers in order to generate a consistent presentation within the thesis.

**Signed:** .....

**Date:** .....

## **Publications and abstracts arising from this thesis**

### **Published Journal Articles**

**Ulrich, D;** Muralitanian, R; Gargett, CE. Towards the use of endometrial and menstrual blood mesenchymal stem cells (MSC) for cell based therapies. *Expert Opinion on Biological Therapy*. 2013; 13(10):1387-400.

**Ulrich, D;** Edwards, SL; Su, C; Tan, KS; White, JF; Ramshaw, JAM.; Lo, C; Rosamilia, A; Werkmeister, JA; Gargett, CE. Human Endometrial Mesenchymal Stem Cells Modulate the Tissue Response and Mechanical Behaviour of Polyamide Mesh Implants for Pelvic Organ Prolapse Repair. *Tissue Engineering A*. 2014; 20(3-4):785-98.

(Featured on the front cover- Appendix 3)

**Ulrich, D;** Edwards, SL; White, JF; Supit, T; Ramshaw, JAM.; Lo, C; Rosamilia, A; Werkmeister, JA; Gargett, CE. A preclinical evaluation of alternative biomaterials for pelvic organ prolapse repair using a rat abdominal hernia model. *PLoS One*. 2012; 7(11):e50044.

Featured on the front cover of the *Journal of Tissue Engineering*

**Ulrich, D;** Edwards, SL; Su, C; White, JF; Ramshaw, JAM; Jenkin, G; Deprest, J; Rosamilia, A; Werkmeister, JA; Gargett, CE. Influence of reproductive status on tissue composition and biomechanical properties of ovine vagina. *PLoS One*. 2014; in press.

### **Submitted Journal Articles**

**Ulrich, D;** Tan, KS; Deane, J; Schwab, K; Cheong, A; Rosamilia, A; Gargett, CE. Mesenchymal stem/stromal cells in Postmenopausal Endometrium. Submitted to *Human Reproduction*.

**Ulrich, D;** Edwards, SL; Letouzey, V; Su, C; White, JF; Rosamilia, A; Gargett, CE; Werkmeister, JA. Regional differences of the connective tissue and biomechanical properties in human and ovine vaginal tissue. Submitted to *AJOG*.

### **Publications arising from collaborations related to my project**

Rajaraman, G; White, JF; Tan, KS; **Ulrich, D;** Rosamilia, A; Werkmeister, JA; Gargett, CE. Optimisation and scale- up culture of human endometrial multipotent mesenchymal

stromal cells: potential for clinical application. *Tissue Eng Part C Methods*. 2013; 19(1):80-92.

**Ulrich, D**; Guzman- Rojas, Dietz, HP; Trutnovsky G. Evaluation of VAS for bother of prolapse. *Ultrasound in Obstetrics and Gynecology*. *Ultrasound Obstet Gynecol*. 2013 Oct 11. doi: 10.1002/uog.13222.

**Ulrich, D**; Dwyer, P; Rosamilia, A; Lim, Y; Lee, J. The effect of vaginal pelvic organ prolapse surgery on sexual function. *Neurourology and Urodynamics* 2014; 5. doi: 10.1002/nau.22569.

Trutnovsky, G; **Ulrich, D**; Rojas, RG; Mann, K; Aigmueller, T; Dietz, HP. The "bother" of urinary incontinence. *Int Urogynecol J*. 2014 Feb 11. [Epub ahead of print].

Edwards, SL; **Ulrich, D**; White, JF; Rosamilia, A; Gargett, CE; Werkmeister, JA. Biomechanical evaluation of novel cell seeded meshes for pelvic organ prolapse repair. In preparation for submission to *Tissue Engineering*.

Edwards, SL; **Ulrich, D**; Rosamilia, A; Werkmeister, JA; Gargett, CE; Letouzey, V. Multi-axial mechanical evaluation of novel and clinical meshes for pelvic organ prolapse repair: an implantation study. In preparation for submission to the *International Urogynecology Journal*.

## **Oral presentations**

**Ulrich, D**; Edwards, SL; Su, C; Tan, KS; White, JF; Ramshaw, JAM.; Lo, C; Rosamilia, A; Werkmeister, JA; Gargett, CE. Biomechanical Properties of Gelatin Coated Polyamide Meshes Seeded with Human Endometrial Mesenchymal Stem Cells. *International Urogynecological Association meeting*, May 25-29, 2013; Dublin, Ireland.

*This abstract was awarded with the IUGA award “Best Oral Poster Presentation by a Fellow”*

**Ulrich, D**; Edwards, SL; Su, C; Tan, KS; White, JF; Ramshaw, JAM; Lo, C; Rosamilia, A; Werkmeister, JA; Gargett, CE. Preclinical Evaluation of a Tissue Engineering Approach for Pelvic Organ Prolapse (POP) Repair comprising Human Endometrial Mesenchymal Stem Cells and Polyamide (PA) Mesh. *Society for Gynecologic Investigation meeting*, March 19-23, 2013; Orlando, FL, USA.

*This abstract was awarded with the “SGI President’s Presenter Award”*

**Ulrich, D;** Dwyer, P; Rosamilia, A; Lim, Y; Lee J. Prolapse and sexual matters symptoms after surgery for pelvic organ prolapse (POP). Australasian Gynaecological Society for Surgery and Endoscopy Meeting. Mar 16-17, 2012: Melbourne, Australia.

### **Poster presentations**

**Ulrich, D;** Tan, KS; Schwab, K; Cheong, A; Rosamilia, A; Gargett, CE Mesenchymal stem/stromal cells in Postmenopausal Endometrium. Australasian Society for Stem Cell Research meeting, Oct 27-29, 2013; Brisbane, Australia.

**Ulrich, D;** Edwards, SL; Supit, T; White, Lo, C; J; Rosamilia, A; Ramshaw, JAM, Werkmeister, JA; Gargett, CE. Novel biomaterials for pelvic organ prolapse (POP) repair. 3rd Tissue Engineering and Regenerative Medicine International Society World Congress. Sep 5-8, 2012; Vienna, Austria.

**Ulrich, D;** Edwards, SL; White, J; Lo, C; Rosamilia, A; Ramshaw, JAM; Werkmeister, JA; Gargett, CE. A novel tissue engineering construct using human endometrial mesenchymal stem cells and Polyamide mesh for pelvic organ prolapse (POP) repair. 3rd Tissue Engineering and Regenerative Medicine International Society World Congress. Sep 5-8, 2012; Vienna, Austria.

Edwards, SL: **Ulrich, D;** Supit, T; White, JF; Ramshaw, JAM; Rosamilia, A; Gargett, CE; Werkmeister, JA. Biomechanical properties of implanted mesh: a rat study for pelvic organ prolapse repair. 3rd Tissue Engineering and Regenerative Medicine International Society World Congress. Sep 5-8, 2012; Vienna, Austria.

Rajaraman, G; White, JF; **Ulrich, D;** Edwards, SL; Rosamilia, A; Supit, T; Ramshaw, JAM; Werkmeister, JA; and Gargett CE. The repair of pelvic organ prolapse using biologically-coated knitted scaffolds for delivery of autologous stem cells. 9th World Biomaterials World Congress. Jun 1-5, 2012; Chengdu, China.

**Ulrich, D;** Supit, T; Edwards, SL; Werkmeister, JA; White, JF; Gargett, CE. Biocompatibility of newly designed meshes in a rat abdominal hernia model. RANZCOG 2011 Annual Scientific Meeting: November 27-30, 2011; Melbourne, Australia.

My work was also presented in these invited presentations given by my supervisors

Gargett, CE; Edwards, SL; **Ulrich, D**; White, JF; Rajaraman, G; Tan, KS; Ramshaw, JAM; Rosamilia, A; Werkmeister, JA. Human endometrial mesenchymal stem cells and novel meshes as an autologous cell-based therapy for pelvic organ prolapse (POP). 3rd Tissue Engineering and Regenerative Medicine International Society World Congress. Sep 5-8, 2012; Vienna, Austria.

Gargett CE, Edwards SL, Rajaraman G, **Ulrich D**, Rosamilia A, Werkmeister, JA. Mesenchymal stem cells as a therapy for pelvic organ prolapse. RANZCOG 2011 Annual Scientific Meeting, Nov 27-30, 2011; Melbourne, Australia.

Gargett, CE; Rajaraman, G; Edwards, SL; **Ulrich, D**; White, J; Supit, T; Rosamilia, A; McLean, K; Werkmeister, JA. Uterine Mesenchymal Stem/Stromal Cells and Novel Biomaterials for Pelvic Floor Regeneration. Australian Society for Stem Cell Research 4th annual Meeting. October 23-25, 2011; Sydney, Australia.

Werkmeister JA, **Ulrich D**, Edwards SL, White JF, Su C, Tan KS, Rosamilia A, Ramshaw JAM, Gargett CE. Immunomodulatory Effects of Endometrial Stromal Cells Seeded onto Composite Meshes for Pelvic Floor Dysfunction Repair. Tissue Engineering and Regenerative Medicine International Society, Oct 22-26, 2013, Wuzhen, China.

**Ulrich D**, Edwards SL, White JF, Su K, Tan KS, Rosamilia A, Ramshaw JAM, Gargett CE, and Werkmeister JA. A New Tissue Engineering Approach to Treat Pelvic Organ Dysfunction using Modified Meshes with Endometrial Mesenchymal stromal cells. 2<sup>nd</sup> International Medical Materials, Devices and Regenerative Medicine, Jan 11-14, 2014, Kathmandu, Nepal.

## CHAPTER 1.

### INTRODUCTION

#### 1.1 Pelvic Organ Prolapse

POP is defined as the descent or herniation of one or more of the urogenital tract organs into the vagina. Depending on the organ herniated, POP is classified into uterine, vaginal vault, anterior and posterior vaginal wall prolapse (Haylen et al. 2010) (Figure 1).

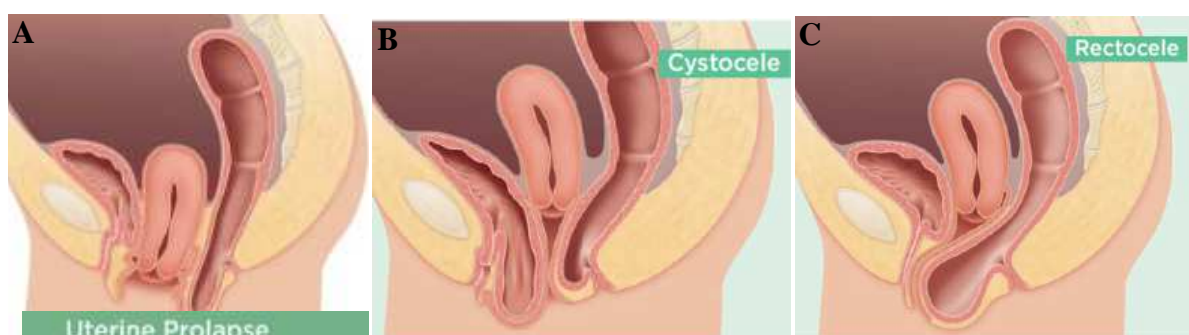


**Figure 1.** Schematic drawings of a female pelvis showing different forms of POP.

A. uterine prolapse. B anterior compartment prolapse (cystocele). C posterior compartment prolapse (rectocele). Reproduced with permission from BARD Medical.

The diagnosis of POP is based on patient's symptoms, clinical examination and can be assisted by imaging. Clinical symptoms of POP include vaginal bulging, pelvic pressure, bleeding, discharge, infection, splinting, backache or urinary incontinence. The clinical examination is based on the POP- quantification (POP-Q) system as shown in Table 1 and Figure 2. Imaging options are ultrasound, radiological as well magnetic resonance imaging (Dietz 2004). The prevalence of POP in developing countries is 19.7% (Walker and Gunasekera 2011) and almost 25% of all women in the US have one or more symptoms of POP, with urinary incontinence the most common (Nygaard et al. 2008). The impact of incontinence on the quality of life and daily functioning can be severe (Hunnskaar and Vinsnes 1991) and comparable to stroke and dementia (Mardon et al. 2006).

**Table 1.** Pelvic Organ Prolapse staging.

Stage	Clinical symptoms
0	prolapse is not demonstrated
I	the most distal portion of the prolapse is more than 1 cm above the level of the hymen
II	the most distal portion of the prolapse is 1cm or less proximal to or distal to the plane of the hymen
III	the most distal portion of the prolapse is more than 1 cm below the plane of the hymen
IV	complete eversion of the total length of the lower genital tract

Reproduced from Haylen et al., 2010

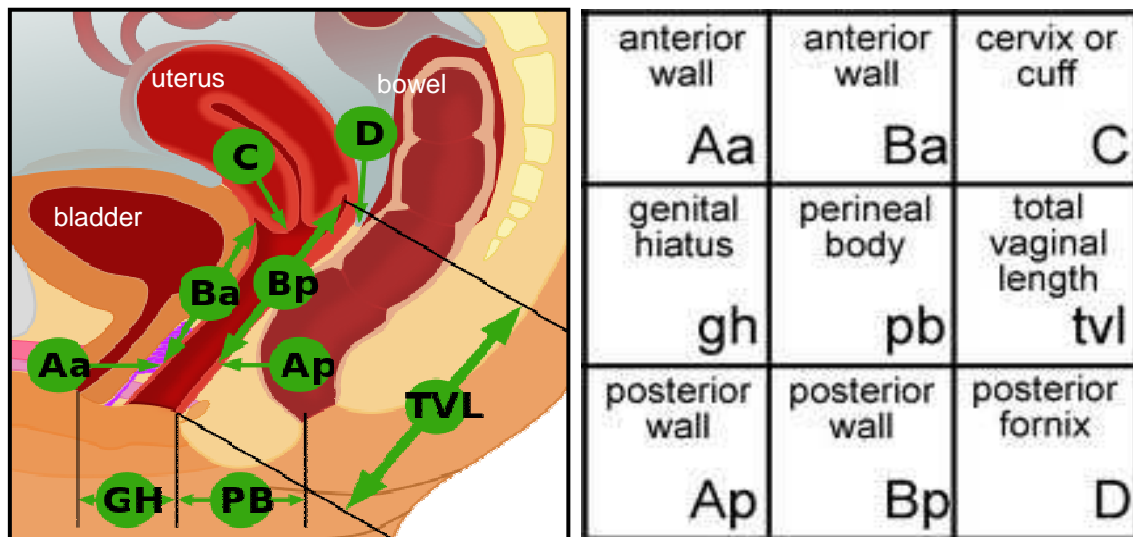


**Figure 2.** Schematic of the POP- Q system, showing the points of reference and their explanation.

Reproduced with permission from BARD Medical.

Incontinence accounts for >\$20 billion pa expenditure in the US, more than the direct costs for breast, ovarian, cervical and uterine cancers combined (Varmus 2008).

Approximately 22,000 POP operations are conducted annually in Australia (Medicare 2010) and cost approximately \$200 million.

### 1.1.1 Anatomy of the pelvis

The pelvis lies between the abdomen and the lower limbs and is divided into the greater and the lesser pelvis. The abdominal organs are hosted by the greater pelvis, the urinary

tract and the internal reproductive organs by the lesser pelvis. The female pelvic viscera in the lesser pelvis include urinary organs, the female internal genital organs and parts of the digestive tract (Figure 3A, B).

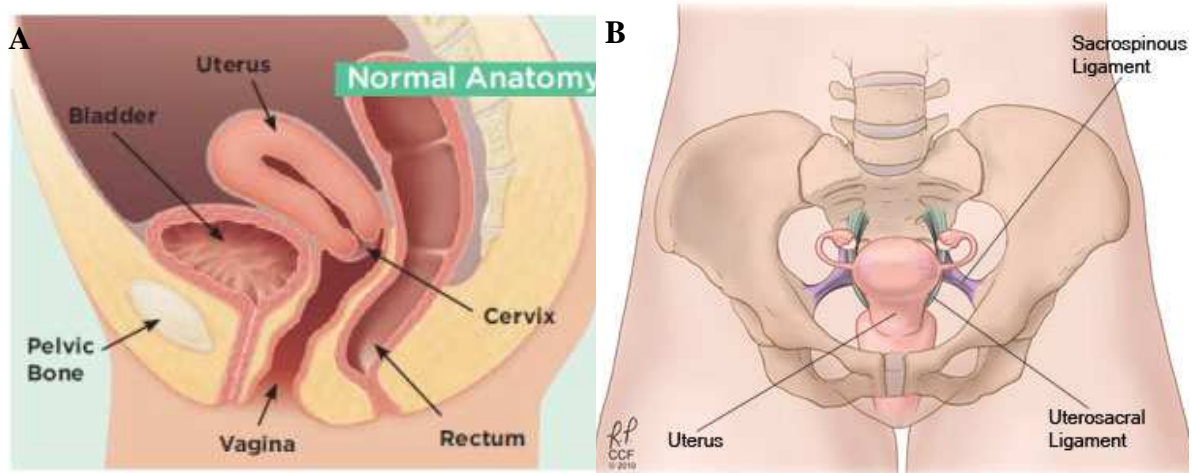


**Figure 3.** Normal Female lower urogenital tract.

A. Median anatomical section. Reproduced with permission from BARD Medical. B superior view of bony pelvis and the pelvic ligaments. Reproduced from [http://my.clevelandclinic.org/obgyn/womenshealth/urogynecology\\_pelvic\\_floor\\_disorders/treatment.aspx](http://my.clevelandclinic.org/obgyn/womenshealth/urogynecology_pelvic_floor_disorders/treatment.aspx).

The female internal genital organs include the ovaries, uterine tubes, uterus and vagina. The lesser pelvis provides the skeletal framework for both the pelvic cavity and the perineum. The anatomic structures in the female that prevent incontinence and POP comprise several muscles of the pelvic floor, the surrounding dense fibromuscular connective tissue of the vagina known as the endopelvic fascia, and the suspensory ligaments. These structures are known as the three levels of support (Delancey 1992, Ashton-Miller and DeLancey 2007) (Figure 4). The levator ani is the most important muscle structure in the pelvis and extends through the whole pelvic cavity. It is composed of the puborectalis muscle, the pubococcygeus muscle, and the iliococcygeus muscle forming a dynamic floor. The pelvic fascia is formed by two layers, the parietal and the visceral pelvic fascia acting as connective tissue surrounding the vaginal walls. The structural support of the uterus is provided by the pelvic diaphragm, as well as by its position on top of the bladder and by the cardinal and the uterosacral ligaments (Figure 3A, B). Any form of prolapse can occur due to weak muscles or any other failure in this complex interaction of the pelvic floor components (e.g. ligaments, endopelvic fascia, pelvic floor muscles).

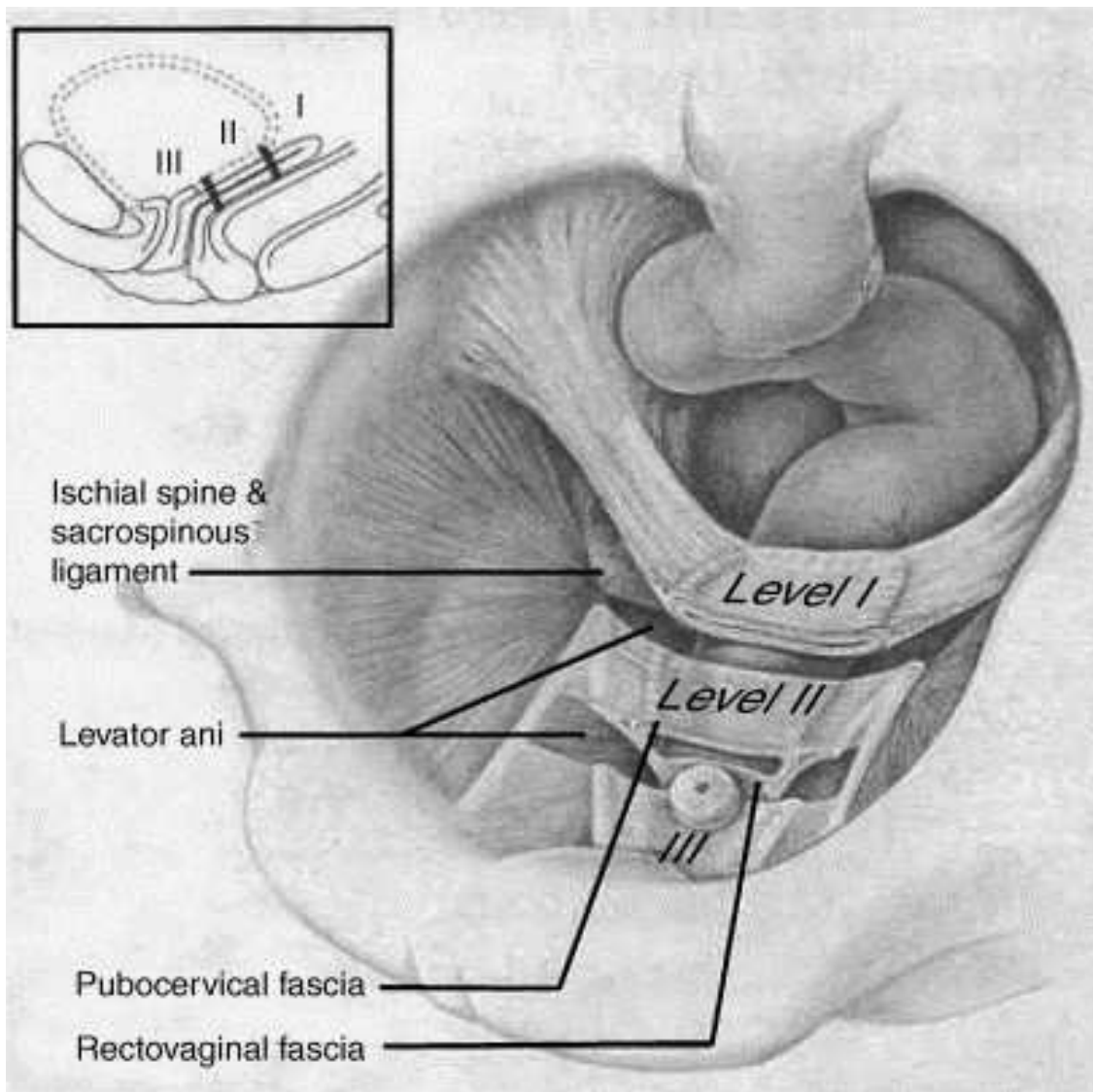


**Figure 4.** Schematic of the three levels of pelvic organ support.

Reproduced with permission from Delancey, AJOG 1992.

### 1.1.2 Causes of Pelvic Organ Prolapse

The causes of POP are likely multifactorial and depend on the individual (Schaffer et al. 2005). The biggest risk factors for POP are childbirth, ageing and obesity, with age at delivery also playing a role (Hunskar et al. 2005, Gyhagen et al. 2013).

Pregnancy and vaginal birth cause strain and injury to the pelvic support structures, including damage and/or denervation of muscle bundles (Dietz and Lanzarone 2005), and overstretching or tearing of the ligaments and endopelvic fascia. A magnetic resonance imaging study showed that 20% of 160 primiparous women sustained damage to levator ani muscles, while 0% of the control 80 nulliparous women had these injuries (Ashton-Miller and Delancey 2009). Single parity is associated with higher risk for the development of POP (Odds Ratio (OR) 2.13) than every additional pregnancy (OR 1.1).

However, no increased risk was shown after more than five parities (Hendrix et al. 2002). All women sustain stretching of their pelvic floor during vaginal birth. However, in 10-20% of women delivering their first child, forceps delivery, prolonged second stage labour, large infant birth weight, anal sphincter laceration and episiotomy exacerbate pelvic floor injury leading to POP (Ashton-Miller and Delancey 2009). Women undergoing caesarean section have a lower risk of developing POP than women after one or more vaginal deliveries (Lukacz et al. 2006) although caesarean section does not protect all women (Gyhagen et al. 2013).

Pelvic floor disorders are more common in obese women (Hendrix et al. 2002); women with a body mass index more than 26 kg/m<sup>2</sup> are more likely to undergo surgery for POP (Moalli et al. 2003). The cause of this may be due to a higher intra-abdominal pressure but is not yet fully understood yet. Women who gained weight at a mean of 4.4 kg had a significantly increased incidence of POP, however weight loss is not associated with a regression of POP (Kudish et al. 2009).

Ethnicity also influences the risk for POP. Compared with white women, African American women have a lower risk for uterine prolapse, cystocele, and rectocele. Hispanic women have the highest rate of uterine prolapse and an increased risk for cystocele, but not rectocele. Asian women have the highest risk of cystocele and rectocele, but not uterine prolapse (Hendrix et al. 2002) in a US based study.

Another important factor in the pathogenesis of POP is the vaginal collagen content. The endopelvic connective tissue in younger women with pelvic organ prolapse has a lower collagen level compared to age-matched controls without POP (Soderberg et al. 2004). A contradicting study found that total collagen was increased in the vaginal apex in women with POP compared to those without (Moalli et al. 2005). Moalli has also suggested, using semi quantitative antibody staining, that collagen type III is elevated in POP and instrumental for increased distensibility of the tissue but another more recent study using a more sensitive biochemical Western blotting assay, found quite the opposite (Zhou et al. 2012). Thus, changes in collagen composition of the vagina in women with POP are still unclear.

Increasing age has been discussed as being a risk factor for POP (Hunskar et al. 2005), however it is unclear whether concomitant changes like an increased rate of diabetes or other co-morbidities are responsible for this phenomenon. A large retrospective study did

not reveal a significant correlation between POP and age, but instead with menopause (Dietz 2008).

### **1.1.3 Treatment options for Pelvic Organ Prolapse**

POP can be treated either conservatively or surgically. For women having few symptoms or a POP-Q of stage 2 or less, observation on a regular basis is acceptable. There is an argument that in the case of a defect of the anterior vaginal wall, the post-void residual volumes should be followed on a 6 monthly basis to detect compromised bladder emptying which could lead to renal damage (Brincat et al. 2010). In practice, regular post void residual assessment does not occur indefinitely or regularly, probably due to the unawareness of many physicians.

Pelvic floor muscle training (PFMT) is one of the conservative possibilities for treating POP. PFMT aims to strengthen the sphincter structures and the supporting muscles of the pelvic floor. PFMT is associated with an improvement in POP symptoms due to an elevation of the bladder and the rectum as well as a reduction in the frequency and bother of symptoms, without causing any harm to the body (Braekken et al. 2010). Primigravid women who performed regular PFMT had a significantly lower rate of postpartum stress urinary incontinence at 3 months, however the positive effects were gone in the long term (Reilly et al. 2002). Similar results were found in a systematic review including several randomised trials (Brostrom and Lose 2008).

The use of a pessary poses another non-surgical treatment. These devices support the structures of the pelvis and relieve the pressure on bladder and bowel. Pessaries are especially suitable for women who decline surgery either in the short or long term, or who are not suitable for anaesthesia. Pessaries are available in different materials and sizes (Figure 5) and require the patient to have regular visits to a gynaecologist (Jelovsek et al. 2007) or to self-manage. There have been reports that complications such as vesicovaginal and rectovaginal fistulas, faecal impaction, hydronephrosis, and urosepsis occur, emphasizing the necessity of regular monitoring. In any case, it is important to detect vaginal bleeding due to tissue erosion or ulceration that may arise during pessary use. No randomized trials have been conducted comparing pessaries with other surgical treatment options. Surgery is indicated when urination or defecation problems, vaginal erosions or other severe conditions occur.

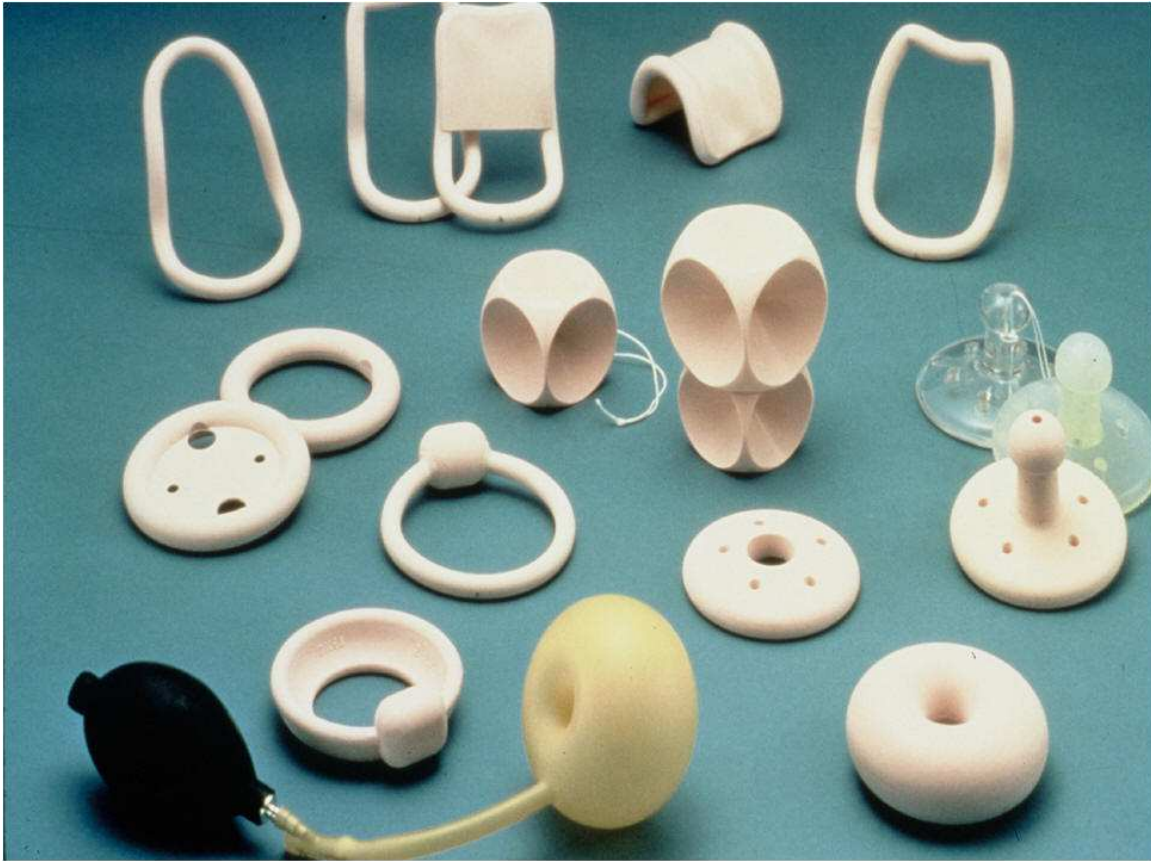


**Figure 5.** Different pessaries.

Reproduced with permission from <http://www.2womenshealth.com/Cystocele-Repair.htm>

### **1.1.3.1 Surgical treatment of Pelvic Organ Prolapse**

The life time risk for women to undergo surgery for POP and/or incontinence is 19% in the general Australian female population (Smith et al. 2010) and 11.1% in a US population based cohort (Olsen et al. 1997). The most frequent component of the pelvic organs affected by POP is the anterior vaginal wall compared to the posterior vaginal wall or the uterus regardless of the uterine status (Hendrix et al. 2002, Handa et al. 2004).

Surgical treatment for POP aims to restore the normal vaginal anatomy and normal bladder, bowel and sexual function. The first operations for prolapse repair were reported by the Egyptians and documented in the Ebers papyrus about 3500 years ago (Barbalat and Tunuguntla 2012). These early procedures were mostly fully obliterative or largely occlusive. The first vaginal hysterectomy for prolapse was performed in the US in 1861 (Young 2009) and the first anterior vaginal repair in 1913 (McCracken and Lefebvre 2007). Since then, prolapse surgery has evolved into various forms of native tissue reconstruction or mesh-based interventions. Native surgical treatment options for POP include hysterectomy, anterior and posterior vaginal repair and vaginal vault suspension,

including McCall culdoplasty, sacrocolposuspension / sacrocolpopexy (Figure 6. ), and uterosacral suspension either vaginally, laparoscopically or abdominally depending on the affected part of the vagina (Young 2009).

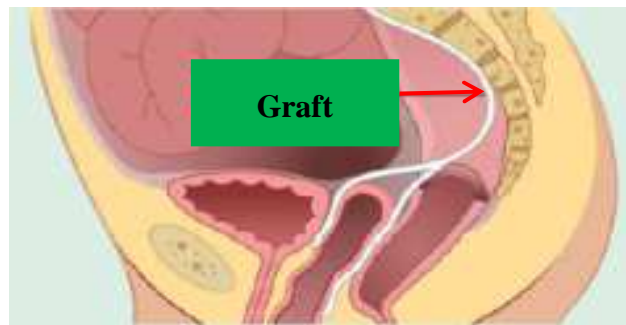


**Figure 6.** Sacrospinous fixation. Reproduced with permission from BARD Medical.

### **1.1.3.2 Anterior vaginal wall repair**

The anterior colporrhaphy is one of the standard surgical treatment options for the repair of an anterior vaginal wall defect, involving central plication of the fibromuscular layer of the anterior vaginal wall. The success rate for this procedure ranges from 40-100%. (Maher and Baessler 2006, Carey et al. 2009, Guerette et al. 2009). However, the recurrence rate is higher compared to techniques using degradable polyglactin mesh or porcine dermal inlays (Maher et al. 2010) (Section 1.1.3.5). Another surgical treatment option is vaginal paravaginal repair which has equally high success rates (67-100%). However, this surgical procedure can have significant complications such as haemorrhage in up to 20% (Mallipeddi et al. 2001, Young et al. 2001). Another surgical approach which is no longer widely practised in Australia is the trans-abdominal internal anterior repair in combination with Burch colposuspension for patients with grade 1 or 2 cystoceles and stress urinary incontinence. It has reasonably good short term results but decreasing efficacy after 5 years (Lovatsis and Drutz 2001).

### **1.1.3.3 Posterior vaginal wall repair**

Only a few treatment options for the posterior vaginal wall repair exist. The original posterior colporrhaphy with plication of the levator ani muscle has a high anatomical success rate but also a high rate of dyspareunia, vaginal and/ or rectal pain (Kahn and Stanton 1997, Ulrich et al. 2014). To minimize this side effect, midline fascial plication (posterior colporrhaphy) without levator ani plication, as well as site-specific rectocele repair operations, is preferred. Both methods result in similar anatomic and functional outcomes with significant improvements in symptoms, quality of life, and sexual function with dyspareunia rates ranging from 8-26% (Maher et al. 2004, Paraiso et al. 2006).

#### **1.1.3.4 Surgical treatment options with synthetic meshes**

Due to the relatively high failure rates of native tissue surgery, synthetic meshes were introduced into POP surgery. Surgical methods for repair of POP have increased in number and complexity since the introduction of synthetic meshes. Their aim is to provide additional support not provided by existing and damaged pelvic floor musculature, ligaments and endopelvic fascia to improve the relatively poor long-term outcomes of native tissue surgery alone (Hiltunen et al. 2007). Synthetic meshes have been used in abdominal POP surgery as part of the abdominal sacral-colpopexy procedure (Kohli 2012). Compared with other disciplines, the use of synthetic materials in vaginal POP surgery has only been introduced within the last two decades (Kohli 2012). The specialties of orthopaedic or general surgery have a long history incorporating the use of synthetic materials in surgical procedures and have provided important knowledge and data. The meshes used in urogynaecology were originally designed for abdominal hernia repair and are well studied for this specific application (Scott et al. 2002, Deprest et al. 2006). Driven by marketing, following the success of the synthetic midurethral slings for stress urinary incontinence, Polypropylene (PP) meshes were introduced quickly into vaginal POP surgery in an attempt to decrease prolapse recurrence rates (De Ridder 2008) without due consideration of mesh suitability, particularly mesh mechanical properties. Meshes for vaginal repair were introduced as Class II devices where a manufacturer only had to demonstrate that a new device was comparable to an existing device, the so called 510k path to market. In contrast, Class III devices have to undergo thorough premarket approval review. It has only very recently been suggested that new meshes should undergo appropriate stringent preclinical testing before entering the market (Deprest and Feola 2013). Synthetic non-degradable meshes are believed to work by inducing an inflammatory foreign body reaction, resulting in fibrosis that provides strength, albeit not necessarily optimal, to the weakened support structures (Deprest et al. 2006, de Tayrac et al. 2007).

#### **1.1.3.5 Anterior vaginal wall repair with mesh**

The success rates for anterior colporrhaphy (Figure 7A) with mesh, not using trocar-based systems range from 92-97% and from 77-97% for trocar-based systems with POP-Q stage  $\leq 1$  as the primary outcome (Hinoul et al. 2008, Milani et al. 2011, Stanford et al. 2011). Trocar mesh placement systems allow the mesh to be fixed to an anatomical structure.

Mesh complications such as erosion or exposure have been reported to occur in up to 25% of cases at an average follow up of 12-24 months. Up to 11% of women with mesh exposure require reoperation usually including the removal of the exposed mesh and epithelial closure (Jia et al. 2010). The largest randomized clinical trial involving 200 study subjects compared the success rates between PP mesh and anterior repair alone and found significantly better success rates for the mesh group (Altman et al. 2011). A recent review also concluded that procedures using mesh in the anterior compartment have better long term anatomical success rates, but with increased risks of complications (Maher et al. 2013). The use of biological materials for anterior defect repairs has shown contradictory results (Maher et al. 2011).

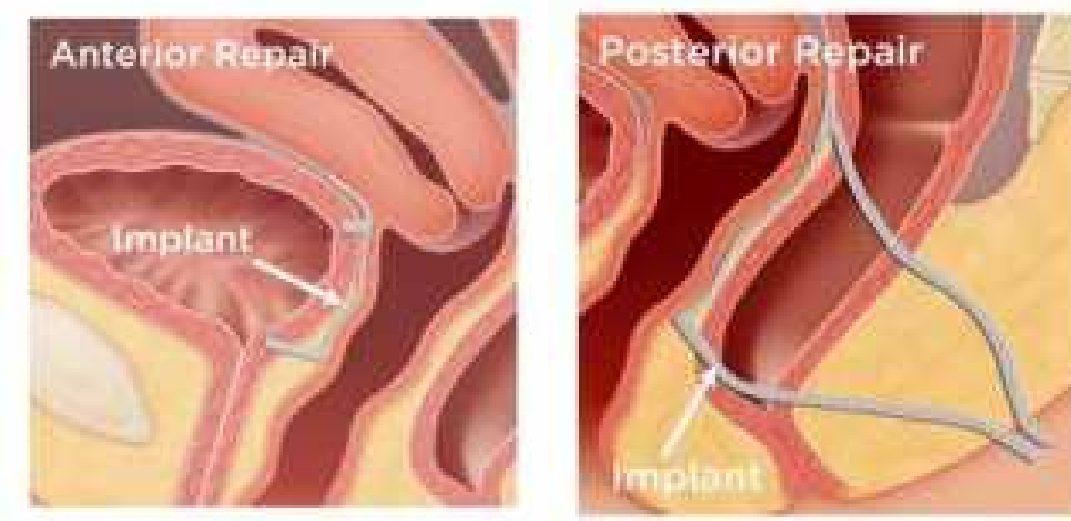


**Figure 7.** Schematic of anterior and posterior vaginal wall repair using mesh.

A. Schematic of anterior vaginal wall repair with a synthetic implant. B. Schematic of posterior vaginal wall repair with a synthetic implant. Reproduced from BARD Medical.

#### **1.1.3.6 Posterior vaginal wall repair with mesh**

Cure rates for posterior vaginal wall repair (Figure 7B) with mesh have been reported between 75-92% without trocar use and 92-97% with trocar-based systems with fixing of the mesh to an anatomical structure (de Tayrac et al. 2006). The mesh complication rate was up to 25% after 1 year (Stanford et al. 2012). Generally, there are not enough randomized clinical trials to draw sufficient conclusions to support mesh use in the posterior compartment (Maher et al. 2013).

### 1.1.3.7 Apical compartment repair with mesh

The most common apical repair surgery is the abdominal sacrocolpopexy (SCP) (Figure 6). The SCP gives support to the vaginal walls and vault by using an interposition graft usually of synthetic mesh and anchoring this to the anterior longitudinal ligament over the periosteum of the sacral promontory (indicated by the white line in Figure 6).

Sacrospinous colpopexy (SSC) fixes the vault or the apex to the sacrospinous ligament, a very strong ligament at the back of the pelvis. Both SCP and SSC provide subjective success rates of 94% and 91%, respectively with no significant differences in re-operation rates for prolapse (RR 0.46, 95% CI 0.19 to 1.11) (Higgs et al. 2005, Maher et al. 2010). Mesh or suture erosions after laparoscopic sacrocolpopexy occur in 3-12% of patients after an average follow up from 6 to 36 months (Drutz and Alarab 2006).

The use of biological materials for apical repair does not appear to be beneficial in terms of the long term outcome due to rapid resorption of the materials (Yurteri-Kaplan and Gutman 2012).

### 1.1.3.8 Mesh classification

Synthetic meshes differ in pore size, composition (polymer type), filament type (monofilament vs. multifilament), knitted mesh design and surface properties (coated versus non coated). Meshes are divided into four groups as shown in

**Table 2.** The foreign body reaction to the mesh is dependent on the various mesh properties, i.e., monofilament meshes generally induce lower inflammation compared to multifilament meshes because immune cells get trapped between the filaments (Klinge et al. 2002). Pore size is another determining factor, with larger pore sizes allowing better tissue ingrowth with lesser inflammation; however, if the pore sizes are too large, tissue ingrowth occurs more slowly and can compromise the structural integrity of the mesh (Klinge et al. 2001, Klinge et al. 2002, Pascual et al. 2008). Microporous meshes (<10 µm pore size) induce a greater foreign body reaction because the immune cells are unable to penetrate the mesh. Overall, a monofilament mesh with a large pore size is the preferable option (Huebner et al. 2006); such a mesh might improve tissue integration and therefore decrease the rate of side effects. Recently our laboratory has shown that meshes knitted from alternative materials (polyether-ether-ketone and polyamide) with similar architecture to the commercially available polypropylene meshes have improved biomechanical

properties with reduced stiffness and a lower bending rigidity (Edwards et al. 2013) (Figure 8).

**Table 2.** The classification of synthetic biomaterials.

Mesh type	Filamentous structure	Pore size
I	Monofilament	Macro ( $> 75\mu\text{m}$ )
II	Multifilament	Micro ( $< 10\ \mu\text{m}$ )
III	Multifilament	Macro/ micro ( $< 10\ \mu\text{m}$ )
IV	Multifilament	Submicro ( $< 1\ \mu\text{m}$ )

Adapted from Huebner et al., 2006

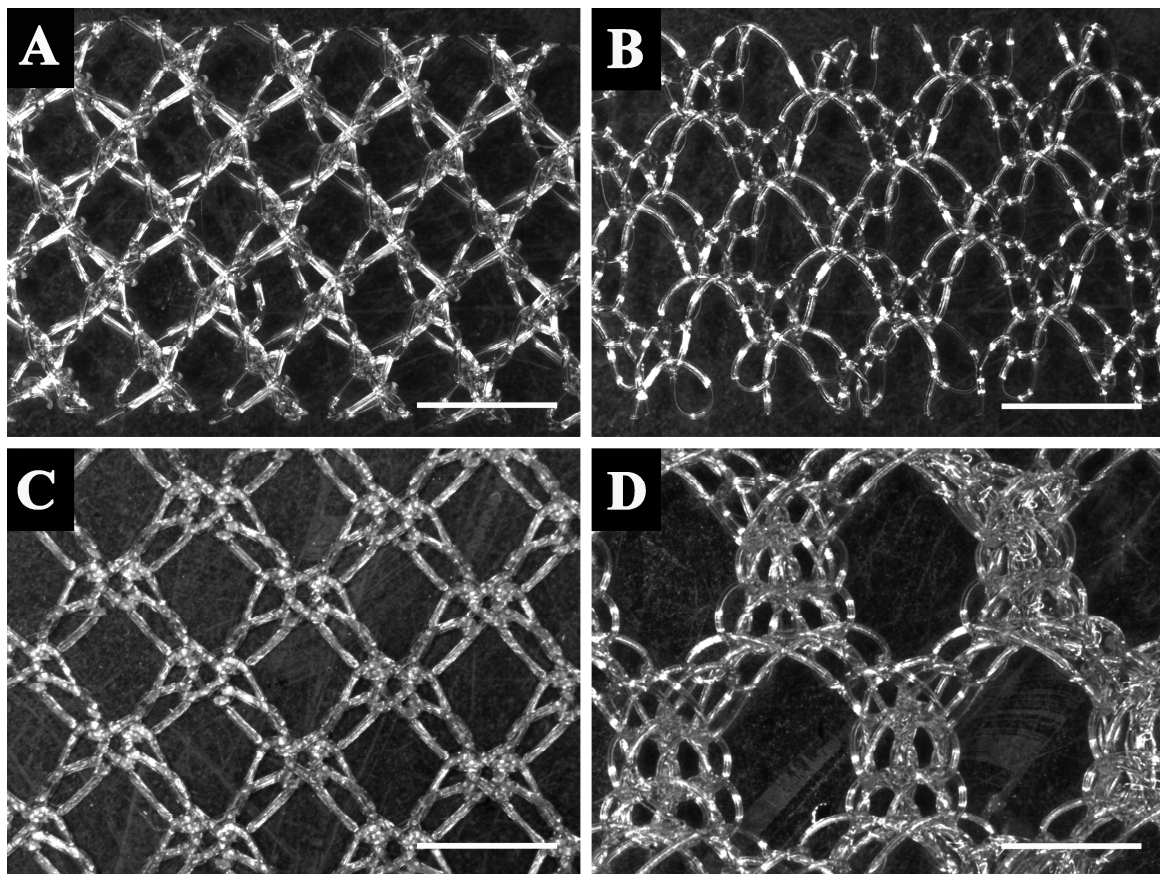


**Figure 8.** Optical micrographs of meshes.

A. Polyamide 1, B. Poly-ether-ether-ketone 1, C. Polyform, D. Poly-ether-ether-ketone 2. Scale bar: 2000  $\mu\text{m}$ . Reproduced and modified with permission from Edwards et al. 2013

#### **1.1.4 The mesh dilemma- The knowledge gap**

The ideal implant should be biocompatible, nontoxic, noncarcinogenic and nonteratogenic (Bringman et al. 2010). Any material will evoke a foreign body reaction due to the body's recognition of the foreign material through the innate immune system. After mesh insertion an inflammatory response occurs. This reaction may reflect poor tissue biocompatibility, depending on the extent and type of response and local host factors. The foreign body reaction, involving tissue macrophages, is primarily responsible for the significant complications arising from the use of synthetic meshes reported in up to 29% of cases, including mesh contraction, pain, and exposure of mesh into the vagina or erosion into adjacent viscera (Lim et al. 2007). It has been shown that vaginally inserted meshes are associated with higher mesh exposure complication rates than abdominally inserted meshes (Ozog et al. 2012). Also, the surgeon's experience, patient selection and operative condition seem to have an influence on the graft-related complications (Deprest and Feola 2013). As a result of reported complications, the US Food and Drug Administration released a warning regarding the use of mesh in urogynaecological applications in 2008 and an update in 2011 (2008, 2011). In response to these warnings, several companies withdrew some of the mesh devices for vaginal surgery from the market in 2012.

The success of a mesh design is, in part, dependant on mesh mechanical properties. An ideal material should have appropriate strength, stiffness, structural integrity, flexibility and elasticity. A big difference between mesh mechanical properties and the native tissue is a known risk factor for poor tissue compliance and complications. The ideal mesh for vaginal POP surgery has not yet been reported (Bringman et al. 2010). When I began this study, there were no reports on the development of new meshes for POP surgery. Only just recently studies have attempted to develop alternative biomaterials to improve tissue regeneration and biocompatibility (Boennelycke et al. 2011). There is an urgent need to develop meshes which match the biomechanical properties of human vaginal tissue for tissue compatibility and optimal tissue integration, to provide adequate treatment for women suffering from POP.

## 1.2 Stem Cells

Stem cells are responsible for the development and regeneration of tissue and organ systems. There are three main types, embryonic stem cells, induced pluripotent stem cells and adult stem cells. Embryonic stem cells are derived from the inner cell mass of the blastocyst embryo and as pluripotent cells they can differentiate into all cell types derived from the three embryonic germ layers, ectoderm, endoderm and mesoderm (Alvarez et al. 2012) (Figure 9). Induced pluripotent (iPS) cells are also pluripotent and are produced by reprogramming somatic cells (Takahashi et al. 2007). In contrast, adult stem cells are rare, long-lived cells found in most adult tissues, for example haematopoietic stem cells are multipotent and were first discovered in 1961 by Till and McCulloch (Till and Mc 1961). Adult stem cells also self-renew but are more restricted in differentiation repertoire (i.e. multipotent) and are less proliferative than embryonic stem cells. Problems associated with embryonic stem cells are their unpredictable differentiation and tendency to generate teratomas (Prokhorova et al. 2009), ethical issues and difficulty of access, therefore making adult stem cells an easier, safer, attractive option for cell-based therapies.

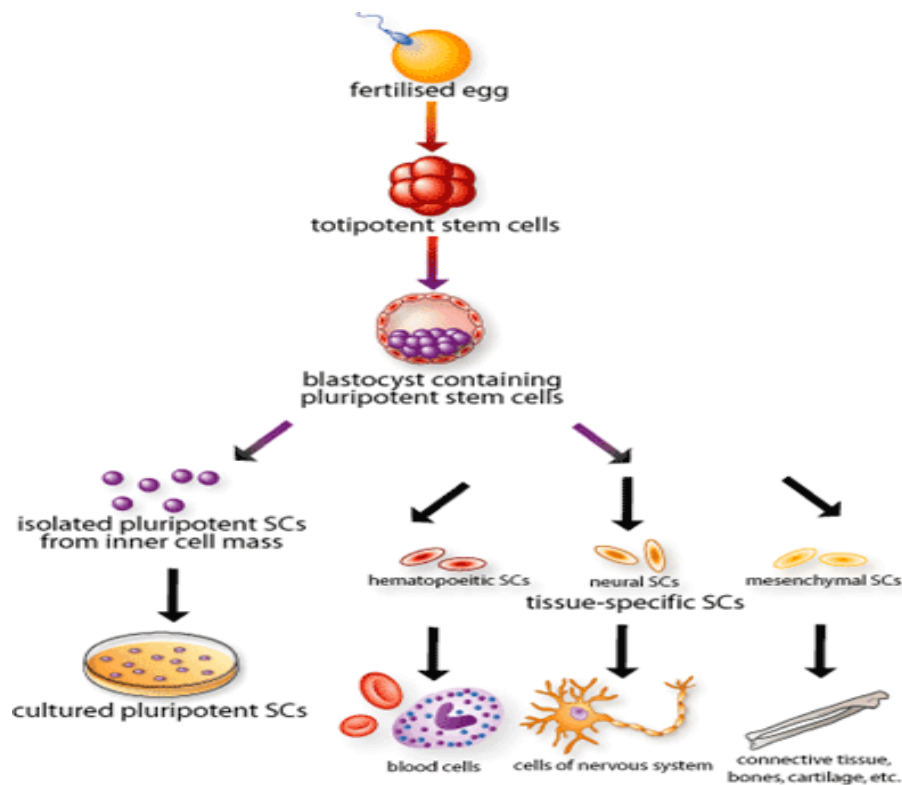


**Figure 9.** The origin and specialisation of stem cells.

Reproduced with permission from <http://www.scq.ubc.ca/stem-cell-bioengineering/>

## 1.2.1 Stem cell properties

Adult stem cells are not readily recognisable in tissues. Until markers are discovered, they are identified by their functional properties; self-renewal, differentiation and proliferative capacity (Gargett 2007).

### 1.2.1.1 Colony-forming unit activity

In contrast to mature cells, stem cells are able to show colony-forming unit (CFU) activity. CFU is defined as the ability of a single cell to form a clone of cells when seeded at extremely low density (Loeffler et al. 1997) (Figure 10).

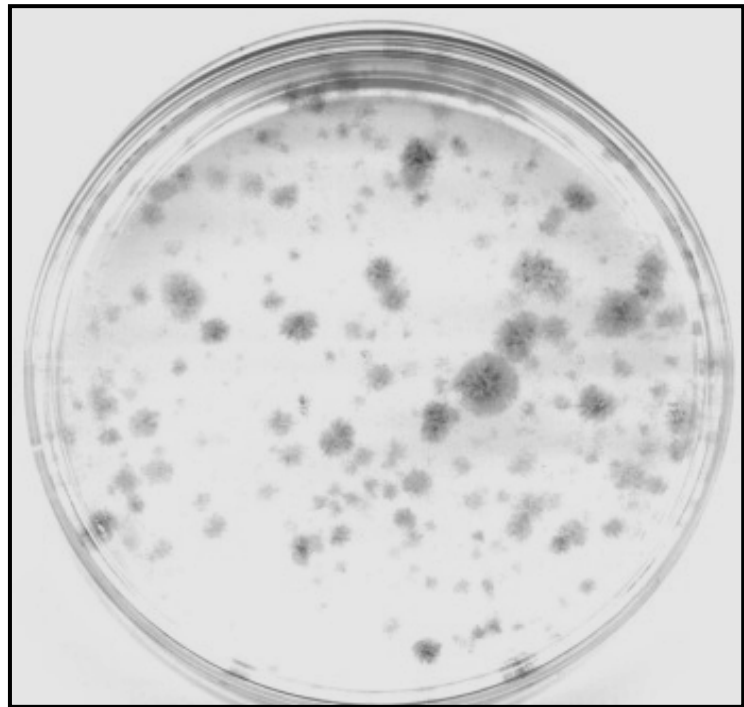


**Figure 10.** Stromal colony forming units from human endometrium.

Reproduced with permission from Chan et al., 2004.

### 1.2.1.2 Self renewal

Only a small number of stem/progenitor cells are present in any adult tissue.

These cells are generally quiescent, and possess the ability to re-enter the cell cycle by certain signalling pathways enabling them to self-renew

and replace themselves and at the same time differentiate into the functional cells of the tissue in which they reside. Several molecular and biochemical pathways are involved in stem/progenitor cell entry into cell cycle, which cell types they differentiate into and the number of progeny produced (Fuchs and Segre 2000). Asymmetric cell division is the process where an identical daughter cell and a more differentiated daughter cell is produced (Fuchs and Segre 2000) (Figure 11). An alternative process is symmetric division leading to either two identical stem cells or two more differentiated daughter progenitor cells, which then differentiate into two transit amplifying cells (Loeffler et al. 1997, Morrison et al. 1997). Stem cells are able to self-renew and replace themselves but also provide populations of differentiated cells that perform the function of a tissue.

Transit amplifying cells are rapidly proliferating cells before their final differentiation into mature functional cells (**Figure 11**).

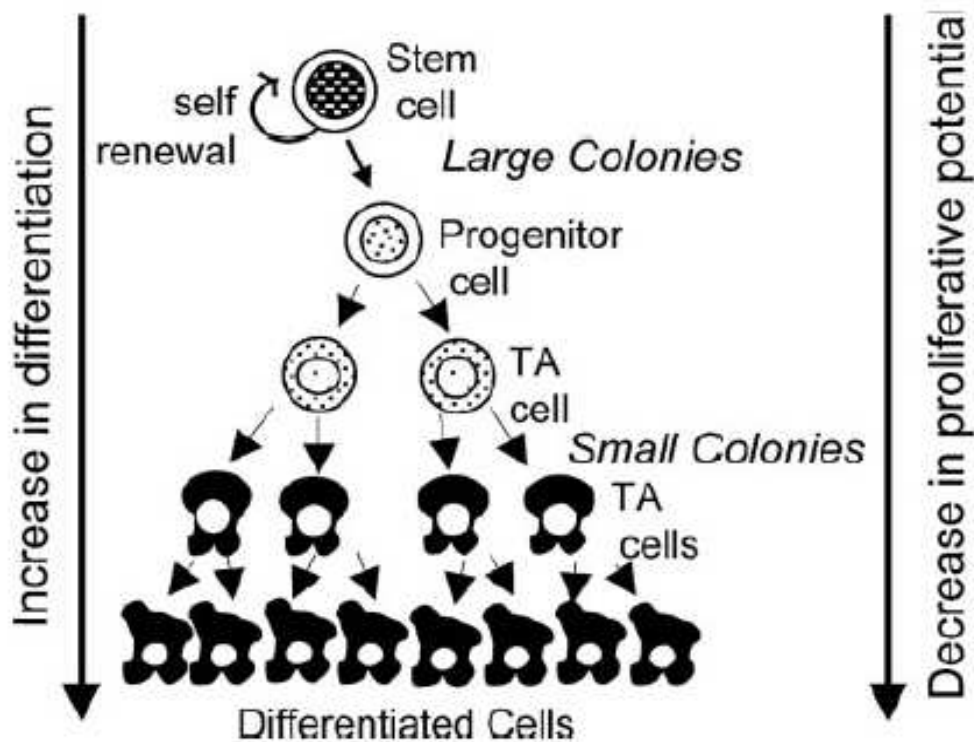


**Figure 11.** Hierarchy of tissue stem cell differentiation.

Stem cells undergo asymmetric cell divisions, which enable them to self-renew and replace themselves or differentiate to give rise to committed progenitors. These proliferate and give rise to more differentiated functional cells with no capacity for proliferation. Reproduced with permission from Chan et al. (2004)

### 1.2.1.3 High proliferative potential

One objective verification of stem cell activity is determining their proliferative potential or cellular output from a single cell, which is greater for stem cells compared to any progenitor or transit amplifying cells (Pellegrini et al. 1999, Gronthos et al. 2003). For example conjunctival keratinocyte stem cells formed holoclones (epidermal stem cells), which had the greatest proliferative capacity compared to their more differentiated progeny cells which generated smaller meroclones (mixture of stem cells and differentiated cells) and paraclones (transit amplifying cells) (Pellegrini et al. 1999).

#### **1.2.1.4 Stem cell differentiation**

Stem cell differentiation includes the change of the cell phenotype and function involving changes to gene expression and signalling pathways. Stem cells undergo several tiers of incremental differentiation with each round of cell division until they produce fully differentiated (specialised) and post-mitotic functional tissue specific cells (Figure 11). During the process of differentiation the original stem cell loses the capacity to self-renew and differentiate into more than one lineage.

#### **1.2.1.5 Tissue reconstitution in vivo**

Another key feature of stem cells is their ability for regenerating tissues by producing replacement cells after tissue damage or cellular loss (Clarke and Smith 2005). This has been elegantly demonstrated in a mouse model where the epithelium of an entire organ (mammary gland) was reconstituted from a single epithelial stem cell using the mammary fat pad assay (Shackleton et al. 2006), however studies in humans are sparse for tissues other than bone marrow and its populations of haemopoietic stem cells (Kapoor et al. 2007).

#### **1.2.1.6 Stem Cell Niche**

The regulation of adult stem cell fate decisions (i.e. to self-renew or differentiate) is determined by the neighbouring niche cells and surrounding extracellular matrix (ECM) (Schofield 1978). Niche cells generate signals that regulate stem cell proliferation and cell fate decisions (Eckfeldt et al. 2005). However, current knowledge on the characteristics and mechanism of niche cells in human stem cell systems is generally sparse. Adhesion molecules like cadherins or integrins play a role in anchoring adult stem cells in the niche during inactivity as well as in managing asymmetric cell divisions (Zhang et al. 2003, Fuchs et al. 2004, Wilson and Trumpp 2006).

### **1.2.2 Mesenchymal Stem Cells**

#### **1.2.2.1 Properties and phenotype of MSC**

Mesenchymal stem cells or mesenchymal stromal cells or multipotent stromal cells (MSC) are defined as plastic adherent, clonogenic cells with a characteristic surface phenotype, capacity to proliferate extensively and differentiate into several mesodermal lineages (Vaananen 2005). MSC were first discovered in bone marrow in 1966 and later described

by Friedenstein *et al.* as adherent fibroblast-like cells (Friedenstein *et al.* 1976). According to the International Society for Cellular Therapy (ISCT), MSC must fulfil three main criteria; plastic-adherence, multilineage differentiation into osteoblasts, adipocytes and chondrocytes, myocytes and other connective tissue cells *in vitro*, and possession of key surface markers, including CD29, CD44, CD73, CD105 and CD146 but not the haematopoietic cell markers CD34, CD45, CD14, CD11b, CD79 $\alpha$ , CD19 and HLA-DR (Dominici *et al.* 2006, Caplan 2007). MSC from different tissue sources may possess unique markers that can be used for their prospective isolation. For example, CD271 and STRO-1 have been used to identify and isolate and enrich bone marrow MSC (Simmons and Torok-Storb 1991, Buhning *et al.* 2007). Therefore, these criteria may not be applicable to MSC from every tissue type since MSC possess different surface markers depending on their origin and the MSC definition may need revision (Keating 2012).

#### **1.2.2.2 Sources of MSC**

MSC have been identified in most tissues including bone marrow, adipose tissue, dental pulp, umbilical cord, corneal stroma, cord blood, skeletal muscle, periosteum, scalp tissue, pancreas, placenta, synovial membrane and endometrium (Gronthos *et al.* 2000, Schwab and Gargett 2007, Crisan *et al.* 2008, Brooke *et al.* 2009). MSC appear to transdifferentiate into several cell lineages other than their mesodermal germ layer of origin, making them an attractive source for cell-based therapies for future treatment options (Pittenger *et al.* 1999). Furthermore, substantial evidence indicates that MSC are a subset of pericytes that line blood vessels (Schwab and Gargett 2007, Caplan 2008, Crisan *et al.* 2008, Masuda *et al.* 2012) and promote tissue repair. MSC are a heterogeneous population, especially when obtained by the plastic adherence method. A more pure population can be obtained when MSC are extracted with antibodies against specific surface markers.

MSCs were originally thought to aid tissue repair by transdifferentiation (Griffin *et al.* 2010, Prockop and Youn Oh 2012) into the cell types required. However, there is increasing recognition that MSC act in a paracrine manner by homing to damaged tissues and secreting copious quantities of bioactive molecules. These molecules promote angiogenesis, limit fibrosis and scarring, inhibit apoptosis and promote tissue specific progenitor cells to proliferate (Caplan 2009, Murphy *et al.* 2013). MSC also dampen the inflammatory response and modulate both the innate and adaptive immune system.

### **1.2.2.3 Anti-inflammatory properties of MSC**

MSCs also function in modulating the inflammatory responses; however the mechanisms are still unclear and these functions are yet to be fully elucidated (Le Blanc and Ringdén 2005, Chen et al. 2006, Kaplan et al. 2011, Le Blanc and Mougiakakos 2012, Prockop and Youn Oh 2012). However, in an inflammatory milieu, cytokines such as tumor necrosis factor alpha (TNF- $\alpha$ ) and IFN- $\gamma$  license MSC (Krampera 2011) to produce anti-inflammatory mediators including prostaglandin E2 (PGE2) (Ylostalo et al. 2012), Indoleamine 2,3-dioxygenase (IDO) (Meisel et al. 2004) and nitric oxide (Ren et al. 2008), which in turn modulate the function of natural killer (NK) cells and macrophages, key cells involved in the innate immune response. When macrophages are co-cultured with MSC, their production of pro-inflammatory cytokines such as TNF- $\alpha$  and IL-6 are diminished and anti-inflammatory cytokines such as IL-10 increased (Kim and Hematti 2009, Maggini et al. 2010). MSC production of PGE2 drives a phenotypic change in macrophages from pro-inflammatory (M1) to anti-inflammatory wound healing (M2) phenotypes (Kim and Hematti 2009) through interaction with macrophage prostanoid receptors. MSC also modulate the inflammatory response through Toll-Like Receptor (TLR) signalling. Viral dsRNA activation of TLR-3 receptors on MSC initiates production of anti-inflammatory effectors that reduce the inflammatory response of macrophages, while a pro-inflammatory macrophage response results from lipopolysaccharide (Gram negative bacterial cell wall component) activation of TLR-4 on MSC. This suggests that there are two different MSC phenotypes, MSC1 (pro-inflammatory) and MSC2 (anti-inflammatory) (Waterman et al. 2010). These phenotypes were speculated to result from stimulation by low concentrations of agonists, levels likely expected *in vivo*. Further studies are needed to confirm the differential effects of TLR-3 and TLR-4 stimulation to confirm these MSC phenotypes, as others have also shown that LPS stimulated MSC exert an anti-inflammatory response (Maggini et al. 2010, Foraker et al. 2011).

### **1.2.2.4 Immunomodulatory properties of MSC**

The immunosuppressive effects of MSC on the adaptive immune system predominantly affect T-cell proliferative responses to foreign, non-self MHC molecules on antigen presenting cells (APC). These immunomodulatory properties of MSC have been exploited for treating graft versus host disease and indeed bone marrow MSC have been used in a successful clinical trial for this purpose (Le Blanc et al. 2008). More recently placental

stromal cells were also successfully used for the treatment for acute graft-versus host disease with a response rate of 75% in a trial of 8 patients (Ringden et al. 2013). Much still remains to be learned about the normal role of MSC in immunomodulation and the role this might play in tissue repair and how this can be manipulated to create new therapeutics.

#### **1.2.2.5 Identification of MSC in human tissues.**

MSC are rare and few are available for harvest from adult tissues, requiring their substantial expansion *ex vivo*. As with most adult stem cells, prolonged culture of MSC results in their spontaneous differentiation to fibroblasts (Li et al. 2011). In addition, the numbers of MSC present in the bone marrow decrease with ageing, with a tenfold loss occurring within the first 10 years of life, and a similar rate of loss continuing into adulthood (Haynesworth et al. 1993). Furthermore, MSC defining surface markers are also expressed on fibroblasts and other cells, making it difficult to identify and purify MSC from adjacent tissue cells (Alvarez et al. 2012). MSC are predominantly identified by their properties in cell culture; CFU activity and multipotency, but flow cytometry phenotyping and fluorescence- activated cell sorting (FACS) using recently identified novel markers (Stro-1, TNAP/W8B2) have also been used by some (Shi and Gronthos 2003, Buhning et al. 2007, Sobiesiak et al. 2010). Furthermore, MSC change their surface marker expression in culture, making it more difficult to obtain pure MSC (Boquest et al. 2005).

Identification of specific markers for MSC purification is a priority of current research, together with optimisation of culture conditions to prevent spontaneous differentiation and loss of MSC activity, and to achieve the desired cell type for transplantation (Tang et al. 2012).

#### **1.2.2.6 Survival of transplanted of MSC**

Many animal and human studies have demonstrated a beneficial effect of MSC infusion or implantation on tissue and organ repair. MSC travel to sites of tissue damage when infused intravenously, where they secrete bioactive molecules that promote tissue repair, with little evidence of engraftment (Prockop 2009). When infused cells are tracked *in vivo* after administration, few are found as they are rapidly trapped in the lungs and cleared from tissues. For example, intravenous injection of bmMSC in a mouse model of coronary artery disease (coronary vessel ligation) significantly improved myocardial parameters after 3 weeks; however, the cells were not detected after 48 hours (Lee et al. 2009). Large

numbers of MSC were found in the lungs where they induced upregulation of 50 genes including TNF- $\alpha$  (Lee et al. 2009). In contrast, the inflammatory response in a rat model of corneal injury was reduced after intraperitoneal infusion of bmMSC. After 10 million cells were injected, <10 were detected on day 3 suggesting that the cells do not engraft but rather release anti-inflammatory cytokines and proteins, including TNF- $\alpha$ –stimulated gene/protein 6 (TSG-6) (Roddy et al. 2011). Similar results were observed in a model of peritonitis and sepsis (Nemeth et al. 2009, Choi et al. 2011).

It has been suggested that MSC act through a “touch and go” mechanism. MSC rapidly migrate to the damaged site and are cleared after release of their anti-inflammatory and immunomodulatory payload (Uccelli et al. 2008). Culture expanded bmMSC do not express HLA class II cell surface molecules indicating their lack of involvement in the specific immune response (Koc et al. 2000). MSC can therefore be used in an allogeneic setting and there are several companies developing “off the shelf” allogeneic products (Mesoblast, Medistem) with the advantage that a single donor can produce thousands of doses. It is currently unclear if immune rejection will be provoked if repeated doses from different individuals are administered. A recent review did not find an increased rate of toxicity events after unmatched heterologous MSC administration, suggesting that MSC are “immune- privileged” (Lalu et al. 2012). In most of these studies, multiple doses of MSC have not been administered and therefore it is still uncertain whether allogeneic MSC might initiate an immune response in these circumstances. Multiple treatments are not an issue for autologous MSC and regulatory requirements are simpler (Murphy et al. 2013).

### **1.2.3 Endometrial MSC**

The endometrium undergoes regular cycles of shedding and regeneration for over 400 times during a woman’s reproductive years (Edwards SL 2010) suggesting that a MSC population may be responsible for generating the stromal vascular compartment each month. Indeed, recently, a small population of clonogenic endometrial stromal cells with typical adult stem cell properties of self renewal, high proliferative potential and multilineage mesodermal differentiation capacity was identified in human endometrium (Gargett et al. 2009). These cells are clonogenic and self-renew as demonstrated by serial cloning in culture. They are also highly proliferative, undergoing 30 population doublings with a total cellular output of several billion cells from a single cell indicating their

capacity for *ex vivo* expansion and potential utility in cell-based therapies. These were defined as endometrial mesenchymal stem-like cells (eMSC). Cells with eMSC properties have also been identified as a component of the Side Population (SP) cells (Cervello et al. 2010, Masuda et al. 2010, Cervello et al. 2011). EMSC can be easily obtained by uterine biopsy from premenopausal women with access via the cervix (Ulrich et al. 2013) (Figure 12). In contrast, the procurement of bmMSC and adipose MSC requires at least local anesthesia, while the endometrium is one source of human MSC that usually does not require an anaesthetic (Gargett et al. 2012). Clonogenic endometrial stromal cells were found in both reproductive age and postmenopausal women, and in the endometrium of women on oral contraceptive therapy (Schwab et al. 2005) indicating that eMSC could be harvested from women of all ages irrespective of hormonal status or treatments.

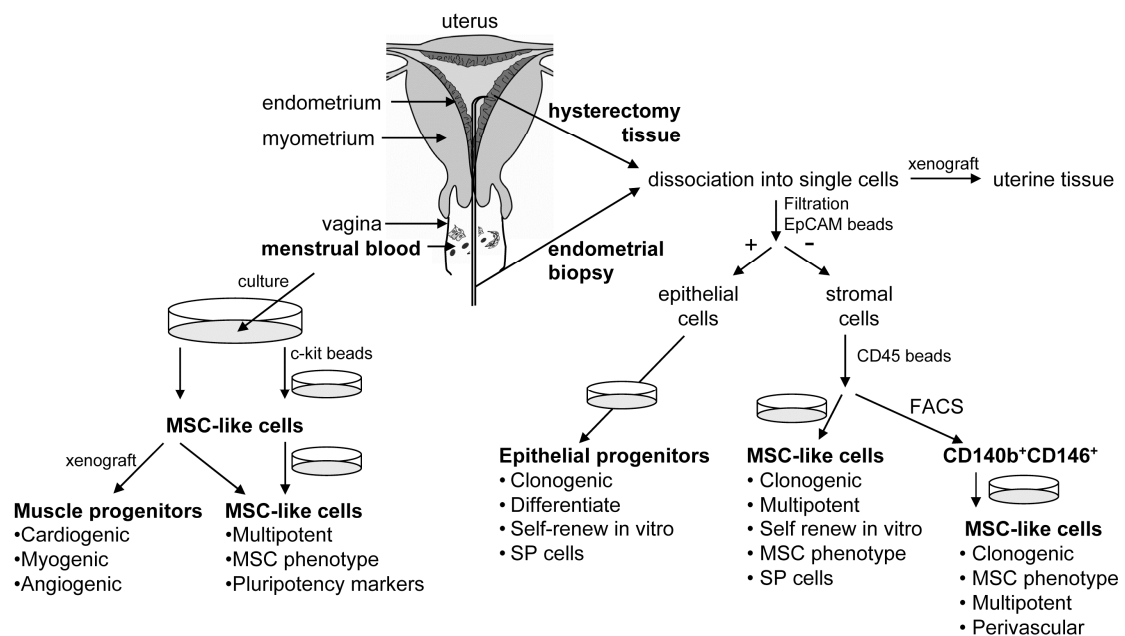


**Figure 12.** Schematic showing isolation procedures for obtaining endometrial stem/progenitor cells from human uterus and menstrual blood.

Endometrial stem/progenitor cells are sourced from hysterectomy, endometrial biopsy and menstrual blood. Culture dishes indicate when culture occurs in the isolation or characterisation procedures. Adult stem cell features conducted on the various cell populations are shown as dot points. Adapted and reproduced with permission from World Scientific Publishers, Singapore (Gargett 2010).

### **1.2.3.1 EMSC Differentiation**

Large endometrial stromal colony forming units (CFU) undergo multilineage differentiation into four mesodermal lineages when cultured under appropriate conditions, including smooth muscle, fat, cartilage and bone (Gargett et al. 2009). Cultured endometrial stromal cells containing eMSC not only differentiate down typical mesodermal lineages, but also into other non-endometrial cells, including platelet releasing megakaryocytes *in vitro* (Wang et al. 2012), possibly by a direct transdifferentiation mechanism that does not involve de-differentiation or transition through distinct hierarchies of haematopoietic stem cells (Ladewig et al. 2013). EMSC also differentiate into ectodermal and endodermal lineages including neural cells *in vitro* and *in vivo* (Wolff et al. 2011, Mobarakeh et al. 2012) and insulin-producing cells *in vitro* (Santamaria et al. 2011) making them a possible source for use in neurodegenerative diseases like stroke, Parkinson's disease, Alzheimer's disease, amyotrophic lateral sclerosis, epilepsy, trauma and intoxications, and for treatment of diabetes. In these studies unfractionated human endometrial stromal cells were used and it is presumed that the approximately 1-5% eMSC that would be present in these cultures were responsible for this differentiation.

### **1.2.3.2 Origin of eMSC**

The precise origin of eMSC is not entirely clear. An endogenous source derived from residual fetal stem cells has been proposed (Gargett 2007), while there is also some evidence that bone marrow cells may incorporate into human and mouse endometrium and contribute to the generation of endometrial cells (Taylor 2004, Du and Taylor 2007). Currently it is not known if these incorporating bone marrow derived cells are haematopoietic stem cells, MSC, myeloid cells or endothelial progenitor cells (Gargett 2007), but they do not contribute to the SP population (Cervello et al. 2012). In women transplanted with a single antigen HLA mismatched bone marrow, significant chimerism ranging from 0.2 to 52% of the endometrial glands and stroma was observed in 4 patients (Taylor 2004). Most glands, however, consisted entirely of either host or donor-derived cells indicating monoclonal derivation. In other studies, chimeric endometrial glands were reported in three women who had received gender mismatched bone marrow transplants (Ikoma et al. 2009). Due to the low levels of engraftment of bone marrow cells in

endometrium, it seems therefore more likely that eMSC originate from resident stem/progenitor cells than bone-marrow derived cells; however more research is needed.

### **1.2.3.3 Prospective isolation and scale up culture of eMSC**

MSC from bone marrow and adipose tissue are frequently obtained from simple culture of adherent cells and contain a mixture of fibroblasts and MSC. STRO 1 has been used to purify bmMSC but this marker did not purify clonogenic eMSC from human endometrium (Schwab et al. 2008). Specific markers have been identified for the prospective isolation of eMSC from human endometrium as the co-expressing CD140b<sup>+</sup> CD146<sup>+</sup> -cell population (Schwab and Gargett 2007). This CD140b<sup>+</sup>CD146<sup>+</sup> population fulfils the minimal criteria for MSC, including multipotency, clonogenicity and surface phenotype (CD29, CD44, CD73, CD90 and CD105 expression). A recent gene profiling study of the 3 populations sorted from endometrial stromal cells on the basis of CD140b and CD146 expression confirmed that eMSC are found in the double positive population and the expressed genes were involved in angiogenesis, inflammation, immunomodulation, cell communication and proteolysis (Spitzer et al. 2012).

A recent development was the identification of a single marker, W5C5 for eMSC (Masuda et al. 2012). The W5C5 antibody detects the SUSD2 transmembrane protein expressed on the cell surface (Sivasubramaniyan et al. 2013). Extracting eMSC via magnetic beads is possible with a single marker and preferable to FACS sorting as it is rapid, uses simpler technology and is less traumatic for the cells (Masuda et al. 2012). On average, 4.2% of endometrial stromal cells are positive for W5C5 (Masuda et al. 2012). The W5C5<sup>+</sup> eMSC fulfil the minimal criteria for MSC (Dominici et al. 2006) making them preferable for use as a cell-based therapy in proof-of-principle animal models (Ulrich et al. 2013).

Furthermore, W5C5<sup>+</sup> cells generate stromal tissue when xenografted into immunocompromised mice (Masuda 2012) (Section 1.2.4.5)

### **1.2.3.4 Ex vivo culture of eMSC for cell-based therapies**

The niche regulates stem/progenitor cells by providing a specific physiological environment. Niche cells produce growth factors and other cytokines that together with extracellular matrix molecules regulate their functional state. Certain growth factors support the growth of eMSC in serum free medium, including fibroblast growth factor 2 (FGF2), epidermal growth factor (EGF), transforming growth factor- $\alpha$  (TGF-  $\alpha$ ) and platelet-derived growth factor-BB (PDGF-BB) (Schwab et al. 2005). Due to their rarity in

tissues, yields of freshly isolated eMSC are small which makes *in vitro* expansion necessary. In preparation for clinical use, protocols have been developed for serum-free, xeno-free culture expansion of eMSC (Rajaraman et al. 2013). In the first steps to achieve clinical grade production of eMSC, a serum free medium comprising several growth factors was developed and cells were cultured in hypoxic O<sub>2</sub> concentrations, without changing surface marker expression, differentiation capacity or proliferative potential (Rajaraman et al. 2013).

#### **1.2.3.5 W5C5+ eMSC Regenerate Stromal Tissue in vivo**

One of the most important functions of stem cell populations is their ability to reconstruct the appropriate tissue *in vivo*. W5C5<sup>+</sup> eMSC reconstituted endometrial stromal tissue after transplantation under the kidney capsule in non-obese diabetic severe combined immunodeficient interleukin-2 receptor  $\gamma$ -deficient (NOD SCID  $\gamma$  or NSG) mice (Masuda et al. 2012). Similarly endometrial stromal tissue was also reconstituted when human endometrial SP cells were transplanted under the kidney capsule of immunocompromised mice (Masuda et al. 2010, Cervello et al. 2011). These findings indicate that prospectively isolated, culture-expanded eMSC have the capacity to regenerate tissue and therefore have utility as a cell-based therapy (Ulrich et al. 2013).

#### **1.2.4 Endometrial Regenerative Cells from menstrual blood**

The endometrium is partially shed during menstruation every month, leaving behind the basal regenerative layer from which the new functional layer grows (Gargett et al. 2012). The markers used to purify eMSC, co-expression of CD140b and CD146 or the single marker, W5C5/SUSD2, reveal their perivascular location in both the basal and functional layer, indicating they will be shed each month during menstruation. It is therefore not surprising that viable MSC have been identified in menstrual blood. These have been isolated and characterized in a similar manner as bmMSC using plastic adherence. These cultures include both MSC and fibroblasts. These adherent cells were described as endometrial regenerative cells (ERC) (Meng et al. 2007) and in this thesis, this term will be used. ERC express key MSC markers (CD9, CD29, CD41a, CD44, CD59, CD73, CD90, and CD105), and lack the haematopoietic cell markers CD14, CD34 and CD45. Similar to cultured eMSC they do not express STRO-1. The ERC retained a stable karyotype for up to 68 passages in culture and doubled every 19 hours, showing a higher proliferation rate than cord blood MSC (Meng et al. 2007). ERC have also been extracted

from cultured menstrual blood mononuclear cells by c-kit selection (Patel et al. 2008). Matrix metalloproteases were highly expressed in ERC; they produced high levels of MMP3, MMP10, and growth factors including granulocyte-macrophage colony stimulating factor (GM-CSF), angiopoietin-2 and PDGF-BB (Meng et al. 2007). ERC differentiated into 9 different cell lineages from the three germ layers, including cardiomyocyte, neuronal, hepatic, and pancreatic lineages (Meng et al. 2007, Patel et al. 2008). ERC express the pluripotent markers OCT-4 and SSEA-4 (Patel and Silva 2008). ERC were also clonogenic, expressed typical MSC surface markers and differentiated into mesodermal lineages (Musina et al. 2008). Myogenic differentiation of ERC was demonstrated by co-culture with rat cardiomyocytes. Some cultured cells started to beat spontaneously, formed sheets of heart muscle and incorporated into cardiac muscle when transplanted as a patch *in vivo* (Hida et al. 2008). Similarly, cardiomyogenic transdifferentiation was observed when ERC were cultured in serum free medium, showing greater physiological similarity to cardiomyocytes compared to those cultured in serum containing medium, likely due to unknown quantities of inhibitory factors present in some batches of serum (Ikegami et al. 2010).

#### **1.2.4.1 ERC and bmMSC have similar properties**

A recent, comprehensive comparative profiling of ERC and bmMSC for gene expression, miRNAs and cytokine production showed similar but not identical profiles (Wang et al. 2012). BmMSC express higher levels of VEGF, IL-6, TGF $\beta$ 1 or TGF $\beta$ 2, whereas ERC express higher levels of IL-8 and ICAM-1 suggesting that ERC may have a role in acute inflammation and may be more suitable for different tissue engineering purposes. Other angiogenic cytokines, PDGF-BB and angiopoietin, were 27-fold and 14-fold higher in ERC compared to bmMSC, respectively, suggesting that alternative angiogenesis pathways may be activated by ERC. Further studies are needed to determine if ERC stimulate more angiogenesis *in vivo* than bmMSC. ERC seeded onto nanofibrous polycaprolactone scaffolds produced proteoglycans and collagen type II *in vitro*, indicating their potential for differentiating into cartilaginous tissue (Kazemnejad et al. 2012). ERC proliferate faster than bmMSC and express the pluripotency marker, OCT-4, but like eMSC (Schwab et al. 2008) lack the MSC marker, STRO1 (Kazemnejad et al. 2012). ERC have been isolated by three independent groups (Meng et al. 2007, Musina et al. 2008, Patel et al. 2008) and appear similar to eMSC. Although comparative studies have not been reported for eMSC and ERC, it is expected that purified eMSC populations

(CD140b<sup>+</sup>CD146<sup>+</sup> or W5C5<sup>+</sup>/SUSD2<sup>+</sup>) would be more potent than unfractionated plastic adherent stromal cells cultured from menstrual blood. Further studies are also needed to compare eMSC directly with bmMSC.

## **1.3 Tissue Engineering**

All of the current surgical procedures used for treating POP provide support of pelvic organs, but do not appropriately repair the damaged tissue. As POP results from damage, injury, and ligament rupture, a new treatment option using a tissue engineering (TE) approach is needed.

TE is the combination of cells and materials for implantation which aims to restore, maintain, or improve tissue function or a whole organ (Langer and Vacanti 1993). Engineered simulated or natural extracellular matrices ("scaffolds") serve as the basis and vary according to the target application. A large variety of synthetic non degradable and degradable polymers as well as biological materials with a wide range of biomechanical properties have been used in TE (Fisher and Mauck 2013). Different cell types can be used for TE purposes; autologous/homologous cells (from the same person/animal), heterologous/allogeneic cells (from the same species but different person/animal), and xenogeneic cells (different species). Cells can be injected or implanted, either alone or with carriers such as hydrogels or in scaffolds as matrix-based tissue engineering approach (Fisher and Mauck 2013). Autologous cells are the preferred types of cells as rejection due to immunological causes do not occur. More recently the usage of mesenchymal stem cells has evolved for allogeneic use considering their potential and their anti-inflammatory and immunomodulatory properties.

### **1.3.1 The potential of TE in the field of regenerative medicine**

Several studies in different medical fields have shown good results with TE approaches.

#### **1.3.1.1 Cell based and tissue engineering approaches**

The properties of collagen meshes before and after stromal cell seeding have been investigated (Ochoa et al 2011). In these studies, human adipose- derived MSC were obtained from human liposuction procedures. After 7 days of co-culture of the meshes with or without MSC the biomechanical strain increased significantly in the cell-seeded

meshes compared to the unseeded meshes indicative that the cells had begun to form new tissue which improve mesh properties (Ochoa et al. 2011).

Transplanted bone- marrow derived stem cells (bmMSC) engineered into a cell-sheet placed onto scarred myocardium improved wall thickness and cardiac function in a myocardial infarction rat model (Miyahara et al. 2006). An angiogenic effect of ERC was observed in a mouse model of muscular dystrophy which resulted in improved muscle repair (Cui et al. 2007). In this study,  $2 \times 10^7$  ERC were injected into the thigh muscle of dystrophic mice and were compared to saline injected controls. Mice treated with cells showed increased dystrophin expression in the affected muscles and improved muscle regeneration determined by quantitative immunohistochemistry. ERC have also been used to treat myocardial infarction in a rat coronary artery ligation model. Rats received  $1-2 \times 10^6$  ERC or bmMSC into the infarct lesion, 2 weeks after artery ligation. The size of the myocardial infarction zone was reduced in ERC-treated rats compared to the control or bmMSC group (Hida et al. 2008) suggesting that ERC have a stronger reparative effect *in vivo* than bmMSC.

More recently it was shown that polyglactin prosthetics seeded with bmMSC are associated with less adhesions in a rat abdominal hernia model compared to non- seeded hernia prosthetics (Dolce et al. 2010).

Only one study so far reports about the preclinical use of eMSC. The potential clinical utility of eMSC for treating an inflammatory disorder was examined in a mouse model of encephalomyelitis (Peron et al. 2012). Fewer infiltrating mononuclear cells were observed in the lesions when eMSC were administered intraperitoneally compared to animals without eMSC due to reduced recruitment of both Th1 and Th17 cells into the central nervous system. The cytokines IL-10 and IL-27 were upregulated in the spleen, suggesting that eMSC exerted a systemic anti-inflammatory effect. It has to be noted that the control group in this study was not properly described, so further studies evaluating the immunomodulatory properties of eMSC are still necessary.

A successful TE approach in a human experimental setting is tracheal reconstruction using PP mesh tubes. The prosthesis was either soaked with peripheral blood, heterologous bone marrow aspirates or autologous bone-marrow- derived cells. The MSC seeded scaffolds resulted in better regeneration of dog tracheal mucosa after 1 and 12 months (Nakamura et al. 2009). Recently a case report of a two year follow up after tracheal replacement in a

young boy was published (Elliott et al. 2012). BmMSC were seeded on a decellularised cadaveric donor tracheal scaffold. The graft revascularised within 1 week after surgery, cytological evidence of restoration of the epithelium was present at one year. The graft developed biomechanical strength at 18 months, and at 2 years the TE construct served as a functional airway.

### **1.3.2 TE used in reproductive tract disorders**

Several studies have investigated the use of MSC seeded scaffolds for bladder reconstruction in animals and humans. Success in terms of less graft shrinkage and functionality was higher in MSC seeded scaffolds (Atala et al. 2006, Jayo et al. 2008, Tanaka et al. 2010). Promising results were also published in repairing urethral defects when using TE constructs comprising tubularized synthetic biomaterials seeded with autologous bladder derived epithelial and muscle cells (Raya-Rivera et al. 2011). The scaffolds seeded with cells showed significantly better tissue development compared to the unseeded scaffolds. Similarly, another study showed successful urethral reconstruction with a biodegradable tubularized polyglycolic acid:poly(lactide-co-glycolide acid) (PGA:PLGA) scaffold seeded with autologous muscle and epithelial cells. All patients received satisfactory urinary flow rate and normal appearing architecture of the urethra (Raya-Rivera et al. 2011).

TE approaches for uterine reconstruction were similarly successful. Autologous rabbit uterine muscle and epithelial cells were grown on uterine-shaped biodegradable polymer scaffolds. The TE constructs were reimplanted into the animals, normal uterine tissue components were confirmed and the development of embryos was supported (Lu et al. 2009).

Preliminary attempts to generate vaginal tissue using TE techniques demonstrated similar success. Rabbit smooth muscle cells and epithelial cells derived from vaginal biopsies were seeded onto PGA polymers. The tubular scaffolds with or without cells were surgically re-implanted into the rabbits as a total vaginal replacement. The seeded constructs developed a normal vaginal tissue architecture, innervation and comparable tensile stress and strain properties compared to unseeded constructs that did not show innervation (De Filippo et al. 2008). Similarly, mouse muscle-derived stem cells (mdSC) were cultured on porcine decellularised collagen material (SIS®) and these TE constructs were implanted into rat vagina. The mdSC scaffolds stimulated vaginal tissue repair by

promoting epithelial regeneration as well as reducing fibrosis (Ho et al. 2009). More recently, smooth muscle and epithelial cells from rabbit vaginal tissue were seeded on biodegradable PGA and implanted into mice. The explanted constructs showed complete layers of vaginal epithelial cells and smooth muscle cells (Dorin et al. 2011).

One study reported on cervical reconstruction. Cervical cells from healthy donors were isolated and seeded on porous silk scaffolds using normal and dynamic culture conditions. After 8 weeks a tissue complex similar to the native tissue in terms of morphology, biochemical and mechanical properties was obtained. The dynamic culture conditions were associated with significantly increased collagen deposition and stiffness (House et al. 2010).

In summary, it seems that human tissue-engineered reproductive organ constructs constitute a novel approach for a range of fundamental medical conditions in women.

### **1.3.3 TE for POP repair surgery- The gap**

The damaged pelvic floor including muscles, endopelvic fascia and ligaments needs to be repaired sufficiently to achieve good long term outcomes for POP surgery. The current treatment options with or without meshes only give structural support and have a high complication rate or poor long term outcomes. No TE approach has been developed for POP treatment to date, but increasing interest is shown by the growing number of conference abstracts and review articles pointing out the need for this a new treatment approach for POP (Bhatia and Ho 2004, Gargett and Chan 2006, Aboushwareb et al. 2011). A TE construct comprising an easily obtainable cell source like eMSC and novel meshes could be a first step towards the development of a novel treatment option for POP.

## **1.4 Experimental approaches for investigating a TE approach for POP repair**

### **1.4.1 Animal Models for investigating POP repair surgery**

Rodents have been used for a wide variety of research applications for many years. Mice and rats have the advantage that they are small in size, easy to work with, relatively cheap and available in large numbers (Abramowitch et al. 2009). However, the reproductive tract in rats is small and the pelvic musculature is different to humans, which does not make them an ideal model for experiments in the pelvic region. However, in urogynaecological

applications rats are the preferred animal to test tissue integration and biomechanical properties of new meshes using the abdominal hernia model (Zheng et al. 2004, Konstantinovic et al. 2005, Konstantinovic et al. 2010). The pressure from the abdominal organs is thought to mimic the movements of the pelvic floor. An additional advantage of rodents is that they are available as gene knock-out mice/ rats, i.e. athymic rats have a greatly reduced or absent cell mediated immunity with a marked reduction in T-lymphocyte function making them ideal models for xenograft applications (Glover et al. 2010). A striking discovery was made in 1992, when human bone marrow injected intravenously into severe combined immunodeficient (SCID) mice repopulated the bone marrow, setting the beginning of post-radiation therapy for leukemic patients (Lapidot et al. 1992). Immunodeficient animals are preferable for tissue engineering constructs because they can host xenografted cells without immune rejection.

Rabbits have similar advantages to rodents with their larger size an additional benefit, facilitating larger implants and providing more tissue for histology. However, they are not an ideal model to study POP as the anatomy of the vagina and the pelvis differs significantly from humans. Additionally, they do not undergo spontaneous estrous cycling (Abramowitch et al. 2009).

Sheep are also relatively cheap and available in large numbers, particularly in Australia, with the advantage that their large size and their similarity to the human pelvic connective tissue anatomy with the same three primary levels of support (Abramowitch et al. 2009). Sheep can be used to model many urogynaecological operations and experiments. Furthermore sheep have prolonged labours with a large head-to-vaginal ratio and have a similar frequency of spontaneous POP (Shepherd 1992). In contrast to humans, sheep are quadruped and not bipedal which may limit their utility for clinical translation. However, their risk in developing POP increases with every pregnancy, but can also occur in virgin sheep similar to nulliparous humans (Couri et al. 2012).

Thorough analysis of the histological and biomechanical properties of the ovine vagina can help us to understand the complexity of POP and provide baseline data for comparison when evaluating TE approaches for treating POP. Sheep vaginal tissue has a similar structure to human vagina comprising of the epithelium, subepithelium, muscularis and adventitia (Ennen et al. 2011). Analysis of the biomolecular structure of vaginal tissue showing that the  $\alpha$ 2-chain of collagen I is decreased in prolapsed sheep compared to

controls (Ennen et al. 2011), however knowledge about vaginal biochemical composition and biomechanical properties is sparse.

Non human primates would also pose a suitable model for POP because they have similar anatomy to humans and develop spontaneous POP. However, ethical restrictions are high as are the costs (i.e. \$13,000 for one macaque at Monash University, Australia).

#### **1.4.2 Connective tissues of the pelvic floor structures**

The cellular components of the endopelvic fascia comprise fibroblasts which produce the majority of the extracellular matrix (ECM) and smooth muscle cells which allow vaginal contractility. The ECM consists of fibrous proteins (egg. collagens, elastin), as well as a range of glycosaminoglycans usually attached to a core protein (proteoglycans) (Couchman and Pataki 2012). The ECM is a dynamic structure that responds to the changing environment by remodelling. Collagen type I comprises the major fibrillar protein found in bone, ligament and interstitial tissues that influences the tensile strength of these tissues (Prockop and Kivirikko 1995, Gelse et al. 2003). Collagen I, together with elastin and smooth muscle cells influence the biomechanical and particularly the viscoelastic properties of the vaginal wall. Collagen type III is also a fibrillar protein that is widely distributed in soft tissues like skin and blood vessels and can contribute to tissue elasticity. An increase in collagen III in healing or regenerative tissues usually reduces the tissue mechanical strength by decreasing the overall collagen fibre diameter of collagen I/III heterofibrils. The relative content of collagen types appears to change as women age. The ratio of collagen I/ (III+V) is decreased in the arcus tendineous fasciae pelvis (ATFP) in postmenopausal women suggesting that tensile strength is compromised and therefore increases the susceptibility for POP in older women (Moalli et al. 2004).

Elastin, a stable rubber-like protein, allows tissue to stretch (Li et al. 1991) and return to its original shape without energy loss (Ritz-Timme et al. 2003). No differences in the amount of elastin detected by immunohistochemistry was found between pre- and post-menopausal women in the ATFP (Moalli et al. 2004). A more recent study using immunoblotting revealed higher tropoelastin (elastin precursor) and as a consequence also higher elastin expression measured by radioimmunoassays in women with POP compared to age matched controls suggesting that vaginal tissue remodels and adapts to mechanical stretch (Zong et al. 2010).

Metalloproteinases (MMPs) play a key role in protein decomposition in the ECM (Woessner 1991). Tissue-derived inhibitors of metalloproteinases (TIMP's) counteract the effect of MMP's by binding and inactivating them and therefore preventing over-degradation. One study correlated histological findings with scanning electron microscopy data and gelatin zymography to assess the role of collagens and MMP's in women with POP. Women suffering from POP had a higher collagen content in their vaginal tissue due to overexpression of collagen III compared to premenopausal controls. Active MMP-9 was also increased in patients with POP, whereas no differences were observed for proMMP-2 or proMMP-9 suggesting that vaginal tissue undergoes remodelling in POP (Moalli et al. 2005). The amount of collagen type I was decreased in biopsies of the uterosacral ligament in women with POP compared to women without, whereas metalloproteinase-1 (MMP-1) was increased (Vulic et al. 2011). Similarly, younger women with POP (<53 years) had a 30% lower collagen than age-matched controls (Soderberg et al. 2004). Histology has been correlated with biomolecular analysis in sheep with or without prolapse (Ennen et al. 2011). Sheep with POP had a decreased expression of the collagen I  $\alpha$ 2-chain compared to controls, and an increased rate of collagenase, MMP 1 activity suggesting that prolapse is associated with malfunction in metabolic processes. Human vaginal tissue of premenopausal women contained more collagen III than postmenopausal tissue determined by Western blot (Zhou et al. 2012). These findings were correlated with scanning haptic microscope measurements (assessment of stiffness on a microscale) evaluating tissue stiffness showing that premenopausal tissue was less stiff and more elastic. Generally women with POP independent of their hormonal status had stiffer vaginal walls which did not correlate- with the quantitative analysis.

Another important protein in the ECM is fibulin with fibulin I being the most widely analysed. Fibulin mutations are present in patients with Marfan's syndrome, a condition associated with prolapse (Carley and Schaffer 2000), curvature of the spine (scoliosis), abnormal joint flexibility or unexplained stretch marks on the skin among other things. Fibulin-3, fibulin-4 and fibulin-5 were more recently characterized and have unique properties inducing synthesis and assembly of elastic fibres and subsequently vaginal recovery (Drewes et al. 2007). It is therefore not surprising that reduced fibulin-5 concentrations in the para-urethral ligaments in pre- and post-menopausal women suffering from POP were lower compared to controls. Fibulin-5 regulates MMP-9 on a

molecular level suggesting that POP is an acquired disorder of ECM metabolism (Budatha et al. 2011).

The muscularis of the vagina also plays a major role in providing support when tonically contracted and stretches to give way for transit of the baby's head during birth. A recent detailed study revealed differences between different regions of the rat vagina (Skoczylas et al. 2013). There was an increase of circumferentially aligned muscle bundles in the distal region compared to the middle and proximal regions in relation to the vaginal length.

## **1.5 Biomechanical properties of pelvic floor tissue**

Biomechanical testing of the vaginal tissue is a relatively new field. Different groups have introduced different testing protocols, which makes it difficult to compare the results. Furthermore, it is often difficult to obtain sufficient human vaginal tissue for testing (Cosson et al. 2004, Zimmern et al. 2009). Common biomechanical parameters measured include stiffness, strength and deformability represented by tangent modulus, tensile strength and tensile strain, respectively. The rat poses an adequate model to test biomechanical properties of the vaginal support structures (Moalli et al. 2005). Similar to the human vagina, collagen I is the predominant structural protein, followed by collagen III. More recently rhesus macaques have been used for biomechanical testing. When combined with quantitative histology, inferior biomechanical properties like decreased stiffness, tensile strength or strain energy density and collagen alignment was demonstrated after vaginal delivery compared to nulliparous controls (Feola et al. 2010).

Hormones, especially estrogen, affect vaginal tissue by increasing the elasticity and height of the epithelium. Estrogen can also improve symptoms of stress urinary incontinence. Similarly, estrogen restores the biomechanical properties of the vagina in ovariectomised "menopausal" rats (Moalli et al. 2008). The same group also examined the effect of pregnancy and vaginal delivery in rats. Vaginal distensibility, measured with a balloon connected to a pressure transducer, was increased in pregnant compared to virgin rats and did not return to virgin levels in postpartum rats (Alperin et al. 2010). Similarly, the effect of hormones on the vagina and its supportive tissues was compared in rats. Tissue stiffness (related to tissue distensibility) and load at failure (the load at which the tissue ruptures) were decreased in pregnant compared to virgin rats, and returned to virgin levels within a month after delivery (Feola et al. 2010). This suggests that the hormonal changes during

pregnancy allow adaptation of the pelvic floor to accommodate the fetus (Lowder et al. 2007). Similar results were found in vaginal tissue of *Fbln5*<sup>-/-</sup> mice, which spontaneously develop prolapse in 91% of females with increasing age and multiparity. The vaginal tissue of *Fbln5*<sup>-/-</sup> mice has higher distensibility with an even lower stiffness during pregnancy compared to virgins (Rahn et al. 2008).

The first biomechanical testing of human vaginal tissue was performed in 2002 with a study comparing pre- with post-menopausal women suffering from POP using uniaxial testing (Goh 2002). Several limitations of this study include differences in POP staging between the two groups compared and that it was restricted to anterior vaginal tissue. However, no significant differences in permanent elongation were found, but a higher elastic modulus (tissue was stiffer and less distensible) was observed in the postmenopausal tissue likely due to ageing. In a similar study the maximal rupture strength and strain of posterior vaginal fundal tissue showed great variability between the 16 postmenopausal women with POP (Cosson et al. 2004). However elastic modulus, which is an important measurement for comparison of these tissues during surgical repair, was not reported. In a comparative study of vaginal tissue from women with and without prolapse, vaginal stress-strain response was non-linear (with regions of different stiffness levels) and hyperelastic (Rubod et al. 2008) (Figure 13). This data provided the first insight into vaginal tissue biomechanical properties (Rubod et al. 2008).

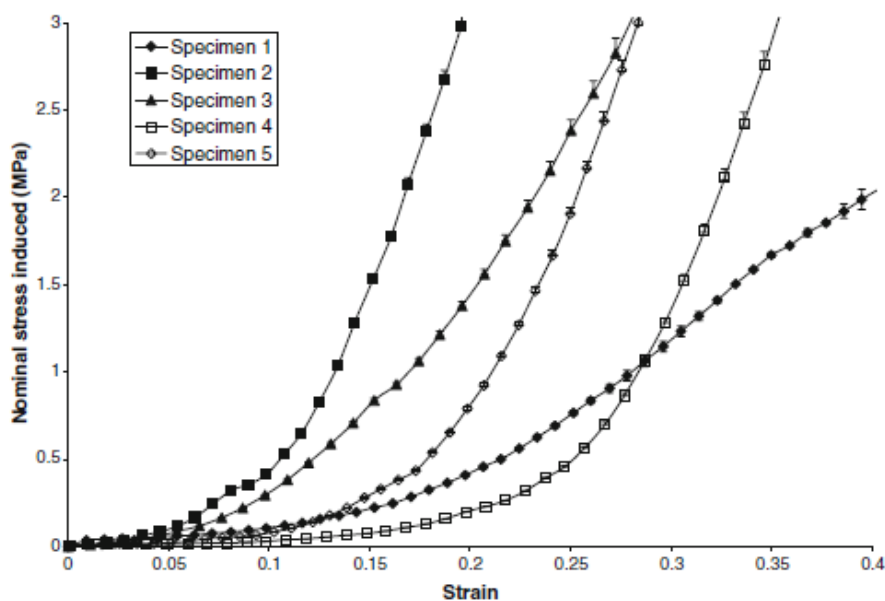


**Figure 13.** Stress strain curves showing variability between different human vaginal samples.

Reproduced with permission from Rubod 2008 et al.

A later study found that vaginal tissue from women with POP was stiffer than from women without POP, in both the anterior and posterior compartments. The non linear region of the stress strain curve, that is arguably more relevant to vaginal tissue function, increased in stiffness in both posterior and anterior prolapsed tissue. This could in part account for the higher rate of relapse with autologous surgical repair. However, differences in the mechanical properties between the anterior and posterior vaginal walls were only found in the transverse direction (Jean-Charles et al. 2010). Another group examined the elasticity (the ability of the tissue to return to its original dimensions following deformation) of human vaginal tissue and found that the tissue in women with POP was less elastic and stiffer compared to controls (Lei et al. 2007).

It is unclear whether the mechanical properties of the vaginal wall influence the incidence of POP, or result from POP. To answer this question, the predictive value of mechanical properties for recurrence after anterior vaginal repair was investigated. However Young's modulus was not predictive for the defined failure criteria suggesting that other pelvic floor factors influence long term anatomical outcomes (Gilchrist et al. 2010). This study used uniaxial testing because it can be done on small pieces of tissue; however it is unclear whether this test method is suitable to determine the complex mechanical properties of vaginal tissue. Multi-axial testing provides more insight into tissue properties but requires larger tissue size (Edwards et al. 2013).

### **1.5.1 Biomechanical properties of mesh following vaginal implantation**

Few studies have implanted synthetic mesh into the vagina for subsequent mechanical testing. Most studies assess mesh following abdominal implantation (Konstantinovic et al. 2007, Spelzini et al. 2007, Konstantinovic et al. 2010, Pereira-Lucena et al. 2010). A feasibility study of vaginal mesh implantation in rabbits and sheep found high erosion rates in both models, however low animal numbers may have influenced the results. In the rabbit model, erosion may also have been complicated by the very thin vaginal epithelium, the proximity of the urethral opening within the urogenital sinus as well as possible contamination (Krause and Goh 2009). Similar high erosion rates into the vagina were found when different meshes were implanted in rabbit vagina for comparison with the abdominal wall (Hilger et al. 2006). These erosion rates were higher than in humans, possibly due to the model itself.

Cross-linked porcine dermis, a degradable tissue collagen-based material, explanted from rabbit abdomen and vagina after 9 months, displayed decreased ultimate tensile strength (strength) and elastic modulus (stiffness) with mesh degradation. Conversely, PP mesh explants showed decreased stiffness but increased strength (Pierce et al. 2009), suggesting that current degradable materials have less favourable biomechanical properties compared to PP in the long-term.

Given that meshes designed for abdominal hernia repair were rapidly introduced to augment POP reconstructive surgery it is important to determine whether the abdominal fascia or the human skin have different mechanical properties compared to vaginal tissue (Gabriel et al. 2011). Such differences might explain the higher adverse effects when meshes are implanted vaginally (Deprest and Feola 2013).

### **1.5.2 The gap in knowledge on biomechanical analyses of vaginal tissues**

The results from the above mentioned studies are often conflicting. Also, different testing methods and specimen sizes used to analyse the connective tissue make it difficult to compare and interpret the results. Information on where the tissue for analysis was taken is often lacking, or it is unclear whether the full thickness of the vaginal wall or only the muscularis was analysed. A structured analysis of vaginal tissue, combining histology, biomechanical and chemical analysis needs to be carried out to draw more comprehensive conclusions from the data and to increase our understanding of the pathophysiology of POP. The sheep model seems to be an ideal model as it allows large samples for tissue collection and for the combination of different analytic tests. Furthermore it poses an ideal model for future preclinical studies due to the similarity in anatomy and physiology to humans (Abramowitch et al. 2009, Couri et al. 2012).

## **RATIONALE**

POP is a major hidden burden affecting millions of women worldwide. Current treatment options are native tissue repair with disappointing long term success rates or synthetic mesh implantation with considerable rates of side effects and re-operations. The FDA has posted several announcements warning about mesh use for vaginal surgery and several meshes have been withdrawn from the market. Meshes of improved mechanical properties, manufactured from alternative polymers are required.

Adult stem cells, particularly MSC are an attractive source of cells for regenerative medicine as they can self-renew, differentiate into several cell lineages and are highly proliferative. Mesenchymal stem-like cells have recently been identified in the human endometrium as an easily accessible source of MSC, obtained with minimal morbidity. As POP occurs predominantly in postmenopausal women it is important to determine whether eMSC are present in postmenopausal endometrium, if they possess key stem cell properties and can be obtained by a relatively non-invasive biopsy procedure.

Tissue Engineering has become the new horizon for future treatment options of chronic diseases. It combines cells and materials and aims to restore the damaged tissue/ cells. Current surgical treatment of POP including implanting synthetic meshes only restores anatomy; however it does not regenerate the damaged tissue. A tissue engineering approach could provide an alternative treatment option for POP addressing these issues.

## **Aims and Hypotheses of this Thesis**

This thesis aimed to investigate the potential use of eMSC combined with new materials in a tissue engineering (TE) construct as a potential cell-based therapy for POP repair.

### **Hypothesis I**

Meshes fabricated from alternative materials to PP to more closely match vaginal tissue mechanical properties integrate and perform better *in vivo*.

### **Aim I**

In Chapter 2, the aim was to assess meshes fabricated from different polymers using a rat abdominal hernia model. Mesh biomechanical properties and biocompatibility, following implantation, were compared to a commonly used clinical PP mesh.

### **Hypothesis II**

EMSC can be prospectively isolated from postmenopausal endometrium in a similar manner to premenopausal eMSC and possess similar MSC properties, enabling their potential use for autologous cell therapies.

## **Aim II**

In Chapter 3, the aim was to characterise the phenotype and biological properties of human postmenopausal eMSC obtained from endometrial biopsies without or with prior exposure to oral oestrogen treatment.

## **Hypothesis III**

A TE construct comprising gelatin-coated PA mesh seeded with eMSC shows superior biocompatibility compared to mesh alone.

## **Aim III**

In Chapter 4, the *in vivo* performance of a novel TE construct was determined including evaluation of tissue response, mesh integration and mechanical properties. This construct comprised of a novel composite PA/gelatin knitted mesh, seeded with eMSC and implanted in an immunocompromised dorsal rat wound repair model.

## **Hypothesis IV**

The histological, biochemical and biomechanical properties vary between different reproductive stages of life in the ovine vagina.

## **Aim IV**

In Chapter 5, the aim was to assess the anatomic, histological, and biomechanical properties of normal sheep vagina and its chemical composition including several collagen types, elastin and glycosaminoglycans in virgin, parous and pregnant sheep to provide baseline data for assessing the utility of sheep as a large animal preclinical model of POP and for POP repair surgery.

## **Hypothesis V**

The vaginal tissue composition and mechanical properties within an individual differs along the vaginal wall length and will be similar between sheep and humans.

## **Aim V**

In Chapter 6, the aim was to analyse the variation in histological, biochemical composition and biomechanical properties of sheep and human vaginal tissue along the full length of the vaginal wall to further define the sheep as a large animal preclinical model of POP.

## CHAPTER 2

### Alternative materials for POP repair

Current meshes for POP repair are associated with the side effects of erosion and pain. Stiffness and nondegradability of the mesh play a role in the development of these side effects, which emanate from an ongoing foreign body reaction and excessive fibrosis. Our collaborators have recently designed and fabricated meshes from alternative non-degradable monofilament polymers. These new polyamide (PA) or polyether-etherketone (PEEK) meshes have lower stiffness, permanent strain and bending rigidity than several commercially available PP meshes (Edwards et al. 2013).

New meshes for abdominal hernia and POP repair are routinely evaluated in a rat model using the abdominal hernia approach. In this chapter I describe the evaluation of the *in vivo* biocompatibility of novel meshes in a rat abdominal hernia model. I implanted the meshes and analysed the explants for adhesions and contraction. I developed protocols for histology and immunohistochemistry to determine the vascularisation, the foreign body reaction and collagen deposition of the explanted mesh/tissue complexes. Previous researchers have scored foreign body cells or collagen deposition subjectively. I was able to establish an objective computer based software programme to analyse the immunostained images objectively and more accurately around individual mesh filaments.

I thank Dr. Tommy Supit for performing animal surgery in a third of the animals and Camden Lo for assisting with the computer program for the image analysis. I acknowledge Dr Sharon Edwards from CSIRO Materials Science and Engineering for undertaking the biomechanical testing and analysis.

## Monash University

### Declaration for Thesis Chapter 2

#### Declaration by candidate

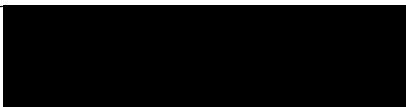
In the case of Chapter 2, the nature and extent of my contribution to the work was the following:

Nature of contribution	Extent of contribution (%)
Animal experiments, Tissue collection, Tissue processing, Tissue staining, Image analysis, Statistical analysis, Paper writing	65

The following co-authors contributed to the work. Co-authors who are students at Monash University must also indicate the extent of their contribution in percentage terms:

Name	Nature of contribution	Extent of contribution (%) for student co-authors only
Dr. Sharon L. Edwards	Biomechanical testing, Data analysis, Data interpretation	
Jacinta F. White	Tissue staining	
Tommy Supit	Animal experiments, Tissue collection, Tissue processing, Tissue staining	15
John AM. Ramshaw	Data interpretation	
Dr. Camden Lo	Image analysis	
Dr. Anna Rosamilia	Study design, Data interpretation	
Dr. Jerome A. Werkmeister	Study design, Data interpretation, Paper writing	
Dr. Caroline E. Gargett	Study design, Data analysis, Data interpretation, paper writing	

Candidate's  
Signature

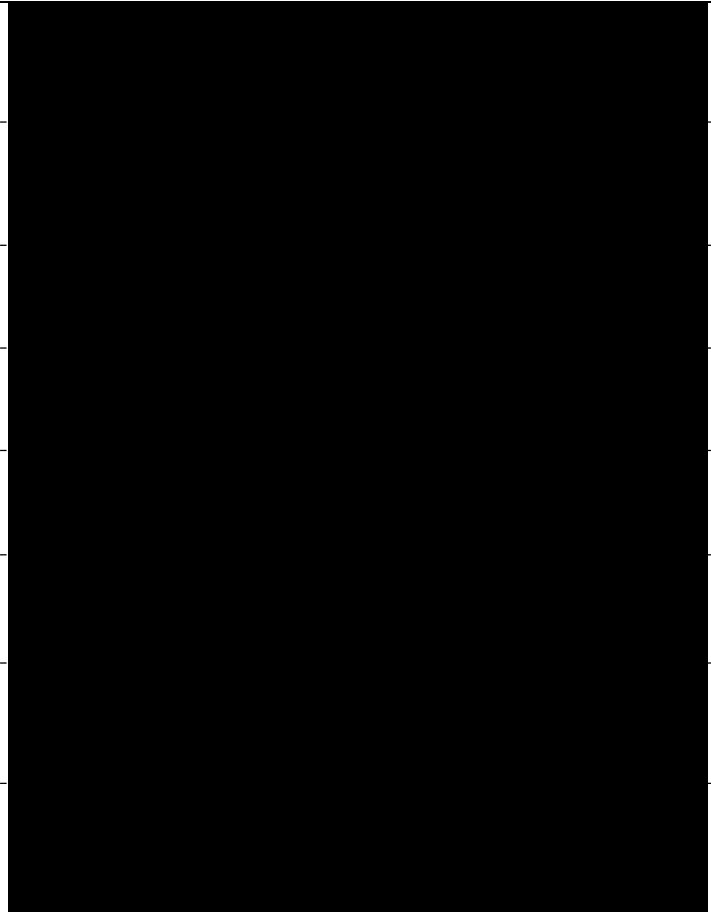
	Date 07.03.2014
--	--------------------

### Declaration by co-authors

The undersigned hereby certify that:

- (1) the above declaration correctly reflects the nature and extent of the candidate's contribution to this work, and the nature of the contribution of each of the co-authors.
- (2) they meet the criteria for authorship in that they have participated in the conception, execution, or interpretation, of at least that part of the publication in their field of expertise;
- (3) they take public responsibility for their part of the publication, except for the responsible author who accepts overall responsibility for the publication;
- (4) there are no other authors of the publication according to these criteria;
- (5) potential conflicts of interest have been disclosed to (a) granting bodies, (b) the editor or publisher of journals or other publications, and (c) the head of the responsible academic unit; and
- (6) the original data are stored at the following location(s) and will be held for at least five years from the date indicated below:

<b>Location(s)</b>	<b>MIMR- PHI Institute of Medical Research, Level 3, Monash University, Melbourne, VIC, Australia; CSIRO Materials Science Engineering, Clayton, Melbourne, VIC, Australia</b>
--------------------	--

	<b>Name</b>	<b>Date</b>
<b>Signature 1</b>		<b>22/12/13</b>
<b>Signature 2</b>		<b>20/12/13</b>
<b>Signature 3</b>		<b>20/12/13</b>
<b>Signature 4</b>		<b>20/12/13</b>
<b>Signature 5</b>		<b>20/12/13</b>
<b>Signature 6</b>		<b>20/12/13</b>
<b>Signature 7</b>		<b>20/12/13</b>
<b>Signature 8</b>		<b>20/12/13</b>

# A Preclinical Evaluation of Alternative Synthetic Biomaterials for Fascial Defect Repair Using a Rat Abdominal Hernia Model

Daniela Ulrich<sup>1,2,4</sup>, Sharon L. Edwards<sup>3</sup>, Jacinta F. White<sup>3</sup>, Tommy Supit<sup>1</sup>, John A. M. Ramshaw<sup>3</sup>, Camden Lo<sup>1</sup>, Anna Rosamilia<sup>4</sup>, Jerome A. Werkmeister<sup>3</sup>, Caroline E. Gargett<sup>1,4\*</sup>

**1** Monash Institute of Medical Research, Clayton, Victoria, Australia, **2** Medical University Graz, Graz, Austria, **3** CSIRO Materials Science and Engineering, Clayton, Victoria, Australia, **4** Department of Obstetrics and Gynaecology and Monash Micro Imaging, Monash Medical Centre, Monash University, Clayton, Victoria, Australia

## Abstract

**Introduction:** Fascial defects are a common problem in the abdominal wall and in the vagina leading to hernia or pelvic organ prolapse that requires mesh enhancement to reduce operation failure. However, the long-term outcome of synthetic mesh surgery may be unsatisfactory due to post-surgical complications. We hypothesized that mesh fabricated from alternative synthetic polymers may evoke a different tissue response, and provide more appropriate mechanical properties for hernia repair. Our aim was to compare the in vivo biocompatibility of new synthetic meshes with a commercial mesh.

**Methods:** We have fabricated 3 new warp-knitted synthetic meshes from different polymers with different tensile properties polyetheretherketone (PEEK), polyamide (PA) and a composite, gelatin coated PA (PA+G). The rat abdominal hernia model was used to implant the meshes (25×35 mm, n=24/ group). After 7, 30, 60, 90 days tissues were explanted for immunohistochemical assessment of foreign body reaction and tissue integration, using CD31, CD45, CD68, alpha-SMA antibodies. The images were analysed using an image analysis software program. Biomechanical properties were uniaxially evaluated using an Instron Tensile<sup>®</sup> Tester.

**Results:** This study showed that the new meshes induced complex differences in the type of foreign body reaction over the time course of implantation. The PA, and particularly the composite PA+G meshes, evoked a milder early inflammatory response, and macrophages were apparent throughout the time course. Our meshes led to better tissue integration and new collagen deposition, particularly with the PA+G meshes, as well as greater and sustained neovascularisation compared with the PP meshes.

**Conclusion:** PA, PA+G and PEEK appear to be well tolerated and are biocompatible, evoking an overlapping and different host tissue response with time that might convey mechanical variations in the healing tissue. These new meshes comprising different polymers may provide an alternative option for future treatment of fascial defects.

**Citation:** Ulrich D, Edwards SL, White JF, Supit T, Ramshaw JAM, et al. (2012) A Preclinical Evaluation of Alternative Synthetic Biomaterials for Fascial Defect Repair Using a Rat Abdominal Hernia Model. PLoS ONE 7(11): e50044. doi:10.1371/journal.pone.0050044

**Editor:** Nuno M. Neves, University of Minho, Portugal

**Received:** May 30, 2012; **Accepted:** October 15, 2012; **Published:** November 20, 2012

**Copyright:** © 2012 Ulrich et al. This is an open-access article distributed under the terms of the Creative Commons Attribution License, which permits unrestricted use, distribution, and reproduction in any medium, provided the original author and source are credited.

**Funding:** Supported by Australian National Health and Medical Research Council grants (1021126) (CEG, JW, AR) and R.D Wright Career Development Award 465121 (CEG), the Australian Stem Cell Centre (SDF5) and South East Melbourne Alliance for Regenerative Therapies (SMART) grants (CEG, JW, AR, SE) the Victorian Government's Operational Infrastructure Support Program and a Monash Postgraduate Award (DU). In kind support as a gift of Polypropylene meshes were kindly provided by Boston Scientific, USA. The funders had no role in study design, data collection and analysis, decision to publish, or preparation of the manuscript.

**Competing Interests:** Polypropylene meshes were kindly provided to Dr. Anna Rosamilia by Boston Scientific, USA for use in this study. This does not alter the authors' adherence to all the PLOS ONE policies on sharing data and materials.

\* E-mail: Caroline.Gargett@med.monash.edu.au

## Introduction

Incisional ventral hernias occur in up to 49% of patients after abdominal surgery for trauma, infection, herniation or surgical resection [1–3]. Similarly, hernias in the female lower urogenital tract known as pelvic organ prolapse (POP) occur in up to 25% of women with childbirth, ageing and obesity being the most common causes [4]. Recurrence rates with tissue approximation procedures occur in up to 17% for abdominal hernias [5] and 30% for POP repair [6], respectively, which has led to the implantation of synthetic meshes to improve surgical outcomes.

Polypropylene (PP) mesh is the most commonly used mesh, and is knitted from monofilament yarn to a relatively large pore size, in order to allow tissue ingrowth [7]. Synthetic non-degradable meshes are used to provide a permanent solution and are believed to work by inducing an inflammatory foreign body reaction, resulting in fibrosis that provides strength, albeit not necessarily mechanically optimal, to the weakened support structures [8,9]. However, the presence of an inflammatory response may reflect poor tissue biocompatibility, depending on the extent and type of response. It is also primarily responsible for the significant complications arising from the use of synthetic meshes reported

in up to 42%, including mesh contraction, infection, pain, and exposure of mesh [10,11].

With PP mesh dominating the market, we believe that mesh manufactured from alternative synthetic polymers may evoke a different biological response, and provide more appropriate mechanical properties for hernia repair. PA and PEEK polymers were chosen as alternative polymers to PP, due to differences in yarn tensile properties. Gelatin coating was also used to further improve tissue integration [12,13]. Gelatin works as a carrier for delivering large number of cells and can be adapted as a basis for cell based therapies in the future [14].

The aim of this study was to compare the *in vivo* host tissue response of synthetic meshes fabricated from alternative polymers and a composite mesh coated with gelatin, with a clinical PP mesh, using a rat abdominal hernia model as a preclinical model for hernia repair surgery.

## Materials and Methods

Polyetheretherketone (PEEK) and polyamide (PA) meshes were warp knitted to the same pattern using 100  $\mu\text{m}$  PEEK (Invibio; UK) and PA (Ri-Thai International; Taiwan) monofilament yarns. Meshes were knitted to possess pore sizes ranging 1310 to 1487  $\mu\text{m}$  and weights ranging 69 to 85  $\text{g}/\text{m}^2$ . A clinical PP mesh (Polyform™; Boston Scientific; USA), of similar knit pattern, filament diameter and pore size, with a weight of 42  $\text{g}/\text{m}^2$  [15], was also used in the study. Additionally, fabricated PA mesh was coated with gelatin (PA+G). Briefly, PA mesh was immersed in a 0.2  $\mu\text{m}$  filter sterilised solution of 12% porcine gelatin (Type A, 300 bloom; Sigma; USA), in water. Once fully wetted the mesh was placed onto ice-cold 2% glutaraldehyde (Sigma) in PBS for 8 minutes on either side. All the subsequent steps were for 15 minutes duration and at room temperature. The mesh was washed, placed into 2% w/v glycine (Merck; Australia) in water, washed, placed in 2% v/v  $\text{H}_2\text{O}_2$  (Merck) in water, washed, then 4% w/v glycerol (Merck) in water. Finally, the mesh was air-dried overnight. All mesh samples were gamma ray irradiated at 25 kGy prior to implantation.

## Animals

The experimental procedures and rat husbandry were approved by the Monash Medical Centre Animal Ethics Committee A (2009/50). Sprague Dawley rats were housed in the animal house of Monash Animal Service facilities in compliance with the National Health and Medical Research guidelines for the care and use of laboratory animals. The rats were provided with food and water *ad libitum* and were kept under controlled environmental conditions at 20°C and a 12 h day/night cycle.

## Surgical Procedure

125 female rats were divided into 5 experimental groups (24 rats/group) and were implanted with one of 4 mesh types; PA, PA+G, PEEK, or PP. A sham operation was used as a negative control as described below. The rats were anaesthetised with 2.5% Isoflurane® and analgesia was provided with Carprofen (5 mg/kg bodyweight). The abdomen was shaved and disinfected and covered with sterile drapes. A longitudinal 3 cm skin incision was performed in the lower abdomen and a full thickness fascial defect of the abdominal wall, 20×30 mm, was created [16] (Fig. S1A). Before implantation, mesh thickness was measured with a calliper. Each mesh (25 mm×35 mm) was implanted using the overlay technique (Fig. S1A) and sutured with PP sutures as previously described [16,17] (Fig. S1C). Rats in the control group were sham-operated without mesh implantation. A 25×35 mm full-thickness

abdominal wall defect was created on the right lateral side of the midline. A muscle flap with preserved vascularisation from the contralateral side was created, rotated 45° clockwise and sutured with 3/0 Surgipro™ II (polypropylene thread) to cover the initial defect (Fig. S1B). Skin closure in all groups was performed by intracutaneous continuous suture with 3/0 Vicryl\* Plus (polyglactin thread).

Following recovery, the animals were monitored daily until they were sacrificed at 7, 30, 60 and 90 days ( $n=6$ / group/ timepoint). Each rat was euthanized in a  $\text{CO}_2$  chamber. The adhesion area of the mesh on the intestinal side was recorded and calculated as a percentage of total mesh area. Adhesion tenacity to the intestinal wall was also recorded as previously described [18]. Adhesion scores were graded from 1–4 with 4 being the most adhesive. The mesh was dissected with a 5 mm border of adjacent tissue and divided into three parts; for biomechanical analysis, histology and immunohistochemistry, using the same pattern of dissection for each mesh. Adhesive organs to the mesh were peeled off manually. The meshes used for biomechanical analysis were stored at –20 degrees prior to testing. Additionally, explant dimensions (length, width and thickness) were measured with a calliper at 3 random regions and the mean recorded. Mesh contraction was calculated by dividing the mesh size after explantation by the original mesh size.

## Biomechanical Analysis

The frozen samples were thawed overnight at 4 degrees and kept moist during testing. Day 7 and day 90 explants and tissue from the control rats were uniaxially tensile tested using an Instron® Tensile Tester (Instron Corp; USA) and a 5 kN load cell. Samples (typically  $n=10$ ), with dimensions of 4×25 mm, were cut in the explant cross direction and tested using a 14 mm gauge length (noted as the initial length). Samples were pre-loaded to 100 mN at an elongation rate of 14 mm/min to remove any sample slack. Subsequent testing was conducted at an elongation rate of 30 mm/min to break. Average load-elongation curves were plotted for each mesh type and the control (failure region not included in curve) from the data obtained. Tensile strain (%) was calculated by dividing mesh elongation by the initial mesh length and multiplying by 100. Mesh stiffness is represented by the slope of the curve, with a steeper curve indicating a stiffer mesh.

## Histology

The explanted tissue for histological analysis was fixed in 4% w/v paraformaldehyde (PFA) for 24 h, then embedded in paraffin and sectioned into 5  $\mu\text{m}$  thick sections. After dewaxing and rehydrating in graded alcohols, sections were stained with haematoxylin and eosin (H+E) or Sirius red F3B (0.1 g/100 ml saturated aqueous picric acid) (Sigma Aldrich®, St. Louis, MO USA) for one hour at room temperature (RT).

## Immunohistochemistry (IHC)

To examine for tissue macrophages, a monoclonal anti rat CD68 antibody (details in Table 1) was used. Sections underwent dewaxing, rehydrating in graded alcohols. Antigen retrieval using citric acid buffer (0.1 M, pH 6.0) was done by microwaving for 5 minutes on high power. After cooling to RT and washes in PBS, endogenous peroxidase was quenched with 3% v/v  $\text{H}_2\text{O}_2$  followed by protein blocking (Protein Block serum free, Dako®, Glostrup, Denmark) for 30 minutes at RT. The primary CD68 antibody and isotype controls (mouse IgG<sub>1</sub>) were incubated overnight at 4°C, sections washed and the secondary Streptavidin HRP-conjugated antibody was applied for 30 minutes at RT, respectively (Table 1). 3,3'-Diaminoben-

**Table 1.** Details of antibodies used for immunohistochemistry.

Primary antibody	Clone	Dilution	Isotype	supplier	Secondary antibody	Dilution	supplier
$\alpha$ smooth muscle actin	1A4	1:400	Mouse IgG2a	Dako <sup>®</sup> , Glostrup, Denmark	Alexa fluor 488 goat anti-mouse IgG	1:200	Invitrogen <sup>®</sup> , Mulgrave, VIC, Australia
CD 31 PECAM-1	TLD-3A12	1:200	Mouse IgG1	BD Pharmingen <sup>®</sup> , NJ, USA	Alexa fluor 568 donkey anti-mouse IgG (H+L)	1:200	Invitrogen <sup>®</sup> , Mulgrave, VIC, Australia
CD 45 Leukocyte common antigen	OX-1	1:200	Mouse IgG1	BD Pharmingen <sup>®</sup> , NJ, USA	Alexa fluor 568 donkey anti-mouse IgG (H+L)	1:200	Invitrogen <sup>®</sup> , Mulgrave, VIC, Australia
CD 68/ MCA341R	ED 1	1:500	Mouse IgG1	AbD Serotec <sup>®</sup> , Oxford, UK	EnVision <sup>®</sup> -System- HRP Labelled Polymer (anti-mouse)	Ready to use	Dako <sup>®</sup> , CA, USA

doi:10.1371/journal.pone.0050044.t001

zidine (Sigma-Aldrich<sup>®</sup>, St. Louis, MO, USA) was used as a chromogen, counterstaining was with haematoxylin. The slides were dehydrated in graded alcohols and mounted with DPX mounting medium.

### Immunofluorescence

4% w/v PFA fixed, paraffin embedded tissues were used for immunofluorescence analysis and 5  $\mu$ m sections dewaxed, dehydrated, blocked and washed as above. Sections were incubated with the primary monoclonal anti-alpha smooth muscle actin ( $\alpha$ SMA) antibody for one hour at 37°C (Table 1) to label smooth muscle cells, myofibroblasts and myoepithelial cells. Mouse IgG<sub>2a</sub> isotype was used for the negative control and applied at the same concentration. Bound antibodies were detected with Alexa-Fluor-488- conjugated secondary antibody (Table 1) for 30 minutes at RT after 3 washes in PBS. Nuclei were stained with Hoechst 33258. The slides were mounted with fluorescent mounting medium (Dako<sup>®</sup>, Glostrup, Denmark).

CD31 and CD45 immunofluorescence was used to visualise endothelial cells and leukocytes, respectively (Table 1). Tissue for frozen sections was snap frozen in optimal compound tissue solution (OCT, Tissue-Tek, Miles, IN, USA). The frozen sections cut (5  $\mu$ m) were thawed at RT, fixed in ice cold acetone for 10 minutes followed by protein block (Dako<sup>®</sup>, Glostrup, Denmark) for 30 minutes at RT. After three washes in PBS, primary antibodies were incubated for 1hr at 37°C and with Alexa-Fluor-568- conjugated secondary antibody (Table 1) for 30 minutes at RT, respectively. The slides were mounted as above.

### Histomorphometric Analysis

Four images were taken per section stained with Sirius red or immunostained with CD68,  $\alpha$ SMA, CD31 or CD45 for each explant at each timepoint using a Leica<sup>®</sup> DMR Fluorescence Microscope at 20X 0.6NA magnification and at 10X 0.3NA for H+E. Images of the 4 most central mesh filaments were captured (Fig. S2A, B, Fig. 1A), to achieve consistency and overcome bias, and to avoid any foreign body reaction associated with anchoring sutures. The images were analysed using the image analysis software, Metamorph<sup>®</sup> (v7.7 Molecular Devices, LLC, CA, USA). The software was programmed to identify individual mesh filaments (Fig. 1B) and trace contoured concentric area bands around filament bundles in 50  $\mu$ m increments (Fig. 1C, D). The positive signal area (pixels) for each shape was recorded and divided by the total tissue area examined (Fig. 1B). Neotissue formation (as indicated by Sirius,  $\alpha$ SMA and CD31) was analyzed using the whole image, assessing the entire surrounding tissue. Foreign body cells were assessed close to the mesh filaments.

### Statistics

GraphPad Prism 5 was used for statistical analysis. Results are reported as mean  $\pm$  SEM for each experimental group (n=6 animals/ group/ timepoint). Since the data was not normally distributed (D'Agostino & Pearson omnibus normality test), non-parametric analysis using Kruskal – Wallis ANOVA, were undertaken to assess differences between timepoints for the various meshes, followed by Bonferroni correction for pairwise comparisons. P values <0.05 were considered as statistically significant. For statistical analysis of load-elongation curves, 95% confidence intervals were plotted as error bars to determine whether the differences were significant at the p <0.05 level of significance.

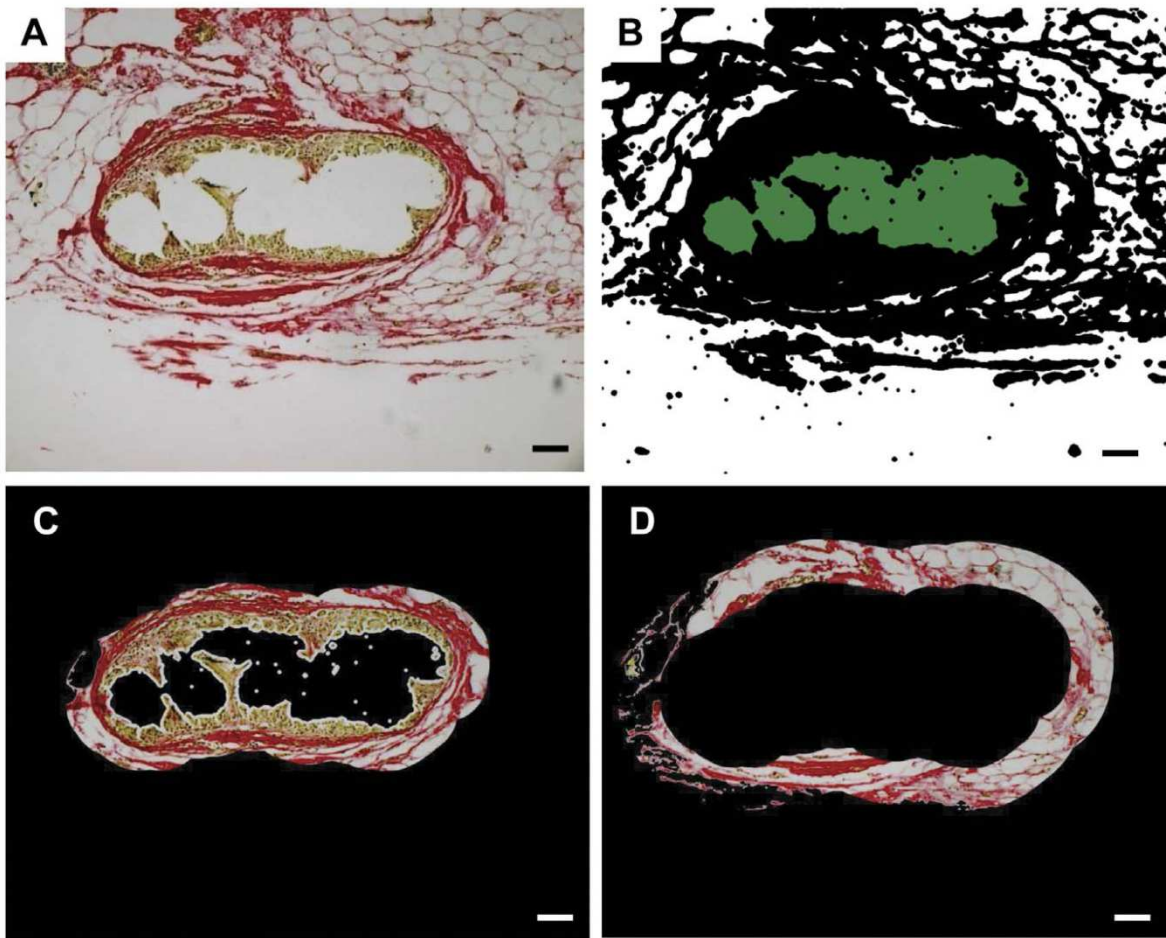


**Figure 1. Image analysis using Metamorph® Software.** A. Original image showing Sirius red staining of tissue around a central filament bundle, scale bar — 100 µm. B. binarized image with mesh recognition. C. First 50 µm increment surrounding filament bundle. D. Second 50 µm increment (50–100 µm) surrounding filament bundle. doi:10.1371/journal.pone.0050044.g001

## Results

### Macroscopic Tissue Compatibility of New Meshes

Two new meshes, warp-knitted from PA and PEEK monofilaments in a similar pattern as commercially available PP mesh, were examined for tissue biocompatibility using a standard rat abdominal hernia model. In addition, a gelatin-coated PA mesh was studied, since this composite could be adapted for delivering cells in future experiments. Of the 125 animals operated, all had a normal post-operative recovery. Five rats developed wound infection or wound dehiscence with no differences between the mesh groups, necessitating killing these animals according to local ethics committee regulations. Therefore a total number of 120 animals (6 per group at each timepoint) were included for analysis.

All mesh types were well tolerated. Rats gained weight 30 days after operation and weight gain increased significantly in rats implanted with PA, PEEK and PP meshes at 60 days ( $p < 0.05$ ) (Fig. 2). At 90 days, rats implanted with PA and PA+G meshes showed significantly greater weight gain compared to control rats, and rats implanted with PEEK and PP meshes ( $p < 0.001$ ). Ninety

days after surgery, weight gain was significantly higher in all groups compared to 7 days (pairwise comparisons  $p < 0.0001$ ).

At the time of necropsy (Fig. S1D, E), intraperitoneal adhesions were noted mainly with the ileum and the omentum over the whole implant surface for all materials as well as to the sutures in all mesh groups. The adhesion scores are shown in Table 2. No differences were observed at 7 and 30 days between the mesh groups. PA meshes showed a significantly lower adhesion score compared to PA+G ( $p < 0.05$ ), PEEK and PP ( $p < 0.001$ ) at 90 days. Adhesion scores for PA+G, PEEK and PP meshes were significantly increased at 60 and 90 days compared to the earlier timepoints for the same mesh type ( $p < 0.05$ ).

While all meshes displayed the greatest adhesion area at 7 days (range 73 to 88%, Table 3), the strength of adhesion was low (adhesion score of 1.0, Table 2). The extent of adhesion was lowest with the PA+G mesh at day 7 without statistically significant differences (Table 3). At 30 days, the extent of adhesion with the PA+G and PEEK meshes was significantly less than observed with PA and PP ( $p < 0.05$ ), with no significant difference by 60 and 90 days. All meshes reached the lowest adhesion area at 60 days, with

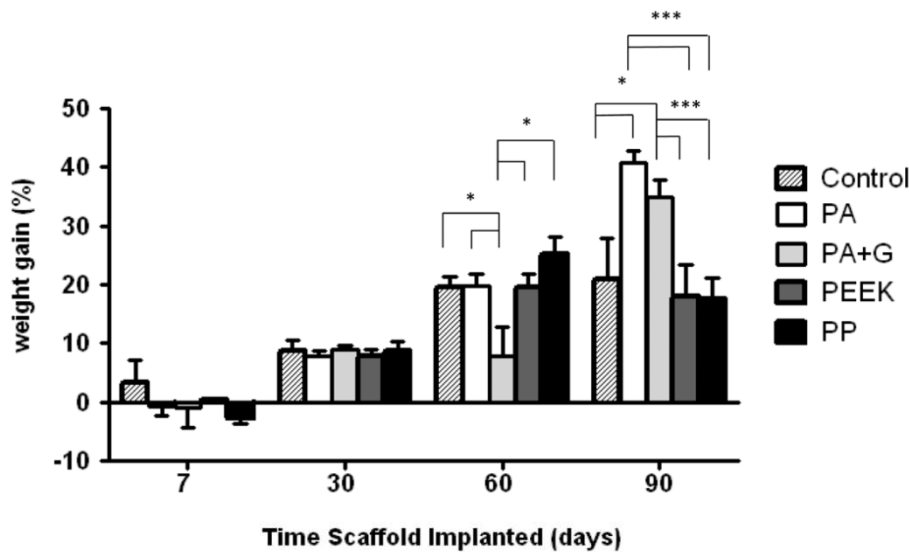


**Figure 2. Body weight gain of rats implanted with different synthetic meshes: PA, PA+G, PEEK or PP and controls.** Data are mean  $\pm$  SEM of n=6 animals/ group, \* p<0.05, \*\*\* p<0.001. PA, polyamide; PA+G, polyamide gelatin composite; PEEK, polyetheretherketone; PP, polypropylene. doi:10.1371/journal.pone.0050044.g002

no further reduction at 90 days, although none of these differences were significant.

Folding of the meshes, which contributes to apparent mesh shrinkage, was occasionally observed, with the highest incidence seen in the PA and PP groups. Folding may have arisen from poor suturing but could also be due to extensive tissue ingrowth. These meshes were included in the analysis of mesh contraction. Contraction was significantly greater at 30 days compared to 7 days for PA+G and PP meshes; no significant differences in mesh contraction for PA and PEEK meshes were observed between these timepoints (Table 4). PEEK meshes shrank significantly less than PA and PP meshes at 30 days; however no significant difference was observed at 60 or 90 days (range at 90 days 9 to 19.4%, Table 4).

**Biomechanical Properties**

The load-elongation curves for the day 7 and day 90 explants are shown in Figure 3 and in Fig. S3. The mechanical properties of meshes prior to implantation were not significantly different to those measured after 7 days implantation. Comparable load-elongation curves, with similar levels of stiffness, were observed for

explanted mesh types and the control tissue on day 7; error bars suggest that curves were not significantly different from each other (p>0.05). The curves of day 7 meshes suggest some bilinearity, with a linear region from 1.7 mm elongation (Fig. 3 inset), however this is less obvious than for the day 90 meshes (which have distinct toe and linear regions). The load-elongation curves of all meshes explanted at day 90 were significantly (p<0.05) different to their day 7 counterparts exceeding 0.9 mm elongation (6.4% strain), and generally had increased stiffness (with steeper slopes) in the linear region of the curves (generally exceeding 0.6 mm elongation: 4.2% strain) (Fig. 3). At day 90, the PA+G explanted meshes were the stiffest of all the explanted meshes, and comparable to the control tissue explants, although this was only significant (p<0.05) at elongations exceeding 2.0 mm (14% strain).

**Tissue Biocompatibility of Meshes**

We examined the microscopic changes induced by the implanted mesh materials using histological stains and immunohistochemistry. As shown in Fig. S2A and B there was substantial cell and tissue formation around the mesh filaments at 7 days. At

**Table 2. Adhesion scores of rats implanted with meshes.**

Time (days)	PA	PA+G	PEEK	PP
7	1.0 $\pm$ 0.0	1.0 $\pm$ 0.0	1.0 $\pm$ 0.0	1.0 $\pm$ 0.0
30	1.0 $\pm$ 0.0	1.0 $\pm$ 0.0	1.0 $\pm$ 0.0	1.0 $\pm$ 0.0
60	2.0 $\pm$ 0.3	2.0 $\pm$ 0.0	1.8 $\pm$ 0.2	2.3 $\pm$ 0.2
90	1.3 $\pm$ 0.2 <sup>a,b</sup>	1.8 $\pm$ 0.2	2.0 $\pm$ 0.0	2.0 $\pm$ 0.0

Data are mean  $\pm$  SEM.  
<sup>a</sup>p<0.05 compared to PA+G.  
<sup>b</sup>p<0.001 compared to PEEK and PP.  
 doi:10.1371/journal.pone.0050044.t002

**Table 3. Percentage adhesion area of meshes implanted into abdominal fascial wound in rats.**

Time (days)	PA	PA+G	PEEK	PP
7	88 $\pm$ 4	73 $\pm$ 14	86 $\pm$ 5	80 $\pm$ 9
30	72 $\pm$ 10 <sup>a</sup>	40 $\pm$ 4	40 $\pm$ 8	73 $\pm$ 8 <sup>b</sup>
60	48 $\pm$ 8	42 $\pm$ 8	43 $\pm$ 8	63 $\pm$ 7
90	52 $\pm$ 8	53 $\pm$ 4	55 $\pm$ 6	72 $\pm$ 4

Data are mean  $\pm$  SEM.  
<sup>a</sup>p<0.05 compared to PA+G and PEEK.  
<sup>b</sup>p<0.05 compared to PA+G and PEEK.  
 doi:10.1371/journal.pone.0050044.t003

**Table 4.** Percentage mesh contraction in rats implanted with meshes.

Timepoints	PA	PA+G	PEEK	PP
7	17.8±2.0	7.1±1.9	19.7±5.1	8.7±2.5
30	29.9±7.0 <sup>a</sup>	21.1±5.0	10.9±4.3	26.7±3.0 <sup>b</sup>
60	13.0±5.0	9.2±2.4	11.2±2.4	14.6±2.0
90	14.7±5.4	9.0±4.3	19.4±3.0	15.1±2.8

Data are presented as percentage reduction in size from original implanted mesh as mean ± SEM.

<sup>a</sup>p<0.01 compared to PEEK.

<sup>b</sup>p<0.05 compared to PEEK.

\*denotes gelatin around PA filaments.

doi:10.1371/journal.pone.0050044.t004

90 days some encapsulation tissue was still apparent around all filament bundles. PA+G meshes had a greater tissue and cell response around the mesh filaments at 90 days compared to the other mesh types. No microscopic differences were apparent in the control group between 7 and 90 days.

To quantify this tissue response, image analysis was undertaken to examine the gradient of positive staining in 50 µm increments from the central mesh filaments. A diminishing gradient, with a significant decrease, in CD45 and CD68 immunostaining was observed with increasing distance from the filaments (Fig. S4A). We therefore studied the immediate area surrounding the mesh (within 50 µm). No continuous gradient was observed for the other stains (Sirius red, αSMA and CD31) (Fig. S4B), which were analysed using the entire micrograph.

**Inflammatory Foreign Body Reaction**

The inflammatory response to the implanted meshes was evaluated by examining the extent of CD45<sup>+</sup> leukocyte distribution in and around the meshes. CD45 is expressed on all hematopoietic cells except erythrocytes. Larger numbers of leukocytes (red fluorescence) were observed around the meshes (Fig. 4A) at all time points (Fig. 4C), compared to controls where no meshes were present (Fig. 4C). There were significantly fewer CD45 positive cells at 7 and 30 days in the control and PA+G groups compared to PA, PEEK and PP (p<0.001) (Fig. 4C). At 60 days PA, PA+G and PEEK attracted significantly more leukocytes than the control (p<0.05), with higher positive staining for PEEK, compared to PP (p<0.05). At 90 days, the new meshes showed greater leukocyte infiltration than the control and PP groups (p<0.001) (Fig. 4C).

To assess macrophage involvement we used the CD68 antibody (Fig. 5). The kinetics of macrophage infiltration varied between mesh types. For example, for the PA mesh, macrophages significantly increased over time from day 7 (Fig. 5A) to day 90 (Fig. 5C) (p<0.001). Significantly more macrophages were observed around the filaments for all mesh types than in the control group (p<0.001), at all timepoints (Fig. 5C). At 90 days PA meshes were surrounded by significantly more macrophages than PP (p<0.05) (Fig. 5C).

**Collagen Deposition**

Collagen deposition was assessed using Sirius red staining which shows the collagen as red stained material in bright-field microscopy (Figure 6A, B). On day 7 PEEK meshes showed pronounced Sirius red staining loosely distributed around a dense cellular infiltrate (Fig. 6A). At day 90, the cellular infiltrate was less and collagen levels were reduced but more localised around the filaments of the porous mesh (Fig. 6B). At 7 days, a significantly lower collagen content was observed in the control and PP groups

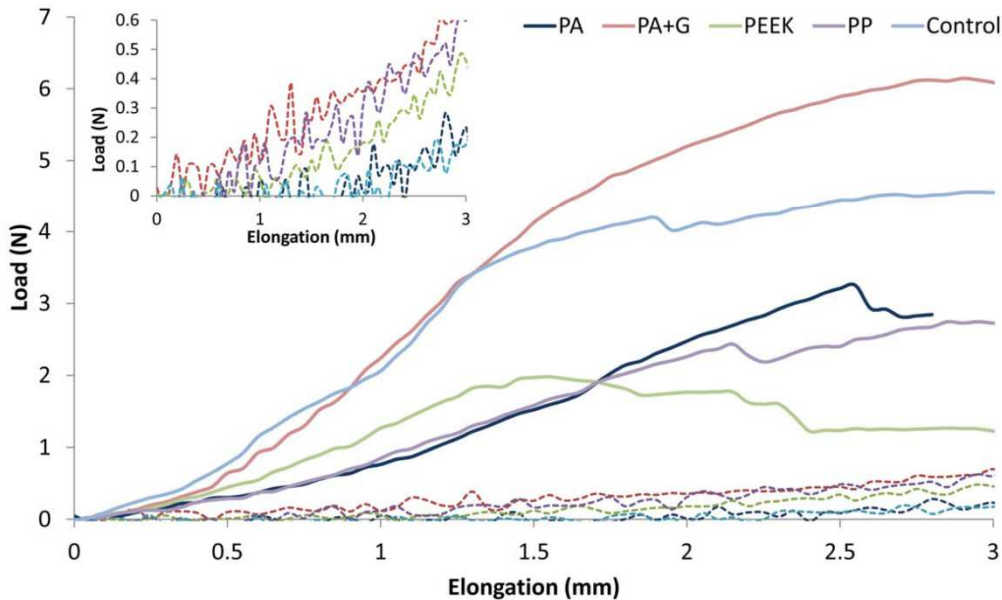


**Figure 3. Biomechanical properties of explanted mesh types and control on day 7 (- - -) and day 90 (—).** Failure region of graph has not been included. Average explant stiffness is indicated by the slope of the curve, with stiffer materials possessing a steeper gradient. Inset is an enlargement of day 7 meshes.  
doi:10.1371/journal.pone.0050044.g003

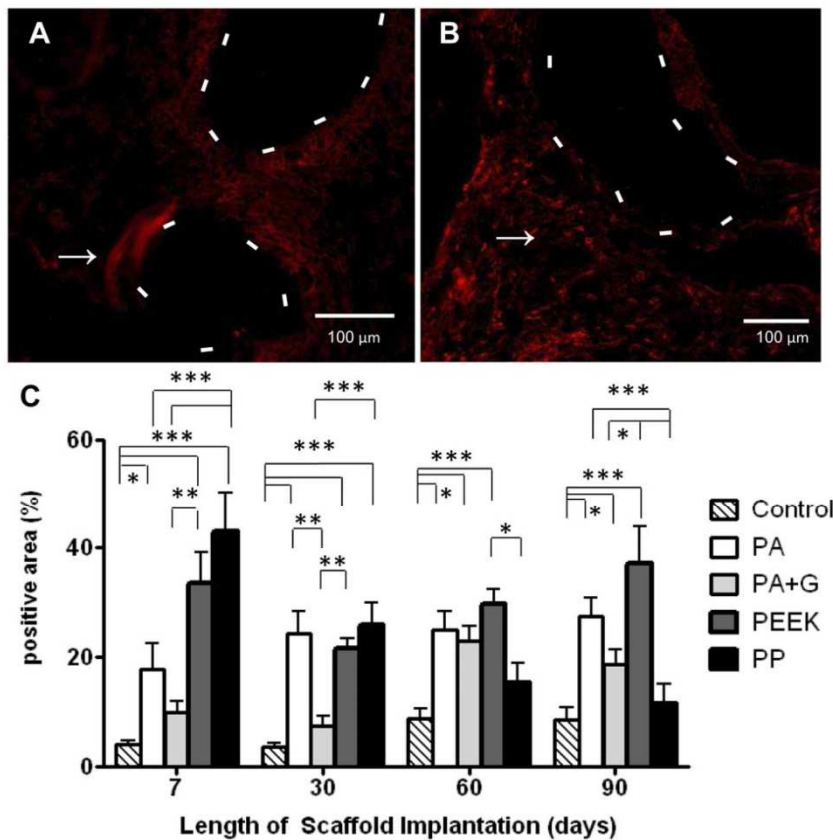


**Figure 4. CD45 immunostaining in rats implanted with synthetic mesh.** A. PA after 7 days (--- line indicates mesh filament) and B. After 90 days implantation (arrow indicates a representative CD45 positive cell). C. Percentage CD45 positive area within the 50 µm radius of central mesh filament bundles. Data are mean ± SEM of n=6 animals/ group \*: p<0.05, \*\*: p<0.01 Scale bar, 100 µm. doi:10.1371/journal.pone.0050044.g004

compared to PA, PA+G and PEEK meshes ( $p<0.001$ ) (Fig. 6C). At 30 days, PA+G mesh induced the highest collagen deposition which was significantly greater than PA, PEEK and PP meshes ( $p<0.001$ ), and comparable to control animals. At 90 days PA, PEEK and PP meshes were all significantly lower in collagen content ( $p<0.001$ ) than the control, whilst the PA+G mesh was significantly higher, and comparable to the control (Fig. 6C). Compared to 7 days, collagen content decreased significantly in both PA and PEEK meshes ( $p<0.05$ ) at 90 days, whereas collagen increased significantly in PP meshes ( $p<0.05$ ).

#### Vascularisation

The development of vascular structures in the explanted meshes was assessed using the marker CD31 which is expressed on endothelial cells, platelets and subsets of leukocytes. It predominantly stains endothelial cells on small and large blood vessels. Similar to all mesh types, the PA+G meshes were vascularised by day 7 (Fig. 7A), with vessels present at each time point, until day 90 (Fig. 7B). The positive area for CD31 (Fig. 7C) was similar between all mesh groups, and comparable with control animals, on day 7. On day 30 the control group and PEEK meshes showed significantly more positive staining than the PP meshes ( $p<0.01$ ,  $p<0.05$  respectively) (Fig. 7C). Vascularisation of PA and PEEK mesh types, and control animals was significantly higher than in

PP meshes, at 60 and 90 days ( $p<0.01$ ) (Fig. 7C). The extent of vascularisation increased with time for the PA meshes, and was significantly greater at 60 and 90 days compared to day 7 and day 30 ( $p<0.05$ ). Vascularisation in the PEEK and PA+G meshes was similar at the different timepoints, as were the PP meshes, which had the least CD31 staining overall. To assess larger (stabilized) vessels having a smooth muscle cell coat,  $\alpha$ SMA staining was performed. Figure 8A shows a large number of immunostained myofibroblasts in the PEEK meshes on day 7, which were similarly observed in all mesh types at 7 and 30 days. Larger vessels were seen at 90 days, for example in PEEK meshes (Fig. 8B). All meshes induced similar levels of myofibroblast differentiation and smooth muscle cells at 7 and 30 days (Fig. 8C). At 60 days, PA, PA+G and PEEK meshes had significantly more  $\alpha$ SMA staining compared to PP meshes ( $P<0.01$ ). At 90 days, all mesh types had a significantly lower positive signal compared to the other time points with no differences between the mesh groups.

#### Discussion

In this study we compared the *in vivo* biocompatibility of alternative synthetic meshes with a clinical PP mesh, and a tissue control, by investigating biomechanics, collagen deposition, vascularisation and foreign body tissue reaction. Synthetic mesh, manufactured from alternative polymers to a clinical PP mesh,

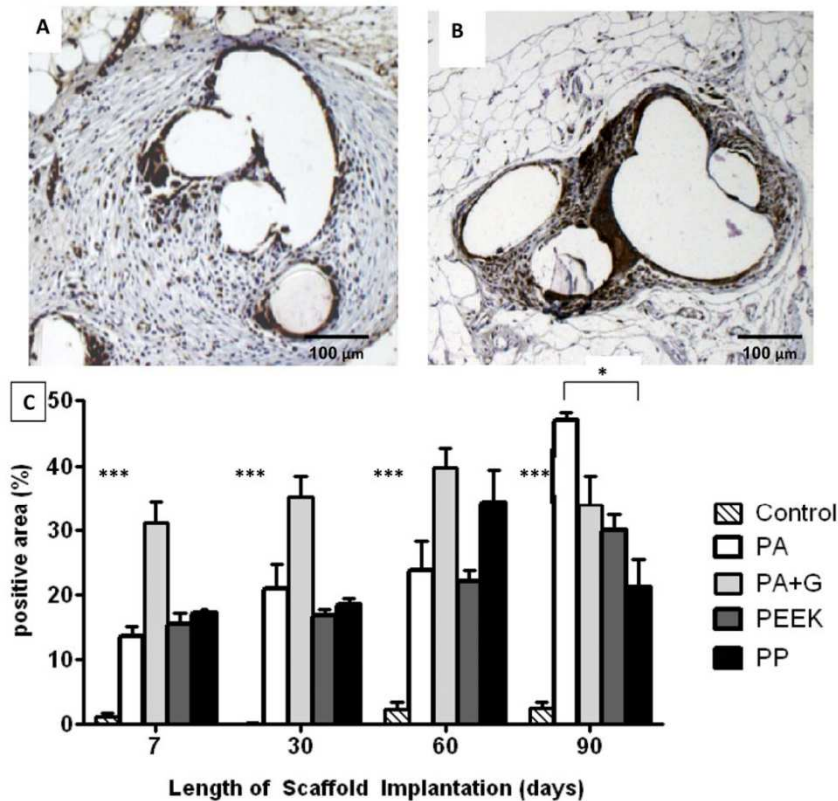


**Figure 5. CD68 immunostaining in rats implanted with synthetic mesh.** A. PA after 7 days and B. after 90 days implantation (--- line around mesh filament). Brown staining indicates CD68<sup>+</sup> macrophages. C. Percentage CD68 positive area within 50 μm radius of central mesh filament bundle. Data are mean ± SEM of n=6 animals/ group, \* p<0.05; \*\*\* p<0.001. Scale bar, 100 μm. doi:10.1371/journal.pone.0050044.g005

were warp knitted to a similar pattern, using yarn of the same diameter. This ensured that mesh pores were similar in size. Any differences in the host biological response were, therefore, a result of the polymer alone or of the coating. We studied the effect of gelatin coating only in the PA mesh as the tissue response to this composite mesh deemed to be representative for all polymers. This study showed that our new meshes induced a typical foreign body reaction over the time course, largely comparable with the PP meshes, but that there were differences with the extent and type of responses associated with inflammation, macrophage infiltration, collagen deposition and neovascularisation over the 90 day period.

In general, the PA+G meshes showed the least early CD45<sup>+</sup> inflammatory response at 7 and 30 days suggesting that the coating acts like a biofilm, while the PEEK and PP meshes were associated with a more acute inflammation that persisted with the PEEK meshes and subsided with the PP meshes over time. Nonetheless, the macrophage CD68 response depicted a general acute response to all implants. Generally, after implantation of a mesh an acute inflammatory reaction occurs, with macrophages dominating the acute phase at 7 days [16]. In our study, the inflammatory response to the foreign materials showed typical temporal differences. The PA+G meshes had notably more macrophages than the other mesh types at Day 7. Given that these mesh types had the lowest CD45 response at the same time point, it is likely that the major acute response here is due to macrophages. The PP response is similar to that described by

Spelzini et al who also showed a lower foreign body reaction at 90 days around the PP implant compared to silk implants [19]. Apart from its role in acute inflammation and early vascularisation, macrophages also have a critical role in the subsequent chronic phase of the host response. In particular, macrophages can potentially differentiate towards two pathways, one leading to an immediate and/or persistent inflammation, the other leading to a constructive remodelling and new tissue generation [20]. This M1/M2 macrophage polarisation has not been studied in this current study. In the case with the PA+G meshes, the gelatin was found to be degrading at the later stages of implantation, associated with more available porous openings allowing fibroblast infiltration and new collagen deposition. It is likely, although speculative, that in these meshes immunoregulatory M2 macrophages are the major type of cell.

Consistent with this, our meshes led to better tissue integration (collagen deposition for PA+G on day 90) and neovascularisation at day 60 compared with the PP meshes. All mesh types were generally well tolerated, with significant weight gain in all rats by 90 days. PA and PA+G implanted rats gained significantly more weight at 90 days compared to the other mesh types and the control, suggesting that these were better tolerated by the animals.

In line with previous studies examining several commercially available mesh types [21,22], both our new meshes and the PP meshes showed contraction at all time points. In general, a correlation can be drawn between collagen deposition and mesh

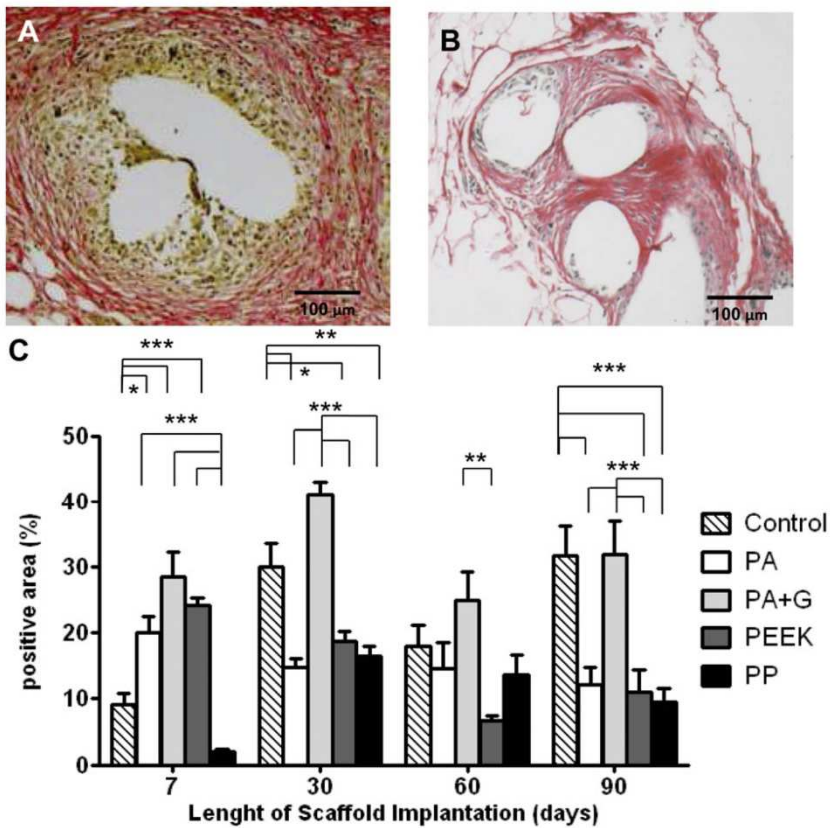


**Figure 6. Sirius red staining of collagen fibres in rats implanted with synthetic mesh.** A. PEEK after 7 days and B. After 90 days implantation. C. Percentage Sirius red stained area within 50 μm radius of central mesh filament bundle. Data are mean ± SEM of n=6 animals/group \*: p<0.05; \*\*: p<0.01, \*\*\*: p<0.001, Scale bar, 100 μm. doi:10.1371/journal.pone.0050044.g006

contraction for the PA+G, PEEK and PP mesh types, with an increase in collagen deposition leading to an increase in mesh contraction. It has been reported that both folding and contraction after implantation are responsible for side effects such as pain and tissue erosion [8]. No major differences in adhesion scores were determined between the mesh types assessed using the Lorenz adhesion scores [18]. PA had a significantly smaller adhesion area at 90 days compared to PEEK and PP, indicating that PA might produce fewer adhesions in the long term. No significant differences were found between the other mesh groups. Similar to our findings Boehm et al. compared Ultrapro® (combined PP and absorbable Monocryl®) and Prolene® (polypropylene) with no significant differences in terms of adhesions between the groups [21].

Uniaxial tensile testing was used to assess the biomechanical properties of explanted meshes, with stiffness represented by the slope of the load-elongation curve. Curves for the day 90 explants were found to be bilinear, with a region of initial low stiffness (toe region), followed by a region of higher stiffness (linear stiffness), as found by Afonso et al [23]. Biomechanical testing found all mesh types to be stiffer on day 90 compared to their day 7 counterparts, when loaded beyond strains of 4.2%. Collagen levels decreased between days 7 and 90 for some mesh types, suggesting that collagen alone did not contribute to increased explant stiffness; nor did mesh contraction since contraction was similar for all mesh

types except PP. The present results are likely due to a combination of innate mesh mechanical properties and the amount, type and orientation of collagen formed, as suggested by the relative differences in stiffness between the 90 day explanted meshes and collagen levels. Separate tensile studies conducted on these meshes gave no indication of mesh creep, and without a necrotic response, it seems unlikely that any plasticizing material in the polymer was released. The large quantity of collagen present on the PA+G meshes at all time points, except day 60 (for which low rat weights were recorded), suggests that the gelatin coating promoted collagen deposition, or was associated with a cellular response that promoted an environment for fibroblast infiltration, collagen secretion and tissue remodelling. When the gelatin coating had almost fully degraded by day 90 (Fig. S2C), mesh pores became accessible to cells (Fig. S2B h), and permitted collagen synthesis, particularly within the large pores, between the filament bundles. Generally, the level of collagen decreased between 30 and 90 days for all mesh types. This outcome could be related to the fact that the meshes themselves do not promote tissue integration in the long term, or the type of tissue response is too rapid and does not allow for gradual cell infiltration, collagen synthesis and tissue remodelling that may be occurring with the PA+G meshes. We have addressed the need for a more objective analysis of collagen in mesh explants as identified in previous studies [17]. However it is difficult to make comparisons with these

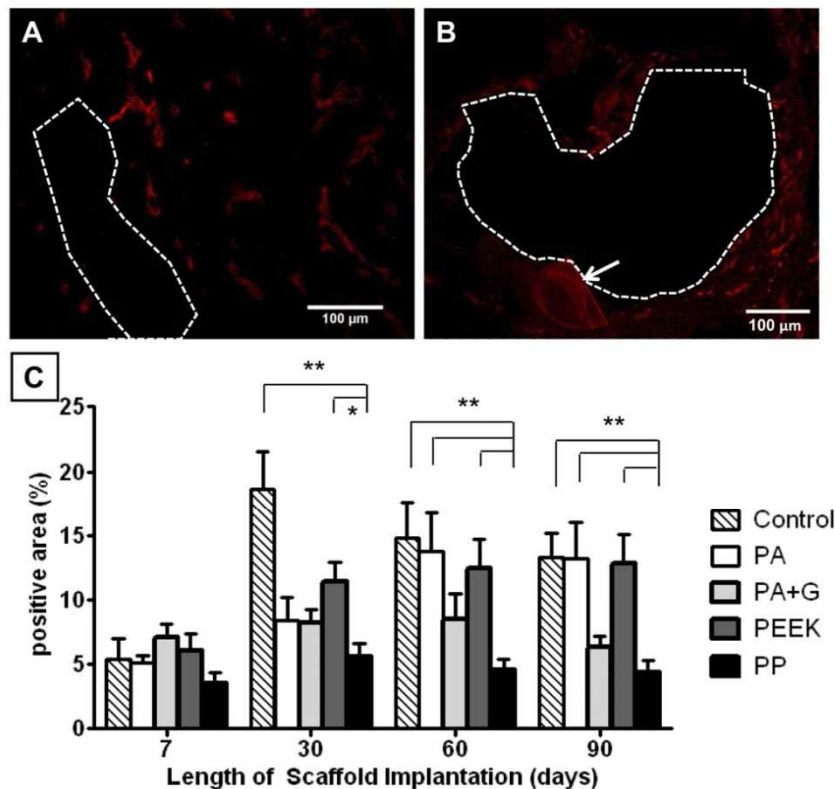


**Figure 7. CD31 immunostaining in rats implanted with synthetic mesh.** A. PA+G after 7 days and B. After 90 days implantation (- - - line around mesh filament). C. Percentage positive CD31 area within 50 µm radius of mesh. Data are mean ± SEM of n=6 animals/ group, \*p<0.05, \*\*p<0.01.

doi:10.1371/journal.pone.0050044.g007

studies and the current quantitative evaluation. Our novel image analysis enables quantification of the amount of collagen and its relationship to the mesh filaments, whereas other studies have scored the organisation of collagen fibres which is also important for mechanical strength [16,24]. Irrespective of this, collagen levels diminish, where in fact, collagen remained more closely associated with mesh filaments, rather than encapsulating the entire implant. In addition, the Sirius red stain does not take into account packing density of collagen fibrils or type of collagen around the mesh filaments, both of which will impact on the mechanical behaviour of the tissue.

Neovascularisation as measured by CD31 immunostaining reached highest levels at 60 and 90 days which is in agreement with previous studies for PP meshes [7,17]. In the current study, PP meshes were consistently less vascularised over the entire time period compared with all new mesh types. In particular, PA and PEEK meshes were superior to PP meshes at 60 and 90 days, perhaps indicating these materials are intrinsically more permissive for angiogenic processes, or are simply comparable to vascularisation in control tissues, and the PP meshes actually inhibit the process. Vascularisation could be further improved by incorporating angiogenic factors onto the mesh filaments during fabrication [25].

Smooth muscle cells and myofibroblasts are cells implicated in wound healing where strengthening wound tissue is important. Our studies show a steady increase in alpha smooth muscle actin

until 60 days. At this time point, all 3 new meshes were associated with significantly elevated smooth muscle cells compared with the PP meshes. These cells are finally lost through apoptosis after healing is complete explaining the significant decrease at 90 days. Acquisition of a smooth muscle cell coat by neovessels increases their stability, a desirable feature in the repair of tissues, including those that have herniated, by providing a stable blood supply to nourish neotissue and maintain its integrity in the long term.

In addition to the novelty of the new types of polymer meshes and biological coating used in this study, the strength of the current study is reflected in the use of computer-based analysis of the immunohistochemically stained slides using image analysis software. Histological analysis is the most commonly used technique in assessing new meshes [9]. Qualitative and semi-quantitative analysis of tissue by histology/immunohistochemistry has its limitations. Apart from the fact that different parts of the meshes are studied for histology making comparisons difficult [26,27] more relevant is the problem of subjectivity during the scoring process. In the current study, subjective bias during the scoring process is excluded as the software detects the positive signal in each immunostained image on the same set of 4 centrally placed mesh filaments and calculates the percentage stained area. Also, for the first time, we report a significant gradient for inflammatory cells surrounding mesh filaments, by using the software to examine staining and cell numbers within 50 µm increments from the surface of the filament bundles. Using the

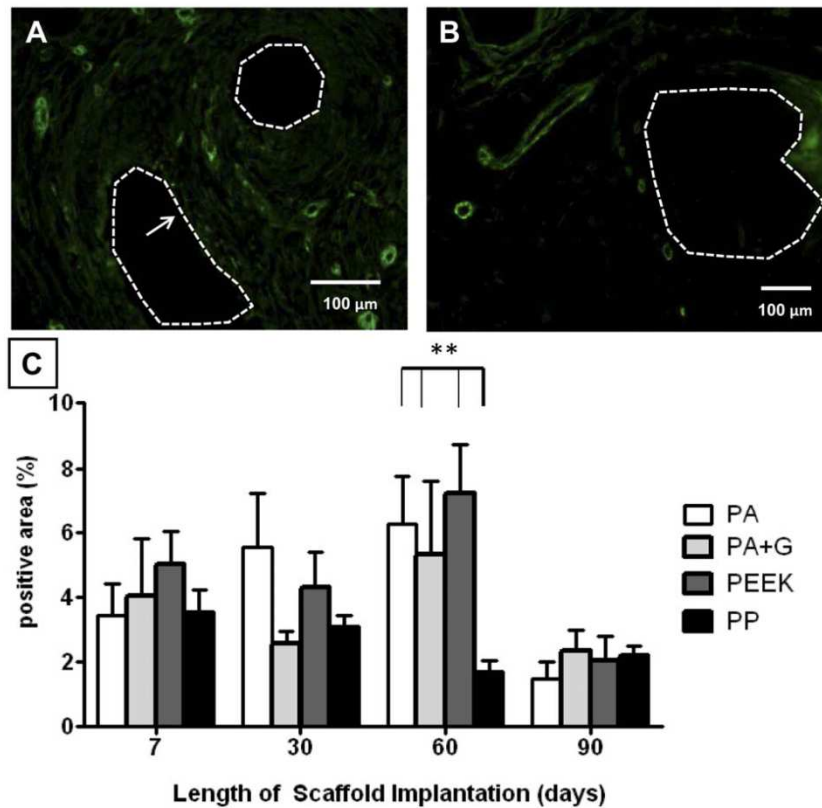


**Figure 8.  $\alpha$ SMA staining in rats implanted with synthetic mesh.** A. PEEK after 7 days and B. after 90 days after implantation (dotted line around mesh filament, arrow indicates vessel). C. Percentage of positive  $\alpha$ SMA staining. Data are mean  $\pm$  SEM of  $n=6$  animals/ group, \*\*:  $p<0.01$ . Scale bar, 100  $\mu$ m.  
doi:10.1371/journal.pone.0050044.g008

image analysis software allowed us to investigate the same area of stained tissue for every image and precisely focus on the area of interest.

A limitation of this study is the choice of model for assessing *in vivo* biocompatibility of mesh to be used for fascial defect repair. The rat abdominal wall hernia model does not mimic the clinical environment. However, this model is well accepted for initial testing of newly designed meshes for both synthetic and biological materials in hernia repair, including pelvic organ prolapse [28]. The clinical interpretation needs to be carefully considered in animals lacking any pathological conditions.

The optimal mesh for hernia or POP repair has not been developed yet [8]. Our ongoing studies indicate that PA+G meshes promote good cell attachment and proliferation for mesenchymal stem cell growth and may be suitable as meshes, (data not published). In conclusion, the new mesh types investigated in this study might form the basis of a new option for the future treatment of fascial defects.

## Supporting Information

**Figure S1 Schematic of overlay technique.** A: Ventral full-thickness abdominal defect involving the transversalis fascia, rectus abdominis muscle, and peritoneum. Meshes (dotted green line), in direct contact with the viscera and skin were sutured with slight overlay to the abdominal wall, B: Rat incisional hernia model in

control groups. The defect (dotted red lines) was repaired by manipulating the contralateral full-thickness abdominal wall (blue line). Photographs of rat abdominal wall C. At time of mesh implantation (PA) B. At 7 days of mesh implantation (PA+G) C. At 90 days of mesh implantation (PA+G) representative for all mesh groups.  
(TIF)

**Figure S2 H+E stained sections from rats implanted with synthetic mesh.** A. Composite picture showing typical distribution of mesh filament bundles of PA at 7 days. B. Composite picture with several mesh filaments of PA at 90 days. C. Single filament bundles at higher power for control, PA, PA+G, PEEK and PP mesh after 7 days and. 90 days implantation. \* denotes gelatin around PA filaments.  
(TIF)

**Figure S3 Biomechanical properties of explanted mesh types and control on day 7 (--- lines) and day 90 (— lines).** Explant stiffness is indicated by the slope of the curve, with stiffer materials possessing a steeper gradient. This is the same data shown in Figure 3 (means) and in addition includes 95% CI error bars.  
(TIF)

**Figure S4 Gradient analysis around the mesh filaments in 50  $\mu$ m increments in PEEK meshes (representative**

**example for all meshes).** A. CD68 positive staining at 7, 30, 60 and 90 days. \*:  $p < 0.05$ , \*\*\*:  $p < 0.001$ . B.  $\alpha$ SMA staining at 7, 30, 60 and 90 days. \*:  $p < 0.05$ , \*\*\*:  $p < 0.001$  (TIF)

## Acknowledgments

We thank Dr Keith McLean for advice and Dr Vincent Letouzey for critical reading of the manuscript.

## References

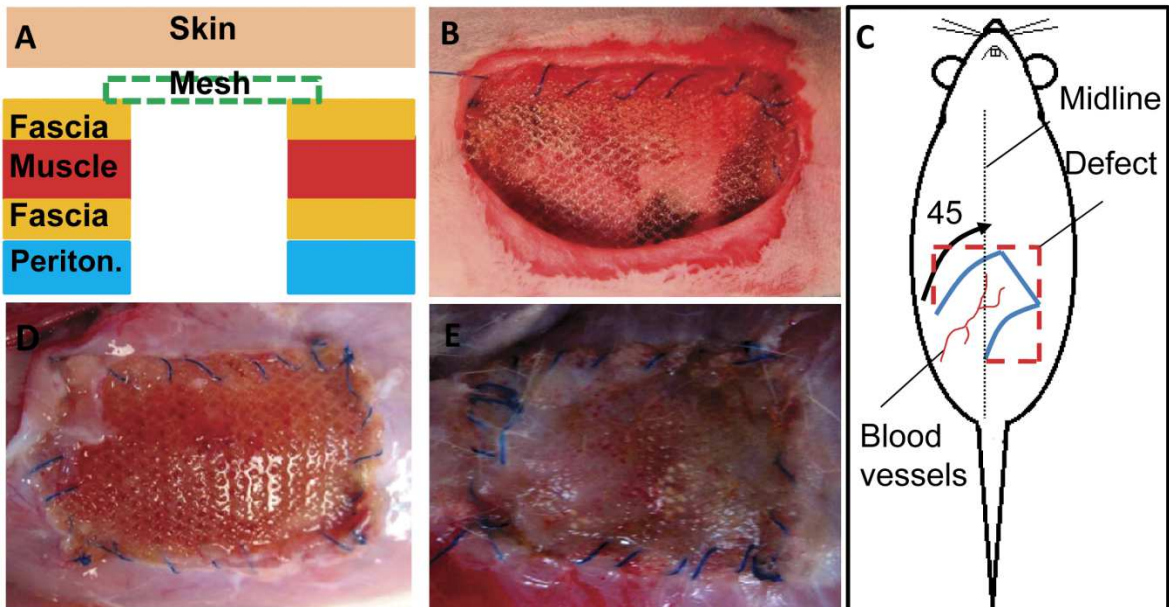
- Mudge M, Hughes LE (1985) Incisional Hernia - A 10 year prospective -study of incidence and attitudes. *Br J Surg* 72: 70–71.
- Sailes FC, Walls J, Guelig D, Mirzabeigi M, Long WD, et al. (2011) Ventral Hernia Repairs: 10-Year Single-Institution Review at Thomas Jefferson University Hospital. *J Am Coll Surg* 212: 119–123.
- Cassar K, Munro A (2002) Surgical treatment of incisional hernia. *Br J Surg* 89: 534–545.
- Hunskar S, Burgio K, Clark A, Lapitan MC, Nelson R, et al. (2005) Epidemiology of urinary (UI) and faecal (FI) incontinence and pelvic organ prolapse (POP); Abrams P, Cardozo L, Khoury S, Wien A, editors. Available: [http://www.icsoffice.org/Publications/ICI\\_3/v1.pdf/chap5.pdf](http://www.icsoffice.org/Publications/ICI_3/v1.pdf/chap5.pdf). 255–312 p. Accessed 22.10.2012.
- Butters M, Redecke J, Koninger J (2007) Long-term results of a randomized clinical trial of Shouldice, Lichtenstein and transabdominal preperitoneal hernia repairs. *Br J Surg* 94: 562–565.
- Stanford EJ, Cassidenti A, Moen MD (2012) Traditional native tissue versus mesh-augmented pelvic organ prolapse repairs: providing an accurate interpretation of current literature. *Int Urogynecol J* 23: 19–28.
- Konstantinovic ML, Pille E, Malinowska M, Verbeken E, De Ridder D, et al. (2007) Tensile strength and host response towards different polypropylene implant materials used for augmentation of fascial repair in a rat model. *Int Urogynecol J Pelvic Floor Dysfunct* 18: 619–626.
- Deprest J, Zheng F, Konstantinovic M, Spelzini F, Claerhout F, et al. (2006) The biology behind fascial defects and the use of implants in pelvic organ prolapse repair. *Int Urogynecol J Pelvic Floor Dysfunct* 17 Suppl 1: S16–25.
- de Tayrac R, Alves A, Therin M (2007) Collagen-coated vs noncoated low-weight polypropylene meshes in a sheep model for vaginal surgery. A pilot study. *Int Urogynecol J Pelvic Floor Dysfunct* 18: 513–520.
- Lim YN, Muller R, Corstiaans A, Hitchins S, Barry C, et al. (2007) A long-term review of posterior colporrhaphy with Vypro 2 mesh. *Int Urogynecol J Pelvic Floor Dysfunct* 18: 1053–1057.
- Robinson TN, Clarke JH, Schoen J, Walsh MD (2005) Major mesh-related complications following hernia repair - Events reported to the Food and Drug Administration. *Surgical Endoscopy and Other Interventional Techniques* 19: 1556–1560.
- Pereira-Lucena CG, Artigiani-Neto R, Lopes GJ, Frazao CVG, Goldenberg A, et al. (2010) Experimental study comparing meshes made of polypropylene, polypropylene plus polyglactin and polypropylene plus titanium: inflammatory cytokines, histological changes and morphometric analysis of collagen. *Hernia* 14: 299–304.
- Felemovicius I, Bonsack ME, Hagerman G, Delaney JP (2004) Prevention of adhesions to polypropylene mesh. *J Am Coll Surg* 198: 543–548.
- Tadokoro M, Matsushima A, Kotobuki N, Hirose M, Kimura Y, et al. (2012) Bone morphogenetic protein-2 in biodegradable gelatin and ss-tricalcium phosphate sponges enhances the in vivo bone-forming capability of bone marrow mesenchymal stem cells. *J Tissue Eng Regen Med* 6: 253–260.
- BostonScientific website. Available: [http://www.bostonscientific.com/templatedata/imports/collateral/Gynecology/broc\\_Polyform\\_01\\_ug\\_us.pdf](http://www.bostonscientific.com/templatedata/imports/collateral/Gynecology/broc_Polyform_01_ug_us.pdf). Accessed 22.10.2012.
- Zheng F, Lin Y, Verbeken E, Claerhout F, Fastrez M, et al. (2004) Host response after reconstruction of abdominal wall defects with porcine dermal collagen in a rat model. *Am J Obstet Gynecol* 191: 1961–1970.
- Ozög Y, Konstantinovic ML, Verschueren S, Spelzini F, De Ridder D, et al. (2009) Experimental comparison of abdominal wall repair using different methods of enhancement by small intestinal submucosa graft. *Int Urogynecol J Pelvic Floor Dysfunct* 20: 435–441.
- Zuhlke HV, Lorenz EMP, Straub EM, Savvas V (1990) PATHOPHYSIOLOGY AND CLASSIFICATION OF ADHESIONS. *Langenbecks Arch Chir*: 1009–1016.
- Spelzini F, Konstantinovic ML, Guelinckx I, Verbist G, Verbeken E, et al. (2007) Tensile strength and host response towards silk and type i polypropylene implants used for augmentation of fascial repair in a rat model. *Gynecol Obstet Invest* 63: 155–162.
- Mantovani A, Sica A, Sozzani S, Allavena P, Vecchi A, et al. (2004) The chemokine system in diverse forms of macrophage activation and polarization. *Trends in Immunology* 25: 677–686.
- Bohm G, Steinau G, Krahling E, Schumpelick V, Hermanns-Sachweh B, et al. (2011) Is Biocompatibility Affected by Constant Shear Stress? - Comparison of Three Commercially Available Meshes in a Rabbit Model. *J Biomater Appl* 25: 721–741.
- Garcia-Urena MA, Ruiz VV, Godoy AD, Perca JMB, Gomez LMM, et al. (2007) Differences in polypropylene shrinkage depending on mesh position in an experimental study. *Am J Surg* 193: 538–542.
- Afonso JS, Martins P, Girao M, Jorge RMN, Ferreira AJM, et al. (2008) Mechanical properties of polypropylene mesh used in pelvic floor repair. *Int Urogynecol J* 19: 375–380.
- Konstantinovic ML, Lagae P, Zheng F, Verbeken EK, De Ridder D, et al. (2005) Comparison of host response to polypropylene and non-cross-linked porcine small intestine serosal-derived collagen implants in a rat model. *Bjog* 112: 1554–1560.
- Oh HH, Lu HX, Kawazoe N, Chen GP (2012) Micropatterned angiogenesis induced by poly(D,L-lactic-co-glycolic acid) mesh-structured scaffolds. *J Bioact Compat Polym* 27: 97–106.
- Bellows CF, Wheatley BM, Moroz K, Rosales SC, Morici LA (2011) The Effect of Bacterial Infection on the Biomechanical Properties of Biological Mesh in a Rat Model. *Plos One* 6(6): e21228.
- Boennelycke M, Christensen L, Nielsen LF, Everland H, Lose G (2011) Tissue response to a new type of biomaterial implanted subcutaneously in rats. *Int Urogynecol J* 22: 191–196.
- Abramowitch SD, Feola A, Jallah Z, Moalli PA (2009) Tissue mechanics, animal models, and pelvic organ prolapse: A review. *EJOG* 144: S146–S158.

## Author Contributions

Conceived and designed the experiments: SLE JAW JAMR AR CEG. Performed the experiments: DU SLE JFW TS. Analyzed the data: DU SLE TS CL. Contributed reagents/materials/analysis tools: CL AR. Wrote the paper: DU SLE AR JAW CEG.

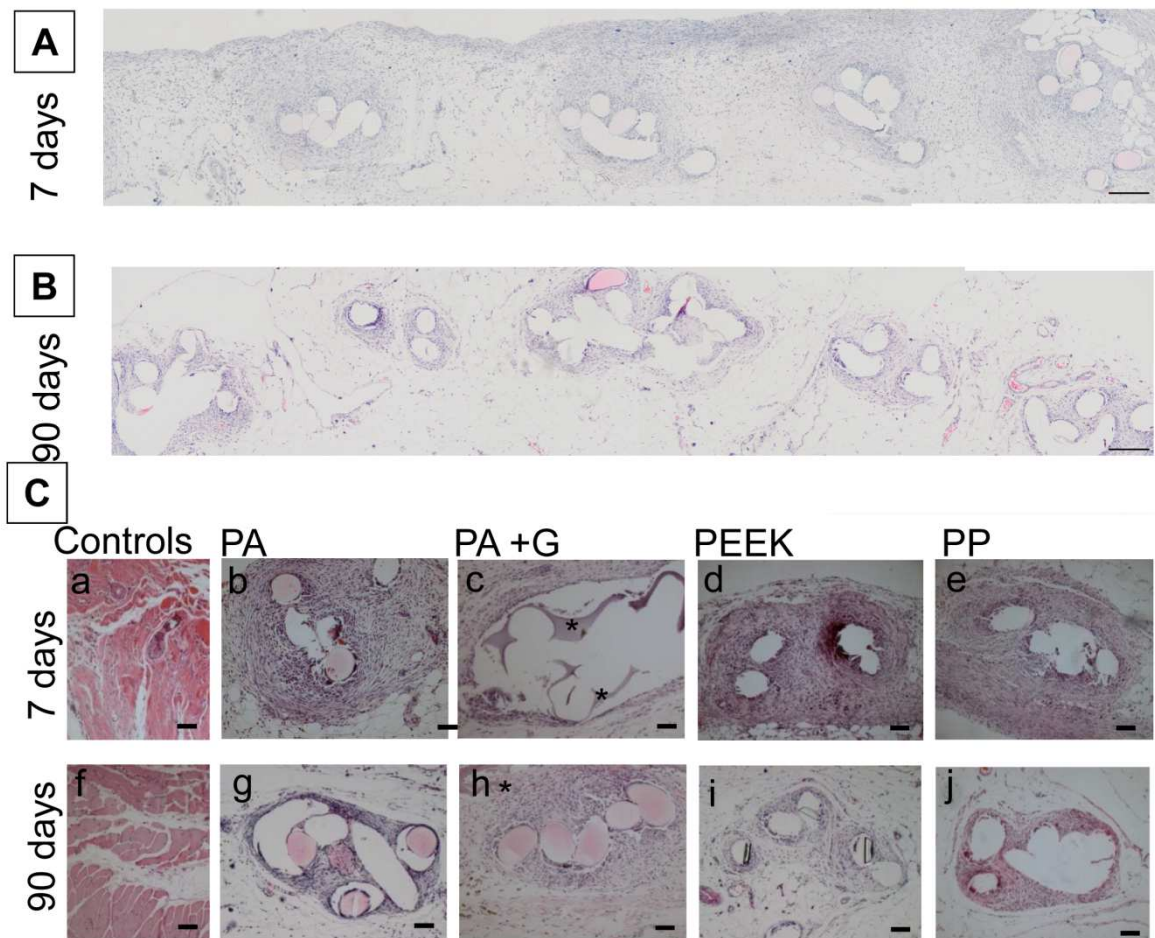
### Supplementary Figure 1.

Schematic of overlay technique. A: Ventral full-thickness abdominal defect involving the transversalis fascia, rectus abdominis muscle, and peritoneum. Meshes (dotted green line), in direct contact with the viscera and skin were sutured with slight overlay to the abdominal wall, B: Rat incisional hernia model in control groups. The defect (dotted red lines) was repaired by manipulating the contralateral full-thickness abdominal wall (blue line). Photographs of rat abdominal wall C. At time of mesh implantation (PA) B. At 7 days of mesh implantation (PA+G) C. At 90 days of mesh implantation (PA+G) representative for all mesh groups.



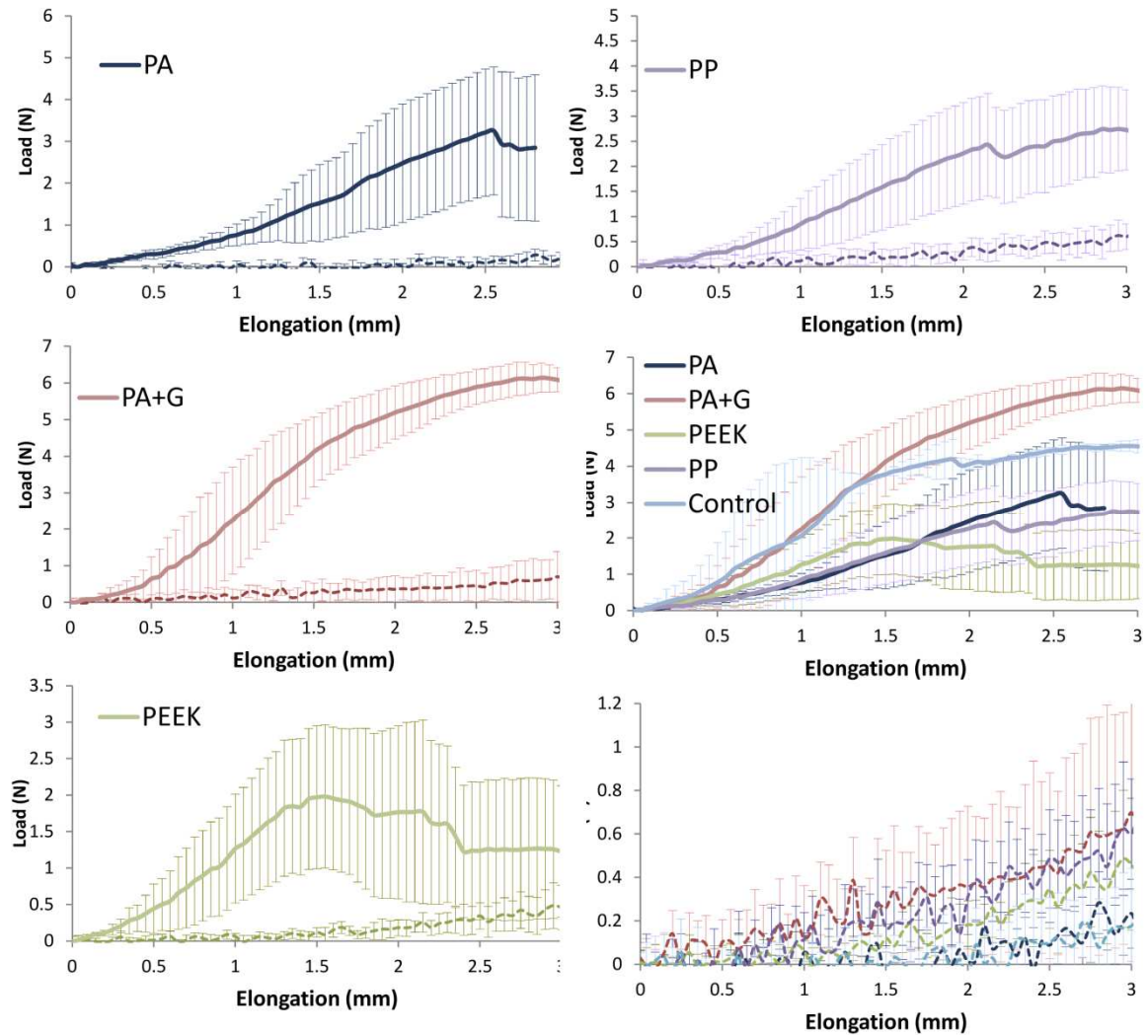
## Supplementary Figure 2.

H+E stained sections from rats implanted with synthetic mesh. A. Composite picture showing typical distribution of mesh filament bundles of PA at 7 days. B. Composite picture with several mesh filaments of PA at 90 days. C. Single filament bundles at higher power for control, PA, PA+G, PEEK and PP mesh after 7 days and 90 days implantation. \* denotes gelatin around PA filaments.



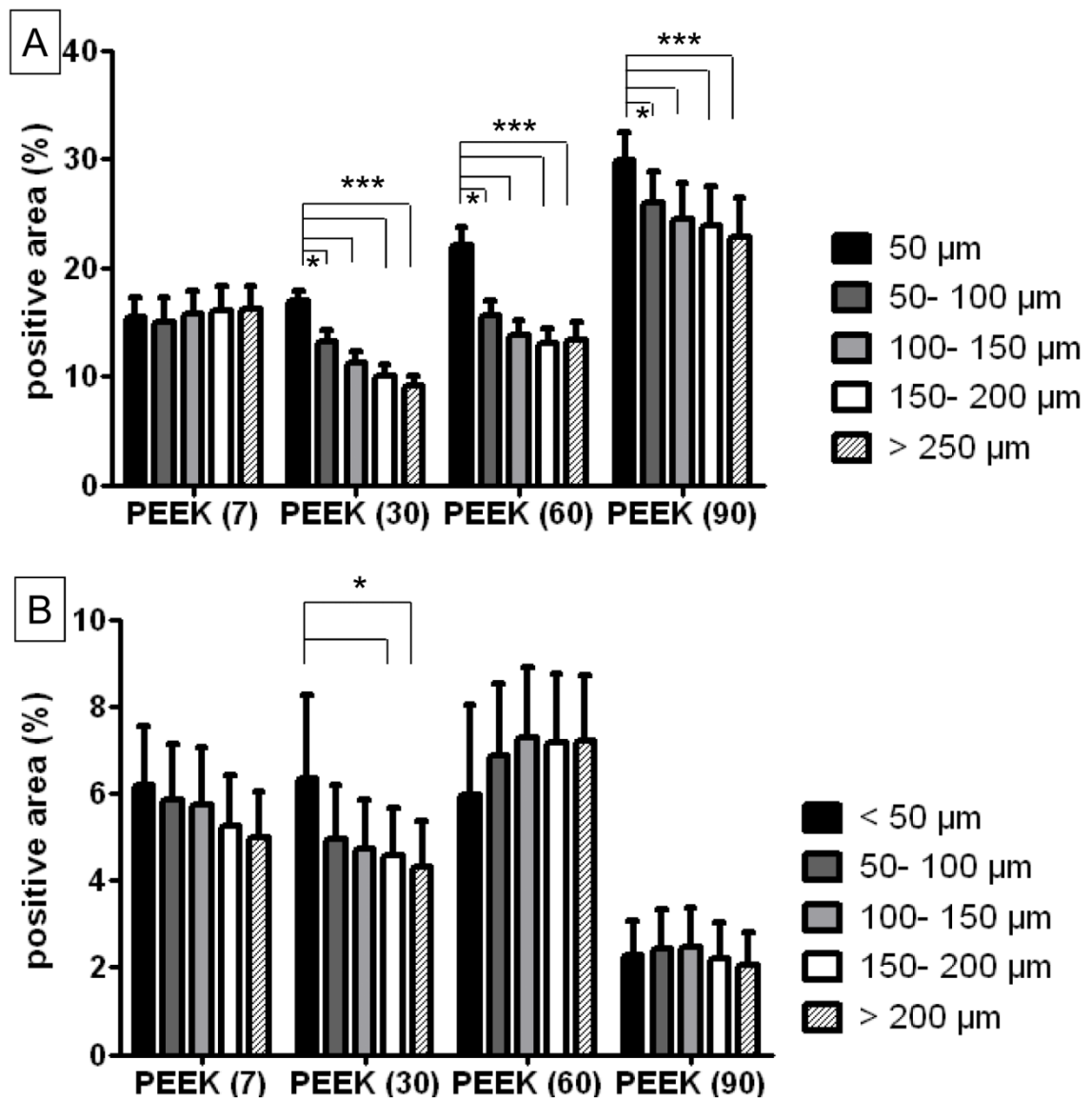
### Supplementary Figure 3.

Biomechanical properties of explanted mesh types and control on day 7 (--- lines) and day 90 (— lines). Explant stiffness is indicated by the slope of the curve, with stiffer materials possessing a steeper gradient. This is the same data shown in Figure 3 (means) and in addition includes 95% CI error bars.



**Supplementary Figure 4.**

Gradient analysis around the mesh filaments in 50  $\mu\text{m}$  increments in PEEK meshes (representative example for all meshes). A. CD68 positive staining at 7, 30, 60 and 90 days. \*:  $p < 0.05$ , \*\*\*:  $p < 0.001$ . B.  $\alpha\text{SMA}$  staining at 7, 30, 60 and 90 days. \*:  $p < 0.05$ , \*\*\*:  $p < 0.001$



## CHAPTER 3

### Endometrial MSC in Postmenopausal Endometrium

Mesenchymal stem cells have anti-inflammatory and immunomodulatory effects when transplanted into animal models and humans. In the presence of pro-inflammatory cytokines, MSC activate chemokines and generate nitric oxide to dampen inflammation (Ren et al. 2008). The clinical utility of intraperitoneal administration of endometrial stromal cells containing eMSC in a mouse model of encephalomyelitis was demonstrated by their anti-inflammatory effect in a pilot study (Peron et al. 2012). Since the adverse effects of mesh implantation are mostly caused by chronic inflammation and fibrosis a TE approach using MSC may provide a mechanism of reducing these unwanted side effects. EMSC are a readily available source of MSC which possess all key adult stem cell properties and can be harvested from premenopausal women without anesthesia by a simple biopsy procedure (Ulrich et al. 2013). Since POP manifests predominantly in postmenopausal women it is important to determine whether eMSC in menopausal endometrium are a suitable source for TE applications.

The endometrium during menopause is thin and atrophic due to lack of circulating hormones, which results in gland inactivity and atrophy. The cell yield from postmenopausal endometrium is low and makes analysis difficult. Drs. Rosamilia and Gargett therefore initiated a phase IV clinical trial of estradiol valerate treatment of eligible postmenopausal women to thicken postmenopausal endometrium to allow the prospectively isolation of eMSC from an endometrial biopsy.

This Chapter investigates the key adult stem cell properties of eMSC in postmenopausal women either with or without estrogen replacement therapy. Specifically, on eMSC purified using W5C5-antibody labelled magnetic beads:

- 1) I determined the cloning efficiency,
- 2) I performed mesodermal differentiation assays to determine multipotency and,
- 3) I used flow cytometric analysis to determine the eMSC surface phenotype.
- 4) I also confirmed that the efficacy of estradiol valerate by measuring endometrial thickness and luminal and glandular epithelial height using image analysis.

Immunohistochemistry was used to determine the microvessel density in the endometrium.

I thank Ker Sin Tan for assisting with cell isolation, cell culture, tissue processing, and staining. I also thank Dr. Anna Rosamilia and Dr. Amy Cheong for patient recruitment. I

acknowledge Dr. Amy Cheong for assistance of image acquisition and image analysis of the histological sections. I also thank Liz Fitzgerald, Yao Han and Pamela Mamers for their contribution in monitoring the clinical trial and collection of tissue samples. My thank also goes to Kjiana Schwab and James Deane for helping with the immunohistochemistry and immunofluorescence.

### Declaration for Thesis Chapter 3

#### Declaration by candidate

In the case of Chapter 3, the nature and extent of my contribution to the work was the following:

Nature of contribution	Extent of contribution (%)
Study design, Cell isolation and processing, Cell staining, Image analysis, Statistical analysis, Data interpretation, Paper writing	85

The following co-authors contributed to the work. Co-authors who are students at Monash University must also indicate the extent of their contribution in percentage terms:

Name	Nature of contribution	Extent of contribution (%) for student co-authors only
<b>Ker Sin Tan</b>	Cell isolation and processing, Cell staining	
<b>James Deane</b>	Tissue staining	
<b>Kjiana Schwab</b>	Patient recruitment, Cell isolation and processing, Cell staining	
<b>Amy Cheong</b>	Image analysis	
<b>Anna Rosamilia</b>	Study design, Patient recruitment, Tissue harvesting	
<b>Caroline E. Gargett</b>	Study design, Data interpretation, Paper writing	

Candidate's Signature

	Date <b>07.03.2014</b>
--	---------------------------

**Declaration by co-authors**

The undersigned hereby certify that:

- (1) the above declaration correctly reflects the nature and extent of the candidate's contribution to this work, and the nature of the contribution of each of the co-authors.
- (2) they meet the criteria for authorship in that they have participated in the conception, execution, or interpretation, of at least that part of the publication in their field of expertise;
- (3) they take public responsibility for their part of the publication, except for the responsible author who accepts overall responsibility for the publication;
- (4) there are no other authors of the publication according to these criteria;
- (5) potential conflicts of interest have been disclosed to (a) granting bodies, (b) the editor or publisher of journals or other publications, and (c) the head of the responsible academic unit; and
- (6) the original data are stored at the following location(s) and will be held for at least five years from the date indicated below:

**Location(s)** **MIMR- PHI Institute of Medical Research, Level 3, Monash University**

	<b>Name</b>	<b>Date</b>
<b>Signature 1</b>		<b>06/01/2014</b>
<b>Signature 2</b>		<b>04/03/2014</b>
<b>Signature 3</b>		<b>31/12/2013</b>
<b>Signature 4</b>		<b>22/12/2013</b>
<b>Signature 5</b>		<b>20/12/13</b>
<b>Signature 6</b>		<b>20/12/13</b>



**Manuscript submitted to Human Reproduction**

**Mesenchymal stem/stromal cells in Postmenopausal Endometrium**

Running title

MSC in postmenopausal endometrium

**AUTHORS**

Ulrich, D<sup>1,2,3</sup> Tan, KS<sup>1</sup>; Deane, J<sup>1</sup>; Schwab, K<sup>1</sup>; Cheong, A<sup>1</sup>, Rosamilia, A<sup>1,2,4</sup>; Gargett, CE<sup>1,2,4\*</sup>

<sup>1</sup> The Ritchie Centre, Monash Institute of Medical Research, 27-31 Wright Street, Clayton, 3168, Clayton, VIC, Australia

<sup>2</sup> Monash University Department of Obstetrics and Gynaecology, Monash Medical Centre, 246 Clayton Road, Clayton, 3168, VIC, Australia

<sup>3</sup> Current address: Department of Obstetrics and Gynaecology, Medical University Graz, 8045 Graz, Austria

<sup>4</sup> equal senior authors

\* Corresponding Author

A/Prof Caroline Gargett, PhD

The Ritchie Centre,

Monash Institute of Medical Research

27-31 Wright Street

Clayton, 3168

Melbourne, VIC, Australia

Email: [REDACTED]

Keywords

Mesenchymal stem cells, mesenchymal stromal cells, endometrial MSC, W5C5, SUSD2, estrogen, postmenopausal, endometrium

## **ABSTRACT**

**Study question:** Are there mesenchymal stem/ stromal cells in postmenopausal endometrium with adult stem cell properties that can be prospectively isolated from a biopsy?

**Summary answer:** Perivascular W5C5<sup>+</sup> cells isolated from postmenopausal endometrial biopsies displayed characteristic mesenchymal stem/stromal cell (MSC) properties of clonogenicity, multipotency and surface phenotype irrespective of whether women are or are not pre-treated with estrogen to regenerate the endometrium.

**What is known already:** Recently MSCs have been identified in human premenopausal endometrium, and can be prospectively isolated using a single marker, W5C5/SUSD2.

**Study design, size, duration:** Endometrial tissue from 17 premenopausal (pre-MP), 19 postmenopausal (post-MP) without hormonal treatment, and 15 postmenopausal women on estrogen replacement therapy (post-MP+ E<sub>2</sub>) was collected through a prospective phase IV clinical trial over 2 years. Endometrial tissue was obtained from women by biopsy (curettage) just prior to undergoing hysterectomy and assessed for histological and in vitro analysis of MSC properties.

**Participants/materials, setting, methods:** Postmenopausal women less than 65 years of age were treated with or without E<sub>2</sub> for 6-8 weeks prior to tissue collection. Serum E<sub>2</sub> levels were determined by estradiol immunoenzymatic assay. The effect of E<sub>2</sub> on endometrial thickness and glandular and luminal epithelial height was determined using image analysis. Endometrial tissue was dissociated into single cell suspensions and MSC properties were examined in freshly isolated and short-term cultured, magnetic bead-purified W5C5<sup>+</sup> cells. MSC properties were assessed using clonogenicity, mesodermal differentiation in adipogenic, chondrogenic, osteogenic and myogenic induction culture media and surface phenotype by flow cytometric assays. Estrogen receptor  $\alpha$  expression in

W5C5<sup>+</sup> cells was examined using dual colour immunofluorescence. Vascularity was analysed using CD34 and alpha smooth muscle actin immunostaining and subsequent image analysis.

**Main results and the role of chance:** Postmenopausal endometrium exposed to E<sub>2</sub> treatment was significantly thicker than untreated post-MP endometrium (p< 0.05).

A small population of stromal cells with MSC properties was purified with the W5C5/SUSD2 antibody from postmenopausal endometrium, whether atrophic from low circulating estrogen or regenerated from systemic estrogen treatment, similar to premenopausal endometrium. The MSC derived from postmenopausal endometrium treated with or without E<sub>2</sub> fulfil the minimum MSC criteria: clonogenicity, surface phenotype (CD29<sup>+</sup>, CD44<sup>+</sup>, CD73<sup>+</sup>, CD105<sup>+</sup>, CD140b<sup>+</sup>, CD146<sup>+</sup>,) and multipotency. Postmenopausal endometrial MSCs (eMSC) also have comparable properties to premenopausal eMSC with respect to self renewal in vitro and SUSD2 expression. The W5C5<sup>+</sup> cells were located perivascularly as expected and did not express estrogen receptor  $\alpha$ .

**Limitations, reasons for caution:** The properties of MSC derived from postmenopausal endometrium were evaluated in vitro and their in vivo tissue reconstitution capacity has not been established as it has for premenopausal eMSC.

**Wider implications of the findings:** The endometrium is an easily accessible source of MSC obtainable with minimum morbidity that could be used for future clinical applications as a cell-based therapy. This study shows that menopausal women can access their eMSC by a simple biopsy for use in autologous therapies whether or not if their endometrium has been regenerated by short-term E<sub>2</sub> treatment, provided they have an intact uterus and are not contraindicated for short-term E<sub>2</sub> treatment. EMSC in

postmenopausal women possess key MSC properties and are a promising source of MSC independent of a woman's age.

**Study funding/competing interest(s):** This study was supported by the National Health and Medical Research Council (NHMRC) of Australia grant (1021126) (CEG, AR) and Senior Research Fellowship (1042298) (CEG), Australian Gynaecological Endoscopic Society grant (AR) and Victorian Government's Operational Infrastructure Support Program.

**Trial registration number:** CTNRN12610000563066

## INTRODUCTION

Human mesenchymal stem cells or multipotent stromal cells (MSC) have been identified in almost every adult tissue; bone marrow, adipose tissue, synovial membrane and the endometrium (da Silva Meirelles et al. 2006, Beltrami et al. 2007, Schwab and Gargett 2007, Crisan et al. 2008). Originally MSC were identified by their adherence to plastic and differentiation into mesodermal lineages; adipocytic, chondrocytic and osteoblastic (Prockop 1997, Pittenger et al. 1999). More recently it has been shown that bone marrow MSC (bmMSC) also differentiate into endodermal and neuroectodermal lineages (Torrente and Polli 2008, Morikawa et al. 2009). Cultured MSC are highly proliferative with capacity to produce millions of cells from a single clonogenic cell (Gargett et al. 2009). MSC have characteristic surface markers including CD29, CD44, CD73, CD105, but not haematopoietic cell markers CD34, CD45, CD14, CD11b, CD79 $\alpha$ , CD19 and HLA-DR (Dominici et al. 2006, Caplan 2007). The identification of more specific markers, Stro-1, CD146, CD271, has enabled the prospective isolation of MSC from bone marrow (Simmons and Torok-Storb 1991, Gronthos et al. 2003, Buhring et al. 2007). BmMSC have anti-inflammatory and immunomodulatory properties which make them an attractive source for tissue engineering and regenerative medicine applications (Salem and Thiemermann 2010, Le Blanc and Mougiakakos 2012).

Endometrial MSC (eMSC) were recently discovered and characterised in premenopausal endometrium where they are thought to regenerate the stromal vascular component of the functional layer each month (Gargett et al. 2009). EMSC also possess high capacity for proliferation, differentiate into mesodermal lineages and express characteristic MSC surface markers, fulfilling the minimal criteria for defining MSC (Dominici 2006). Originally eMSC were prospectively isolated from hysterectomy tissue using co-

expression of 2 markers (CD140b/ PDGFR $\beta$  and CD146) by FACS sorting (Schwab and Gargett 2007). EMSC can now be prospectively isolated from endometrial biopsy tissue using the single marker W5C5 using magnetic bead sorting (Masuda et al. 2012). W5C5 recognises an epitope of Sushi Domain containing 2 (SUSD2) molecule (Sivasubramaniyan et al. 2013). Almost all clonogenic endometrial stromal cells were found in the W5C5<sup>+</sup> fraction. Similar to CD140b<sup>+</sup>CD146<sup>+</sup> cells, W5C5<sup>+</sup> cells meet the defining criteria for MSC (Masuda et al 2012). Clonogenic stromal cells have also been identified in postmenopausal endometrium, although the sample size examined was small (n=4) (Schwab et al. 2005). EMSC are an attractive source of MSC as they can be easily obtained through an office biopsy procedure without anaesthesia or scarring (Gargett et al. 2012) or a simple curettage for many women. Protocols are being developed for culture expansion of eMSC under clinical grade Good Manufacturing Practices (cGMP) conditions making them an ideal source for future clinical applications, particularly in women's health, where they could be used autologously (Rajaraman et al. 2013).

Clinical conditions for which eMSC could be utilised as a cell-based therapy may affect postmenopausal women, for example pelvic organ prolapse (Hunskar et al. 2005, Boennelycke et al. 2013, Ulrich et al. 2013). To date, eMSC have only been characterised in premenopausal women. Due to hormonal depletion, postmenopausal endometrium is thin and atrophic, difficult to biopsy without anaesthesia, and we hypothesized a low yield of eMSC. However, postmenopausal endometrium has significant regenerative potential, particularly when systemic estrogen is administered. A thick functional endometrium can be generated and indeed postmenopausal women in their 60s have born children via IVF (Paulson et al. 2002).

Therefore, the aim of this study was to determine whether postmenopausal endometrium contains a population of eMSC and to characterize these postmenopausal eMSC for

clonogenicity, mesodermal differentiation, self renewal and surface phenotype. We hypothesized that eMSC can be prospectively isolated from endometrial biopsies of postmenopausal endometrium, that they would be present at similar frequency as in premenopausal endometrium and that they possess similar properties to premenopausal eMSC.

## **MATERIALS AND METHODS**

### **Human tissue and ethical approval**

Human endometrial tissue including underlying myometrium was collected from 17 premenopausal (pre-MP) and 19 postmenopausal (post-MP) (longer than 12 months since last period) undergoing hysterectomy who were not taking hormones (Table 1). We also collected endometrial biopsies from 15 postmenopausal women on oral estrogen replacement therapy (post- MP+E<sub>2</sub>). Due to the low endometrial stromal cell yield from atrophic postmenopausal endometrium, a single arm phase IV clinical trial was registered with the Therapeutic Goods Association (CTNRN12610000563066) to treat postmenopausal women with short term estrogen to regenerate the endometrium and obtain higher cell yields for the collection and analysis of eMSC. The enrolled women (n= 15) took oral estrogen replacement therapy (Progynova 2mg daily for 6-8 weeks) which was ceased 2 days prior to scheduled hysterectomy. The biopsy was obtained by curettage just prior to surgical removal of the uterus. Inclusion criteria were at least 12 months since the last period and age less than 65 years. Exclusion criterion was any condition where systemic oestrogen use was contra-indicated, including current/past history of breast cancer, other oestrogen responsive tumours, liver adenoma, thrombo-embolism, undiagnosed vaginal bleeding, uncontrolled hypertension or ongoing oral hormone replacement therapy (HRT). The women were assessed for these exclusion criteria by

urogynaecologist AR. Informed written consent was obtained from each patient and ethics approval was obtained from the Monash Health Human Research and Ethics Committee B and Cabrini HREC.

The collected tissues (n=51) were used for histological and/ or cell culture analysis. Serum samples were also collected to determine the hormonal status of the postmenopausal women (n=10) and determine circulating estrogen levels in the estrogen-treated women (n=10). Endometrial samples (n=26) collected in collection medium (HEPES-buffered DMEM/F12 medium containing 5% fetal calf serum and 5% antibiotics-antimycotics) were immediately transported to the laboratory and processed within 24 hours. Samples (n=32) were also frozen in OCT for cryostat sections and fixed for paraffin sections. Blood from Post-MP and Post-MP+E<sub>2</sub> was drawn and centrifugated at 2000 g for 20 minutes at 4° C to collect serum. Estrogen levels were determined by a competitive binding estradiol immunoenzymatic assay performed by Monash Health Pathology Laboratory.

### Histology

Tissues collected for histological analysis were fixed in 10% formalin for 24 hours, then embedded in paraffin and oriented so that the full thickness endometrium from myometrium to the lumen could be examined (Figure 1A-C). These were sectioned into 5µm sections and stained with haematoxylin and eosin (H+E) to determine endometrial thickness.

### Immunohistochemistry

To determine the estrogen effect on the luminal and glandular epithelial height, sections from postmenopausal endometrium were stained with the epithelial marker Cytokeratin 18. To determine the total blood vessel area as a measure of vascularity, sections were

immune-stained with anti-human CD34, and vessels invested with pericytes and smooth muscle cells were immune-stained with anti-human  $\alpha$ SMA (Abberton et al. 1999). Sections underwent dewaxing, rehydrating in graded alcohols and antigen retrieval using citric acid buffer (0.1M, pH 6.0) by microwaving for 5 minutes on high power. After cooling to RT and three washes in PBS, endogenous peroxidase was quenched by 3% H<sub>2</sub>O<sub>2</sub>, followed by a protein block step (Protein Block serum free, ready to use, Dako®, Glostrup, Denmark) for 30 minutes at RT. The primary antibodies (1:100 for CK18 and CD34, 1:400 for  $\alpha$ SMA) and isotype controls at the same concentration (IgG<sub>1</sub>, IgG<sub>2a</sub>) (all from Dako) were incubated overnight at 4° C, sections were then washed and the Envision<sup>+</sup> System HRP secondary antibody (Mouse Envision Kit, Dako) applied for 30 minutes at RT, respectively as done previously (Ulrich et al. 2012) . Colour was developed with 3,3'-Diaminobenzidine (DAB).

#### Immunofluorescence

To determine the location of the SUSD2<sup>+</sup> cells and their estrogen receptor- $\alpha$  status, endometrial tissue was sequentially immunostained with anti-estrogen receptor- $\alpha$  (clone 6F11, Leica Microsystems, Australia) followed by phycoerythrin (PE)-conjugated anti-SUSD2 (BioLegend, USA) (Masuda et al. 2012). Frozen sections were cut at 8 $\mu$ m from OCT embedded tissues, thawed at RT, fixed in 4% paraformaldehyde for 10 minutes, washed in PBS and treated with 0.2% Triton X-100 in PBS for 15 minutes. Protein block (Dako ®) was applied for 30 minutes and sections were incubated with anti-estrogen receptor- $\alpha$  (1:100) in PBS for 2 hours at RT followed by secondary anti-mouse Alexa Fluor 488 (Life Technologies, Australia). Sections were washed three times in PBS, blocked with mouse IgG for 30 minutes, incubated with PE-anti-SUSD2 (1:100) for 2

hours at RT, washed three times with PBS, counterstained with Hoechst 33258 and imaged on a Nikon C1 confocal microscope.

#### Image analysis

Three consecutive sections per patient were photographed using the Leica® DMR Microscope at 5- 40x magnification and analysed using ImageJ software. Endometrial thickness was measured in 3 randomly located regions on each of 3 H&E sections using the software micrometer and the mean of the 9 measurements obtained for each of the samples examined. These were used to generate means for each of the experimental groups (pre- MP, n= 8; post- MP, n=10; post- MP+E<sub>2</sub>, n=10). Similarly, luminal and glandular epithelial height was measured on 3 different locations or gland profiles from 3 separate sections and the mean of 9 measurements from each sample was obtained and used to generate means for the same 3 groups for both luminal and glandular height.

To assess vascularity, the positive area for CD34 and  $\alpha$ SMA stained samples (n=8 for post- MP, n=10 for post- MP+E<sub>2</sub>) was analysed using Metamorph ® image analysis software (Ulrich et al. 2012). The percentage area was calculated as the positive area detected by Metamorph divided by the total endometrial area from 4 images obtained from 2 sections for each sample.

#### Endometrial stromal cell isolation and culture

Single cells were obtained as published previously (Chan et al. 2004, Schwab and Gargett 2007) from 8 pre-MP, 13 post- MP, and 8 post- MP+E<sub>2</sub> samples. Briefly, the endometrium was finely minced, then dissociated in 5% collagenase I (Worthington Biochemical Corporation, Lakewood, NJ, USA), 40  $\mu$ g/ml deoxyribonuclease type I (Worthington Biochemical Corporation), and DMEM/F-12 medium containing 15 mM HEPES buffer (Invitrogen, Auckland, New Zealand). Following dissociation, the cells were filtered

through a 40µm cell strainer (BD Biosciences, Durham, NC, USA) to obtain the stromal fraction. Stromal single cell suspensions were layered over Ficoll-Paque PLUS (GE healthcare Bio-Sciences AB, Uppsala, Sweden) and centrifuged to remove red blood cells. The endometrial stromal cells were used fresh or cultured for 1 passage in DMEM medium containing 10% fetal calf serum (Invitrogen), 5% antibiotics-antimycotics and 2 mM glutamine (Invitrogen) to obtain sufficient cell numbers for experiments. Cells were harvested by TrypLE Express (Life Technologies, Auckland, New Zealand) and eMSC were extracted using magnetic beads conjugated to the W5C5 antibody as described (Masuda et al. 2012). Briefly, cell suspensions (up to  $1 \times 10^7$  cells / 100 µl) were labelled with the phycoerythrin (PE)-conjugated W5C5 antibody (Biolegend, San Diego, CA, USA) in 0.5 % Fetal Calf Serum in PBS (Bead Medium) for 30 minutes at 4C followed by 3 washing steps in PBS, then incubated for 30 minutes in the dark with the anti-PE antibody-conjugated MACS MicroBeads (Miltenyi Biotec, Bergisch Gladbach, Germany). Up to  $1 \times 10^8$  cells / 500 µl were applied to MS columns (Miltenyi Biotec) in a magnetic field, followed by washing the column with 500µl Bead Medium three times. The W5C5<sup>-</sup> cells passed through the column, magnetically labelled W5C5<sup>+</sup> cells were retained. The columns were removed from the magnetic field and W5C5<sup>+</sup> cells were flushed out with 1 ml of Bead Medium. The W5C5<sup>+</sup> cells were assayed for cloning efficiency, and the remaining cells were cultured for one more passage for differentiation assays and phenotyping.

#### MSC functional properties

Clonogenicity was determined by seeding fresh and cultured W5C5<sup>+</sup> cells at clonal density (10 and 50 cells/cm<sup>2</sup>) on fibronectin-coated 100 mm tissue culture plates (BD Biosciences, San Jose, California, USA). Cells were incubated at 37°C in 5% CO<sub>2</sub> incubator for at least

2 weeks; DMEM<sup>+</sup> media supplemented with 10ng/ml human fibroblast growth factor 2 (FGF2; Millipore, Billerica, MA) (F-DMEM<sup>+</sup>) was changed weekly. Colonies were monitored microscopically to ensure they were derived from single cells. Large clones were harvested in cloning rings using TrypLE Express and subcloned twice, at seeding densities of 5-10 cells/cm<sup>2</sup> (Gargett et al. 2009).

For differentiation, P2 W5C5<sup>+</sup> cells were cultured in 4 well plates on coverslips at 1 X 10<sup>4</sup> cells/ cm<sup>2</sup> using specific induction media to obtain adipocytes, osteoblasts and chondrocytes and smooth muscle cells as previously described (Gargett et al. 2009).

Controls were cultured in DMEM<sup>+</sup> medium. After 4 weeks, adipogenic differentiation was evaluated by detection of lipid accumulation using oil red O staining; osteogenic differentiation was evaluated by histochemical detection of mineral calcium with Alkaline Phosphatase staining; myogenic differentiation was evaluated by detection of myofibroblasts and smooth muscle cells using alpha-smooth muscle staining as described previously (Rajaraman et al. 2013). For chondrogenic differentiation, 3-5x10<sup>5</sup> cells were cultured as a micromass pellet in a centrifuge tube in chondrogenic differentiation medium for 4 weeks. The pellet was fixed in 10% formalin, embedded in 4% Agar, processed through graded alcohols and xylene, then embedded in paraffin and cut into 5um sections.

Chondrocyte matrix production was visualized using Alcian blue staining and photographed using a Leica microscope at 10x magnification (Rajaraman et al. 2013) .

Differentiation capacity was scored as 0 (no differentiation), 1(< than 50% of the cells differentiated), and 2 (> 50% of the cells differentiated).

To determine the phenotype of the postmenopausal W5C5<sup>+</sup> cells, single-colour flow cytometry on P1 cells was used for known MSC surface phenotype markers (W5C5, CD140b (PDGFR $\beta$ ) (R&D Systems, Minneapolis, MN, USA), CD146 (CC9 culture supernatant, kind gift from Prof David Haylock, CSIRO, Clayton, Victoria, Australia),

CD29 (BD Biosciences, San Jose, California, USA), CD44 (BD Biosciences), CD73 (BD Biosciences), CD105 (BD Biosciences) as previously described (Masuda et al. 2012). Contaminating cells were analysed using haematopoietic (CD34; BD Biosciences) and myeloid cell makers (CD45; BD Biosciences). Controls were isotype matched IgG used at the same concentration as primary antibodies. A minimum of  $5 \times 10^4$  cells for controls and for surface markers of interest were incubated with individual antibodies in separate tubes for 30 min at 4C, followed by incubation with a PE-labelled anti-mouse IgG<sub>1</sub> secondary antibody (BD Biosciences). Cells were centrifuged and washed at 4C with Bench Medium after each incubation and examined in a MoFlo® XDP cell sorter (Beckman Coulter). The initial selection of cells for analysis was based on the forward versus side scatter profile. The percentage of positive cells was based on IgG control setting of gates to < 2% positive cells (Masuda et al. 2012) and analysed by Summit Software v5.2.

### Statistics

GraphPad Prism v5 was used for statistical analysis. Results are reported as median (range) or mean  $\pm$  SEM for each group. Since the data were normally distributed (D'Agostino & Pearson omnibus normality test), one way ANOVA and Holm- Sidak post hoc test for pairwise comparisons were undertaken for assessment of differences between groups. P values < 0.05 were considered as statistically significant.

## RESULTS

The mean age of the patients and other demographic parameters are shown in Table 1. The premenopausal women were significantly younger compared to the two postmenopausal groups ( $p < 0.01$ ). Median time since the last menstrual period was 13 (10-20) years for the E<sub>2</sub> treated women and 9 (1-15) for the non E<sub>2</sub> treated women ( $p < 0.05$ ).

Mean serum E<sub>2</sub> levels for women treated with E<sub>2</sub> were significantly higher than for postmenopausal women without E<sub>2</sub> treatment (Table 1).

#### Evidence of estrogen effects on estrogen-treated postmenopausal endometrium

To demonstrate that postmenopausal endometrium was responsive to E<sub>2</sub> (Progynova) treatment we examined endometrial thickness and endometrial epithelial cell height. To assess the thickness of the postmenopausal endometrium we used H+E stained sections (Figure 1 A-C). Pre- MP and post- MP+E<sub>2</sub> endometrium were significantly thicker than post-MP ( $p < 0.05$ ) (Figure 1D). Systemic estrogen levels also influence the height of endometrial epithelium (Gomes et al. 1997). In CK18 immunostained tissue, there was a trend towards higher luminal epithelium (LE) in the premenopausal women compared to the postmenopausal groups, although this was not significant ( $p > 0.05$ ) (Figure 1E). Glandular epithelial (GE) height was measured in the basalis layer of pre-MP endometrium since there was no clearly distinguishable functionalis layer in the post- MP groups and previous studies have shown that postmenopausal epithelium has a similar gene expression profile as the basalis of postmenopausal epithelium (Nguyen et al. 2012). GE height was similar in the menopausal tissues and there was no difference between pre- MP and postmenopausal women treated with or without E<sub>2</sub> (Figure 1F). There was also no significant difference between the GE height of basal glands and those adjacent to the LE (results not shown).

#### Quantification SUSD2/W5C5<sup>+</sup> cells in postmenopausal endometrium

We next measured the proportion of endometrial stromal cells that expressed the eMSC marker, SUSD2 in freshly dissociated samples. The mean stromal cell yield from endometrial tissue of estrogen treated women was  $1.6 \times 10^6 \pm 4.8 \times 10^5$  (n=4) and  $0.7 \times 10^5$

$\pm 0.3 \times 10^5$  (n=4) for the untreated women per 1 gram of tissue. Insufficient cell numbers were obtained from 3 postmenopausal samples without estrogen treatment after the isolation procedure and could not be used for the further experiments. To determine the percentage of W5C5<sup>+</sup> cells present in stromal cells cultured from PostMP endometrium, cells at passage one (P1) were harvested by trypsin, labelled with W5C5 antibodies and passed through a magnetic bead column to select the W5C5<sup>+</sup> cells, which were then counted. In post- MP+ E<sub>2</sub> P1 cultures,  $3.7 \pm 1.8\%$  (n=7) of the cells were W5C5<sup>+</sup> cells which compares with  $7.7 \pm 6.3\%$  (n=8) in post- MP cultures (p=0.69).

#### Surface phenotype of human postmenopausal endometrial W5C5<sup>+</sup> cells

Cultured W5C5<sup>+</sup> cells were analysed for expression of typical MSC phenotypic markers (Dominici et al. 2006) using flow cytometry (Figure 2A). The postmenopausal W5C5<sup>+</sup> cells expressed MSC markers as shown in Table 2 without any significant differences between the two postmenopausal groups.

#### Multi-lineage differentiation of postmenopausal endometrial W5C5<sup>+</sup> cells

We next examined whether the postmenopausal W5C5<sup>+</sup> cells could undergo multilineage differentiation, a key MSC property (Dominici et al. 2006). W5C5<sup>+</sup> cells derived from postmenopausal endometrium from women treated with (n= 6) or without estrogen (n= 6) differentiated into adipocytes to a similar extent when cultured in adipogenic induction medium (Figure 2B, Table 3). Similarly, W5C5<sup>+</sup> cells derived from women treated with and without E<sub>2</sub> differentiated into chondrocytes producing a cartilaginous-like Alcian Blue stained matrix (Figure 2C). W5C5<sup>+</sup> cells cultured in osteogenic induction medium differentiated into osteocytes, shown by alkaline phosphatase reactivity (Figure 2D). Similarly W5C5<sup>+</sup> cells cultured in myogenic induction medium differentiated into  $\alpha$ -SMA-

expressing smooth muscle cells (Figure 2E). There was no difference in the capacity of W5C5<sup>+</sup> cells obtained from postMP or postMP+E<sub>2</sub> endometrium to undergo multilineage differentiation (Table 3).

Clonogenicity and serial cloning of postmenopausal endometrial W5C5<sup>+</sup> cells

MSC are clonogenic and we therefore examined the clonogenicity of P1 W5C5<sup>+</sup> cells derived from pre- and postmenopausal endometrium (Figure 3A, B). The mean cloning efficiency for W5C5<sup>+</sup> cells from Post- MP+ E<sub>2</sub> was  $3.4 \pm 0.9 \%$ , n=6), and comparable to Post- MP ( $3.7 \pm 0.4 \%$ , n=8) but statistically lower than P1 Pre-MP ( $8.83 \pm 0.4$ , n=6) (Figure 3C). The clonogenicity of fresh (P0) pre- MP and post-MP+ E<sub>2</sub> was similar with cloning efficiencies of  $3.8 \pm 0.9 \%$  vs  $1.8 \pm 0.1 \%$ , respectively. Both Post-MP and Post-MP+E<sub>2</sub> W5C5<sup>+</sup> cells underwent substantial self renewal by undergoing serial cloning at least three times (Figure 3D). The cloning efficiency of secondary (S1) and tertiary (S2) clones was significantly higher in premenopausal compared to postmenopausal samples as shown in Figure 3D. The cloning efficiency of P1 pre-MP and post-MP+ E<sub>2</sub> W5C5<sup>+</sup> was double that of freshly isolated Pre-MP cells (results not shown).

Location of SUSD2/W5C5 in postmenopausal endometrium-

Since premenopausal eMSC reside in a perivascular location in both functionalis and basalis (Schwab and Gargett 2007, Masuda et al. 2012), we investigated the localization of the W5C5<sup>+</sup> cells in postmenopausal sections by dual- colour immunofluorescence.

Postmenopausal W5C5<sup>+</sup> cells were similarly identified in a perivascular location in both small and large vessels throughout the endometrium (Figure 4A, B). Since estrogen drives endometrial growth in postmenopausal women we examined whether they expressed estrogen receptor-  $\alpha$  (ER $\alpha$ ). None of the W5C5<sup>+</sup> cells expressed ER $\alpha$ , even though ER $\alpha$

stained some glandular epithelial and stromal cells in both Post- MP and Post- MP+ E<sub>2</sub>. We then looked at the effect of estrogen treatment on vessel density in postmenopausal endometrium. We stained the endometrium with CD34 to mark the endothelial cells (Figure 5A, B) and detect both capillaries and larger vessels, and  $\alpha$ SMA to distinguish larger vessels from capillaries (Figure 5D, E). We found no significant differences between the postmenopausal groups with or without estrogen treatment (Figure 5C, F).

## **DISCUSSION**

In this study we report the first characterisation of an eMSC population in postmenopausal endometrium from women treated with or without estrogen for 8 weeks. We show that postmenopausal endometrium, whether atrophic from low circulating estrogen levels or regenerated from short term systemic estrogen treatment, contains a small population of stromal cells with MSC properties. These postmenopausal eMSC can be obtained by magnetic bead sorting with the W5C5/SUSD2 antibody used to purify eMSC from premenopausal endometrium. We also demonstrated that postmenopausal eMSC can be obtained from a biopsy as is the case for premenopausal eMSC, particularly after 6-8 weeks oral E<sub>2</sub> treatment. As the endometrium is an easily accessible source of MSC, obtainable with minimum morbidity for potential use in future clinical applications, it is important to know whether postmenopausal women can access their eMSC for autologous cell-based therapies provided they have an intact uterus.

The eMSC derived from postmenopausal endometrium fulfil the defining MSC criteria: clonogenicity, surface phenotype and multipotency, suggesting that eMSC are retained in the endometrium following menopause. The postmenopausal eMSC also have comparable properties to premenopausal eMSC with respect to self renewal in vitro and SUSD2 expression. We demonstrated that the postmenopausal eMSC derived from women treated

with or without E<sub>2</sub> had comparable clonogenicity, albeit at lower levels compared to that of cultured premenopausal eMSC. Due to low cell yields, we could only determine clonogenicity in P1 W5C5<sup>+</sup> cells in most samples of untreated post-MP endometrium. The clonogenicity (cloning efficiency) in P1 W5C5<sup>+</sup> cells was double that of fresh (P0) W5C5<sup>+</sup> cells from pre- MP and post-MP+ E<sub>2</sub> indicating selection for clonogenic cells in primary cultures.(Masuda et al. 2012).The surface phenotype of W5C5<sup>+</sup> cells was also similar between premenopausal and the two postmenopausal groups suggesting that eMSC remain in postmenopausal endometrium and may be responsible for E<sub>2</sub> mediated regeneration of the stromal vascular components. The eMSC of either estrogen-treated or non-treated postmenopausal endometrium differentiated to a similar degree, but less than for premenopausal eMSC. This together with the lower cloning efficiencies and self renewal properties suggests that postmenopausal eMSC may lose some potency as they age, similar to MSC from other sources such as bone marrow. A tenfold loss of bmMSC activity occurs during the first 10 years of life and continues to decrease over the lifespan (Haynesworth et al. 1993). Whether eMSC potency diminishes to the same extent as bmMSC over the lifespan is unknown.

Short term estrogen treatment appears to be effective for obtaining adequate yields of endometrial cells because post-MP endometrium rapidly regenerated to more than double its original thickness. As demonstrated previously (Ettinger et al. 1997), we found a thicker endometrium in the estradiol-treated women compared to postmenopausal controls. The percentage of W5C5<sup>+</sup> after magnetic bead selection was similar in the endometrium of E<sub>2</sub> treated and non-treated women suggesting that a defined pool of eMSC is maintained per unit volume of tissue. However the increased absolute volume of endometrial tissue in E<sub>2</sub> treated women allows for greater yields of eMSC, an important consideration for future cell-based therapies. The high degree of variability in the yield of W5C5<sup>+</sup> cells in post-MP

compared to post-MP+E<sub>2</sub> samples indicates the difficulty in harvesting cells from non-treated women and also suggests that dietary xenoestrogens and other undocumented supplements could also have an influence. Alternatively, there may be a dilution effect of W5C5<sup>+</sup> cells in regenerating endometrial “functionalis” after E<sub>2</sub> treatment, perhaps suggesting that the basalis layer may be the main source of MSC responsible for endometrial regeneration.

Small and large vessel profiles are present in similar numbers in the endometrium of postmenopausal women treated with and without E<sub>2</sub> suggesting that short term estrogen therapy does not remodel the vasculature, but provides the regenerating “functionalis” layer with a similar degree of vascularity as atrophic endometrium. Our study, also confirms a previously reported lack of difference in vascularity observed between hormone-treated and non-treated premenopausal endometrium as determined by semiquantitative CD34 immunohistochemistry (Hickey et al. 1996). This study also reported a similar vascularity between atrophied and cycling endometrium.

The luminal epithelial height did not differ between the two postmenopausal groups in contrast to previous findings (Gomes et al. 1997). This could be due to the shorter E<sub>2</sub> treatment time in our study, 6-8 weeks versus three months in the Gomes et al study, possibly not long enough to remodel the surface epithelium. The glandular epithelial height did not show significant differences either and was measured in the basalis layer of premenopausal women. These findings suggest that short term E<sub>2</sub> treatment has little impact on the endometrial epithelium, suggesting that this approach is safe for those women who are not contraindicated for taking E<sub>2</sub>.

Hormone replacement therapy (HRT) is offered to postmenopausal women to relieve menopausal symptoms (Pines et al. 2012), with estrogen replacement therapy confined to hysterectomised women. Short term oral E<sub>2</sub> rapidly increases endometrial growth

suggesting that an approximately 8 week treatment is sufficient to obtain a reasonably thick endometrium (Ettinger et al. 1997). Long term (>12 months) unopposed estrogen given to postmenopausal women may result in endometrial hyperplasia or even endometrial malignancies (Furness et al. 2012), but this is unlikely in an 8 week treatment for harvesting eMSC. It is not quite clear how E<sub>2</sub> regenerates the endometrium since W5C5+ perivascular cells did not express ER $\alpha$ , a finding which agrees with studies in mouse endometrium where epithelial and stromal label retaining cells (marker of slow cycling stem/progenitor cells) are also ER $\alpha$  negative do not express estrogen receptors (Chan et al. 2012). It was hypothesized that estrogen-induced endometrial growth is mediated by stem/progenitor cells indirectly mediated via estrogen receptors on their neighbouring niche cells (Gargett 2007). Our study also showed that eMSC survived in the absence of estrogen and do not require E<sub>2</sub> for trophic support as they were present in similar proportion in untreated atrophic and E<sub>2</sub> treated post- MP endometrium. For this study we only supplemented women without contraindicated medical conditions with 2 mg Progynova daily for 6- 8 weeks and found no associated adverse effects. The participants were closely monitored. An initial dose of one mg Progynova was insufficient to increase endometrial thickness to yield significant numbers of cells (unpublished observation).

Premenopausal endometrium is a highly regenerative tissue, undergoing shedding and regeneration on a 4 weekly basis during the menstrual cycle generating up to 10 mm of new mucosa during each proliferative stage (Gargett et al. 2012). Endometrium is one of the few tissues where MSC can be obtained without anaesthesia, invasive and painful interventions, particularly in parous women. MSC from the endometrium provide a readily accessible alternate source of MSC for use in cell-based therapies as there are no ethical

issues compared to embryonic stem cells (Ulrich et al. 2013). It appears that eMSC reside in the endometrium after a woman's fertile years have ceased. We show for the first time that these eMSC can be readily harvested from postmenopausal women using an office based biopsy, irrespective of whether they are or are not particularly if they are pre-treated with estrogen to regenerate the endometrium, although yields are greater in E2-treated women. The human endometrium is therefore a promising source of MSC independent of a woman's age.

#### **Declaration of Author's roles**

DU: participation in study design, execution, analysis, manuscript writing and critical discussion

KST: execution, analysis and critical discussion

KS: execution, analysis and critical discussion

AC: execution, analysis and critical discussion

AR: participation in study design, manuscript editing and critical discussion

CEG: conception and participation in study design, manuscript editing and critical discussion

#### **ACKNOWLEDGMENTS**

The authors acknowledge Liz Fitzgerald for managing the clinical trial, Yao Han and Pamela Mammers for collection of the tissue.

#### **FUNDING**

This study was supported by the National Health and Medical Research Council (NHMRC) of Australia grant (1021126) (CEG, AR) and Senior Research Fellowship (1042298) (CEG), Australian Gynaecological Endoscopic Society grant (AR) and Victorian Government's Operational Infrastructure Support Program.

#### **CONFLICT OF INTEREST**

The authors have nothing to declare.

## FIGURE LEGENDS

**Figure 1** Effect of oral estrogen on postmenopausal endometrium compared with premenopausal endometrium.

H+E stained endometrium from hysterectomy tissues in (A) pre- MP, (B) post- MP, (C) post- MP+E<sub>2</sub>. Dotted line indicates border between endometrium and myometrium. Scale bar 200  $\mu$ m. (D) endometrial thickness, (E) luminal epithelial (LE) height, and (F) glandular epithelial (GE) height measured in the basalis layer of Pre-MP endometrium .

Bars are mean  $\pm$  SEM of n =6 samples/group. \*P < 0.05.

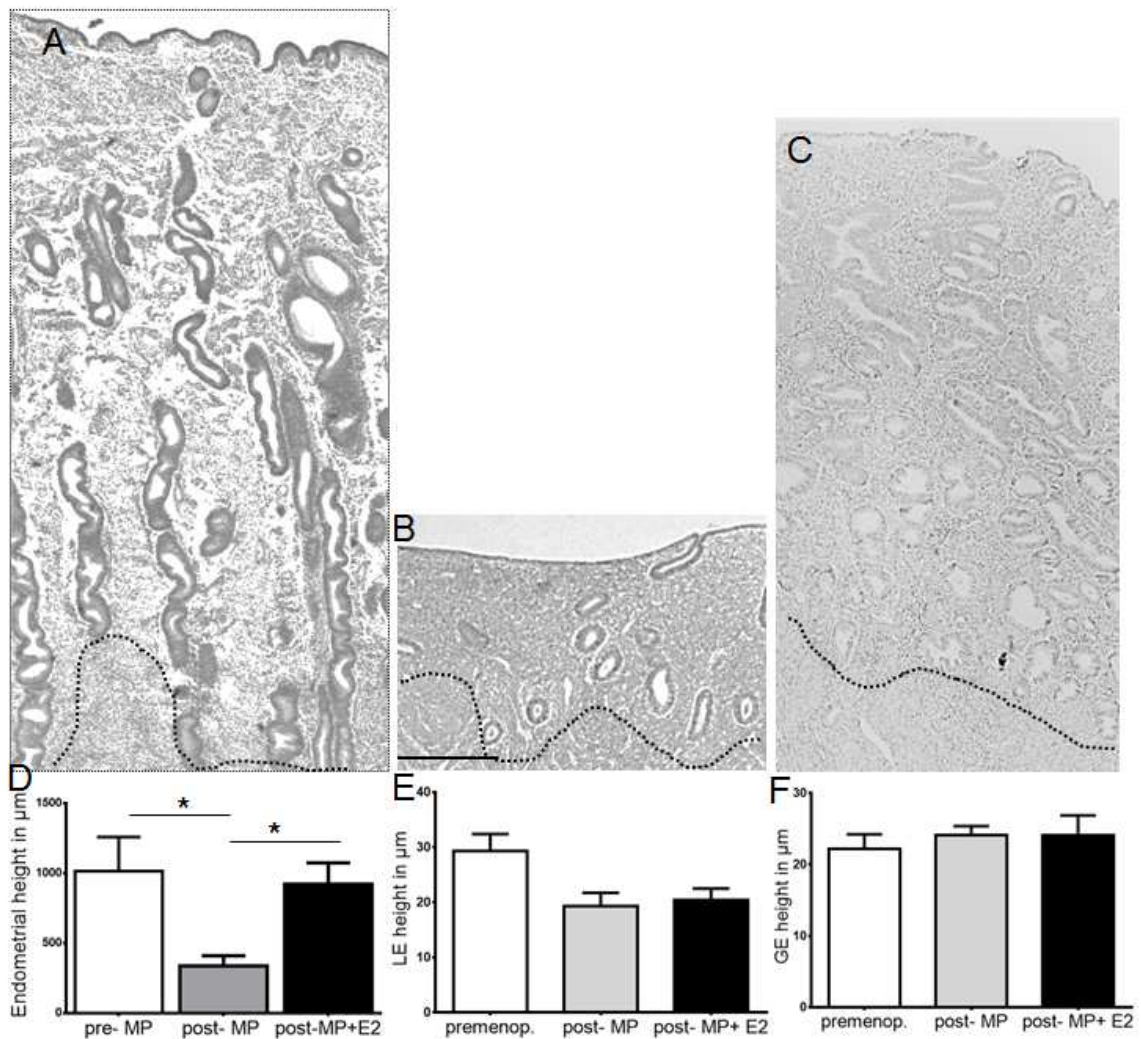


**Figure 2**

Properties of postmenopausal eMSC: (A) surface phenotype showing representative flow cytometric analysis of P1 cultured postmenopausal W5C5<sup>+</sup> cells from a single representative sample from a woman treated with (+E<sub>2</sub>) or without (-E<sub>2</sub>) oral estrogen for 6-8 weeks. Aggregate data is shown in Table 2. Multilineage differentiation of P1 W5C5<sup>+</sup> cells from post- MP+E<sub>2</sub> endometrium in various induction media for 4 weeks (B) adipocytes stained with Oil Red O, (C) chondrocytes (red nuclei) showing production of Alcian Blue stained cartilage-like matrix, (D) alkaline phosphatase positive osteoblasts and (E) smooth muscle cells immunostained with  $\alpha$ -smooth muscle actin. Insets are stained control cultures. Scale bars; B, D and E 100  $\mu$ m; C 25 $\mu$ m.

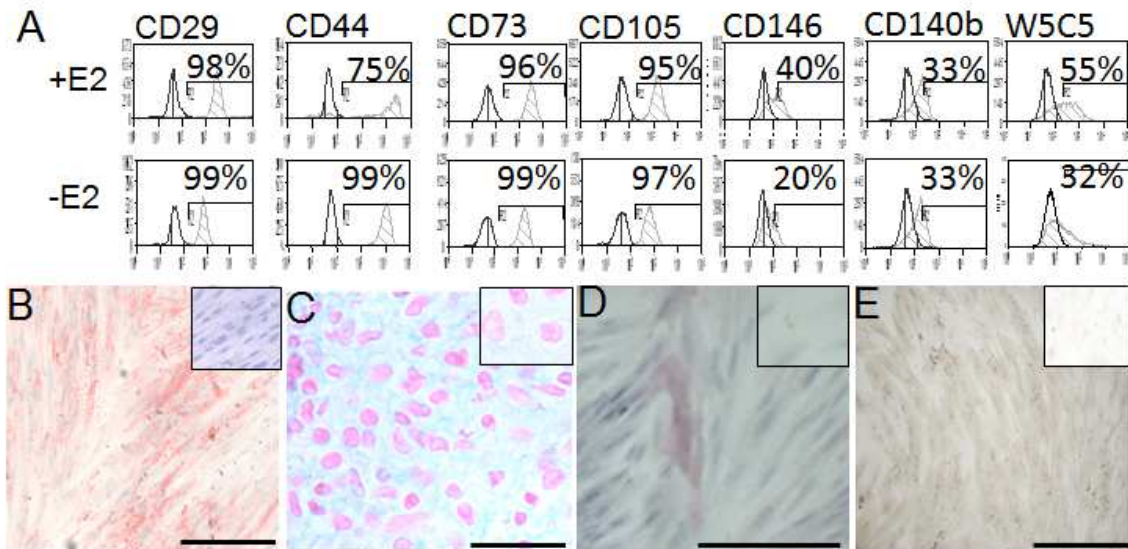


### Figure 3

Cloning efficiency and serial cloning analysis for measuring clonogenicity and self-renewal of human endometrial pre- and postmenopausal eMSC. Representative cloning plates of (A) post-MP and (B) post-MP+E<sub>2</sub> W5C5<sup>+</sup> cells. Arrows show individual clones removed for serial cloning. Clonogenicity of (C) P1 W5C5<sup>+</sup> cells from pre-MP, post-MP and post-MP+ E<sub>2</sub> samples and (D) at each round of serial cloning. Results are means  $\pm$  SEM (n=6/group). \*\*Significant difference between pre-MP and post-MP (P < 0.01) and post-MP+E<sub>2</sub> (\*\* P < 0.01). \*P < 0.05, \*\*\*P<0.001. S0, first cloning; S1, first serial cloning (secondary clones); S2, second serial cloning (tertiary clones).

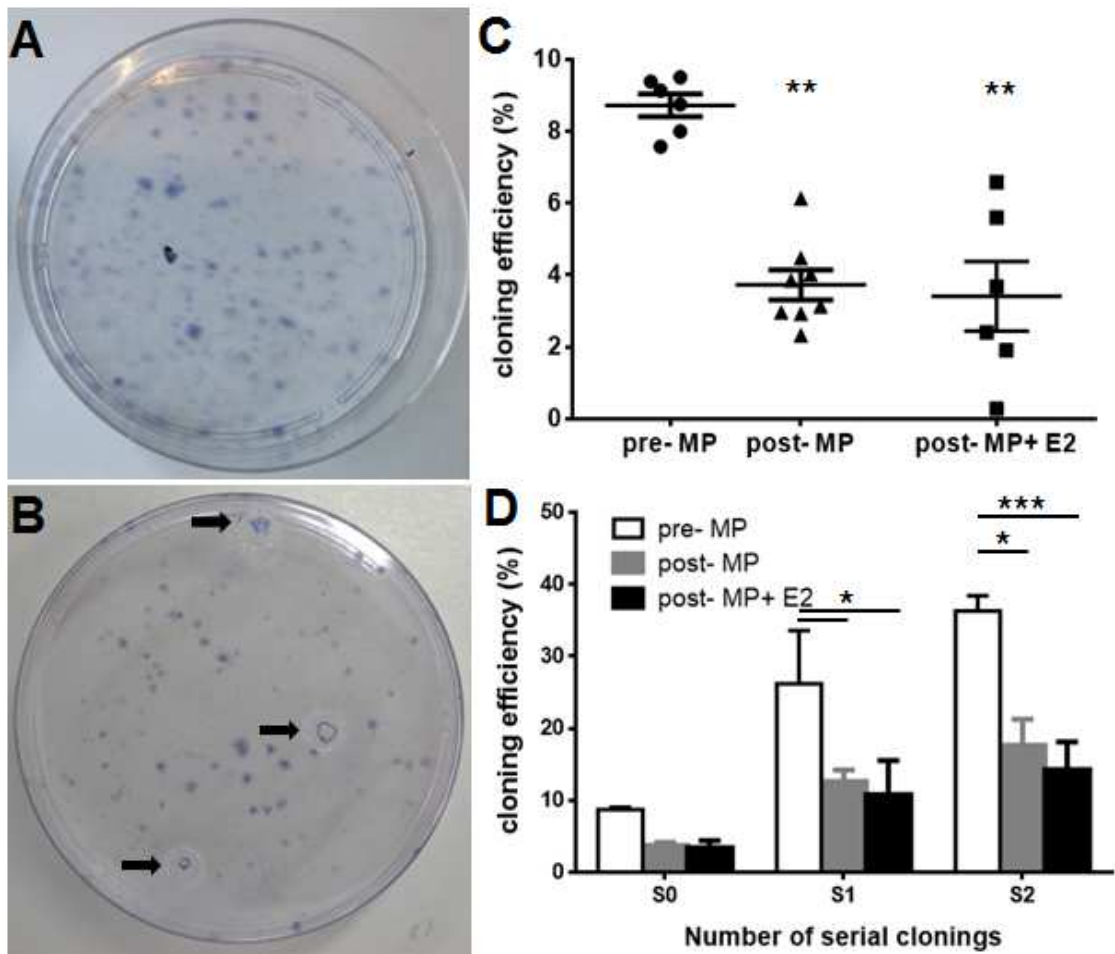


**Figure 4**

W5C5<sup>+</sup> perivascular cells do not express ER $\alpha$ . Dual colour immunofluorescence of (A) post- MP and (B) post- MP+E<sub>2</sub> endometrial tissue. W5C5<sup>+</sup> cells around blood vessels fluoresce red, nuclei ER $\alpha$  fluoresces green. Scale bar 20  $\mu$ m. Arrow indicates representative perivascular W5C5<sup>+</sup> cells.

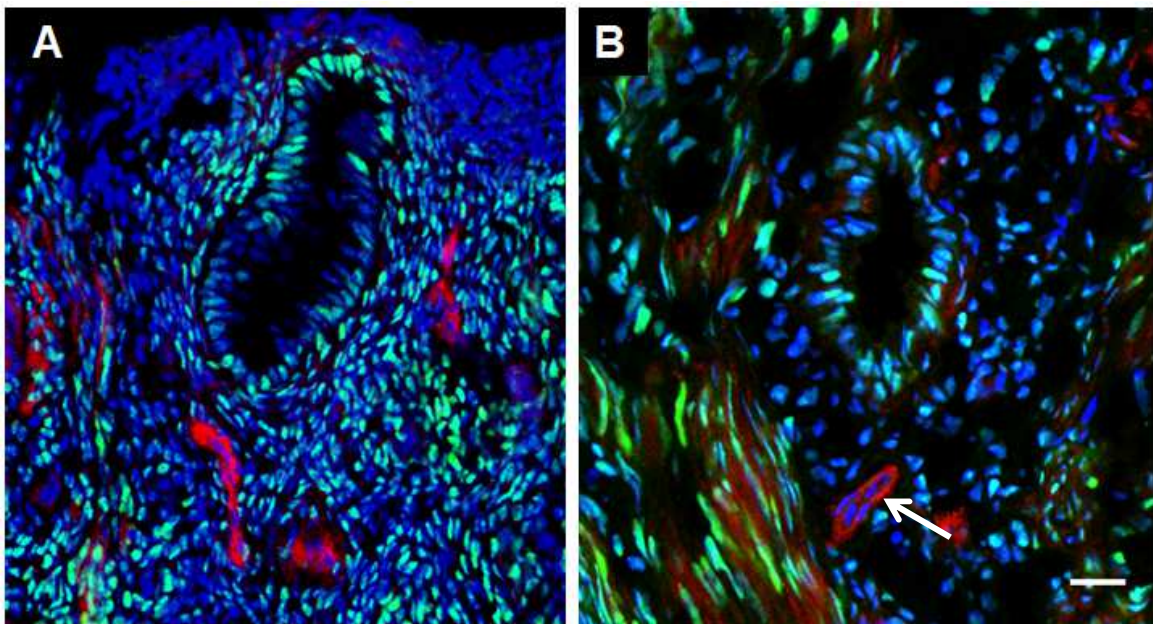


### Figure 5

Vessel profiles in postmenopausal endometrium. CD34 immunostained (A) post- MP and (B) post- MP+E<sub>2</sub> endometrium with (C) immunoquantification showing % of CD34 positive area. Dotted lines show endometrial myometrial border. Alpha-SMA immunostained (D) post- MP, and (E) post- MP+E<sub>2</sub> endometrium counterstained with haematoxylin, with (F) immunoquantification showing %  $\alpha$ SMA positive area. Scale bar in A+B 100  $\mu$ m, D+E 200  $\mu$ m. Bars are means  $\pm$  SEM of n= 8 post-MP and n= 10 post-MP+E<sub>2</sub>.

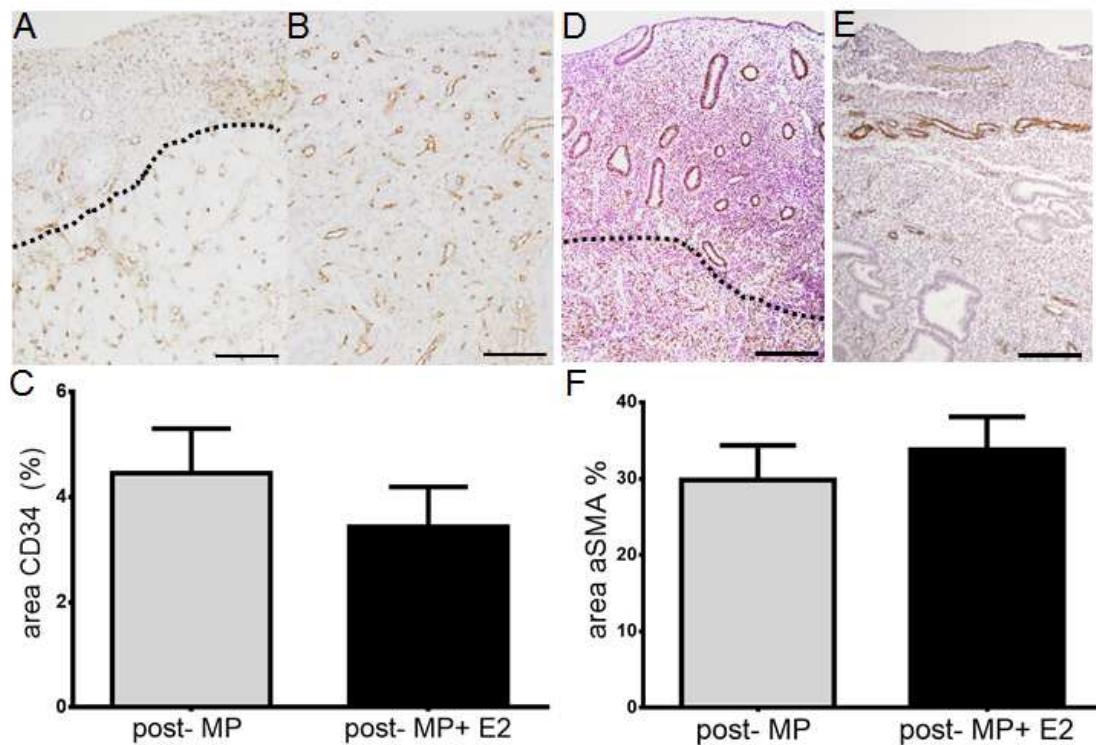


**Table 1.** Patient characteristics

	Pre- MP (n=17)	post- MP (n=19)	post- MP+E <sub>2</sub> (n=15)	p-value
Age (yr)	43±3	60±1	64±3	P < 0.01
BMI (kg/m <sup>2</sup> )	26.4 ± 1.6	25.4 ± 2.0	25.4 ± 4.3	NS
POP-Q stage*	1.2 ± 0.2	1.6 ± 0.2	1.7 ± 0.2	NS
Serum E <sub>2</sub> (pmol/L)	n.d.	88± 9.6	273± 58.2	P < 0.05

Data are presented as mean (± SEM). Pre- MP, premenopausal, post- MP, postmenopausal, post- MP+ E<sub>2</sub>, postmenopausal with E<sub>2</sub> treatment, E<sub>2</sub>, estrogen. NS, not significant. \* reference for POP-Q (Bump et al. 1996). N.D., not done.

**Table 2** MSC surface marker characteristics of P1 postmenopausal samples.

	Post- MP (n=9)	Post- MP+ E <sub>2</sub> (n=8)	p- value
CD29	98.7 ± 0.26	96.0 ± 1.6	Ns
CD44	94.5 ± 3.5	92.8 ± 2.8	Ns
CD73	85.8 ± 12.0	93.3 ± 2.6	Ns
CD105	73.3 ± 16.3	83.7 ± 7.4	Ns
CD146	27.2 ± 5.6	42.0 ± 5.9	Ns
CD140b	32.0 ± 14.1	39.8 ± 14.5	Ns
W5C5	35.4 ± 27.2	53.1 ± 27.2	Ns
CD34	0.8 ± 0.8	0.1 ± 0.1	Ns
CD45	6.1 ± 2.0	1.3 ± 0.6	0.02

Data are from single colour flow cytometric analysis and presented as mean ± SEM. Ns, not significant

**Table 3** Differentiation score of P1 postmenopausal samples cultured in mesodermal induction media.

	Post- MP (n=6)	Post- MP+ E <sub>2</sub> (n=6)	p- value
Adipogenic	1.2 ± 0.3	1.3 ± 0.2	Ns
Chondrogenic	1.3 ± 0.3	1.8 ± 0.2	Ns
Myogenic	1.6 ± 0.2	2.0 ± 0.0	Ns
Osteogenic	1.6 ± 0.2	1.8 ± 0.2	Ns

Data are presented as mean ± SEM. Ns, not significant

Score; 0 no differentiation; 1, <50% of the cells showed differentiation; 2, >50% of the cells showed differentiation.

## CHAPTER 4

### A Tissue Engineering Construct for POP repair

TE uses the combination of cells and materials to generate an implantable construct which aims to restore, maintain, or improve tissue function or a whole organ (Langer and Vacanti 1993). As POP occurs through damage to the vaginal wall fascia, injury to the pelvic musculature and ligament rupture, a new treatment option using a TE approach is needed to repair and replace the damaged tissue. Alternatively a TE approach using eMSC may improve tissue integration and modify the foreign body reaction to new materials. A large number of studies have shown beneficial effects of TE approaches for other injuries. No TE attempts have been undertaken for POP repair at the commencement of this thesis. There were only trials to generate a vaginal replacement for congenital disorders (De Filippo et al. 2008).

In this chapter I developed a preclinical animal model to test TE constructs, comprising eMSC and our novel materials (Chapter 2) in an immunocompromised nude rat model of wound repair. This model was designed to purely examine the effect of eMSC on fascial repair in contrast to the abdominal hernia model where the pressure of the abdominal organs could influence mesh properties. The W5C5<sup>+</sup> cells were tested for MSC properties using cloning efficiency, differentiation assays and phenotype analysis (FACS). I thank Ker Sin Tan for assisting in the evaluation of the eMSC stem cell properties. Prior to implanting the TE construct, I tested various cell labelling techniques to identify the label with the least adverse effects on cell viability and also remained in the cells for a prolonged period in culture. I surgically implanted the meshes with the labelled eMSC or without (control) into nude rats and evaluated a number of outcomes. Cell survival was determined using flow cytometric analysis. Vascularisation, inflammation and collagen deposition were evaluated using immunohistochemistry and image analysis I had developed for aim 1 (Chapter 2). In this study I included hydroxyproline assays and SDS PAGE gel analysis to quantify the amount of collagen and the collagen type I/III ratio as developed by our collaborators at CSIRO. I thank Dr. Kai Su for developing and optimizing these assays and protocols and for performing large parts of these experiments. I also thank Dr. Sharon Edwards for performing the mechanical testing and analysis to evaluate the mechanical properties of the meshes after explantation.

**Declaration for Thesis Chapter 4**

**Declaration by candidate**

In the case of Chapter 4, the nature and extent of my contribution to the work was the following:

<b>Nature of contribution</b>	<b>Extent of contribution (%)</b>
Study design, Animal experiments, Tissue collection, Tissue processing, Tissue staining, Image analysis, Statistical analysis, Data interpretation, Paper writing	75

The following co-authors contributed to the work. Co-authors who are students at Monash University must also indicate the extent of their contribution in percentage terms:

<b>Name</b>	<b>Nature of contribution</b>	<b>Extent of contribution (%) for student co-authors only</b>
<b>Dr. Sharon L. Edwards</b>	Biomechanical testing, Data analysis, Data interpretation	
<b>Dr. Kai Su</b>	Biochemical testing	
<b>Ker Sin Tan</b>	Animal experiments, Tissue collection, Tissue processing, Tissue staining	
<b>Jacinta F. White</b>	Tissue staining, Image analysis	
<b>John AM. Ramshaw</b>	Data interpretation	
<b>Dr. Camden Lo</b>	Image analysis	
<b>Dr. Anna Rosamilia</b>	Data interpretation	
<b>Dr. Jerome A. Werkmeister</b>	Study design, Data analysis, Data interpretation, Paper writing	
<b>Dr. Caroline E. Gargett</b>	Study design, Data analysis, Data interpretation, paper writing	

**Candidate's Signature**

	<b>Date</b> 07.03.2014
--	---------------------------

**Declaration by co-authors**

The undersigned hereby certify that:

- (1) the above declaration correctly reflects the nature and extent of the candidate's contribution to this work, and the nature of the contribution of each of the co-authors.
- (2) they meet the criteria for authorship in that they have participated in the conception, execution, or interpretation, of at least that part of the publication in their field of expertise;
- (3) they take public responsibility for their part of the publication, except for the responsible author who accepts overall responsibility for the publication;
- (4) there are no other authors of the publication according to these criteria;
- (5) potential conflicts of interest have been disclosed to (a) granting bodies, (b) the editor or publisher of journals or other publications, and (c) the head of the responsible academic unit; and
- (6) the original data are stored at the following location(s) and will be held for at least five years from the date indicated below:

**Location(s)**

**MIMR- PHI Institute of Medical Research, Level 3, Monash University, Melbourne, VIC, Australia;  
CSIRO Materials Science Engineering, Clayton, Melbourne, VIC, Australia**

	Name	Date
<b>Signature 1</b>		20/12/13
<b>Signature 2</b>		20/12/13
<b>Signature 3</b>		06/01/14
<b>Signature 4</b>		20/12/13
<b>Signature 5</b>		20/12/13
<b>Signature 6</b>		20/12/13
<b>Signature 7</b>		20/12/13
<b>Signature 8</b>		20/12/13
<b>Signature 9</b>		20/12/13

## Human Endometrial Mesenchymal Stem Cells Modulate the Tissue Response and Mechanical Behavior of Polyamide Mesh Implants for Pelvic Organ Prolapse Repair

Daniela Ulrich, MD,<sup>1,2,\*</sup> Sharon Lee Edwards, PhD,<sup>3</sup> Kai Su, PhD,<sup>3</sup> Ker Sin Tan, MSc,<sup>1</sup> Jacinta F. White, BAppSci,<sup>3</sup> John A.M. Ramshaw, PhD,<sup>3</sup> Camden Lo, PhD,<sup>1</sup> Anna Rosamilia, MD, PhD,<sup>2</sup> Jerome A. Werkmeister, PhD,<sup>3,†</sup> and Caroline E. Gargett, PhD<sup>1,2,†</sup>

**Background:** Pelvic organ prolapse (POP) is defined as the descent of one or more of the pelvic structures into the vagina and includes uterine, vaginal vault, and anterior or posterior vaginal wall prolapse. The treatment of POP may include implantation of a synthetic mesh. However, the long-term benefit of mesh surgery is controversial due to complications such as mesh exposure or pain. The aim of this study was to use a tissue engineering (TE) approach to assess the *in vivo* biological and biomechanical behavior of a new gelatin/polyamide mesh, seeded with a novel source of mesenchymal stem cells in a subcutaneous rat model of wound repair.

**Methods:** W5C5-enriched human endometrial mesenchymal stem cells (eMSC) were seeded onto meshes (gelatin-coated polyamide knit) at 100,000 cells/cm<sup>2</sup>. Meshes, with or without cells were subcutaneously implanted dorsally in immunocompromised rats for 7, 30, 60, and 90 days. Flow cytometry was used to detect DiO labeled cells after explantation. Immunohistochemical assessment of foreign body reaction and tissue integration were conducted. Total collagen and the levels of collagens type III and type I were determined. Uniaxial tensiometry was performed on explanted meshes, originally seeded with and without cells, at days 7 and 90.

**Results:** Implanted meshes were well tolerated, with labeled cells detected on the mesh up to 14 days postimplantation. Meshes with cells promoted significantly more neovascularization at 7 days ( $p < 0.05$ ) and attracted fewer macrophages at 90 days ( $p < 0.05$ ). Similarly, leukocyte infiltration was significantly lower in the cell-seeded meshes at 90 days ( $p < 0.05$ ). Meshes with cells were generally less stiff than those without cells, after 7 and 90 days implantation.

**Conclusion:** The TE approach used in this study significantly reduced the number of inflammatory cells around the implanted mesh and promoted neovascularization. Seeding with eMSC exerts an anti-inflammatory effect and promotes wound repair with new tissue growth and minimal fibrosis, and produces mesh with greater extensibility. Cell seeding onto polyamide/gelatin mesh improves mesh biocompatibility and may be an alternative option for future treatment of POP.

### Introduction

PELVIC ORGAN PROLAPSE (POP) is defined as the descent of one or more of the anterior or posterior vaginal wall, the uterus, or the apex of the vagina after hysterectomy.<sup>1</sup> POP commonly occurs several years after childbirth, but aging and obesity also contribute to the pathophysiology.<sup>2</sup> Almost one in four women in the United States suffers from one or more symptoms of POP, with urinary incontinence the most common.<sup>3</sup> Other symptoms include sexual dysfunction, discomfort due to tissue protrusion, back pain, and voiding or defecatory difficulty. Symptoms range in severity and

depend, in part, on the degree and type of prolapse. While less severe stages of POP can be managed conservatively, more severe stages, or symptoms affecting the patient's quality of life, often require surgical repair. Due to reports of the high objective failure rate of native tissue surgery reconstruction (up to 35% in the long term), synthetic meshes were introduced to augment POP surgery, with better anatomical success rates in the long term.<sup>4,5</sup> Polypropylene (PP) meshes are the most commonly used meshes and are knitted from monofilaments to produce a relatively large pore size for allowing tissue ingrowth.<sup>6</sup> These current therapies provide support but do not replace lost or damaged tissues of

<sup>1</sup>The Ritchie Centre, Monash Institute of Medical Research, Clayton, Victoria, Australia.

<sup>2</sup>Department of Obstetrics and Gynaecology, Monash Medical Centre, Monash University, Clayton, Victoria, Australia.

<sup>3</sup>Materials Science Engineering, CSIRO, Clayton, Victoria, Australia.

\*Current affiliation: Department of Obstetrics and Gynaecology, Medical University of Graz, Austria.

†These authors are equal senior authors.

the pelvic support structures including the pelvic floor musculature, endopelvic fascia, and ligaments.<sup>7</sup> A recent FDA report warned of the complications associated with the use of PP mesh for vaginal surgery.<sup>8,9</sup> Implanted meshes initiate an inflammatory reaction involving cells of the innate immune system, which results in the initial production of neotissue. However, the new tissue develops into scar tissue, which is weaker and more rigid than normal healthy tissue.<sup>10,11</sup> This may translate into significant long-term complications of varying severity including mesh contraction, pain, and vaginal exposure or rarely erosion to adjacent viscera; these complications have been reported in up to 29% of cases.<sup>12</sup>

Tissue engineering (TE) approaches have been used in different medical areas to improve long-term outcomes of surgical interventions. Bone marrow mesenchymal stem cells (bmMSC) are believed to regulate the repair process in injured tissue sites by interacting with essential endogenous cells involved in the healing process; fibroblasts, endothelial, and epithelial cells.<sup>13</sup> Mouse muscle-derived stem cells cultured on porcine small intestinal submucosa (SIS) collagen (Cook, Biotech<sup>®</sup>), and implanted as a TE construct into rat vaginal defects, stimulated vaginal tissue repair by promoting epithelial regeneration and reducing fibrosis.<sup>14</sup> Clinically, SIS has been trialed for POP restoration with very limited success compared with conventional synthetic mesh types.<sup>15</sup> More recently, it was shown that Vicryl<sup>®</sup> hernia meshes seeded with bmMSC were associated with less adhesions in a rat abdominal hernia model compared with cell-free hernia meshes.<sup>16</sup> This study also found that mesh pore size played a major role in cell attachment and proliferation, with mesh pores larger than 3 mm prohibiting cell attachment.<sup>16</sup> We have identified and characterized human endometrial mesenchymal stem cells (eMSC) as an easily obtainable source of mesenchymal stem cells (MSC) by minimal invasive procedures not requiring an anesthetic.<sup>17,18</sup> In contrast, bmMSC and adipose tissue MSC require procurement methods necessitating local or general anesthesia and significant discomfort. Methods have been developed to isolate the eMSC prospectively using the CD146 and CD140b<sup>19,24</sup> or the W5C5 markers.<sup>20</sup> We have recently shown that it should be possible to prepare suitable quantities of eMSC under good manufacturing practice (GMP) for clinical application.<sup>21</sup> More recently, given the perceived issues with some of the clinical PP meshes, we have also developed new meshes from alternative biomaterials, with some improved mechanical properties<sup>22</sup> and shown that a gelatin-coated polyamide mesh had improved tissue integration in a rat abdominal hernia model, compared with a conventional PP clinical mesh.<sup>23</sup>

The aim of this study was to determine the *in vivo* host tissue response and biomechanical properties of a new gelatin-coated polyamide knitted mesh seeded with eMSC using a rat wound model as a preclinical model for POP repair surgery.

## Materials and Methods

### Human tissue

Informed written consent was obtained from each patient and ethics approval was obtained from the Southern Health Human Research and Ethics Committee B. Human endometrial tissue was collected from two patients undergoing hysterectomy and isolated cells were obtained as published previously.<sup>20</sup> Briefly, the endometrium was scraped from the myometrium and finely minced, then digested in collagenase

I and DNase I in Dulbecco's modified Eagle's medium (DMEM)/F12 culture medium (Life Technologies) in 5% CO<sub>2</sub> in air at 37°C. Following digestion, the cells were filtered through a cell strainer to obtain the stromal fraction followed by Ficoll Paque to remove red blood cells. The eMSC were extracted using magnetic beads and the single marker antibody, W5C5 as described recently.<sup>20</sup> The cells were cultured in DMEM/F12 medium containing 10% fetal calf serum, 1% antibiotic-antimycotic (100 U/mL penicillin, 100 µg/mL streptomycin, 0.25 µg/mL fungizone; Life Technologies), and 2 mM glutamine (culture medium) up to passage 6 (P6) to obtain sufficient cell numbers for implantation into rats.

### Properties of cultured W5C5<sup>+</sup> adherent cells

As MSC are known to change their properties in culture, analysis of colony-forming unit activity and differentiation assays were performed on P6 cells to determine MSC properties as previously described.<sup>18,21</sup> Briefly, cloning efficiency was determined by seeding the W5C5 bead-sorted cells at clonal densities (50–200 cells/cm<sup>2</sup>) on fibronectin (10 µg/mL)-coated 100 mm diameter culture dishes. Cells were incubated at 37°C in 5% CO<sub>2</sub> for at least 2 weeks with weekly media changes. Cloning efficiency was compared with P0 W5C5<sup>+</sup> eMSC, as previously published.<sup>20</sup>

To assess multipotency, the P6 cells were cultured in four-well plates in specific adipogenic, chondrogenic, smooth muscle cell, and osteoblast differentiation induction media for 4 weeks as described previously.<sup>18,20</sup> Adipogenic differentiation was evaluated using Oil red O staining to detect lipid droplet accumulation; chondrogenic differentiation by Alcian blue staining; myogenic differentiation by alpha-smooth muscle actin (αSMA) immunostaining; and osteogenic differentiation by alkaline phosphatase histochemistry (Sigma-Aldrich).

### Surface marker phenotyping by flow cytometry

Phenotyping of eMSC was done by single-color flow cytometry using known eMSC surface phenotypic markers (W5C5, CD140b, and CD146)<sup>20,24</sup> and more general MSC markers (CD29, CD44, CD73, and CD105)<sup>25</sup> and for negative markers CD34 (hematopoietic marker) and CD45 (myeloid cells) as previously published<sup>20,26</sup> (details of antibodies shown in Table 1). A minimum of 50,000 P6 eMSC were incubated with individual antibodies in separate tubes. Phycoerythrin-labeled secondary antibodies were used to detect labeled cells using a MoFlo<sup>®</sup> XDP cell sorter (Beckman Coulter). Data were analyzed using Summit Software v5.2. The percentage of positive cells was based on IgG isotype antibodies used for control setting of gates.

### Cell labeling

Before implantation, P6 cells were labeled with Vybrant<sup>™</sup> DiO reagent (Life Technologies) according to the manufacturer's instructions. Briefly, cells were incubated with 5 µL DiO for 2 min at 37°C and excess dye was then removed by three washes in phosphate-buffered saline (PBS). The labeled cells were detected using a 540/30 bandpass filter.

### Preparation of eMSC-seeded mesh constructs

Polyamide meshes were warp knitted and gelatin coated (PA+G) by dip-coating in 12% porcine gelatin, as previously

TABLE 1. ANTIBODIES USED FOR FLOW CYTOMETRY

Primary antibody	Clone	Concentration ( $\mu\text{g/mL}$ )	Isotype	Supplier
CD29	mAb13	10	Rat IgG2a	BD Pharmingen
CD31	M89D3	10	Mouse IgG2a	BD Pharmingen
CD44	G44-26	10	Mouse IgG2b	BD Pharmingen
CD45	HI30	10	Mouse IgG1	CALTAG Laboratories
CD73	AD2	10	Mouse IgG1	BD Pharmingen
CD90	5E10	10	Mouse IgG1	BD Pharmingen
CD105	266	10	Mouse IgG1	BD Pharmingen
CD140b (PDGFR $\beta$ )	PR7212	25	Mouse IgG1	R&D Systems
CD146	CC9	25	Mouse IgG2a	Donated by P. Simmons, Peter MacCallum Cancer Centre
W5C5	W5C5	25	Mouse IgG1	Donated by Dr. Hans-Jörg Bühning, Tübingen University

described,<sup>23</sup> but in the present study were cross-linked with 0.025% (w/v) glutaraldehyde. PA+G meshes were cut into samples of dimensions 10×25 mm, with the longitudinal axis cut in either the machine (warp) or cross (weft) direction of the knitted mesh. Meshes were gamma sterilized at 25 kGy. Prior to cell seeding, meshes were rehydrated in PBS, transferred to culture medium overnight at 4°C, and rinsed with medium. Meshes were manually seeded using a pipette at a seeding density of 100,000 cells/cm<sup>2</sup> (250,000 cells/mesh) in 100  $\mu\text{L}$  of medium per mesh and cultured for 24–48 h. The cells were seeded on top of the stabilized gelatin coating of the PA mesh, which was regularly checked for cell adherence. At the time of implantation, a confluent layer of cells was observed on the mesh surface (Fig. 1B). Control meshes of PA+G, without cells were incubated in culture medium only (Fig. 1A).

#### Implantation of eMSC-seeded mesh constructs

The experimental procedures and rat husbandry were approved by the Monash Medical Centre Animal Ethics Committee A (2011/61). CBH-rnu/Arc rats were housed in the animal house of Monash Animal Service facilities in compliance with the National Health and Medical Research Council guidelines for the care and use of laboratory animals. The rats were kept in closed cages with continuous automated air flow. The rats were provided with sterile food and water *ad libitum* and were kept under controlled environmental conditions at 20°C and a 12-h day/night cycle.

Seventy-four CBH-rnu/Arc immunodeficient nude rats were randomly divided into two experimental groups (37 rats/group) and were implanted with PA+G meshes, either

with or without (controls) eMSC. The rats were anesthetized with 2.5% w/v Isoflurane<sup>®</sup> and analgesia was provided with Carprofen<sup>®</sup> (5 mg/kg bodyweight). The dorsum was disinfected with 0.5% Chlorhexidine<sup>®</sup> in 70% v/v ethanol and covered with sterile drapes. A longitudinal 30 mm skin incision was performed along the spine in the middle of the dorsum. Subcutaneous pockets were achieved by blunt dissection to both sides. Each mesh construct was subcutaneously implanted into each pocket. For each animal two meshes were inserted, one with the longitudinal axis cut in the machine direction of the knitted mesh, and the other cut in the cross direction. This was done to analyze the mechanical properties of both directions, since warp-knitted mesh is anisotropic. The animal ethics committee preferred the insertion of two smaller pieces of mesh on each side of the animal rather than one large piece of mesh across the dorsum. Each animal received either eMSC seeded or unseeded meshes. Meshes were secured in place using Vicryl 3-0<sup>®</sup> sutures on both ends. Skin closure was performed with a single intracutaneous Vicryl 3-0 suture. Following recovery, the animals were monitored daily until they were sacrificed at 7, 30, 60, and 90 days ( $n=8$ /group/timepoint) and 14 days ( $n=5$ ) to track DiO-labeled cells on an additional time point. Each rat was euthanized in a CO<sub>2</sub> chamber. The animals were immediately inspected for signs of infection or seroma. Explanted meshes were dissected with a 0.5-cm border of adjacent tissue including skin and underlying muscles and divided into four parts, for biomechanical analysis, histology, immunohistochemistry, and flow cytometry, using the same pattern of dissection for each mesh.

Additionally, eMSC/PA+G construct dimensions were measured using electronic callipers and mesh contraction

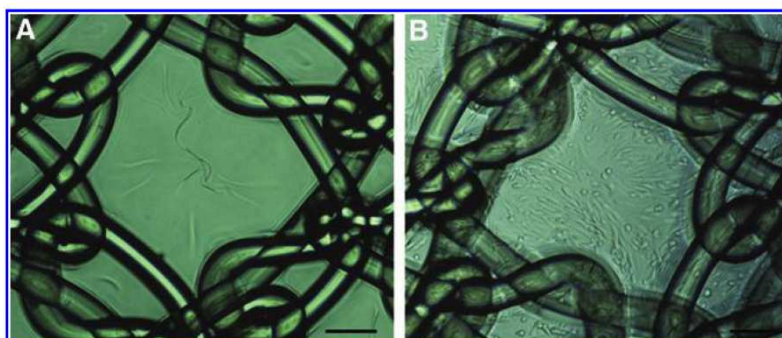


FIG. 1. PA+G mesh seeded (A) without and (B) with 100,000 cells/cm<sup>2</sup> 48 h after cell seeding/noncell seeding, just prior to implantation. PA+G, polyamide mesh with gelatin coating. Scale bar indicates 200  $\mu\text{m}$ . Color images available online at [www.liebertpub.com/tea](http://www.liebertpub.com/tea)

calculated by dividing mesh area after explantation by the original mesh area. Explanted mesh pieces for biomechanical analysis were frozen at  $-20^{\circ}\text{C}$  for subsequent testing.

#### Flow cytometry

A portion of the mesh with the surrounding tissue was collected for flow cytometry at 7, 14, 30, 60, and 90 days. A single cell suspension was obtained after fine mincing and filtering through a  $10\text{-}\mu\text{m}$  cell strainer. Similarly, a  $5\times 5\times 5\text{-mm}$  piece of brain, heart, lung, liver, and kidney were harvested, finely chopped, and filtered through the cell strainer. DiO-prelabeled cells were analyzed as described above. Rats without eMSC were used as the negative control.

#### Histology

For histological analysis, the explanted tissue from days 7, 30, 60, and 90 was fixed in 4% w/v paraformaldehyde (PFA) for 24 h, then embedded in paraffin and sectioned into  $5\text{-}\mu\text{m}$  thick sections. After dewaxing and rehydrating in graded alcohols, sections were stained with hematoxylin and eosin (H&E) or Sirius Red F3B (0.1 g/100 mL saturated picric acid solution) (Sigma-Aldrich) for 1 h at room temperature (RT) to determine total collagen content, as described previously.<sup>23</sup> For the morphometric analysis, the stained slides were washed in running water (nonacidified) to remove the yellow picric acid counterstain and the residual red color imparted by the Sirius Red was quantified by image analysis.<sup>23</sup>

Paraffin sections were stained with anti rat CD68 antibody (details in Table 2) to identify tissue macrophages, and lightly counterstained with hematoxylin as described above. Sections underwent dewaxing, rehydrating in graded alcohols followed by antigen retrieval using citric acid buffer (0.1 M, pH 6.0), and microwaving for 5 min on high power. After cooling to RT and three washes in PBS, endogenous peroxidase was quenched by 3% w/v  $\text{H}_2\text{O}_2$  followed by a protein block step (Protein Block; Dako) for 30 min at RT. The primary antibody and isotype controls (mouse IgG1) were incubated overnight at  $4^{\circ}\text{C}$ , sections washed, and the secondary antibody applied for 30 min at RT, as detailed in Table 2. Color was developed with 3,3'-diaminobenzidine (DAB) (Life Technologies). The slides were mounted with DPX (Scharlab).

#### Immunofluorescence

Tissue samples snap frozen in OCT were used for immunofluorescence and stained with antibodies to CD45 to visualize leukocytes, CCR7 for pro-inflammatory M1 macrophages, CD163 anti-inflammatory M2 macrophages, and anti-rat and anti-human collagen type I (Table 2). PFA fixed tissue was used to stain with  $\alpha\text{SMA}$  to label smooth muscle cells. Thawed frozen sections ( $5\text{-}\mu\text{m}$ ) were fixed in ice-cold acetone for 10 min. Pretreatment was performed for human collagen I according to the manufacturer's protocol. For  $\alpha\text{SMA}$ , tissue was fixed and processed as described above, followed by protein block (Dako) for 30 min at RT. After three washes in PBS, primary antibodies were incubated for 1 h at  $37^{\circ}\text{C}$ ; isotype-matched antibodies were used as negative controls and applied at the same concentration. Alexa-Fluor-488 and Alexa-Fluor-568-conjugated secondary antibodies (Table 2) were incubated for 30 min at RT, respectively. Nuclei were stained

TABLE 2. DETAILS OF ANTIBODIES USED FOR IMMUNOHISTOCHEMISTRY

Primary antibody	Clone	Concentration	Isotype	Supplier	Secondary antibody	Concentration	Supplier
Alpha-smooth muscle actin	1A4	1:400	Mouse IgG2a	Dako	Alexa fluor 488-goat anti-mouse IgG	1:200	Life Technologies®
CD 45 leukocyte common antigen	OX-1	1:200	Mouse IgG1	BD Pharmingen	Alexa fluor 568-donkey anti-mouse IgG (H+L)	1:200	Life Technologies
CD 68	ED1	1:500	Mouse IgG1	AbD Serotec	EnVision + System-HRP Labeled Polymer (anti-mouse)	Ready to use	Dako
Rat Collagen I	AB755P	1:60	Polyclonal IgG	Millipore	Alexa fluor 488-Goat anti-rabbit IgG	1:500	Life Technologies
Human Collagen I	MAB3391 (5D8-G9)	1:20	Mouse IgG <sub>1</sub>	Millipore	Alexa fluor 488-donkey anti-mouse IgG (H+L) Ab150109	1:500	Sapphire Biosciences
CCR7 M1 marker		1:100	Polyclonal IgG	Sapphire Bioscience Pty. Ltd	Alexa568-goat anti-rabbit IgG	1:100	Life Technologies
CD163 M2 marker	ED2	1:400	Mouse IgG1	AbD Serotec	Alexa fluor 488 goat anti-mouse IgG	1:400	Life Technologies

with Hoechst 33258. The slides were mounted with fluorescent mounting medium (Dako).

#### *Histomorphometric analysis of explanted tissues*

Four images were taken per section stained with Sirius Red or immunostained for CD68, CCR7, CD163,  $\alpha$ SMA, and CD45 for each explant at each time point using a Leica<sup>®</sup> DMR Fluorescence Microscope at 20 $\times$  magnification. Images were captured from the four most central mesh filaments to achieve consistency; areas at anchoring sutures were excluded. The images were analyzed using image analysis software Metamorph (Molecular Devices, LLC) to measure positive staining around mesh filaments in 50  $\mu$ m increments, as described previously.<sup>23</sup> The positive signal area (pixels) for every image was recorded and divided by the total tissue area examined. Cell numbers were calculated as positive area divided by the size of one representative cell using the Metamorph software. Collagen alignment was assessed using birefringence microscopy on the Sirius Red-stained slides and scored according to the presence of predominantly thick or thin birefringent fibers (0=predominantly thin fibers, 1=predominantly thick fibers).<sup>27</sup>

#### *Biochemical analysis of collagens I and III*

Sodium dodecyl sulfate–polyacrylamide gel electrophoresis (SDS-PAGE) using delayed reduction<sup>28</sup> was used to determine collagen type III/I ratio. Frozen tissue explants were thawed to RT for 15 min, and 5 $\times$ 5 mm pieces adjacent to the meshes were digested for 4 h (0.25 mg/mL pepsin (Sigma-Aldrich) in 100 mM acetic acid, pH 2.5) at 4 $^{\circ}$ C followed by brief homogenization with a IKA T10 basic Ultra-Turrax<sup>®</sup>. Samples were then allowed to further digest in the pepsin solution for 16 h. Samples were then centrifuged, 10  $\mu$ L of each sample mixed with 40  $\mu$ L NuPAGE<sup>®</sup> LDS sample buffer (Life Technologies), heated to 90 $^{\circ}$ C for 1–2 min, and then loaded onto NuPAGE 4%–12% Bis-tris gels (Life Technologies) with MES running buffer (Life Technologies); 50 mM (2-[N-morpholino]ethanesulfonic acid), 50 mM Tris base, 1 mM EDTA, 0.1% SDS; pH 7.3. Samples were electrophoresed for 1 h at 130 V, the power was then turned off, and 5% v/v 2-mercaptoethanol (Sigma-Aldrich) was added to each well and allowed to stand for 1 h. Finally, electrophoresis was continued for 3 h at 130 V at 4 $^{\circ}$ C. Gels were stained with Coomassie Blue R-250 solution, destained in 20% ethanol and 5% acetic acid. Images were taken using FujiFilm LAS-3000 software. The percentage of type III collagen in type I and III collagen mixtures was calculated from peak sizes using the formula: percentage type III collagen =  $\frac{\text{Area } \alpha 1(\text{III}) \times 1.12 \times 100}{[\text{Area } \alpha 1(\text{III}) \times 1.12] + \text{Area } \alpha 1(\text{I})}$ ,<sup>29</sup> where a calibration factor of 1.12 was used to correct for the color yield from equal weights of the two collagen types.<sup>29</sup>

#### *Mechanical analysis of explanted mesh constructs*

Frozen explants were thawed at 4 $^{\circ}$ C overnight and tested within 24 h of defrosting. We used a standard method of freezing and thawing the tissue, as published previously for urogynecological applications, which does not alter the tissue tensile properties.<sup>30</sup> Samples, of dimensions 4 $\times$ 25 mm, were punched from the explanted mesh piece along the longitudinal axis of the explanted mesh and kept moist using

PBS until testing. Uniaxial tensiometry was performed on day 7 and 90 explants, with and without cells, using an Instron<sup>®</sup> Tensile Tester (5567<sup>®</sup> Instron Corporation) with a 5-kN load cell. Samples were secured in pneumatic serrated jaws to a 14-mm gauge length and extended to break at an elongation rate of 30 mm/min. Samples of the same dimensions were also punched from the preimplanted PA+G mesh in the knit machine and cross directions. PA+G mesh was soaked in PBS for at least 12 h and tested wet using the same procedure. Average load–elongation curves were plotted from the data generated. Mesh stiffness (N/mm) is represented by the slope of the load–elongation curve, with a steeper gradient indicating a stiffer mesh.

#### *Statistics*

GraphPad Prism 5.03.0001 was used for statistical analysis. Results are reported as mean  $\pm$  SEM for each experimental group ( $n=8$  meshes/group/time point). For the biomechanical study, separate analyses were reported for the machine and cross direction meshes ( $n=8$ /group/time point/mesh direction).

Since the data were not normally distributed (D'Agostino and Pearson omnibus normality test), nonparametric analysis using Kruskal–Wallis ANOVA for pairwise comparisons was undertaken followed by Bonferroni correction for assessment of differences between time points for the various meshes.  $p$ -Values < 0.05 were considered statistically significant.

#### *Results*

All animals had a normal postoperative recovery; none developed mesh erosion or any other side effects or died in the course of the experiment. All meshes, with and without seeded eMSC, were well tolerated as rats gained weight at all time points. Mesh contraction was rare and did not significantly differ between the rats treated with eMSC and the controls (without eMSC) or between the different time points.

#### *Properties of passage 6 eMSC*

W5C5<sup>+</sup> sorted-cells from the two samples cultured to P6 were pooled and analyzed as a single cell suspension. Colony forming unit activity was 0.04%  $\pm$  0.02% ( $n=3$  replicates), compared with 3.60  $\pm$  1.56 for P0 W5C5<sup>+</sup> sorted cells. The P6 sorted cells differentiated into adipocytes, chondrocytes, myocytes, and osteocytes (Supplementary Fig. S1A–D; Supplementary Data are available online at [www.liebertpub.com/tea](http://www.liebertpub.com/tea)), similar but to a lesser degree than P0 sorted cells. The P6 W5C5<sup>+</sup> population comprised 14.7% of cells, CD140b 15%, CD146 8.4%, CD29 97%, CD44 95%, CD73 97%, CD105 97%, CD34 0%, and CD45 0%, respectively (Supplementary Fig. S1E).

#### *eMSC survival and tracking after implantation on the PA+G mesh*

The fate of DiO-labeled eMSC implanted on the PA+G mesh was examined by flow cytometry. Before implantation 95% of cells were DiO<sup>+</sup> (Fig. 2A). Seven days after implantation DiO-labeled cells were found on the mesh (Fig. 2B); at 14 days a low percentage of cells were still present (Fig. 2C), but no cells were detected on day 30, 60, or 90 (Fig. 2D–F).

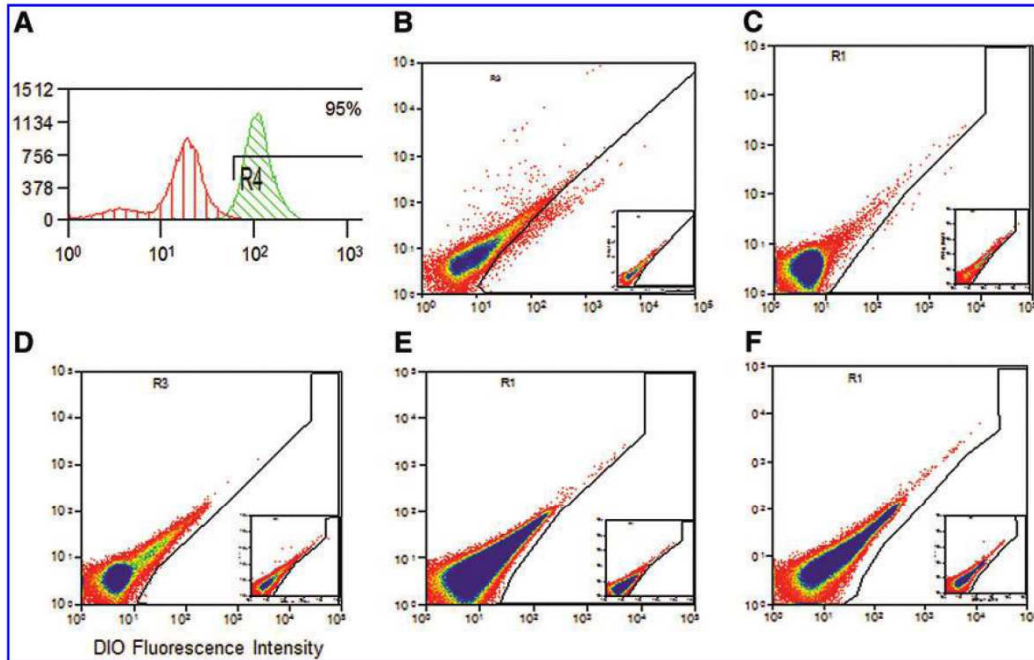


**FIG. 2.** Flow cytometric analysis of DiO-labeled cells. **(A)** Endometrial mesenchymal stem cells (eMSC) labeled with DiO prior to implantation. DiO<sup>+</sup> cells isolated from tissue explants at **(B)** 7 days, **(C)** 14 days, **(D)** 30 days, **(E)** 60 days, and **(F)** 90 days. Insets negative control (unlabeled cells). Representative plots from  $n = 6$  replicates showing DiO fluorescence intensity on the  $x$ -axis. Color images available online at [www.liebertpub.com/tea](http://www.liebertpub.com/tea)

To determine whether eMSC had migrated from the implanted mesh constructs, the brain, lung, heart, liver, spleen, and kidney tissue at every time point was also analyzed by flow cytometry. No DiO<sup>+</sup> cells were observed in any of these organs at any time point.

#### *Effect of eMSC on tissue response to the PA+G mesh*

To examine the effect of implanted eMSC/PA+G constructs on histological changes we undertook a detailed analysis of the explanted TE constructs using histological stains, immunohistochemistry, and SDS gel electrophoresis. Representative images of H&E stained sections are shown in Supplementary Figure S2. As expected, at day 7 there was a vigorous cellular response between and around the mesh filaments in both cell-seeded and unseeded meshes (Supplementary Fig. S2A, B); in the cell-seeded meshes the response appeared more intense and may have been attributed to the presence of the seeded eMSC or a more apparent degradation of the gelatin in the presence of these cells. The degree of cellularity decreased with time but still persisted in both groups of meshes by day 90 (Supplementary Fig. S2C, D), although there was visually more new tissue formation within the implanted meshes in both groups. The connective tissue around the mesh filaments seems to be more organized in the meshes with eMSC on day 7 compared with the mesh alone. However, by day 90 there appeared less inflammatory cells around the filament bundles in the mesh with eMSC compared with the mesh alone. The gelatin was still present on day 7 in both groups as indicated by the arrows, whereas it was fully degraded by day 90.

#### *Effect of eMSC on vascularization into the implanted PA+G mesh*

To assess the extent of vascularization, we determined the profile area of  $\alpha$ SMA immunostaining. At 7 days rats implanted with eMSC produced significantly more SMA positive vessel profiles compared with the controls ( $p < 0.05$ ) (Fig. 3A–C). There was no difference in the average content of smooth muscle cells for either eMSC treated or control rats at the later time points.

#### *Effect of eMSC on inflammatory foreign body reaction to the PA+G mesh*

The inflammatory response to the implanted TE constructs was evaluated by examining CD45<sup>+</sup> leukocyte density around mesh filaments (Fig. 4A, B) using image analysis.<sup>23</sup> CD45 leukocytes were concentrated both around the mesh perimeter and between the mesh filaments. The highest labeling index of the leukocyte infiltration was observed at 7 days with no significant differences between rats implanted with or without eMSC (Fig. 4C). At 30 and 60 days there was a decrease in both groups but no significant differences between the groups were observed. At 90 days, there were significantly fewer leukocytes surrounding the mesh filaments in rats treated with eMSC compared with controls ( $p < 0.05$ ) (Fig. 4A–C).

Since macrophages are the major leukocyte involved in the foreign body reaction,<sup>23</sup> we further quantified the level of CD68<sup>+</sup> cells. A similar pattern of labeling indices around the mesh filaments was observed for CD68 as for CD45<sup>+</sup> cells (Fig. 5). The highest macrophage accumulation was

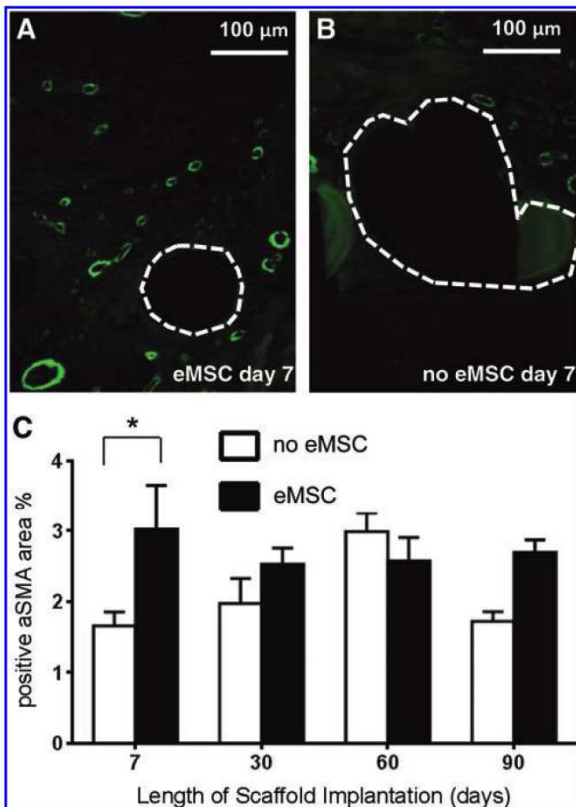


FIG. 3. Alpha-smooth muscle actin ( $\alpha$ SMA) vessel immunostaining in explanted mesh constructs comprising PA+G meshes with (■) and without eMSC (□). At 7 days (A) with eMSC, (B) without eMSC. (C)  $\alpha$ SMA positive area of vessel profiles (%), data are mean  $\pm$  SEM of  $n=8$  animals/group,  $*p<0.05$ . Color images available online at [www.liebertpub.com/tea](http://www.liebertpub.com/tea)

observed at 7 days, which significantly diminished by 90 days for both groups. Rats implanted with eMSC had significantly fewer macrophages at 90 days than rats without eMSC ( $p<0.05$ ) (Fig. 5A–C). To determine whether the macrophages were pro-inflammatory or anti-inflammatory we stained the tissue with CCR7 and CD163 antibodies to detect M1 and M2 macrophages, respectively. The pro-inflammatory M1 cells were significantly higher in rats treated with eMSC at 7 days ( $p<0.05$ ) with no significant differences at later time points (Fig. 5D). At 7 days, there was no difference in the level of M2 cells between the two groups. In the unseeded meshes, the total M1 plus M2 macrophage content was less than the CD68 levels, indicating that a significant proportion of infiltrating macrophages were uncommitted at this early stage. At 30 days M2 macrophages predominated in the eMSC-treated rats ( $p<0.05$ ) (Fig. 5E). The number of anti-inflammatory M2 cells did not differ between groups at 7, 60, or 90 days. The M2/M1 ratio was significantly decreased at 7 days in the eMSC group ( $p<0.001$ ), but no significant differences were observed at the later time points between the two groups (Fig. 5F).

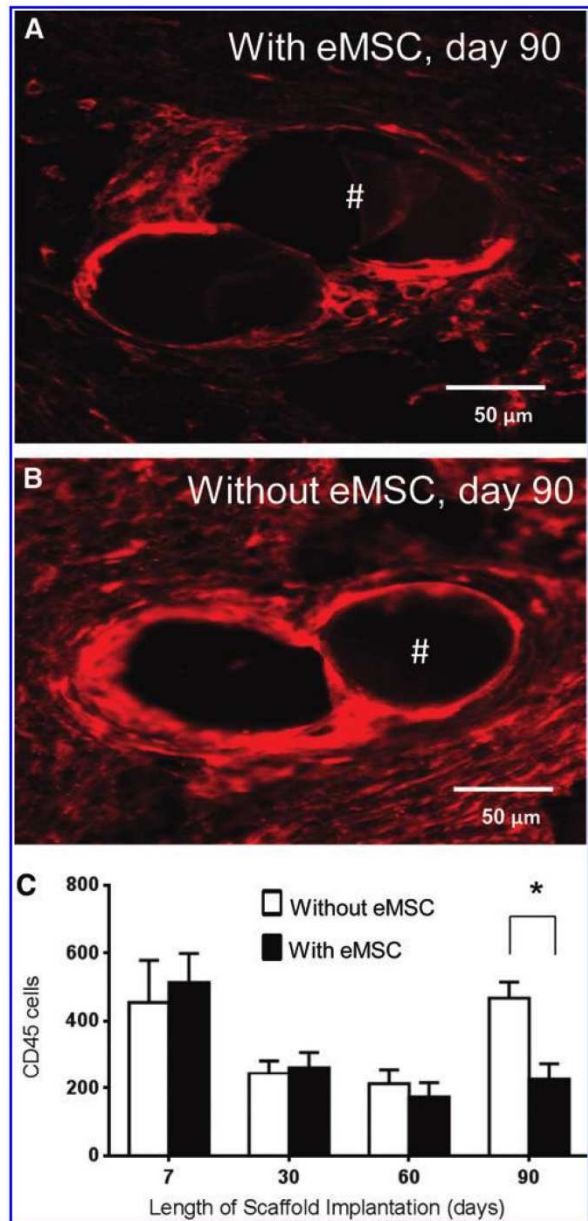
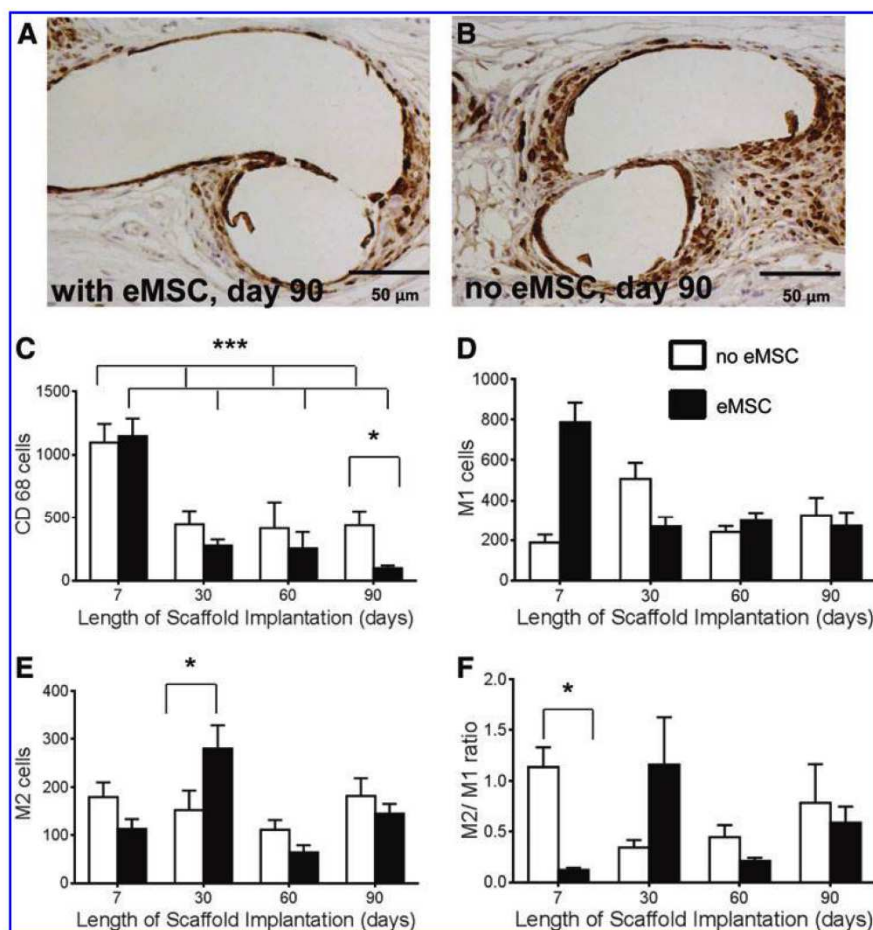


FIG. 4. CD45 immunostaining in explanted mesh constructs comprising PA+G meshes with and without eMSC. Day 90 explant (A) with eMSC, (B) without eMSC; Red staining indicates CD45 leukocytes. #, mesh filament. (C) Number of CD45-positive cells around mesh filaments from explants with (■) and without (□) eMSC. Data are mean  $\pm$  SEM of  $n=8$  animals/group.  $*p<0.05$ . Color images available online at [www.liebertpub.com/tea](http://www.liebertpub.com/tea)

*Effect of eMSC on collagen deposition around the PA+G mesh*

Sirius Red staining of total collagen deposition around mesh filaments (Fig. 6A, B) increased between day 7 and 60 in both eMSC treated and control meshes. Thereafter,

**FIG. 5.** Macrophage immunostaining in explanted mesh constructs comprising PA+G meshes with (■) and without (□) eMSC. Day 90 explant (A) with eMSC, (B) without eMSC. Positive cell numbers around mesh of (C) CD68 macrophages, (D) M1 macrophages (CCR7+), (E) M2 macrophages (CD263+), (F) M2/M1 ratio. Data are mean  $\pm$  SEM of  $n=8$  animals/group. \* $p < 0.05$ , \*\*\* $p < 0.001$ . Color images available online at [www.liebertpub.com/tea](http://www.liebertpub.com/tea)



the amount of collagen plateaued to 90 days (Fig. 6C). The percentage collagen type III within and around the meshes changed little with time in both meshes with and without cells, nor were there temporal differences (Fig. 6D). There were no significant differences in the percentage collagen type III in both seeded and unseeded meshes at any time point. Another important consideration is collagen organization. Our birefringence analysis showed that rats implanted with eMSC-seeded meshes had a greater number of thin collagen fibers, imaged with polarizing filters as green, after 90 days implantation, compared to meshes alone, where the fibers were thick and dense and yellow under polarized light (Fig. 6F, G). On day 90 explants, thin human fibers could be observed (Fig. 7B). The increased new collagen deposition seen at day 90 in Figure 7A was all rat collagen. Using antibodies that were specific to either rat or human collagen type I, cell-seeded 90 day explants showed uniform rat collagen type I within the PA fiber bundles (Fig. 7A) but no human collagen type I (Fig. 7B). Human endometrial tissue was used as a positive control for the anti-human collagen type I antibody (Fig. 7C) and the isotype control was always negative (Fig. 7D).

#### *Effect of eMSC on the biomechanical properties of PA+G mesh*

The average load–elongation curves for the day 7 and 90 explants, and the preimplanted PA+G mesh, in machine and the cross directions, are shown in Figure 8A–D. These load–elongation curves consisted of toe and linear regions, representing an initial region of low stiffness (toe region) followed by a region of higher stiffness (linear region), prior to failure (not shown). Explants without cells were stiffer (less extensible) than cell seeded explants, with increased stiffness in both toe and linear regions, at both time points and in both directions. For statistical analysis of load–elongation curves, 95% confidence intervals were plotted as error bars (Supplementary Fig. S3) to determine whether the differences were significant at the  $p=0.05$  level. Curves for day 7 and 90 explants originally seeded with cells were significantly different exceeding 2 mm elongation, in the cross (Supplementary Fig. S3A) and machine (Supplementary Fig. S3D) directions, respectively. Preimplanted PA+G meshes were generally of intermediate stiffness; between that of the explanted eMSC/PA+G and PA+G meshes. However, this result was only significant ( $p < 0.05$ ) compared to the cell

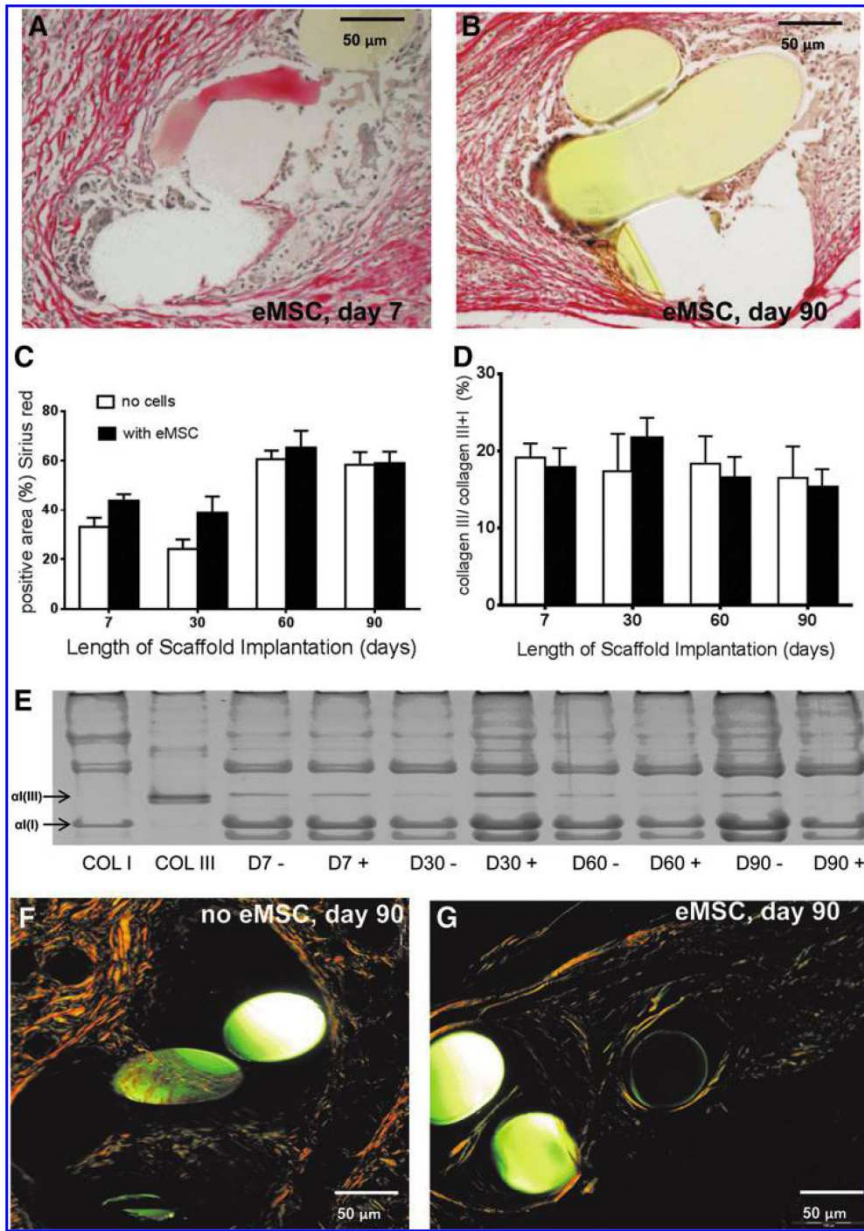


**FIG. 6.** Collagen quantification in explanted mesh constructs comprising PA+G meshes with (■) and without eMSC (□). Sirius Red staining of eMSC-seeded meshes at (A) 7 days, (B) 90 days. (C) Area of total collagen determined by Sirius Red staining (D) Percentage collagen type III determined by (E). Sodium dodecyl sulfate–polyacrylamide gel electrophoresis (SDS-PAGE) gel analysis. Sirius Red birefringence at 90 days in explants (F) without eMSC and (G) with eMSC. Data are mean ± SEM of n=8 animals/group.

seeded construct on day 7, in the cross direction (results not shown).

**Discussion**

The concept of delivering autologous differentiated cells or adult stem cells for POP repair has not been extensively validated, with only a few scattered reports<sup>14,31–33</sup> and no indications of ongoing or future clinical trials.<sup>34,35</sup> We previously showed that PA+G meshes induced a moderate foreign body reaction, neovascularization, and increased collagen deposition.<sup>23</sup> In this study, we have investigated the host inflammatory response, tissue integration, and me-

chanical properties of a novel mesh construct comprising PA+G, with and without seeded eMSC. The presence of seeded eMSC on the meshes was associated with clear quantitative differences in the type and extent of the tissue response, with controlled neotissue formation resulting in a more extensible and compatible integrated mesh. We showed that these eMSC delivered on novel PA+G meshes could be detected for up to 14 days after implantation, inducing higher initial neovascularization and acute inflammation, followed by a significantly reduced inflammatory response that was accompanied by a more organized collagen deposition. Seeded meshes were of decreased mechanical stiffness and higher extensibility compared with

**FIG. 7.** Immunofluorescent detection of collagen type I in 90 day cell-seeded explants specifically stained for (A) rat collagen type I, and (B) human collagen type I; and in control human endometrial tissue stained for (C) human collagen type I or (D) isotype negative control.

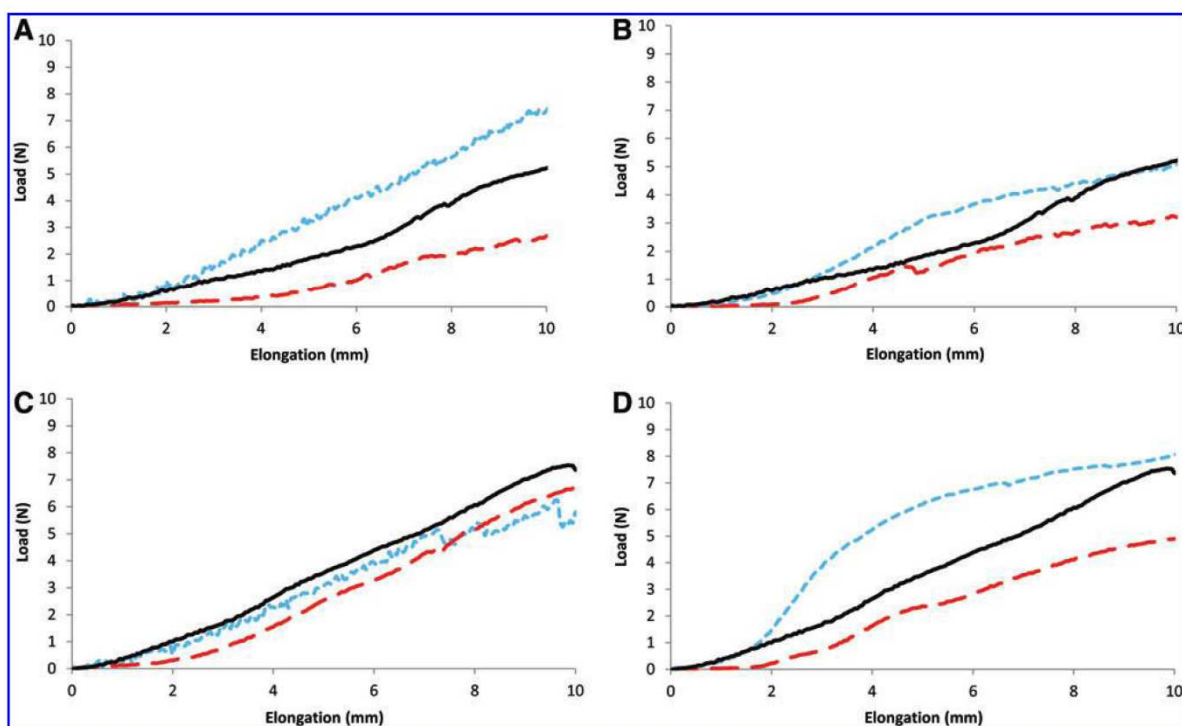
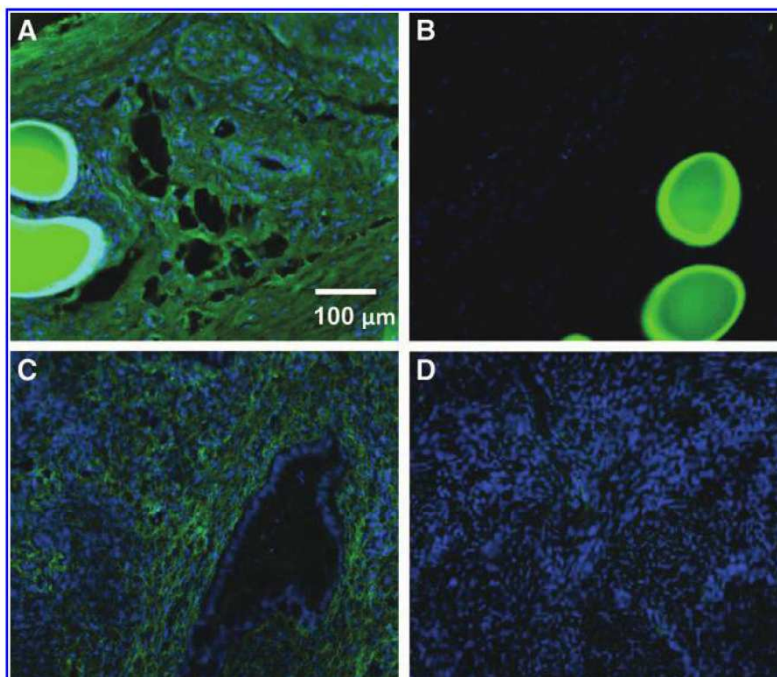


**FIG. 8.** Average load–elongation curves of explanted meshes ( $n=8$ ) on (A, C) day 7 and (B, D) day 90 in mesh cross direction (A, B) and mesh machine direction (C, D). Dashed line indicates meshes implanted with eMSC, dotted line indicates meshes implanted without eMSC, and solid line indicates preimplanted mesh ( $n=6$ ). Color images available online at [www.liebertpub.com/tea](http://www.liebertpub.com/tea)

unseeded mesh explants. Despite the lack of persistence of cells around the mesh filaments at the later time points, their initial modulatory effects appear to have influenced the nature of the chronic inflammatory response and mechanical tissue behavior in the long term. Meshes with eMSC had significantly reduced numbers of macrophages and leukocytes at 90 days suggesting that the eMSC may exert long-term anti-inflammatory effects. It is well known that bmMSC promote tissue repair via secreted soluble factors that recruit endogenous tissue stem cells to the site of injury,<sup>36</sup> and downregulating innate inflammatory and acquired immune responses, for example, by suppressing T lymphocytes, dendritic cells, and natural killer cells.<sup>13,37</sup> The exact immunomodulatory mechanism of MSC is still unclear; however, it has been shown that bmMSC can induce immunosuppression in the presence of IFN- $\gamma$  and the concomitant presence of any of the three other proinflammatory cytokines, TNF- $\alpha$ , IL-1 $\alpha$ , or IL-1 $\beta$ .<sup>13</sup> As the eMSC were not detected at 90 days it appears that these eMSC, like bmMSC, modulate the healing microenvironment through its paracrine or trophic effects, release signaling factors that reduce the inflammatory response even in the long term.<sup>36</sup> In our current study, it also appears that eMSC cytokines might influence the type of macrophage activity in the wound healing response as assessed by M1 and M2 phenotypic polarization.<sup>38</sup> Classically, the M1 macrophage phenotype and function is associated with pro-inflammatory responses, for example, activated by IFN- $\gamma$ , microbial products, or antigens and can also lead to chronic inflammation, whereas the M2 phenotype encourages immunoregulation, tissue repair, and constructive tissue remodeling.<sup>38,39</sup> We observed that the meshes with eMSC had a significantly higher number of M1 macrophages at 7 days suggesting that in the nude xenograft animal model there is still substantial innate immunity with an influx of M1 macrophages either in response to the foreign human MSC or to the gelatin, which might more rapidly degrade in the presence of these cells. However, at 30 days a shift occurs and a significantly higher number of M2 macrophages were present in the rats implanted with eMSC suggesting that the eMSC may have promoted differentiation of the M1 to the M2 type macrophage. A recent study found that a high number of M2 macrophages at day 14 after intra-abdominal mesh implantation in a rat model was associated with preferable histological outcomes.<sup>40</sup> In our study, the M2/M1 ratio was highest in the seeded meshes at 30 days, but decreased at day 60 before again increasing at the later 90 day time point. This has been observed with biological cross-linked SIS implants where it was speculated that the transient relative increase in M1 or decrease in the M2/M1 ratio was due to degradation of the cross-links with time<sup>39</sup>; in our study, this may reflect the degradation peak of the gelatin substrate.

We also showed that neovascularization occurred more rapidly in the rats treated with eMSC as shown by the significantly higher number of  $\alpha$ SMA-positive vessel profiles in the surrounding tissue at 7 days. In a recent study, a range of MSC populations from bone marrow, adipose, and dermal tissues were found to exert strong paracrine effects on neovascularization, promoting migration and proliferation of microvascular endothelial cells due to enhanced expression of the angiogenic factors, VEGF-A, bFGF, and others.<sup>41</sup> In our study, the level of vascularization remained constant

over the course of implantation for the seeded meshes showing a trend to better vascularization even at 90 days compared with unseeded meshes. This early and sustained neovascularization induced by eMSC may promote neotissue formation from endogenous cells that accounts for the longer term improvement in tissue integration and mechanical properties of the newly formed tissue around the PA+G mesh.

Generally, the host wound healing response to implants occurs in various overlapping phases comprising inflammation, proliferation, tissue matrix formation, and remodeling.<sup>31</sup> Fibroplasia and collagen deposition begin in the proliferation zone and continues as the tissue becomes less cellular and remodels to a mature tissue or scar.<sup>42</sup> We found a slightly higher collagen content around the meshes in rats that had been seeded with eMSC although this was not statistically significant, suggesting that the eMSC might promote collagen production. The new collagen deposited within the mesh fibers over the course of implantation was of rat origin with no human collagen type I. This is consistent with our finding that the seeded human eMSC were only detected up to 14 days suggesting no trans-differentiation of these stem cells to collagen-producing human fibroblasts. It is more likely and consistent with the paracrine effects associated with these cells that the increased collagen results directly from the influx of surrounding rat fibroblasts. Collagen type I resides in most tissues, providing tensile strength and stiffness,<sup>43,44</sup> and collagen type III is abundant in extensible tissues.<sup>44</sup> Differences in fiber diameter, between types I and III, may account for differences in mechanical properties between them, with a reduction in collagen fiber diameter leading to a reduction in tensile strength.<sup>45</sup> In our study, collagen ratio did not significantly alter over time; however, there was a trend of decreasing collagen type III with time. This trend is in agreement with other studies that showed increased collagen type I/III over time in implants comprising PP, polyester, or a PP/polyglactin composite<sup>46</sup> and indicates normal physiological wound healing. What factors result in a normal physiological tissue is influenced not only by the collagen levels and types of collagens, but also by the quality of collagen and how it is remodeled.<sup>47</sup> Increased quantities of thin collagen fibers on eMSC seeded meshes on day 90, as determined by birefringence analysis, may have contributed to differences in observed biomechanical properties of the explants. The lower stiffness levels of the eMSC/PA+G meshes at all time points may have been due to these thinner, more deformable collagen fibers. However, as no difference in the collagen ratio was determined between eMSC/PA+G and PA+G meshes, differences in collagen fiber thickness may have been due to collagen packing and alignment.<sup>48</sup> In terms of collagen analysis not only is the amount of collagen important, but also the orientation or alignment of the collagen.<sup>47</sup> Both the unseeded and seeded meshes contained significant proportions of well aligned and packed collagen fiber bundles necessary for effective tensile strength within the new tissue. But, unlike the unseeded meshes where thicker fibers dominated, there was a good mix of thick orange fibers and a significant increase in green thinner fibers in meshes with cells at 90 days, indicative of a gradual remodeling that occurs in healthy new tissue formation as opposed to the continual expression of only overly thick fibers often

associated with scarring.<sup>27</sup> Scarless healing is important in the long term as scar tissue has less favorable mechanical properties than healthy tissue.<sup>49</sup> The endometrium is shed every month and heals without scarring<sup>50</sup> suggesting that eMSC could have a similar effect when transplanted in a xenogeneic model. It should be noted that our mechanical differences are related to the physiological stiffness of the new tissue formed; while we have not directly reported on the ultimate tensile strength, it is highly unlikely that this would have changed between the two mesh types (data not shown). It has recently been reported in POP repair that mesh stiffness is a primary clinical concern in the deterioration in biomechanical properties of the vagina;<sup>51</sup> so, our results on the role of eMSC on controlling tissue stiffness could impact on prevention of a common clinical sequelae.

The fate of implanted MSC after implantation is not yet clear, however, long-term engraftment seems to be rare.<sup>52</sup> We did not find eMSC in any of the organs, which is reassuring for future clinical applications. Similar to previous studies implanting MSC from other sources we found DiO-positive eMSC in the rats up to 14 days, but not in the long term.<sup>53</sup> Despite this they exert long-term effects that promote the biocompatibility of foreign bodies like synthetic mesh. It is unclear whether the cells die or rapidly proliferate leading to a dilution of the dye. However, we found that DiO-labeled eMSC retain the dye for up to 35 days *in vitro* (unpublished observation). In other studies, using DAPI-labeled muscle-derived stem cells onto SIS scaffolds<sup>14</sup> or DiI-labeled vaginal fibroblasts onto PLGA scaffolds,<sup>32</sup> visualization was found up to 4 and 12 weeks, respectively. The cell labeling itself needs to be validated; PKH126 and CFDA-SE labeling can reduce cell metabolic activity,<sup>54</sup> while there is a degree of variability in the use of the lipophilic membrane dyes.

A strength of this study was the use of image analysis software, which allows objective assessment of the cellular content, vascular tissue, and collagen.<sup>23</sup> However, the software was not able to detect differences in the collagen alignment, which was manually scored by using Sirius Red birefringence.

A limitation of this study is the choice of model for assessing *in vivo* biocompatibility of mesh to be used for endopelvic fascial defect repair as it does not mimic the vaginal milieu. However, we chose a skin wound repair model representative of vaginal skin repair using dorsal surface of the rat as proof of principle. The critical need for preclinical animal validation of new meshes and, in our current study, for cell-seeded meshes in POP repair, has been recently emphasized in the light of the high incidence of clinical implant failures.<sup>55</sup> However, this model can be used as a simulation of vaginal skin repair. We chose the rat dorsal wound model to exclude any effects due to loads or pressure as in the abdominal hernia model,<sup>23,56</sup> and therefore the effects observed would be due to the eMSC alone. In our previous evaluation of the new PA+G meshes in immunocompetent rats, we reported significant differences in the tissue response compared with the conventional PP meshes.<sup>21</sup> The rat is considered an ideal nonfunctional screening model for preclinical experiments to test the performance of new POP meshes.<sup>57</sup> The next step will be to test this TE construct in a large functional animal model of vaginal repair.<sup>58</sup>

Current treatment options for POP are either unsatisfactory when native tissue repair is used or are accompanied by

high rates of adverse side effects when PP meshes are used for augmenting surgical reconstruction. A new treatment approach seems to be necessary. MSC have been shown to have great potential for soft tissue reconstruction<sup>59</sup> and if applied to vaginal surgery these cells might improve the long-term outcome by releasing factors that lead to a repair of the prolapsed tissue and improve biocompatibility by decreasing the foreign body reaction to implanted supporting meshes.

Our study reports that these new PA+G meshes seeded with eMSC are well tolerated, promote tissue integration, and reduce inflammatory reactions toward the implanted mesh in the longer term and may be a possible future treatment option for POP.

#### Acknowledgments

The authors acknowledge grant support from the Australian National Health and Medical Research Council grant 1021126 (C.E.G., J.A.W., A.R.) and Senior Research Fellowship 1042298 (C.E.G.), the CASS Foundation, South East Melbourne Alliance for Regenerative Therapies (C.E.G., J.A.W., A.R., S.L.E.), and the Victorian Government's Operational Infrastructure Support Program.

#### Disclosure Statement

No competing financial interests exist.

#### References

- Haylen, B.T., de Ridder, D., Freeman, R.M., Swift, S.E., Berghmans, B., Lee, J., *et al.* An International Urogynecological Association (IUGA)/International Continence Society (ICS) Joint Report on the Terminology for Female Pelvic Floor Dysfunction. *Neurourol Urodyn* **29**, 4, 2010.
- Hunnskaar, S., Burgio, K., Clark, A., Lapitan, M.C., Nelson, R., Sillen, U., *et al.* Epidemiology of urinary (UI) and faecal (FI) incontinence and pelvic organ prolapse (POP). Available at: [www.icsoffice.org/Publications/ICI\\_3/v1.pdf/chap5.pdf](http://www.icsoffice.org/Publications/ICI_3/v1.pdf/chap5.pdf) 2005. Last accessed August 18, 2013.
- Nygaard, I., Barber, M.D., Burgio, K.L., Kenton, K., Meikle, S., Schaffer, J., *et al.* Prevalence of symptomatic pelvic floor disorders in US women. *Jama* **300**, 1311, 2008.
- Stanford, E.J., Cassidenti, A., and Moen, M.D. Traditional native tissue versus mesh-augmented pelvic organ prolapse repairs: providing an accurate interpretation of current literature. *Int Urogynecol J* **23**, 19, 2012.
- Maher, C., Feiner, B., Baessler, K., Adams, E.J., Hagen, S., and Glazener, C.M. Surgical management of pelvic organ prolapse in women. *Cochrane Database Syst Rev* **4**, CD004014, 2010.
- Konstantinovic, M.L., Pille, E., Malinowska, M., Verbeken, E., De Ridder, D., and Deprest, J. Tensile strength and host response towards different polypropylene implant materials used for augmentation of fascial repair in a rat model. *Int Urogynecol J Pelvic Floor Dysfunct* **18**, 619, 2007.
- Delancey, J.O.L. Anatomic aspects of vaginal eversion after hysterectomy. *Am J Obstet Gynecol* **166**, 1717, 1992.
- FDA Public Health Notification: Serious Complications Associated with Transvaginal Placement of Surgical Mesh in Repair of Pelvic Organ Prolapse and Stress Urinary Incontinence. 2008. Available at [www.fda.gov/MedicalDevices/](http://www.fda.gov/MedicalDevices/)

- Safety/AlertsandNotices/PublicHealthNotifications/UCM061976.htm. Last accessed August 18, 2013.
9. FDA Safety Communication: UPDATE on Serious Complications Associated with Transvaginal Placement of Surgical Mesh for Pelvic Organ Prolapse. 2011. Available at: [www.fda.gov/MedicalDevices/Safety/AlertsandNotices/UCM262435.htm](http://www.fda.gov/MedicalDevices/Safety/AlertsandNotices/UCM262435.htm). Last accessed August 18, 2013.
  10. Deprest, J., Zheng, F., Konstantinovic, M., Spelzini, F., Claerhout, F., Steensma, A., *et al.* The biology behind fascial defects and the use of implants in pelvic organ prolapse repair. *Int Urogynecol J Pelvic Floor Dysfunct* **17**(Suppl 1), S16, 2006.
  11. de Tayrac, R., Alves, A., and Therin, M. Collagen-coated vs noncoated low-weight polypropylene meshes in a sheep model for vaginal surgery. A pilot study. *Int Urogynecol J Pelvic Floor Dysfunct* **18**, 513, 2007.
  12. Lim, Y.N., Muller, R., Corstiaans, A., Hitchins, S., Barry, C., and Rane, A. A long-term review of posterior colporrhaphy with Vypro 2 mesh. *Int Urogynecol J Pelvic Floor Dysfunct* **18**, 1053, 2007.
  13. Shi, Y., Hu, G., Su, J., Li, W., Chen, Q., Shou, P., *et al.* Mesenchymal stem cells: a new strategy for immunosuppression and tissue repair. *Cell Res* **20**, 510, 2010.
  14. Ho, M.H., Heydarkhan, S., Vernet, D., Kovanecz, I., Ferrini, M.G., Bhatia, N.N., *et al.* Stimulating vaginal repair in rats through skeletal muscle-derived stem cells seeded on small intestinal submucosal scaffolds. *Obstet Gynecol* **114**, 300, 2009.
  15. Deprest, J., De Ridder, D., Roovers, J.P., Werbrouck, E., Coremans, G., and Claerhout, F. Medium term outcome of laparoscopic sacrocolpopexy with xenografts compared to synthetic grafts. *J Urol* **182**, 2362, 2009.
  16. Dolce, C.J., Stefanidis, D., Keller, J.E., Walters, K.C., Newcomb, W.L., Heath, J.J., *et al.* Pushing the envelope in biomaterial research: initial results of prosthetic coating with stem cells in a rat model. *Surg Endosc* **24**, 2687, 2010.
  17. Gargett, C.E., Nguyen, H.P.T., and Ye, L. Endometrial regeneration and endometrial stem/progenitor cells. *Rev Endocr Metab Disord* **13**, 235, 2012.
  18. Gargett, C.E., Schwab, K.E., Zillwood, R.M., Nguyen, H.P., and Wu, D. Isolation and culture of epithelial progenitors and mesenchymal stem cells from human endometrium. *Biol Reprod* **80**, 1136, 2009.
  19. Gargett, C.E., Chan, R.W.S., and Schwab, K.E. Endometrial stem cells. *Curr Opin Obstet Gynecol* **19**, 377, 2007.
  20. Masuda, H., Anwar, S.S., Buehring, H.-J., Rao, J.R., and Gargett, C.E. A novel marker of human endometrial mesenchymal stem-like cells. *Cell Transplant* **21**, 2201, 2012.
  21. Rajaraman, G., White, J., Tan, K.S., Ulrich, D., Rosamilia, A., Werkmeister, J.A., *et al.* Optimisation and scale up culture of human endometrial multipotent mesenchymal stromal cells: potential for clinical application. *Tissue Eng Part C Methods* **19**, 80, 2013.
  22. Edwards, S.L., Werkmeister, J.A., Rosamilia, A., Ramshaw, J.A.M., White, J.F., and Gargett, C.E. Characterisation of clinical and newly fabricated meshes for pelvic organ prolapse repair. *J Mech Behav Biomed Mater* **23**, 53, 2013.
  23. Ulrich, D., Edwards, S.L., White, J.F., Supit, T., Ramshaw, J.A.M., Lo, C., *et al.* A preclinical evaluation of alternative synthetic biomaterials for fascial defect repair using a rat abdominal hernia model. *PLoS One* **7**, 2012.
  24. Schwab, K.E., and Gargett, C.E. Co-expression of two perivascular cell markers isolates mesenchymal stem-like cells from human endometrium. *Hum Reprod* **22**, 2903, 2007.
  25. Buhring, H.J., Battula, V.L., Trembl, S., Schewe, B., Kanz, L., and Vogel, W. Novel markers for the prospective isolation of human MSC. *Ann N Y Acad Sci* **1106**, 262, 2007.
  26. Dominici, M., Le Blanc, K., Mueller, I., Slaper-Cortenbach, I., Marini, F., Krause, D., *et al.* Minimal criteria for defining multipotent mesenchymal stromal cells. The International Society for Cellular Therapy position statement. *Cytotherapy* **8**, 315, 2006.
  27. Junqueira, L.C.U., Bignolas, G., and Brentani, R.R. Picrosirius staining plus polarization microscopy, a specific method for collagen detection in tissue-sections. *Histochem J* **11**, 447, 1979.
  28. Sykes, B., Puddle, B., Francis, M., and Smith, R. Estimation of 2 collagens from human dermis by interrupted gel-electrophoresis. *Biochemical and Biophys Res Commun* **72**, 1472, 1976.
  29. Chan, D., and Cole WG. Quantitation of type I and type-III collagens using electrophoresis of alpha chains and cyanogen-bromide peptides. *Anal Biochem* **139**, 322, 1984.
  30. Rubod, C., Boukerrou, M., Brieu, M., Dubois, P., and Cosson, M. Biomechanical properties of vaginal tissue. Part 1: new experimental protocol. *J Urol* **178**, 320, 2007.
  31. De Philippo, R.E., Bishop, C.E., Freitas, L., Yoo, J.J., and Atala, A. Tissue engineering a complete vaginal replacement from a small biopsy of autologous tissue. *Transplantation* **86**, 208, 2008.
  32. Hung, M.J., Wen, M.C., Hung, C.N., Ho, E.S.C., Chen, G.D., and Yang, V.C. Tissue-engineered fascia from vaginal fibroblasts for patients needing reconstructive pelvic surgery. *Int Urogynecol J* **21**, 1085, 2010.
  33. de Filippo, R.E., Yoo, J.J., and Atala, A. Engineering of vaginal tissue *in vivo*. *Tissue Eng* **9**, 301, 2003.
  34. Martin, I., Baldomero, H., Bocelli-Tyndall, C., Passweg, J., Saris, D., and Tyndall, A. The Survey on Cellular and Engineered Tissue Therapies in Europe in 2010. *Tissue Eng Part A* **18**, 2268, 2012.
  35. Ulrich, D., Muralitharan, R., and Gargett, C. Toward the use of endometrial and menstrual blood mesenchymal stem cells for cell-based therapies. *Expert Opin Biol Ther* **13**, 1387, 2013.
  36. Caplan, A.I., and Dennis, J.E. Mesenchymal stem cells as trophic mediators. *J Cell Biochem* **98**, 1076, 2006.
  37. Di Nicola, M., Carlo-Stella, C., Magni, M., Milanese, M., Longoni, P.D., Matteucci, P., *et al.* Human bone marrow stromal cells suppress T-lymphocyte proliferation induced by cellular or nonspecific mitogenic stimuli. *Blood* **99**, 3838, 2002.
  38. Mantovani, A., Sica, A., and Locati, M. Macrophage polarization comes of age. *Immunity* **23**, 344, 2005.
  39. Badylak, S.F., Valentin, J.E., Ravindra, A.K., McCabe, G.P., and Stewart-Akers, A.M. Macrophage phenotype as a determinant of biologic scaffold remodeling. *Tissue Eng Part A* **14**, 1835, 2008.
  40. Brown, B.N., Londono, R., Tottey, S., Zhang, L., Kukla, K.A., Wolf, M.T., *et al.* Macrophage phenotype as a predictor of constructive remodeling following the implantation of biologically derived surgical mesh materials. *Acta Biomater* **8**, 978, 2012.
  41. Hsiao, S.T.-F., Asgari, A., Lokmic, Z., Sinclair, R., Dusting, G.J., Lim, S.Y., *et al.* Comparative analysis of paracrine factor expression in human adult mesenchymal stem cells derived from bone marrow, adipose, and dermal tissue. *Stem Cells Dev* **21**, 2189, 2012.

42. Midwood, K.S., Williams, L.V., and Schwarzbauer, J.E. Tissue repair and the dynamics of the extracellular matrix. *Int J Biochem Cell Biol* **36**, 1031, 2004.
43. Prockop, D.J., and Kivirikko, K.I. Collagens—molecular-biology, diseases, and potentials for therapy. *Annu Rev Biochem* **64**, 403, 1995.
44. Gelse, K., Poschl, E., and Aigner, T. Collagens—structure, function, and biosynthesis. *Adv Drug Deliv Rev* **55**, 1531, 2003.
45. Doillon, C.J., Dunn, M.G., Bender, E., and Silver, F.H. Collagen fiber formation in repair tissue—development of strength and toughness. *Coll Relat Res* **5**, 481, 1985.
46. Junge, K., Klinge, U., Klosterhalfen, B., Mertens, P.R., Rosch, R., Schachtrupp, A., *et al.* Influence of mesh materials on collagen deposition in a rat model. *J Invest Surg* **15**, 319, 2002.
47. Feola, A., Abramowitch, S., Jones, K., Stein, S., and Moalli, P. Parity negatively impacts vaginal mechanical properties and collagen structure in rhesus macaques. *Am J Obstet Gynecol* **203**, 2010.
48. Dayan, D., Hiss, Y., Hirshberg, A., Bubis, J.J., and Wolman, M. Are the polarization colors of Picrosirius Red-stained collagen determined only by the diameter of the fibres. *Histochemistry* **93**, 27, 1989.
49. Jean-Charles, C., Rubod, C., Brieu, M., Boukerrou, M., Fasel, J., and Cosson, M. Biomechanical properties of prolapsed or non-prolapsed vaginal tissue: impact on genital prolapse surgery. *Int Urogynecol J* **21**, 1535, 2010.
50. Salamonsen, L.A. Tissue injury and repair in the female human reproductive tract. *Reproduction* **125**, 301, 2003.
51. Feola, A., Abramowitch, S., Jallah, Z., Stein, S., Barone, W., Palcsey, S., *et al.* Deterioration in biomechanical properties of the vagina following implantation of a high-stiffness prolapse mesh. *BJOG* **120**, 224, 2013.
52. von Bahr, L., Batsis, I., Moll, G., Hagg, M., Szakos, A., Sundberg, B., *et al.* Analysis of tissues following mesenchymal stromal cell therapy in humans indicates limited long-term engraftment and no ectopic tissue formation. *Stem Cells* **30**, 1575, 2012.
53. Zimmermann, C.E., Gierloff, M., Hedderich, J., Acil, Y., Wiltfang, J., and Terheyden, H. Survival of transplanted rat bone marrow-derived osteogenic stem cells *in vivo*. *Tissue Eng Part A* **17**, 1147, 2011.
54. Polzer, H., Volkmer, E., Saller, M.M., Prall, W.C., Haasters, F., Drosse, I., *et al.* Long-term detection of fluorescently labeled human mesenchymal stem cell *in vitro* and *in vivo* by semi-automated microscopy. *Tissue Eng Part C Methods* **18**, 156, 2012.
55. Deprest, J., and Feola, A. The need for preclinical research on pelvic floor reconstruction. *BJOG* **120**, 141, 2013.
56. Konstantinovic, M.L., Lagae, P., Zheng, F., Verbeken, E.K., De Ridder, D., and Deprest, J.A. Comparison of host response to polypropylene and non-cross-linked porcine small intestine serosal-derived collagen implants in a rat model. *BJOG* **112**, 1554, 2005.
57. Abramowitch, S.D., Feola, A., Jallah, Z., and Moalli, P.A. Tissue mechanics, animal models, and pelvic organ prolapse: A review. *Eur J Obstet Gynecol Reprod Biol* **144**, S146, 2009.
58. Frey-Vasconcelis, J., Whittlesey, K.J., Baum, E., and Feigal, E.G. Translation of stem cell research: points to consider in designing preclinical animal studies. *Stem Cells Transl Med* **1**, 353, 2012.
59. Atala, A. Tissue engineering of reproductive tissues and organs. *Fertil Steril* **98**, 21, 2012.

Address correspondence to:

Caroline E. Gargett, PhD  
 Monash Institute of Medical Research  
 27-31 Wright Street  
 Clayton, VIC 3168  
 Australia

E-mail: caroline.gargett@monash.edu

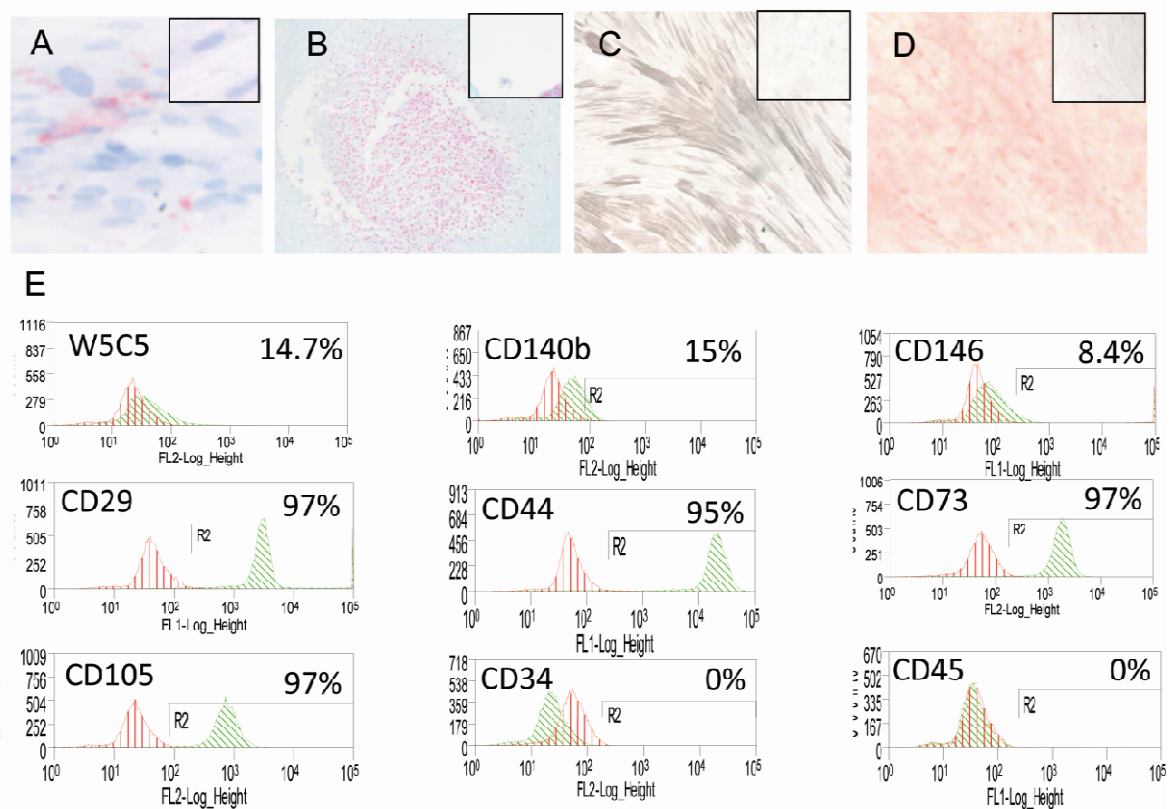
Received: March 15, 2013

Accepted: September 25, 2013

Online Publication Date: November 11, 2013

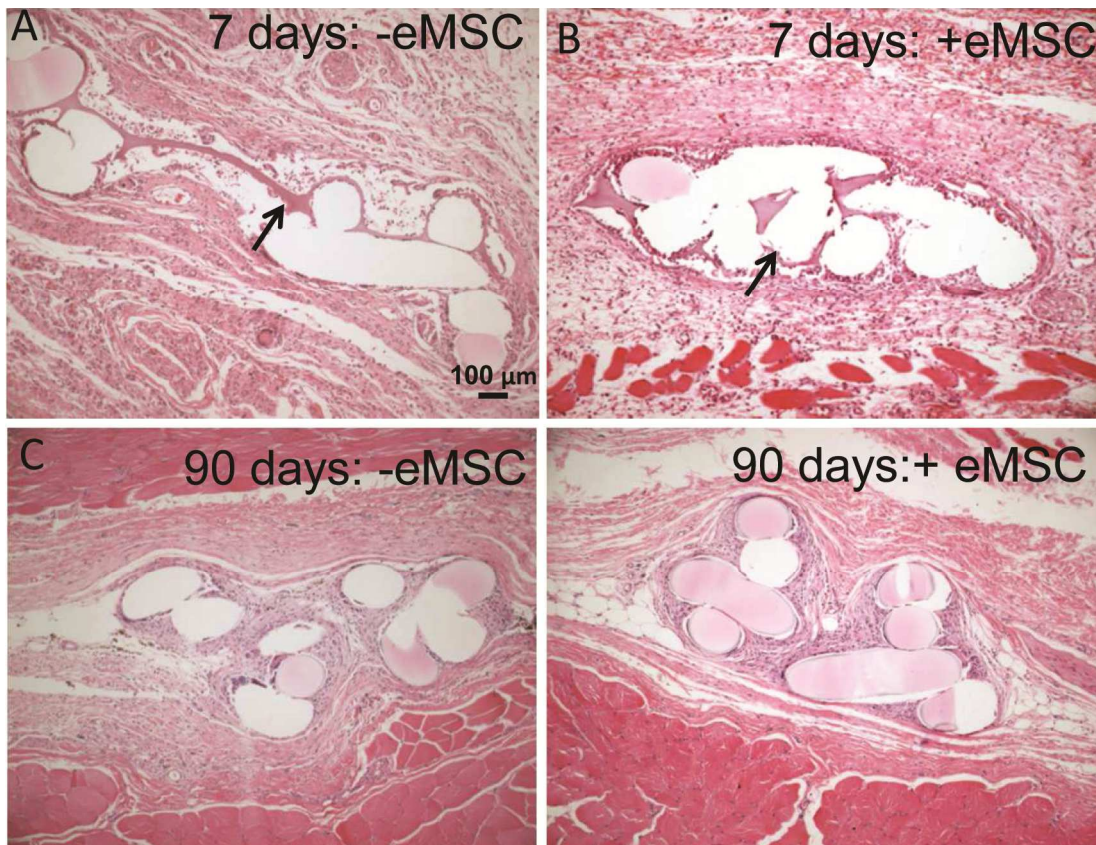
## Supplementary Figure 1

Histological staining of P6 W5C5+ eMSC after 4 weeks culture in (A) adipogenic, (B) chondrogenic, (C) myogenic, and (D) osteogenic induction media stained for (A) Oil Red O, (B) Alcian blue, (C)  $\alpha$ SMA, (D) and Alkaline Phosphatase . (E) Flow cytometric analysis of P6 W5C5+ eMSC showing MSC positive and negative markers as indicated. Scale bar in A, C and D indicates 200  $\mu$ m, in B 100  $\mu$ m.



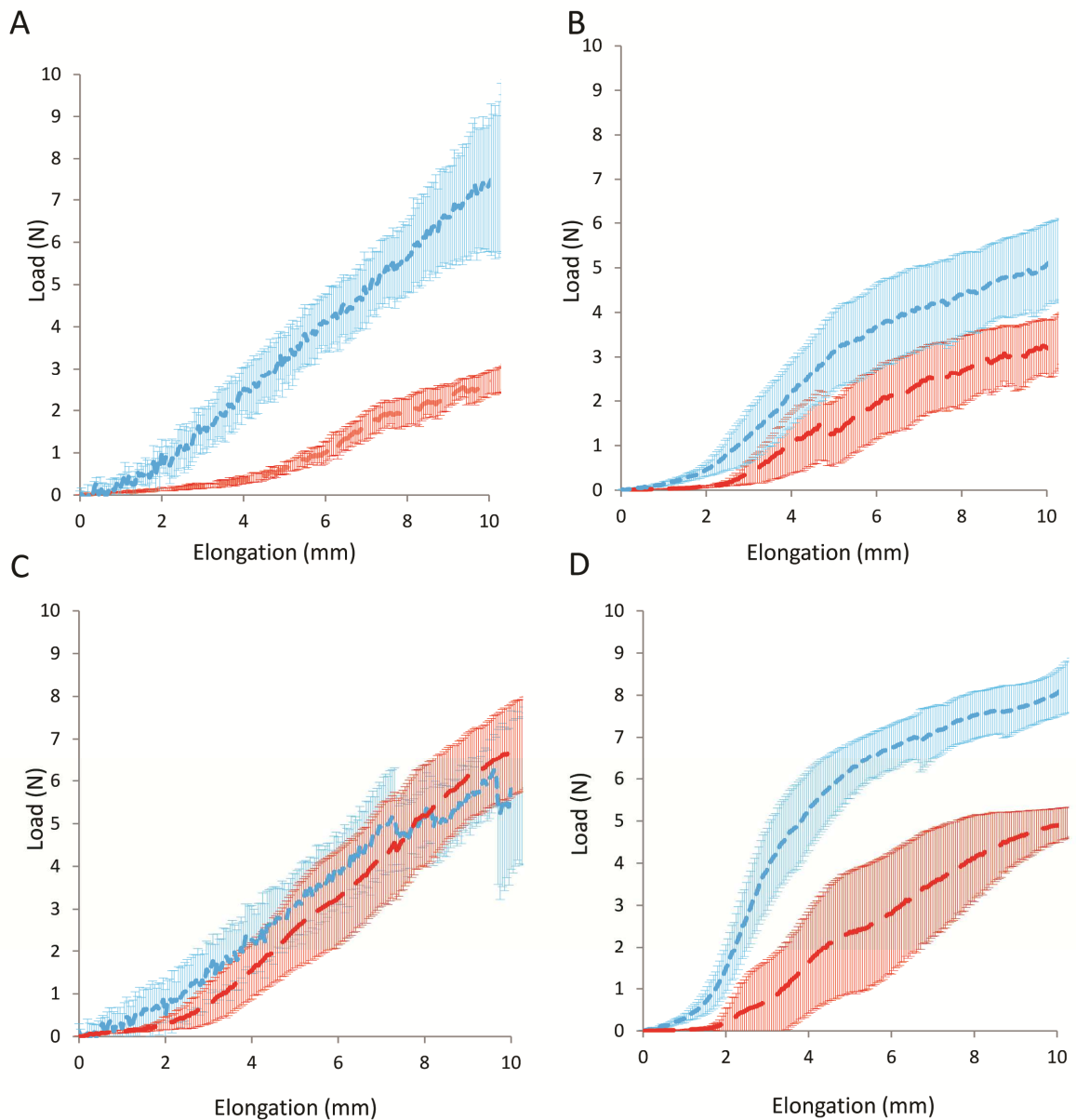
## Supplementary Figure 2

Histological staining of rat explants with H+E at (A) 7 days without eMSC, (B) 7 days with eMSC, showing residual gelatine at the implant site (→), (C) 90 days without eMSC; and (D) 90 days with eMSC, showing the integration of the implant with the surrounding tissue.



### Supplementary Figure 3

Average load-elongation curves of explanted meshes (n=8) on (A and C) day 7 and (B and D) day 90 in mesh cross direction (A, B) and mesh machine direction (C, D). Dashed line indicates meshes implanted with eMSC, dotted line indicates meshes implanted without eMSC (n=6). Error bars are 95% confidence intervals.



## **CHAPTER 5**

### **Ovine Vaginal Tissue Analysis**

In chapter 4 I demonstrated that a TE approach for POP repair in a rat model improves the tissue integration and biocompatibility of the PA+G mesh. Paracrine immunomodulatory effects from the seeded eMSC controlled the extent and type of tissue response. The next step is to test this proof of principle model in a large animal. This autologous large animal study is currently being developed by our research group. To understand the effect of eMSC/PA+G TE constructs in a preclinical ovine model it is necessary to generate baseline data. Current literature on vaginal tissue composition is not comprehensive as tissue collection is often not stated or inconclusive.

For this chapter I performed a comprehensive analysis of vaginal tissue in a sheep model at different reproductive stages using numerous techniques.

First, after dissecting the vaginal tissue I determined its general structure and vascularisation using immunohistochemistry protocols as developed for chapter 2 and 4. I thank Ms Jacinta F. White for teaching me the Masson's trichrome technique and helping with the staining.

Second, together with CSIRO I performed analysis of the extracellular matrix proteins (including collagen, GAG and elastin) using SDS PAGE gel electrophoresis, hydroxyproline assay, dimethylmethylene blue assay, and indirect amino acid elastin quantification. I thank Dr Kai Su for developing and optimizing these protocols and for helping with the testing.

Lastly, based on the methods described in Aims 1 and 3 and on the recent literature Dr Sharon L. Edwards and I developed a novel protocol for testing the biomechanical properties of ovine vaginal tissue. I performed biomechanical testing on the explanted tissue using the Instron machine and I thank Dr. Sharon Edwards for performing the analysis and educating me on the interpretation of the data.

**Declaration for Thesis Chapter 5**

**Declaration by candidate**

In the case of Chapter 5, the nature and extent of my contribution to the work was the following:

<b>Nature of contribution</b>	<b>Extent of contribution (%)</b>
Study design, Animal experiments, Tissue harvesting, Tissue processing, Tissue staining, Image analysis, Biomechanical testing, Biochemical testing, Data analysis, Statistical analysis, Data interpretation, paper writing	70

The following co-authors contributed to the work. Co-authors who are students at Monash University must also indicate the extent of their contribution in percentage terms:

<b>Name</b>	<b>Nature of contribution</b>	<b>Extent of contribution (%) for student co-authors only</b>
<b>Dr. Sharon L. Edwards</b>	Biomechanical testing, Data analysis	
<b>Dr. Kai Su</b>	Biochemical testing	
<b>Jacinta F. White</b>	Tissue staining, Image analysis	
<b>Dr. John AM. Ramshaw</b>	Data interpretation	
<b>Dr. Graham Jenkin</b>	Animal experiments, Tissue harvesting	
<b>Dr. Jan Deprest</b>	Study design, Data interpretation	
<b>Dr. Anna Rosamilia</b>	Data interpretation	
<b>Dr. Jerome A. Werkmeister</b>	Study design, Data analysis, Data interpretation, Paper writing	
<b>Dr. Caroline E. Gargett</b>	Study design, Data analysis, Data interpretation, paper writing	

**Candidate's Signature**

	<b>Date</b> 07.03.2014
--	---------------------------

**Declaration by co-authors**

The undersigned hereby certify that:

- (1) the above declaration correctly reflects the nature and extent of the candidate's contribution to this work, and the nature of the contribution of each of the co-authors.
- (2) they meet the criteria for authorship in that they have participated in the conception, execution, or interpretation, of at least that part of the publication in their field of expertise;
- (3) they take public responsibility for their part of the publication, except for the responsible author who accepts overall responsibility for the publication;
- (4) there are no other authors of the publication according to these criteria;
- (5) potential conflicts of interest have been disclosed to (a) granting bodies, (b) the editor or publisher of journals or other publications, and (c) the head of the responsible academic unit; and
- (6) the original data are stored at the following location(s) and will be held for at least five years from the date indicated below:

<b>Location(s)</b>	<p><b>MIMR- PHI Institute of Medical Research, Level 3, Monash University, Melbourne, VIC, Australia;</b></p> <p><b>CSIRO Materials Science Engineering, Clayton, Melbourne, VIC, Australia</b></p>
--------------------	---

	<b>Name</b>	<b>Date</b>
<b>Signature 1</b>		20/12/13
<b>Signature 2</b>		20/12/13
<b>Signature 3</b>		20/12/13
<b>Signature 4</b>		20/12/13
<b>Signature 5</b>		04/03/14
<b>Signature 6</b>		06/01/14
<b>Signature 7</b>		20/12/13
<b>Signature 8</b>		20/12/13
<b>Signature 9</b>		20/12/13



TITLE PAGE

Influence of reproductive status on tissue composition and biomechanical properties of ovine vagina

AUTHORS

Daniela Ulrich MD<sup>1,2,6</sup>, Sharon L. Edwards PhD<sup>3</sup>, Kai Su PhD<sup>3</sup>, Jacinta F. White BSc<sup>3</sup>, John AM. Ramshaw PhD<sup>3</sup>, Graham Jenkin PhD<sup>1</sup>, Jan Deprest MD PhD<sup>4</sup>, Anna Rosamilia MD, PhD<sup>2</sup>, Jerome A. Werkmeister PhD<sup>3,5</sup>, Caroline E. Gargett PhD<sup>1,2,5</sup>

<sup>1</sup> The Ritchie Centre, Monash Institute of Medical Research, Melbourne, VIC, Australia

<sup>2</sup> Monash University Department of Obstetrics and Gynecology, Melbourne, Victoria, Australia

<sup>3</sup> CSIRO Materials Science Engineering, Clayton, Melbourne, VIC, Australia

<sup>4</sup> Department of Obstetrics and Gynecology, University Hospitals Leuven, Belgium

<sup>5</sup> equal senior authors

<sup>6</sup> current address, Medical University Graz, Austria

CORRESPONDING AUTHOR:

Jerome Werkmeister, PhD

CSIRO Materials Science Engineering

Clayton, Melbourne, VIC, Australia

Email: [REDACTED]

Phone: [REDACTED]

FINANCIAL DISCLOSURE:

JD has the following financial disclosures: AMS: paid travel expenses or honoraria, payment for research and consultant. BARD: paid travel expenses or honoraria and consultant. Ethicon J& J: paid travel expenses or honoraria, payment for research and consultant. Dynamesh: payment for research.

SHORT TITLE: Biomechanics and composition of ovine vagina

KEYWORDS: extracellular matrix; smooth muscle; quantification; collagen; elastin; virgin; parous; pregnancy; stiffness; distensibility; ovine

## **ABSTRACT**

### **Objective**

To undertake a comprehensive analysis of the biochemical tissue composition and passive biomechanical properties of ovine vagina and relate this to the histo-architecture at different reproductive stages as part of the establishment of a large preclinical animal model for evaluating regenerative medicine approaches for surgical treatment of pelvic organ prolapse.

### **Methods**

Vaginal tissue was collected from virgin (n=3), parous (n=6) and pregnant sheep (n=6; mean gestation; 132 d; term=145d). Tissue histology was analyzed using H+E and Masson's Trichrome staining. Biochemical analysis of the extracellular matrix proteins used a hydroxyproline assay to quantify total collagen, SDS PAGE to measure collagen III/I+III ratios, dimethylmethylene blue to quantify glycosaminoglycans and amino acid analysis to quantify elastin. Uniaxial tensiometry was used to determine the Young's modulus, maximum stress and strain, and permanent strain following cyclic loading.

### **Results**

Vaginal tissue of virgin sheep had the lowest total collagen content and permanent strain. Parous tissue had the highest total collagen and lowest elastin content with concomitant high maximum stress. In contrast, pregnant sheep had the highest elastin and lowest collagen contents, and thickest smooth muscle layer, which was associated with low maximum stress and poor dimensional recovery following repetitive loading.

### **Conclusion**

Pregnant ovine vagina was the most extensible, but the weakest tissue, whereas parous and virgin tissues were strong and elastic. Pregnancy had the greatest impact on tissue composition and biomechanical properties, compatible with significant tissue remodeling as demonstrated in other species. Biochemical changes in tissue protein composition coincide with these altered biomechanical properties.

## **INTRODUCTION**

Pelvic organ prolapse (POP) is a common condition affecting millions of women worldwide. Up to 35% of all women in the US have one or more symptoms of POP frequently involving urinary incontinence (Nygaard et al. 2008). POP is defined as the herniation of the bladder, the uterus or the bowel into the lower genital tract (Haylen et al. 2010) caused by several known and unknown factors. The etiology is not fully understood, but vaginal childbirth trauma is a known risk factor; hormonal status may also be relevant (Lukacz et al. 2006). The support structures of the pelvic floor include the pelvic floor muscles, the cardinal and uterosacral suspensory ligaments and the dense fibromuscular connective tissue of the vaginal wall (Delancey 1992). The cellular components of the vaginal wall comprise fibroblasts which produce the majority of the extracellular matrix (ECM), and smooth muscle cells which function in vaginal contractility. The ECM consists of fibrous proteins (e.g. collagens, elastin), as well as a range of glycosaminoglycans (GAGs) (Couchman and Pataki 2012). The ECM is dynamic and responds to changes in the environment by remodeling. Collagen type I comprises the major fibrillar protein found in bone, ligaments and interstitial tissues and contributes to their tensile strength (Ramshaw et al. 2009). Collagen I, together with elastin and smooth muscle cells influence the biomechanical and particularly the viscoelastic properties of the vaginal wall. Collagen type III is also a fibrillar protein widely distributed in soft tissues and can contribute to

tissue elasticity. An increase in collagen III in healing or regenerating tissues usually reduces its mechanical strength by decreasing the overall collagen fiber diameter of collagen I/III heterofibrils (Hulmes 2002).

Studies of the human vaginal wall especially in the non-prolapsed state have been limited by lack of information on the exact site of tissue acquisition and are often restricted to one type of analysis. Sheep have been suggested as a convenient model for assessing surgical treatments for POP (Couri et al. 2012). The advantage of the ovine vaginal model is that the pelvic tissue anatomy is similar in size and structure to humans. Sheep have prolonged labors with relatively large fetuses and spontaneously develop prolapse related to vaginal birth (Shepherd 1992, Couri et al. 2012). Similar to humans, sheep develop POP over a wide range of ages, but predominantly in the months following delivery. The incidence is greatest in multiparous sheep and increases with parity (Couri et al. 2012). However the model is still poorly defined despite these similarities between sheep and humans.

The aim of this study was to undertake a comprehensive analysis of the biochemical tissue composition and biomechanical properties of ovine vagina and relate this to histo-architecture at different reproductive stages as part of the establishment of a large preclinical animal model for evaluating regenerative medicine approaches for transvaginal surgical treatment of pelvic organ prolapse. A secondary aim was to determine if there were any differences in these parameters between the anterior and posterior vaginal walls, given that bladder involvement occurs in nearly half the cases of ovine POP.

## **MATERIALS AND METHODS**

The experimental procedures and sheep husbandry were approved by the Monash Medical Centre Animal Ethics Committee A (MMCA 2011 45). Border Leicester Merino (BLM)

sheep were housed in the animal house of Monash Animal Service facilities in compliance with the National Health and Medical Research Council of Australia guidelines for the care and use of laboratory animals. The sheep were housed in barns with unlimited food and water supply.

Vaginal tissue was harvested from 3 groups of BLM sheep, virgin, parous (sheep that delivered at least three singleton lambs vaginally), and parous pregnant (3rd stage of pregnancy in sheep that also had delivered 3 singleton lambs vaginally prior to the current pregnancy). All animals were humanely euthanized according to the current guidelines by intravenous administration with Pentobarbitone sodium into the jugular vein (150mg/kg).

A measure of maximum displacement of the vaginal wall was established to quantify vaginal wall distensibility. Ewes were placed in the dorsal recumbency position and values were obtained for points corresponding to Ba, Bp and C of the POP-Q in humans (Bump et al. 1996) by clamping the tissue and traction applied to the vaginal walls approximately 3 cm above the external urethral meatus and to the cervix. The level of maximum displacement was measured in centimeters with a ruler. The complete vaginal tract was immediately excised and full thickness vaginal tissue was collected in a longitudinal manner from the upper third of the anterior and posterior vaginal wall and divided into 3 parts for biomechanical, biochemical, and histological analysis as shown in Figure 1.

The explanted tissue for histological analysis was fixed in 4% paraformaldehyde (PFA) for 24 hours, then oriented and embedded in paraffin to obtain full vaginal thickness, sectioned into 5 $\mu$ m sections and stained with hematoxylin and eosin (H+E) and with Masson's Trichrome. For measurements, only images that showed a full depth (complete set of histological components) were analysed. The four zones in the images were readily

identified using a Trichrome stain. In all cases measurements were taken on the axis perpendicular to the epithelium. The height of the muscularis was measured using NIS-elements RA3.2® software. The maximum and minimum thickness for the muscularis and vaginal wall (epithelium to adventitia) was measured on a single section for each sample for both anterior and posterior walls, and the mean and SEM calculated for each experimental group. For immunohistochemistry the tissue was fixed, embedded and sectioned as above and stained with alpha smooth muscle actin ( $\alpha$ SMA) (Dako, Glostrup, Denmark,) to label smooth muscle cells and myofibroblasts. Sections were dewaxed and rehydrated, and protein block (Dako®) was applied for 30 minutes at RT. After three washes in PBS, sections were incubated with the primary antibody for one hour at 37° C at 1:400 dilution. Mouse IgG1 isotype (Dako) was used for the negative control and applied at the same concentration. Bound antibodies were detected with secondary Streptavidin HRP-conjugated antibody (AbD Serotec®, Oxford, UK) for 30 minutes at RT after 3 washes in PBS. 3,3'-Diaminobenzidine (Sigma-Aldrich®, St. Louis, MO, USA) was used as a chromogen. The slides were dehydrated in graded alcohols and mounted with DPX mounting medium.

The biochemical components were determined in triplicate for each sample for the following assays. Total collagen content was measured by hydroxyproline (Hyp) assay. Freshly excised tissue pieces (5 x 5 mm) were frozen at -20° C. Tissue pieces were then pre-weighed and lyophilized for 4 hours, wet weight is shown in suppl. Figure 1. The dry weight ( $W_{dry}$ ) was recorded and the water content of the original tissue calculated. The dried tissue was digested with papain (0.5 mg/ml in 0.1 M Na<sub>2</sub>HPO<sub>4</sub>, 5 mM EDTA, 5 mM L-Cysteine HCl, pH 7.4) for 16 hours. After centrifuging, the supernatants were hydrolyzed in 6N HCl at 115° C for 4 hours and then desiccated overnight. Hyp was

measured spectrophotometrically at 560 nm after reaction with 0.05 mol/L chloramine-T (Sigma) and 10% (w/v in 2-methoxyethanol)  $\rho$ -dimethylaminobenzaldehyde (Sigma). (Woessner 1961) A standard curve using L-hydroxyproline (0-10  $\mu$ g/mL) (Sigma) was used to calculate the Hyp concentration. Total collagen was calculated using a hydroxyproline to collagen ratio of 0.143:1 (Woessner 1961).

The ratio of collagen type III to collagen type I was determined by an SDS-polyacrylamide gel electrophoresis (SDS-PAGE) using delayed reduction (Sykes et al. 1976) as previously described (Ulrich et al. 2013). Frozen vaginal tissue was thawed to room temperature (RT) for 15 min, and 5 x 5 mm pieces adjacent to the area excised for biomechanical analysis (Fig. 1) were digested for 4 h in pepsin (Sigma) (0.5 mg/ml in 100 mM acetic acid, pH 2.5) at 4 °C followed by brief homogenization with an T10 basic Ultra-Turrax® (IKA®, USA) homogenizer. Samples were further digested in the pepsin solution for 16 h. After centrifugation, 10  $\mu$ l of each sample was mixed with 40  $\mu$ l NuPAGE® LDS sample buffer (Life Technologies), heated to 90 °C for 1-2 min and then loaded onto NuPAGE 4-12% Bis-tris gels (Life Technologies) with MES running buffer (Life Technologies); 50 mM (2-[N-morpholino] ethane sulfonic acid) in 50 mM Tris base (1 mM EDTA, 0.1% SDS; pH 7.3). Samples were electrophoresed for 1 h at 130 V, the power turned off, and 5% v/v 2-mercaptoethanol (Sigma) was added to each well for 1 h. Finally electrophoresis was continued for 3 h at 130 V at 4 °C. Gels were stained with Coomassie Blue R-250 solution destained in 20% ethanol and 5% acetic acid. Images were taken using FujiFilm LAS-3000 software. The percentage of collagen III was calculated from peak sizes using the formula: Percentage type III collagen =  $\text{Area } \alpha 1(\text{III}) \times 1.12 \times 100 / [\text{area } \alpha 1(\text{III}) \times 1.12] + \text{area } \alpha 1(\text{I})$  (Chan D 1984), where a calibration factor of 1.12 was used to correct for the color yield from equal weights of the two collagen types (Chan D 1984).

The insoluble precipitate from the papain-digested and centrifuged sample as described above, comprising insoluble collagen and insoluble elastic tissue associated proteins (ETAP) was used for indirect ETAP analysis. The residual insoluble tissue extract was rinsed in PBS three times and distilled water once before freezing and lyophilization for 4 hours. After weighing ( $W_{res}$ ), the residual tissue was sent to Australian Proteome Analysis Facility (APAF, Macquarie University, NSW, Australia) for amino acid analysis. The weight of insoluble collagen in the residual tissue ( $W_{res-col}$ ) was calculated based on its corresponding Hyp amino acid amount. The percentage of ETAP in the original tissue samples was calculated using the following formula:  $ETAP \% = [(W_{res} - W_{res-col}) / W_{dry}] \times 100$ . Elastin and ETAP distribution in tissues were also visualized with a histological stain (Verhoeff Van Gieson).

Glycosaminoglycan (GAG) content was determined using the colorimetric dimethylmethylene blue (DMMB) assay. Sample preparation was the same as for collagen measurement. After centrifuging, the supernatant was combined with DMMB reagent solution [40 mM NaCl, 40 mM glycine, 0.1 M HCl, 46 mM DMMB (Sigma), pH 3.0] for 2 mins (Chandrasekhar et al. 1987). The concentration of GAG in papain digests was determined spectrophotometrically at 525 nm. Chondroitin sulfate C from shark cartilage (Sigma) was used as the standard (0-0.5 mg/mL).

Vaginal tissue for mechanical testing was dissected from virgin (n=3), parous (n=7), and pregnant (n=6) sheep, and stored at -20 °C until testing. Frozen tissues were thawed overnight at 4 °C and tested within 24 hours of thawing. Testing of frozen-thawed vaginal tissue does not alter the mechanical properties and is more reliable as the same conditions are used for each specimen (Rubod et al. 2007). Dog-bone shaped samples of central dimensions 4x34 mm were punched from the sheep anterior and posterior tissues in the

longitudinal axis (Fig. 1) and kept moist using PBS. Prior to testing, sample thickness (n=3) was measured using digital calipers and used to calculate the initial cross sectional area of the sample. Uniaxial tensiometry was performed using an Instron® Tensile Tester (5567® Instron Corp, USA) and a 5 kN load cell. To avoid tissue slippage, samples were secured in pneumatic serrated jaws, which were set to a gauge length of 14 mm. Samples were then preloaded at 10 mm/min to 100 mN and then cyclically loaded from 0 to 1 N, 0 to 2 N, and 0 to 3 N, for 5 cycles each, at 20 mm/min and finally extended to break. This test method is based on the assessment of human vaginal tissue (Rubod et al. 2007, Rubod et al. 2008, Jean-Charles et al. 2010, Rubod et al. 2012), with loading values chosen to avoid damage to the ovine tissues.

Stress-strain curves were plotted from the force and elongation data generated, calculating nominal stress (MPa, where  $1\text{Pa} = 1\text{N}/\text{mm}^2$ ) by dividing the force (N) by the initial cross sectional area ( $\text{mm}^2$ ) and the strain by dividing the extension (mm) by the initial gauge length (mm). The Young's modulus (MPa) was determined from the slope of the stress-strain curve in the linear region (Ozog et al. 2011, Edwards et al. 2013). This was identified as the region immediately following cyclic loading and prior to yielding (Fig. 2). Permanent strain (%) was calculated as the percentage increase in sample length following cyclic loading (Edwards et al. 2013). Maximum stress (MPa) was derived from the stress-strain curve and maximum strain (%) was calculated from the corresponding maximum strain, derived from the stress-strain curve (Fig. 2).

GraphPad Prism 6 was used for statistical analysis. Results are reported as mean  $\pm$  SEM for each of the three experimental groups. Since the data was not normally distributed (D'Agostino & Pearson omnibus normality test), non-parametric analysis using Kruskal – Wallis ANOVA and post hoc test for comparisons between the different groups (Tukey's

correction). Differences between the anterior and posterior wall was determined by paired t-tests. P values < 0.05 were considered statistically significant.

## **RESULTS**

Virgin sheep were one year old, while parous and pregnant sheep were 4 to 5 years old and had delivered 3 lambs prior to the study. The mean gestational age of the fetus in the pregnant sheep was  $132 \pm 8$  days. We developed a clinical score for vaginal wall distensibility by measuring the maximum displacement under traction as shown in Table 1. There was hardly any displacement of the anterior and posterior walls at points 3cm above the urethral orifice in virgin and parous sheep. In pregnancy, the mean displacement was 3.3 cm with traction of both vaginal walls. There was no difference in displacement of the cervix with traction in any of the sheep.

Histologically, the vaginal wall from all groups showed the typical 4 zones from the superficial stratified squamous epithelium, dense connective tissue lamina propria, a muscularis of smooth muscle cells and connective tissue, to the loose connective adventitia (Fig. 3). The virgin sheep (Fig. 3A, B) had a dense connective tissue with moderate uniform cell infiltrates and blood vessels in the lamina propria with densely packed collagen (Fig. 3 C, D). The vaginal architecture of the parous sheep was similar to that of virgin sheep with respect to epithelial height, vessel density (Fig. 3 E, F), and densely packed collagen (Fig. 3 G, H). Pregnant ovine vaginal tissue was strikingly different with fewer cells but similar density of blood vessels in the lamina propria (Fig, 3 I, J) and markedly less dense tissue and collagen packing in all layers (Fig. 3 K,L).

The relative amount of smooth muscle cells (SMC) was quantified by measurement of the extent of the muscularis layer from Masson Trichrome-stained sections of each anterior

and posterior vaginal tissue from each group. Alpha smooth muscle actin ( $\alpha$ SMA) staining was used to confirm SMC presence within the muscularis (Fig. 4). There were extensive variations in the absolute thickness of the muscularis within and between each group, due to inter subject variation. In most sections, the different zones of lamina propria, muscularis and adventitia were not uniform in thickness, so Table 2 shows the mean minimum and maximum thickness ( $\mu\text{m}$ ) from sections from replicate animals. The pregnant group showed the highest proportion of muscularis in the vaginal wall (71.1% and 76.5%, anterior and posterior, respectively) and was significantly greater ( $p < 0.05$ ) than vaginal tissue from virgin sheep (50.5% and 45.0%, anterior and posterior, respectively). Tissue from parous sheep showed the greatest variation in muscularis thickness between anterior (65.1%) and posterior (50.7%) location, although these were not significant. The muscularis of parous posterior vaginal tissue was also significantly less than the posterior vaginal wall of pregnant animals ( $p < 0.05$ ).

The percentage of total collagen relative to tissue dry weight in the anterior wall of parous sheep was significantly higher than in the anterior walls of virgin and pregnant sheep ( $p < 0.001$ ,  $p < 0.0001$ ), respectively (Fig. 5A). Similarly, the posterior vaginal wall from parous sheep had greater total collagen content than tissues from both the virgin and pregnant sheep ( $p < 0.05$ ). The total collagen content was similar between the anterior and posterior vaginal wall for the virgin, parous and pregnant sheep (Fig. 5A). The collagen ratio type III/ total collagen type I + III, did not reveal any significant differences between virgin, parous or pregnant groups (Fig. 5B) or between the anterior and posterior vaginal walls (Fig. 5B).

The ETAP protein content of the parous group was significantly lower in both the anterior and posterior vaginal wall compared to that of the virgin ( $p < 0.01$ ,  $p < 0.05$ , respectively)

and pregnant ( $p < 0.0001$ ,  $p < 0.01$ ) ovine tissue (Fig. 5C). The ETAP content of the anterior vaginal wall of the pregnant sheep was significantly higher than the virgin sheep ( $p < 0.05$ ). The anterior and posterior vaginal wall ETAP content was similar within each of the three groups (Fig. 5C). In addition the distribution of elastin and ETAP is demonstrated by a Verhoeff Van Gieson histological stain (Fig. 6). The staining points out that elastin (and ETAP) are really a minor component in these tissues with very low levels in the lamina propria and mainly localised in pockets within the deep muscularis.

The total GAG content of virgin, parous and pregnant ovine vaginal tissues was low compared with the other ECM proteins. The virgin sheep showed significantly lower values ( $p < 0.05$ ) in the anterior wall compared to the parous sheep (Fig. 5D). However no differences were observed in the posterior vaginal walls between the groups (Fig. 5D). In contrast to virgin and parous sheep, pregnant sheep showed significantly less GAG in the anterior compared to the posterior vaginal wall. All ECM quantitation were based on %ECM/  $\mu\text{g}$  dry weight of tissue. The water content remained similar in all groups (Supplementary Fig. 1).

The non-linear stress strain curves showed an immediate region of low stiffness, followed by a region of higher stiffness in the linear region (Fig. 2); cyclic loading occurred in the transitioning region between the low and higher stiffness parts of the curve (Fig. 2). The Young's modulus (Fig. 7A) of the pregnant tissue was smaller than virgin and parous tissue types, but results were not significant. Pregnant tissue also had the smallest maximum stress (Fig. 7B), which was significantly lower than for the anterior tissue of the virgin group ( $p < 0.05$ ). Permanent strain was highest for the pregnant sheep, with significantly higher strains compared to the parous and virgin groups for both anterior ( $p < 0.05$ ,  $p < 0.01$ ) and posterior ( $p < 0.0001$ ,  $p < 0.01$ ) tissues respectively (Fig. 7C). The

virgin posterior tissue had significantly higher permanent strain than the parous tissue ( $p < 0.01$ ). Similarly, maximum strain was highest for the posterior tissue of the pregnant group compared to the posterior tissues of the parous ( $p < 0.001$ ) and virgin ( $p < 0.05$ ) groups (Fig 7D). Significant differences between anterior and posterior tissues were found for permanent strain in virgin and pregnant tissues (both  $p < 0.05$ ), and maximum strain for pregnant tissues ( $p < 0.05$ ), but none were observed for parous tissue for any of the biomechanical parameters examined. Tissues studied exhibited the Mullins effect, showing an increased strain at the same stress level for subsequent loading cycles. Although not quantified, it was observed that this effect was more pronounced for the pregnant tissue than the other tissue types (Fig. 2).

## **DISCUSSION**

In this study we provide the first comprehensive analysis of normal ovine vaginal tissue composition combining histological, biochemical and biomechanical analyses at different reproductive stages. We also described the first clinical assessment of vaginal wall and cervical displacement with traction. We found that parous sheep had the lowest ETAP and highest collagen content relative to tissue dry weight, and that pregnant sheep had the highest ETAP content and thickest musculature. Pregnant ovine vagina was the most extensible, but weakest tissue, with least dimensional recovery following repetitive loading. The parous and pregnant groups were of equivalent parity, indicating that pregnancy has the greatest influence on ovine vaginal ECM tissue composition and biomechanical properties. In general, there was a trend toward increased stiffness of anterior, compared to posterior tissue, reflecting the findings of other studies, in which anterior POP and non-POP vaginal tissues were stiffer than their posterior tissue

counterparts (Jean-Charles et al. 2010). However, anterior tissue was less extensible and more elastic than posterior vaginal tissue.

A recent review concluded that the clinical data on vaginal tissue composition was inconclusive due to the heterogeneity of reported data and inadequate standardization and quantification of the changes (De Landsheere et al. 2013). We showed that the vagina predominantly comprises collagen type I which is largely responsible for its tensile strength. Parous vaginal tissue had the highest total collagen content relative to dry tissue weight which was associated with a high maximum (breaking) stress. In contrast, pregnant tissue had significantly less collagen, which may be associated with the lower maximum stress. We did not find any quantitative differences in the level of collagen type III between pregnant, virgin and parous sheep. Ennen et al examined sheep with antepartum prolapses and found that mRNA expression for collagen type I was decreased, implying that elevated collagen type III may be associated with POP (Ennen et al. 2011).

Elastin is the other major fibrillar protein found in soft viscoelastic tissues. The ETAP content was significantly lower in vaginal tissues from parous sheep. Elastic fibres are normally intended to last a lifetime except in reproductive tissue where high degradation and re-synthesis was observed (Abramowitch et al. 2009). The muscles and connective tissue of the vaginal wall are responsible for its mechanical integrity and functionality. Both the lamina propria and the muscularis contribute to the strength and visco-elasticity of the vagina. The changes in the vaginal connective tissue ETAP composition were consistent with our mechanical assessment of these tissues. Pregnant vaginal tissue contained the highest ETAP and thickest muscularis and associated smooth muscle cell content; it was the least stiff (Young's modulus) and most extensible tissue (maximum strain), with an average four-fold decrease in stiffness and two-fold increase in maximum strain, compared to parous sheep of similar parity, and to virgin vaginal tissue. These

findings are in agreement with studies in mice (Rahn et al. 2008) and rats (Lowder et al. 2007) where the supportive perivaginal tissues decreased in stiffness and strength during pregnancy and returned to virgin levels four weeks after delivery (Lowder et al. 2007). However, another rat study showed increased vaginal distensibility during pregnancy compared to virgins, which did not return to virgin levels four weeks postpartum (Alperin et al. 2010). We also found a higher level of induced permanent strain following cyclic loading in pregnant vaginal tissue, indicating it was the least elastic by this measure and the least likely to return to its original dimensions. Previous studies characterizing hysteresis by cyclic loading found vaginal tissue visco-hyperelastic (Abramowitch et al. 2009) and to exhibit the Mullins effect (Diani et al. 2009); with a smaller stress required to reach a prescribed strain in subsequent loading cycles. In our study, the Mullins effect was more pronounced for pregnant vaginal tissue compared to that from virgin and parous ewes. We suggest that such a large elastic deformation permits the passage of the fetus through the vagina during delivery as described in other studies.

An ideal animal model for prolapse research has not yet been established. Rats and rabbits are cost effective and available in large numbers (Abramowitch et al. 2009), however, their reproductive tract is small and the pelvic musculature is different from humans (Abramowitch et al. 2009). The reproductive tract of sheep is large with similar vaginal dimensions as humans, and with similar pelvic organ support by the three primary levels although the pelvic musculature differs (Abramowitch et al. 2009). Furthermore, sheep experience high internal pressure on the pelvic structures compared to other quadruped species due to their ruminant anatomy (Couri et al. 2012). The ovine model may therefore be a more suitable preclinical model (Abramowitch et al. 2009, Deprest and Feola 2013) for evaluating regenerative medicine approaches for transvaginal surgical treatment of

POP. Macaques would be an ideal model, but their prohibitive costs and ethical restrictions are much greater than for sheep (Abramowitch et al. 2009).

In conclusion, our data showed that vaginal tissue is dynamic, undergoing profound changes in connective tissue composition that influence the biomechanical behavior, particularly during pregnancy. We speculate that varying degrees of vaginal tissue recovery might explain why some females develop POP and others do not.

#### ACKNOWLEDGMENTS

The authors wish to thank Dr. Keith McLean and Dr. Joseph Lee for helpful advice.

**Table 1** Measurements of vaginal wall and cervical maximum displacement under traction

	Virgin	Parous	Pregnant	p- value
Ba	0.8 ± 0.3	1 ± 0.4	3.3 ± 1	< 0.05*
Bp	0.8 ± 0.3	1 ± 0.4	3.2 ± 0.8	< 0.05*
C	1.5 ± 0.9	1.5 ± 0.6	1.6 ± 0.8	ns

Data are reported as mean ± SEM in cm for n=3 virgin and n=6 each for parous and pregnant ewes. \* compared between virgin versus pregnant and parous versus pregnant. Ba, reference point 3 cm proximal of the external urethral meatus of the anterior wall. Bp, reference point on the posterior wall opposite Ba. C, Cervix. Ns, not significant.

**Table 2.** Measurements of the muscularis thickness in virgin, parous and pregnant sheep.

Tissue		Muscularis thickness, ( $\mu\text{m} \pm \text{SEM}$ )		Total muscularis (% of total wall thickness <sup>1</sup> ± SEM )
		Min <sup>2</sup>	Max <sup>2</sup>	
Virgin	Anterior	1359 ± 144	1970 ± 149	50.5 ± 6.2*
	Posterior	1037 ± 271	2201 ± 439	45.0 ± 9.3**
Parous	Anterior	2047 ± 356	3325 ± 598	65.1 ± 8.1
	Posterior	1537 ± 311	2747 ± 146	50.7 ± 6.9**
Pregnant	Anterior	1983 ± 377	2440 ± 486	71.1 ± 5.9*
	Posterior	2436 ± 193	3428 ± 596	76.5 ± 5.5**

<sup>1</sup> Total thickness was measured from the surface, including the epithelium, to the serosal border.

<sup>2</sup> numerous measurements (>20) were taken to establish minimum and maximum values for each slide.

p < 0.05 (\*pregnant anterior compared to virgin anterior; \*\*pregnant posterior compared to virgin posterior and to parous posterior)

## FIGURE LEGENDS

**Figure 1.** Schematic showing dissection of ovine vaginal tissue for 1 biomechanical testing, 2 histology, 3 biochemical analysis.

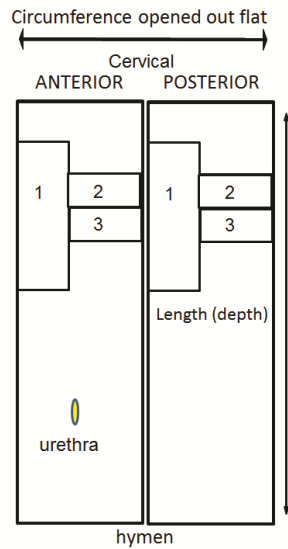


**Figure 2.** Typical stress-strain curves for parous, virgin and pregnant ovine vaginal tissue, indicating maximum stress and strain, Young's modulus, and permanent strain for the virgin tissue curve.

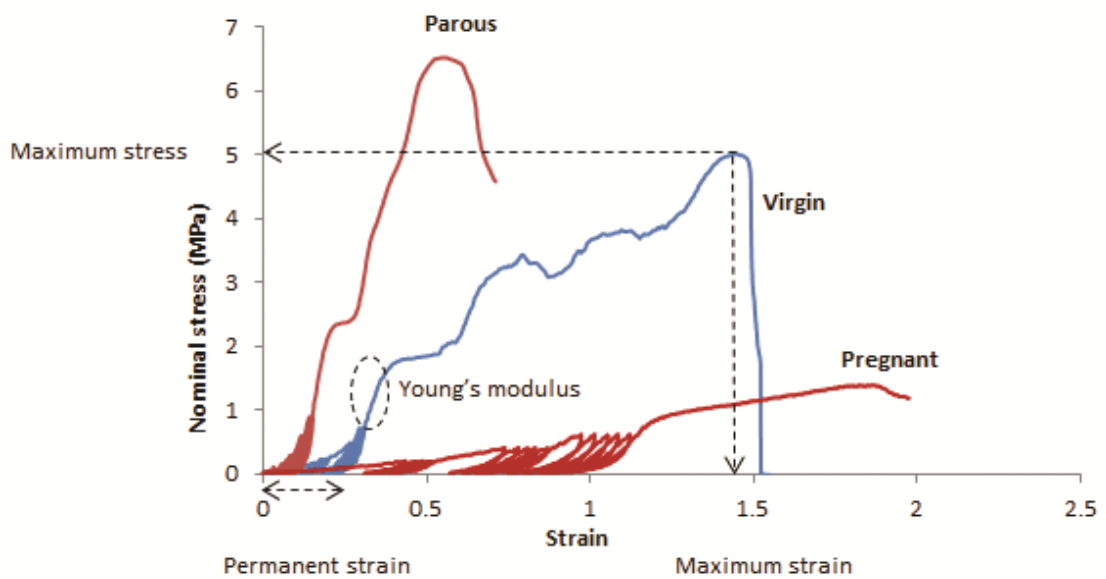


**Figure 3.** Histological structure of ovine vaginal wall. H+E and Masson stained sections showing the anterior and posterior vaginal walls of virgin (A-D), parous (E-H) and pregnant sheep (I-L). \* indicates blood vessels. In image E arrows indicate the 3 vaginal layers. Scale bar for H+E sections 100  $\mu$ m, for Masson sections 250  $\mu$ m.

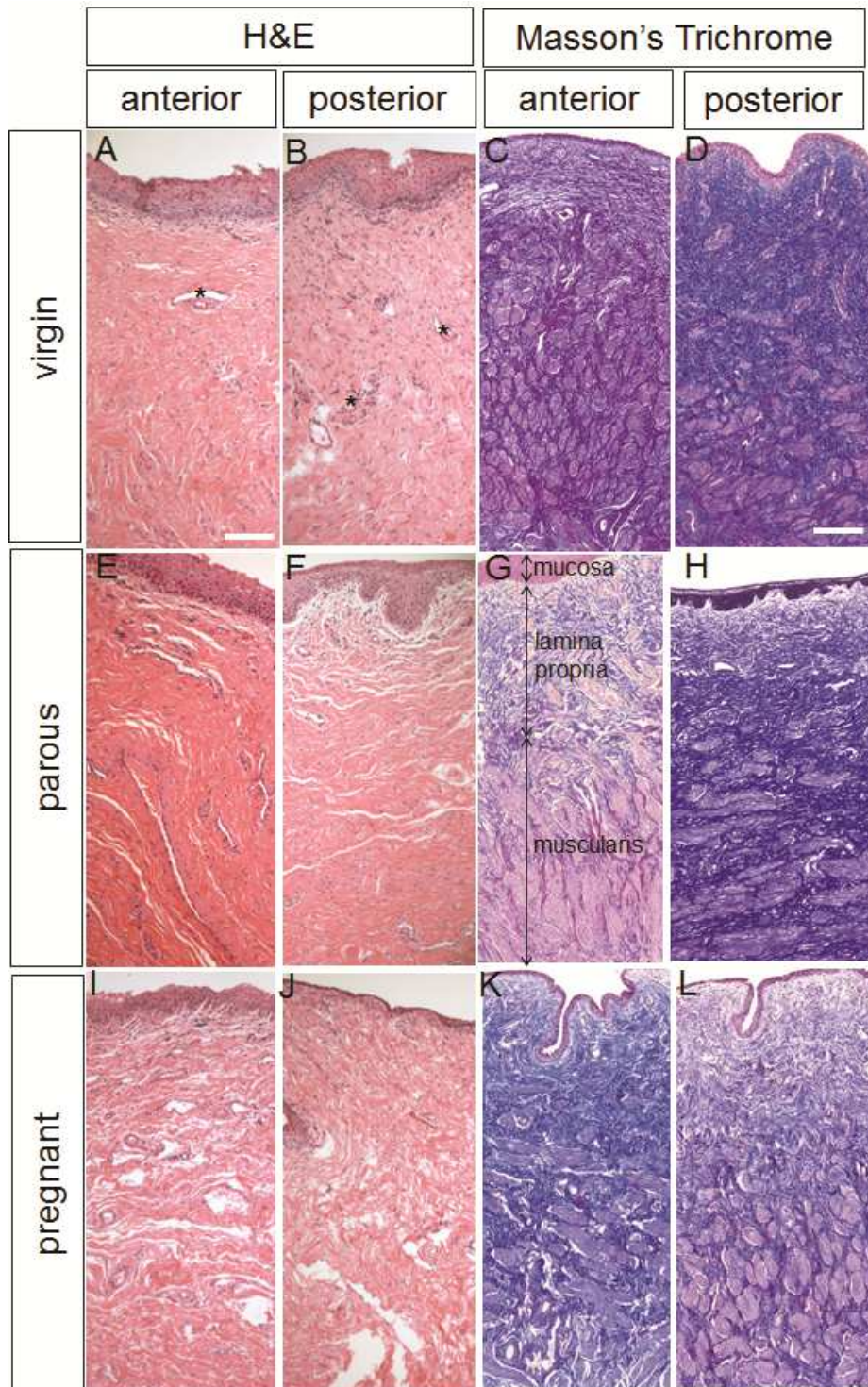


**Figure 4.**  $\alpha$ SMA immunohistochemical staining of ovine vaginal wall. A. virgin, B. parous, C. pregnant ovine vaginal tissue. Dotted lines indicate the muscularis layer. Scale bar 200  $\mu$ m.

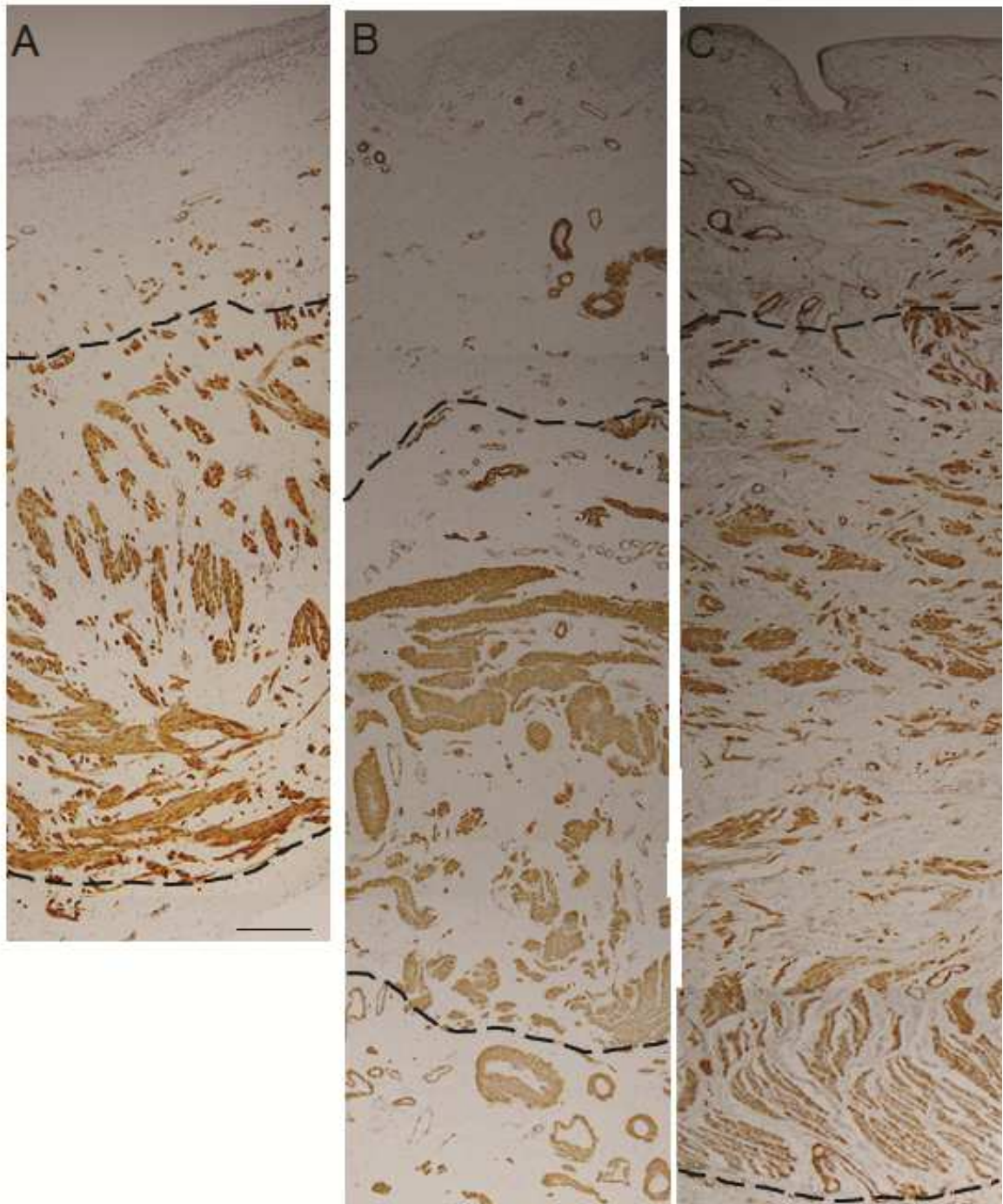


**Figure 5.** Biochemical analysis of the ECM content of the vaginal wall of virgin, parous and pregnant sheep. A. % total collagen per dry weight assessed by hydroxyproline assay in the anterior (black bars) and posterior (grey bars) vaginal wall. B. % collagen III/ (I+III) analysed by SDS-PAGE. C. % Elastin per dry weight by Amino Acid Analysis. D. % GAG per dry weight by DMMB assay. Data is presented as mean ( $\pm$ SEM), n=6/ group for parous and pregnant and n = 3 for virgin ewes. \*  $p < 0.05$ , \*\*\*  $p < 0.001$ , \*\*\*\*  $p < 0.0001$ .

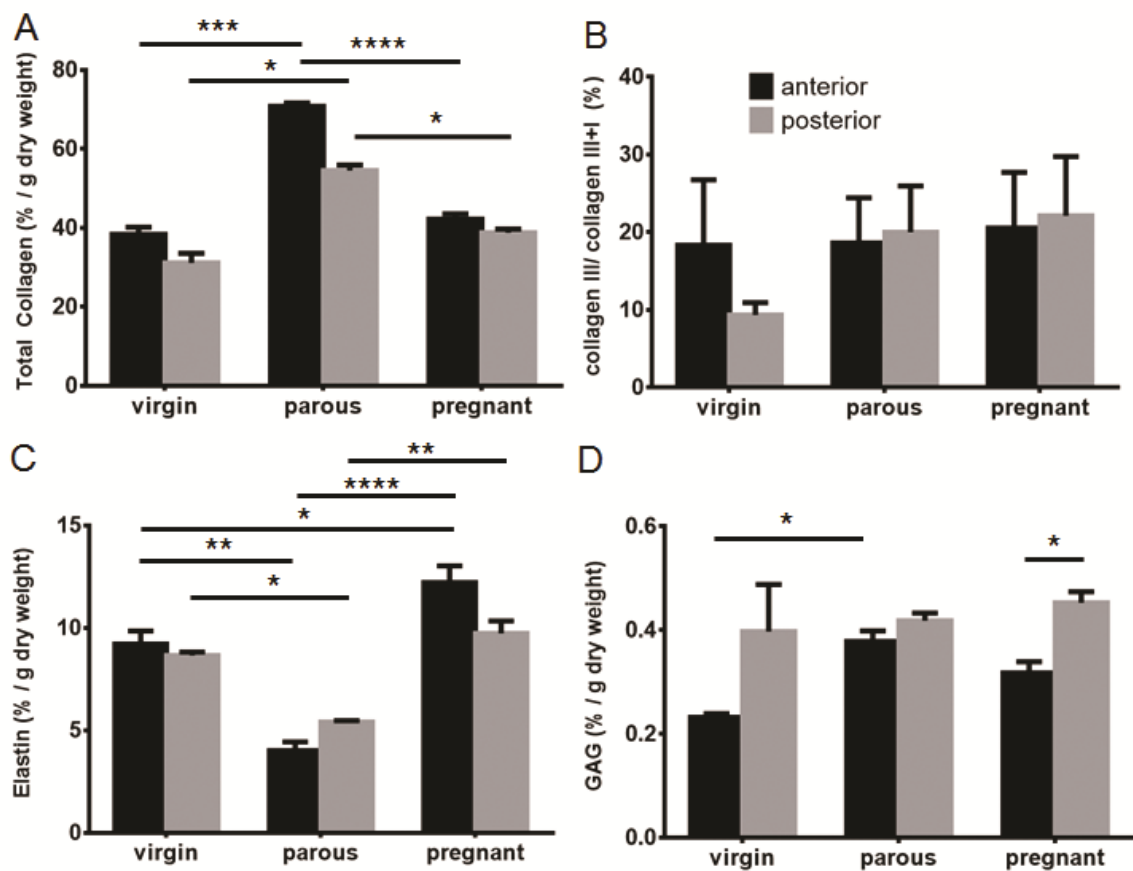


**Figure 6.** Verhoeff- Van Gieson staining for elastic fibres (black) on virgin (anterior), parous (posterior) and pregnant (posterior) vaginal tissues. The white arrows on the full thickness images A, D, G denote the region where the higher magnification images were taken in the lamina propria (B, E, H) and deep muscularis (C, F, I). The green arrows indicate regions of elastic fibres. Scale bars 500  $\mu\text{m}$  (full thickness images) and 50  $\mu\text{m}$  (high magnification images).

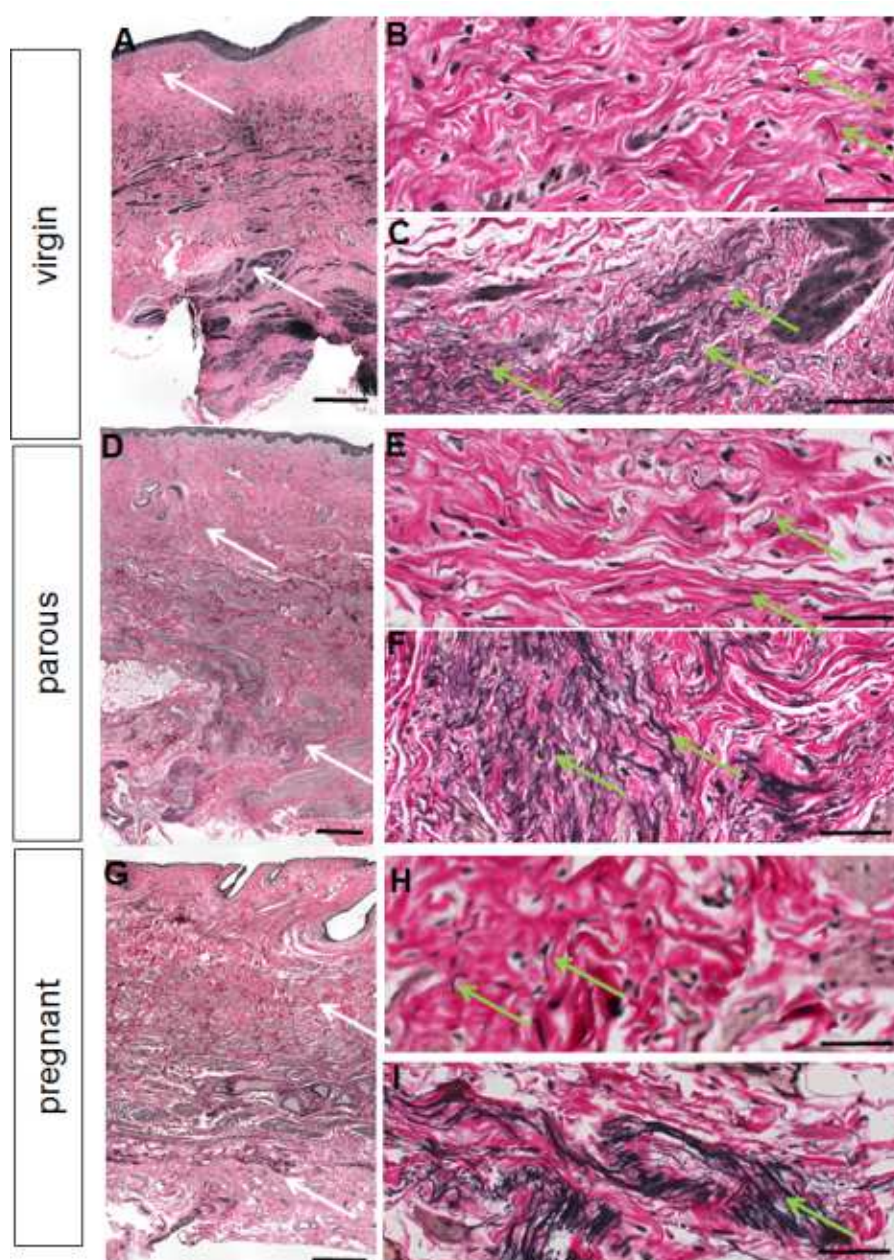
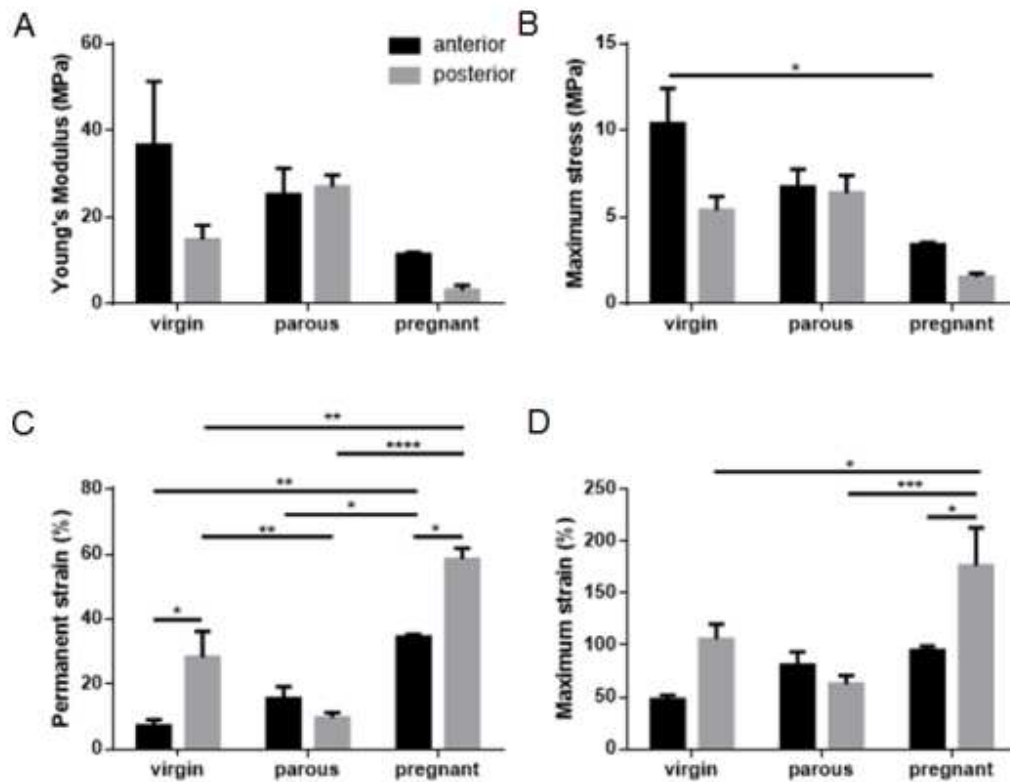
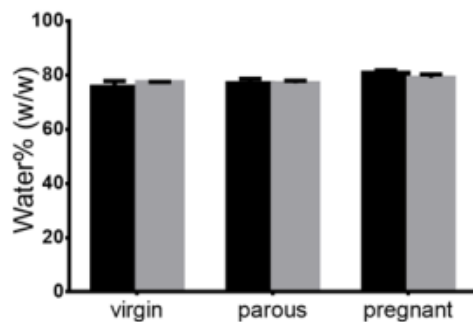


**Figure 7.** Biomechanical properties of ovine vaginal wall. A. Young's modulus (MPa) B. Maximum stress (MPa). C. Permanent strain (%). D. Maximum strain (%) in virgin, parous and pregnant ewes in the anterior (black bars) and posterior (grey bars) vaginal wall, calculated as described in Figure 2. Data is presented as mean ( $\pm$ SEM), n=2-7 replicates/group. \* p< 0.05, \*\*p<0.01, \*\*\* p< 0.001, \*\*\*\* p< 0.0001.



**Supplementary Figure 1.** Wet weight of virgin, parous and pregnant sheep, anterior (black bars) and posterior (grey bars) vaginal wall. Data is presented as mean ( $\pm$ SEM), n=6/ group for parous and pregnant and n = 3 for virgin ewes.



## **CHAPTER 6**

### **Comparison of ovine and human vaginal tissue composition and properties**

In chapter 5 I demonstrated that there are complex differences in ovine vaginal tissue dependent on the different reproductive stages in terms of collagen, GAG and elastin composition as well as in the biomechanical properties with pregnancy having the greatest effect on tissue composition and biomechanical properties.

To establish a reliable preclinical model we wanted to compare ovine and human vaginal tissue. We further wanted to determine whether there are regional differences in the vaginal wall. In humans, vaginal tissue collection in young, healthy women without POP is unethical. We therefore decided to set up a postmenopausal sheep model as a surrogate matched control group to postmenopausal women.

For this chapter I established a model of postmenopausal sheep by removing the ovaries in a surgical setting and leaving the sheep for 3 months. I thank Dr. Vincent Letouzey for his intellectual input and help with the study design. My thank also goes to Dr. Jan Deprest and Graham Jenkins for their advice.

I performed a comprehensive analysis of vaginal tissue in ovine and human tissue using the same techniques as described in chapter 5 with similar contributions of the co-authors.

## Monash University

### Declaration for Thesis Chapter 6

#### Declaration by candidate

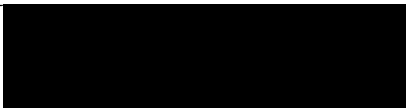
In the case of Chapter 6, the nature and extent of my contribution to the work was the following:

<b>Nature of contribution</b>	<b>Extent of contribution (%)</b>
Study design, Animal experiments, Tissue harvesting, Tissue processing, Tissue staining, Image analysis, Biochemical testing, Biomechanical testing, Data analysis, Statistical analysis, Data interpretation, Paper writing	70

The following co-authors contributed to the work. Co-authors who are students at Monash University must also indicate the extent of their contribution in percentage terms:

<b>Name</b>	<b>Nature of contribution</b>	<b>Extent of contribution (%) for student co-authors only</b>
<b>Dr. Sharon L. Edwards</b>	Biomechanical testing, Data analysis	
<b>Dr. Vincent Letouzey</b>	Study design, Animal experiments, Tissue harvesting, Data interpretation	
<b>Dr. Kai Su</b>	Biochemical testing	
<b>Jacinta F. White</b>	Tissue staining, Image analysis	
<b>Dr. Anna Rosamilia</b>	Tissue harvesting	
<b>Dr. Caroline E. Gargett</b>	Study design, Data analysis, Data interpretation, paper writing	
<b>Dr. Jerome A. Werkmeister</b>	Study design, Data analysis, Data interpretation, Paper writing	

**Candidate's Signature**

	<b>Date</b> 07.03.2014
--	---------------------------

**Declaration by co-authors**

The undersigned hereby certify that:

- (1) the above declaration correctly reflects the nature and extent of the candidate's contribution to this work, and the nature of the contribution of each of the co-authors.
- (2) they meet the criteria for authorship in that they have participated in the conception, execution, or interpretation, of at least that part of the publication in their field of expertise;
- (3) they take public responsibility for their part of the publication, except for the responsible author who accepts overall responsibility for the publication;
- (4) there are no other authors of the publication according to these criteria;
- (5) potential conflicts of interest have been disclosed to (a) granting bodies, (b) the editor or publisher of journals or other publications, and (c) the head of the responsible academic unit; and
- (6) the original data are stored at the following location(s) and will be held for at least five years from the date indicated below:

<b>Location(s)</b>	<b>MIMR- PHI Institute of Medical Research, Level 3, Monash University, Melbourne, VIC, Australia;</b> <b>CSIRO Materials Science Engineering, Clayton, Melbourne, VIC, Australia</b>
--------------------	--

	<b>Name</b>	<b>Date</b>
<b>Signature 1</b>		<b>20/12/13</b>
<b>Signature 2</b>		<b>20/12/13</b>
<b>Signature 3</b>		<b>20/12/13</b>
<b>Signature 4</b>		<b>20/12/13</b>
<b>Signature 5</b>		<b>20/12/13</b>
<b>Signature 6</b>		<b>20/12/13</b>
<b>Signature 7</b>		<b>20/12/13</b>



TITLE PAGE

**Regional variation in tissue composition and biomechanical properties of postmenopausal ovine and human vagina**

AUTHORS

Daniela ULRICH, MD <sup>1,5</sup>, Sharon L. EDWARDS, PhD <sup>2</sup>, Vincent LETOUZEY MD, PhD <sup>1,3</sup>, Kai SU, PhD <sup>2</sup>, Jacinta F. WHITE, Ms <sup>2</sup>, Anna ROSAMILIA MD, PhD <sup>4</sup>, Caroline E. GARGETT, PhD <sup>1,4,6</sup>, Jerome A. WERKMEISTER, PhD <sup>2,6</sup>

<sup>1</sup> The Ritchie Centre, MIMR-PHI Institute of Medical Research, Clayton, 3168, Melbourne, VIC, Australia

<sup>2</sup> CSIRO Materials Science and Engineering, Clayton, 3168, Melbourne, VIC, Australia

<sup>3</sup> Department of Gynecology and Obstetrics, Caremeau University Hospital, Nîmes, France.

<sup>4</sup> Monash University Department of Obstetrics and Gynaecology, Monash Medical Centre, Melbourne, VIC, Australia

<sup>5</sup> Current address: Medical University Graz, Auenbruggerplatz 14, 8036 Graz, Austria

<sup>6</sup> equal senior authors

DISCLOSURE STATEMENT: The authors do not report any conflicts of interest.

SOURCES of FINANCIAL SUPPORT: This study was supported by the National Health and Medical Research Council (NHMRC) of Australia grant (1021126) (CEG, JAW, AR) and Senior Research Fellowship (1042298) (CEG), South East Melbourne Alliance for Regenerative Therapies (CEG, JAW, AR, SE), Australian Gynaecological Endoscopic Society grant (AR) and Victorian Government's Operational Infrastructure Support Program.

CORRESPONDING AUTHOR:

Jerome Werkmeister, PhD

CSIRO Materials Science Engineering

Clayton, Melbourne, VIC, Australia

[REDACTED]

[REDACTED]

Word count abstract: 246

Word count main text: 2999

#### CONDENSATION

Ovine and human vaginal tissues show comparable biochemical composition suggesting that sheep are a suitable animal model for preclinical prolapse research.

#### SHORT TITLE

Ovine and human vaginal tissue characterisation

## **ABSTRACT**

### **Objective**

There are increasing numbers of reports describing human vaginal tissue composition in women with and without pelvic organ prolapse with conflicting results. The aim of this study was to compare ovine and human posterior vaginal tissue in terms of histological and biochemical tissue composition and to assess passive biomechanical properties of ovine vagina to establish a suitable animal model for pelvic organ prolapse research.

### **Study design**

Vaginal tissue was collected from ovariectomised sheep (n=6) and from postmenopausal women (n=7) from the proximal, middle and distal thirds. Tissue histology was analysed using Masson's Trichrome staining; total collagen was quantified by hydroxyproline assays, collagen III/I+III ratios by delayed reduction SDS PAGE, glycosaminoglycans by dimethylmethylene blue assay, and elastic tissue associated proteins (ETAP) by amino acid analysis. Young's modulus, maximum stress/strain, and permanent strain following cyclic loading were determined in ovine vagina.

### **Results**

Both sheep and human vaginal tissue showed comparable tissue composition. Ovine vaginal tissue showed significantly higher total collagen and glycosaminoglycan values ( $p < 0.05$ ) nearest the cervix. No significant differences were found along the length of the human vagina for collagen, GAG or ETAP content. The proximal region was the stiffest (Young's modulus,  $p < 0.05$ ), strongest (maximum stress,  $p < 0.05$ ) compared to distal region, and most elastic (permanent strain).

### **Conclusion**

Sheep tissue composition and mechanical properties showed regional differences along the postmenopausal vaginal wall not apparent in human vagina, although the absolute content of proteins was similar. Ovariectomised sheep may be a suitable preclinical model for POP surgery.

### **Key Words**

Extracellular matrix, human vagina, mechanical properties, pelvic organ prolapse, ovine vagina

## MAIN TEXT

### INTRODUCTION

Pelvic organ prolapse (POP), the herniation of the pelvic organs into the vagina, affects up to 25% of all women (Nygaard et al. 2008). POP predominantly results from vaginal childbirth injury and is exacerbated by ageing, obesity and other factors. However, due to multifactorial reasons the exact aetiology is unclear since young or nulliparous healthy women also develop POP, although at much lower frequency than parous women (Gyhagen et al. 2013).

The pelvic organs are supported at three different levels by the pelvic floor muscles, the cardinal and uterosacral ligaments and the dense fibromuscular connective tissue of the vaginal wall, termed the endopelvic fascia (Delancey 1992). The connective tissue of the endopelvic fascia is derived from resident fibroblasts. The main proteins of the extracellular matrix (ECM) are collagen and elastin (Gerhard Meisenberg 2006). The muscularis mainly comprises smooth muscle cells, and along with ECM, is a dynamic structure that undergoes changes in response to the environment. Together collagen type I and III, elastin and smooth muscle cells are mostly responsible for the biomechanical properties of the tissue.

Sheep may be a suitable model for preclinical studies to perform POP research (Abramowitch et al. 2009, Couri et al. 2012); sheep have a similar sized pelvic region, large fetal head-maternal pelvis ratio and spontaneously develop POP pre- and postpartum. There are an increasing number of reports on the composition of sheep and human vaginal tissue; however, most studies only perform one type of analysis or do not describe the exact location. It is therefore difficult to accurately compare the results and draw conclusions (Ennen et al. 2011, Gabriel et al. 2011). To date, no study has compared human and ovine tissue to justify sheep as a suitable model for basic scientific research in the field of urogynaecology. Regional differences have been observed in the vaginal tissue of rats (Skoczylas et al. 2013) where the contractility and gross anatomy varied along the vagina. Prolapse repair with synthetic meshes is often associated with severe side effects like pain, infection or erosion. It is necessary to define the tissue at different parts of the vagina to understand prolapse repair and to introduce a large animal model for future preclinical studies. The aim of this study was to assess the variation of histoarchitectural,

ECM and biomechanical properties along the length of the vagina of postmenopausal ovine vagina and to compare these findings to human tissue from postmenopausal women.

## **MATERIALS AND METHODS**

### **ANIMALS**

The experimental procedures and sheep husbandry were approved by the Monash Medical Centre Animal Ethics Committee A. Border Leicester Merino sheep were housed in the Monash Animal Service facilities in compliance with the National Health and Medical Research guidelines for the care and use of laboratory animals.

Vaginal tissue was harvested from 6 postmenopausal sheep that had delivered 3 lambs vaginally with the last lamb being delivered at least 12 months prior. A postmenopausal model was achieved by surgical removal of the ovaries. The animals were sedated with Medetomidine; anaesthesia was induced with Pentobarbitone sodium followed by isoflurane inhalation with ventilation (1.5-2.5%) in 100% O<sub>2</sub>. Antibiotics (Amoxicillin 1g) were administered. The sheep were placed in dorsal recumbency and the wool shaved on the abdomen followed by skin prepping using Chlorhexidine, 70% alcohol and Betadine. A fentanyl patch was applied to secure pain relief. A 10 cm lower abdominal midline incision was performed and the ovaries removed. The abdominal fascia and subcutis were closed continuously, respectively, with 3/0 Vicryl followed by local anaesthetic (Bupivacaine, 5 ml) infiltration under the skin. 16 weeks after ovariectomy, animals were humanely euthanized by intravenous administration of Pentobarbitone sodium (150mg/kg). A measure of maximum displacement of the vaginal wall was performed on the posterior vaginal wall 3 cm above the muco-cutaneous junction zone corresponding to point Bp of the POP-Q and by traction on the cervix (Bump et al. 1996). The complete vaginal tract was removed from the 6 sheep immediately after euthanization; full vaginal thickness tissue was collected in a longitudinal manner from the posterior vaginal wall starting at the muco-cutaneous junction zone to the cervix. Tissue for biochemical, histological and biomechanical analysis was obtained at 20% (p20), 50% (p50) and 80% (p80) of the posterior vagina with p20 representing the distal third close to the hymen and p80 the proximal third close to the cervix (Fig. 1).

## HUMANS

Human tissue collection was approved by the Monash Health Human Research Ethics committee B. All women gave written informed consent. A thorough clinical history and pre-operative POP-Q parameters were obtained. Vaginal tissue was obtained from 7 women undergoing vaginal pelvic organ prolapse reconstructive surgery. Redundant vaginal tissue was excised from the midline and obtained at 20, 50, and 80% (at point of excision, Fig.1) of the vagina in a similar manner to the sheep tissue acquisition for histology and biochemical analysis.

## HISTOLOGY

The explanted tissue was processed and stained with Masson's Trichrome to measure the percentage muscularis in each zone; p20, p50 and p80. Sections were viewed at X2 magnification and an area of muscularis was outlined in relation to the total area of the full vaginal wall thickness. Vaginal wall area was measured in  $\mu\text{m}^2$  from the epithelial to the adventitial margin using NIS-elements RA3.2 software.

The tissue was also stained with alpha smooth muscle actin ( $\alpha\text{SMA}$ ). Sections underwent dewaxing, rehydrating and antigen retrieval in citric acid buffer as described (Ulrich et al. 2013). Endogenous peroxidase was quenched followed by Protein block (Dako®, Denmark). The primary antibody (1:400, Dako) was incubated for 1 hour, isotype control was applied at the same concentration (IgG2a, Dako). Secondary antibody (Mouse Envision Kit with HRP, Dako) was applied (Ulrich et al. 2012), colour was developed with 3,3'-Diaminobenzidine (DAB).

## BIOCHEMICAL ANALYSIS

Collagen content was measured by a hydroxyproline (Hyp) assay using 5×5 mm frozen tissue pieces. These were weighed, lyophilized for 4 hours, then digested with 1 ml papain (0.5 mg/ml in 0.1 M  $\text{Na}_2\text{HPO}_4$ , 5 mM EDTA, 5 mM Cysteine. HCl, pH 7.4) for 16 hours; supernatant was collected and total collagen content determined by hydrolysing in 6N HCl at 115°C for 4 hours followed by desiccation overnight (Woessner 1961). After reaction with 0.05 mol/L chloramine-T (Sigma) and 10% (w/v in 2-methoxyethanol)  $\rho$ -dimethylaminobenzaldehyde (Sigma), Hyp was measured spectrophotometrically at 560

nm using a standard curve (L-Hyp standards (0-10 µg/mL) (Sigma)) and total collagen calculated using a Hyp to collagen ratio of 0.143:1 (Woessner 1961).

The collagen type III/type I ratio was determined using a SDS-polyacrylamide gel electrophoresis (SDS-PAGE) using delayed reduction (Sykes et al. 1976) as described (Ulrich et al. 2013). Frozen tissue was thawed to room temperature, and 5 x 5 mm pieces were digested for 4 h in pepsin (Sigma) (0.5 mg/ml in 100 mM acetic acid, pH 2.5) at 4°C. Samples were electrophoresed for 1 h at 130 V. 5% v/v 2-mercaptoethanol (Sigma) was added to each well for 1 h; electrophoresis was then continued for 3 h at 130 V at 4°C. Gels were stained with Coomassie Blue R-250 solution, destained in 20% ethanol and 5% acetic acid. Images were taken using FujiFilm LAS-3000 software. The percentage of collagen III in each tissue was calculated from peak sizes using: Percentage type III collagen =  $\text{Area } \alpha 1(\text{III}) \times 1.12 \times 100 / [\text{Area } \alpha 1(\text{III}) \times 1.12] + \text{Area } \alpha 1(\text{I})$  (Chan D 1984); the calibration factor 1.12 corrects for the colour yield from equal weights of the two collagen types (Chan D 1984).

The insoluble precipitate from the above papain-digested, centrifuged sample was used for indirect elastic tissue associated proteins (ETAP) analysis. This sample contains remaining insoluble collagen and ETAP (primarily elastin but also includes insoluble elastic-associated proteins fibulin, fibrillin and latent TGF binding protein) and was rinsed in PBS and distilled water. After freezing and lyophilization for 4 hours, the residual tissue was weighed ( $W_{\text{res}}$ ), and sent to Australian Proteome Analysis Facility for amino acid analysis. The weight of insoluble collagen in the residual tissue ( $W_{\text{res-col}}$ ) was calculated based on its corresponding Hyp amino acid amount. The percentage of ETAP in the tissue samples was calculated using:  $\text{ETAP \%} = [(W_{\text{res}} - W_{\text{res-col}}) / W_{\text{dry}}] \times 100$ .

Glycosaminoglycans (GAG) were measured by dimethylmethylene blue (DMMB) assay (Chandrasekhar et al. 1987) using the same sample preparation as for collagen measurement. The GAG concentration in papain treated tissue digests was determined spectrophotometrically at 525 nm; Chondroitin sulfate C from shark cartilage (Sigma) was used as the standard (0-0.5 mg/mL).

## MECHANICAL TESTING

The tissue was stored at -20°C until testing, thawed overnight at 4°C and tested within 24 hours of defrosting. Freezing and thawing allows a more reliable assessment as

specimens are tested under the same condition (Rubod et al. 2007). Vaginal tissue was dissected from sheep (n=4-6) in the p20, p50, and p80 regions. Dogbone shaped samples (n=1 replicate/region), central width and total length, 4 and 34 mm, respectively, were punched from the sheep tissue in the longitudinal axis and kept moist using PBS.

Sample thickness was measured at 3 positions using digital callipers for calculation of the initial cross sectional area. Uniaxial tensiometry was performed using an Instron<sup>®</sup> Tensile Tester (5567<sup>®</sup>Instron Corp, USA) and a 5 kN load cell. Samples were secured in pneumatic serrated jaws to prevent slippage and were set to a gauge length of 14 mm. Samples were preloaded at 10 mm/min to 100 mN and cyclically loaded from 0 to 1 N, 0 to 2 N, and 0 to 3 N, for 5 cycles each, at 20 mm/min and then extended to break (Rubod et al. 2007, Rubod et al. 2008, Jean-Charles et al. 2010, Rubod et al. 2012). Loading values were chosen to avoid damage to ovine tissue.

Stress-strain curves were plotted from the generated force and elongation data. Nominal stress (MPa,  $1\text{Pa} = 1\text{N}/\text{mm}^2$ ) was calculated by dividing the force (N) by the initial cross sectional area ( $\text{mm}^2$ ) and strain by dividing the extension (mm) by the initial gauge length (mm). Young's modulus (MPa) was determined from the slope of the stress-strain curve in the linear region, immediately following cyclic loading and prior to yielding (Fig. 2). Permanent strain was calculated as the percentage increase in sample length following cyclic loading (Fig. 2). Maximum stress (MPa) was derived from the stress-strain curve and maximum strain (%) was calculated from the corresponding maximum strain, derived from the stress-strain curve (Fig. 2).

## STATISTICS

GraphPad Prism 6 was used for statistical analysis of the biochemical data, and R software (open source) for the biomechanical data. Results are reported as mean  $\pm$ SEM for each experimental group. Two way ANOVA and post hoc test (Tukey's correction) were used for comparisons of biochemical and muscularis data between regions and between species, and for analysis of biomechanical data comparing sheep and region. Kolmogorov-Smirnov tests showed the normality required for each ANOVA was satisfied. P values  $< 0.05$  were considered statistically significant. Based on the total collagen as the primary outcome of interest with a power of 80% and an alpha level of 0.05, it was estimated that 6

subjects were necessary in each group (p20, p50, and p80) to detect a difference of 15% in the total amount.

## RESULTS

All sheep were 4-5 years old and had delivered 3 lambs. The point corresponding to Bp could be moved to  $-1 \pm 0.1$  cm, the cervix  $1.5 \pm 0.3$  cm indicating no significant prolapse in sheep.

The women's (n=7) mean age was  $71 \pm 8$  years, median parity was 2 (1-4); mean time since menopause was  $17 \pm 8$  years. The human vaginal tissue showed stage 2 to 3 pelvic organ prolapse (Ba:  $0.2 \pm 2.5$ , Bp:  $0.0 \pm 1.8$ , C:  $-0.8 \pm 4.7$ ).

Both ovine and human vaginal tissue showed the typical 4 vaginal wall zones of epithelium, lamina propria, muscularis and adventitia at the 3 regions examined (Fig 3A-C). Masson's Trichrome (Fig. 3 A-C) and  $\alpha$ SMC immune-staining (Fig. 3 D-F) demonstrated the extent of muscularis in each full thickness vaginal tissue section for the 3 regions along the vaginal length (Fig 1), with no significant difference in percent of muscularis between the anatomical regions from p20 to p80 in either human or ovine vaginal walls. In sheep, the percent muscularis varied from  $39.7 \pm 4.2\%$  at p20 to  $45.6 \pm 5.8\%$  (n=6) at p80; in human samples, from  $44.4 \pm 4.8\%$  at p20 to  $41.5 \pm 5.8\%$  (n=7) at p80 (Fig. 3G, H) with no significant difference between the two species for the 3 regions.

The total collagen content was significantly higher ( $p < 0.01$ ) in the proximal region (p80) of ovine vagina compared to the distal (p20) and middle (p50) ( $p < 0.05$ ) regions (Fig. 4A). This difference was not observed in the human vagina; however the average total collagen content was comparable between the ovine and human regions of the vagina (Fig. 4A). Collagen type III, as measured by the collagen III/III+I percentage was  $29 \pm 4.5\%$  at p20, and  $21 \pm 5.5\%$  at p80 in the ovine vagina (Fig. 4B). There was no such trend in the human samples with all regions showing comparable levels of collagen type III, around 40% (Fig. 4B), which was significantly higher at p50 and p80 compared to ovine tissue ( $p < 0.05$ , and  $p < 0.01$ ), respectively.

Similarly, no significant difference in total ETAP content was found along the ovine and human vagina (Fig. 4C). ETAP content was comparable between ovine and human tissue, approximating 15%.

In ovine vagina the GAG content was significantly higher ( $p < 0.01$ ) in the p80 compared to the p20 region (Fig. 4D). In the human samples, there were no regional differences. In both ovine and human tissue samples, the % GAG content was not significantly different at p50 and p80 but at p20 GAG was significantly higher in human compared to sheep ( $p < 0.01$ ), but in both very low levels between 0.5 to 1.2% were observed.

Due to small human sample sizes, biomechanical analysis was only possible for the ovine tissue. Young's modulus was highest in the p80 region indicating the proximal third of the vagina is the stiffest following cyclic loading ( $p < 0.05$ ) compared to p20 and p50 regions, which were of similar stiffness (Fig. 5A). Maximum stress (strength) was also highest in the proximal region, with significant differences between p20 and p80 regions ( $p < 0.05$ ) (Fig. 5B). Permanent strain, an indicator of tissue elasticity, did not show statistical differences along the vaginal length, however a trend of increasing elasticity was observed, with the proximal region being the most elastic (Fig. 5C). Maximum strain (extensibility) produced a similar non-significant trend, with the proximal region being the least extensible (Fig. 5D).

## **DISCUSSION**

In this study we performed a detailed comparative analysis of the histological, biochemical and biomechanical properties (ovine only) along the postmenopausal ovine and human posterior vaginal walls. We found significant differences between sheep and human vaginal tissues for collagen ratio and GAG, whereas there were no differences for total collagen and ETAP between the species at any of the vaginal regions suggesting the sheep to be a suitable animal model for POP research.

Several of the major ECM components were highest in the proximal region of the ovine vagina, particularly total collagen and GAG, although ETAP and collagen ratio did not differ significantly. In human tissue there were no significant differences along the vaginal wall for collagen, GAG or ETAP content. The p80 point in humans may sometimes have been 70-75% of the vaginal length, which may contribute to the lack of differences between the regions.

The vaginal wall consists of four layers, of which its major components have been quantified in several studies, however, it is difficult to compare existing studies given the

range of techniques used; histology, immunohistochemistry and biomechanical analyses, and that the exact origin of the tissue is often not stated (De Landsheere et al. 2013). Many studies have relied on immunohistochemistry, which can only be regarded as semi-quantitative. In this study for the first time we undertook quantitative biochemical assays to accurately measure the major ECM proteins of vaginal tissue. We combined this quantitative biochemical analysis with histomorphometry to provide a comprehensive analysis of both ovine and human vagina. In ovine vagina we further compared this with biomechanical analyses.

Previous studies showed conflicting results in terms of human vaginal wall collagen content; some found no differences between women with or without POP (Kannan et al. 2011), whereas others found a higher collagen content in women with POP (Moalli et al. 2005). Prolapse predominantly occurs in postmenopausal women and tissue analyses is often available for this reproductive status (De Landsheere et al. 2013). Our study has not included women without POP and neither has it compared with premenopausal controls, which are limitations. Collagen type I was the major ECM protein in a previous study (Ulrich et al. 2014) and in ovine and human vaginal tissue in this study, in contrast to others which showed collagen III as the dominant protein using immunoquantification (Moalli et al. 2005). Our quantitative biochemical analysis of ovine vaginal tissue indicated that total collagen was highest in the proximal region, which was associated with the highest maximum stress and Young's modulus, suggesting that the vaginal apex is the strongest and stiffest region, likely due to Collagen type I, known for conferring tissue strength (Ramshaw et al. 2009).

Elastin is a major fibrillar protein of viscoelastic tissues (Woessner and Brewer 1963). ETAP, mainly elastin but also fibulin, fibrillins and latent TGF binding proteins, showed a trend towards higher values in the proximal ovine vagina, which was also the most elastic biomechanically (least permanent strain) compared to the distal regions. Higher ETAP contents were also found in women with POP compared with controls (Zong et al. 2010), whereas no differences were found in another study (Kannan et al. 2011).

The regional differences in biomechanical and biochemical properties observed along the length of the vagina could have developed through different forces experienced during previous deliveries. Our results in sheep are in line with a study in rats which showed significant regional differences of vaginal wall contractility (Skoczylas et al.

2013). We restricted our testing to the posterior vaginal wall tissue due to the different anatomical location of the urethral orifice between sheep and humans.

The sheep used in this study did not have significant prolapse in contrast to the women, however were comparable to the human study subjects in terms of parity and reproductive stage of life. Sheep have been recognized as a relatively suitable animal model for POP research (Abramowitch et al. 2009, Couri et al. 2012) due to similarities in the labour process, head- pelvis ratio and spontaneously develop POP. For the first time, we have directly compared the ECM composition with mechanical data.

Although the tissue composition varied along the vaginal length more in sheep, the similarity in content for most components between sheep and women suggest that sheep can serve as a good model of POP research.

## **ACKNOWLEDGMENTS**

The authors thank Ker Sin Tan, employed at MIMR- PHI Institute of Monash University, Melbourne, Australia, for technical assistance and Dr David L.J. Alexander, employed at CSIRO Computational Informatics, Clayton, Australia for his assistance in statistical analysis.

**FIGURE LEGENDS**

**Figure 1.** Schematic showing dissection of ovine posterior vaginal wall. Specimen 1 was used for mechanical analysis, specimen 2 for biochemical analysis and, specimen 3 for histological analysis. Each was obtained at 20% (p20), 50% (p50) and 80% (p80) of total vaginal length.

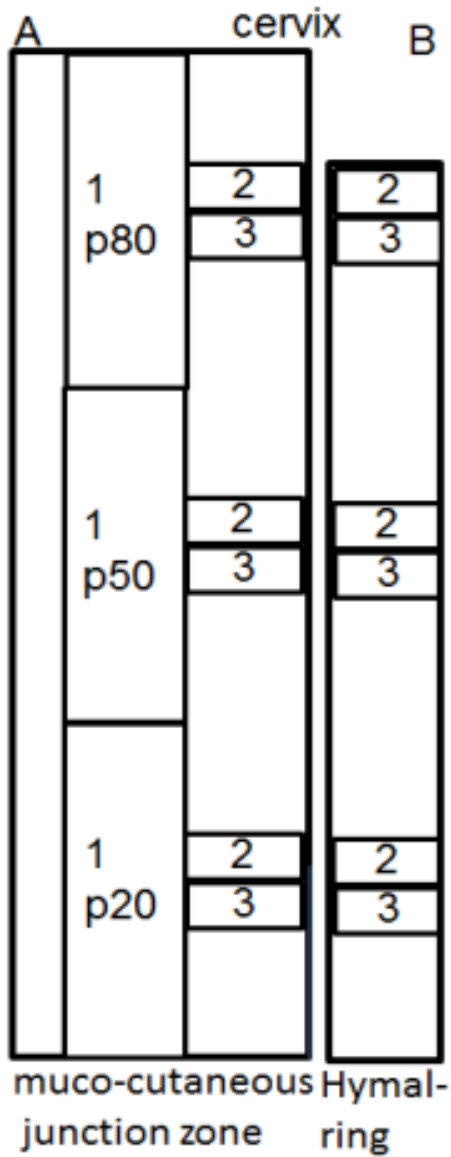


**Figure 2.** Typical nominal stress strain curves for a model of postmenopausal ovine tissue (ovariectomised parous ewes), indicating maximum stress and strain, Young's modulus, and permanent strain for the p80 curve.

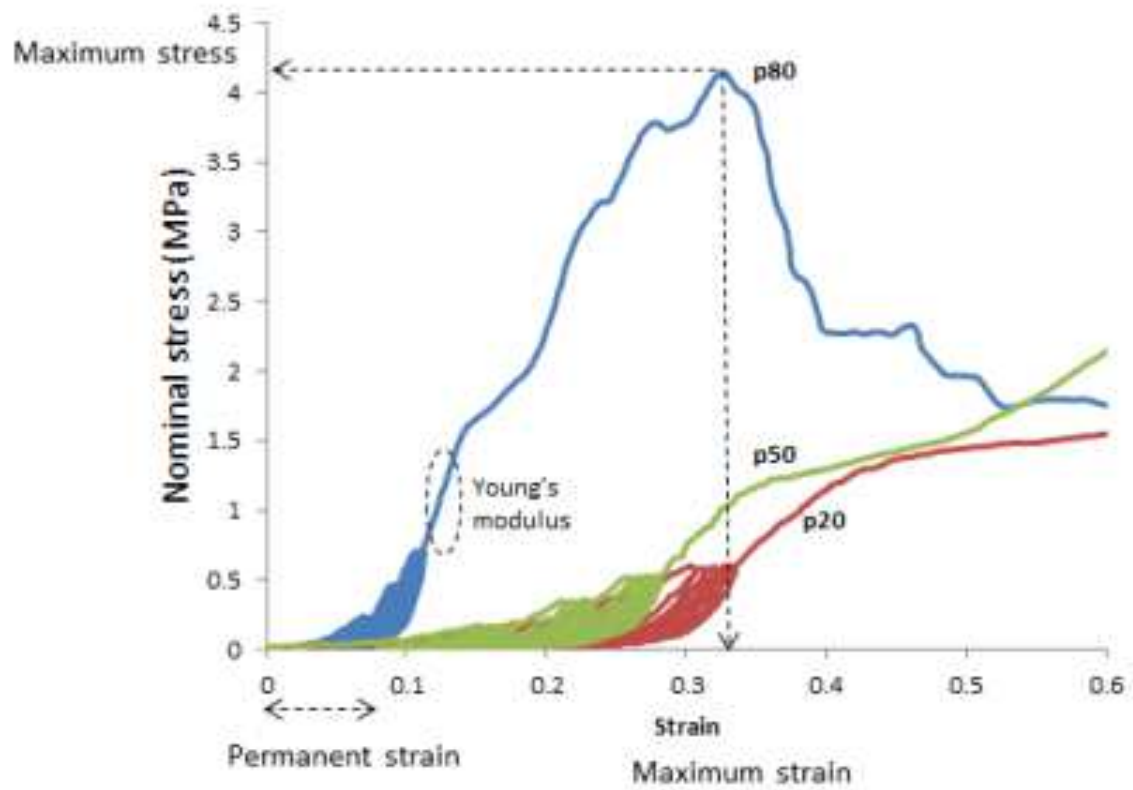


**Figure 3.** Masson staining of postmenopausal ovine vaginal wall at A. p20, B. p50, C. p80. D shows % muscularis in sheep in p20 (white bars), p50 (grey bars) and p80 (black bars). E. p20, F. p50, G. p80 images of human vaginal wall with  $\alpha$ SMA staining. H shows % muscularis in humans in p20 (white bars), p50 (grey bars) and p80 (black bars). Data are presented as mean ( $\pm$ SEM), n=6/ group each for sheep and for human. Scale bar is 250  $\mu$ m.

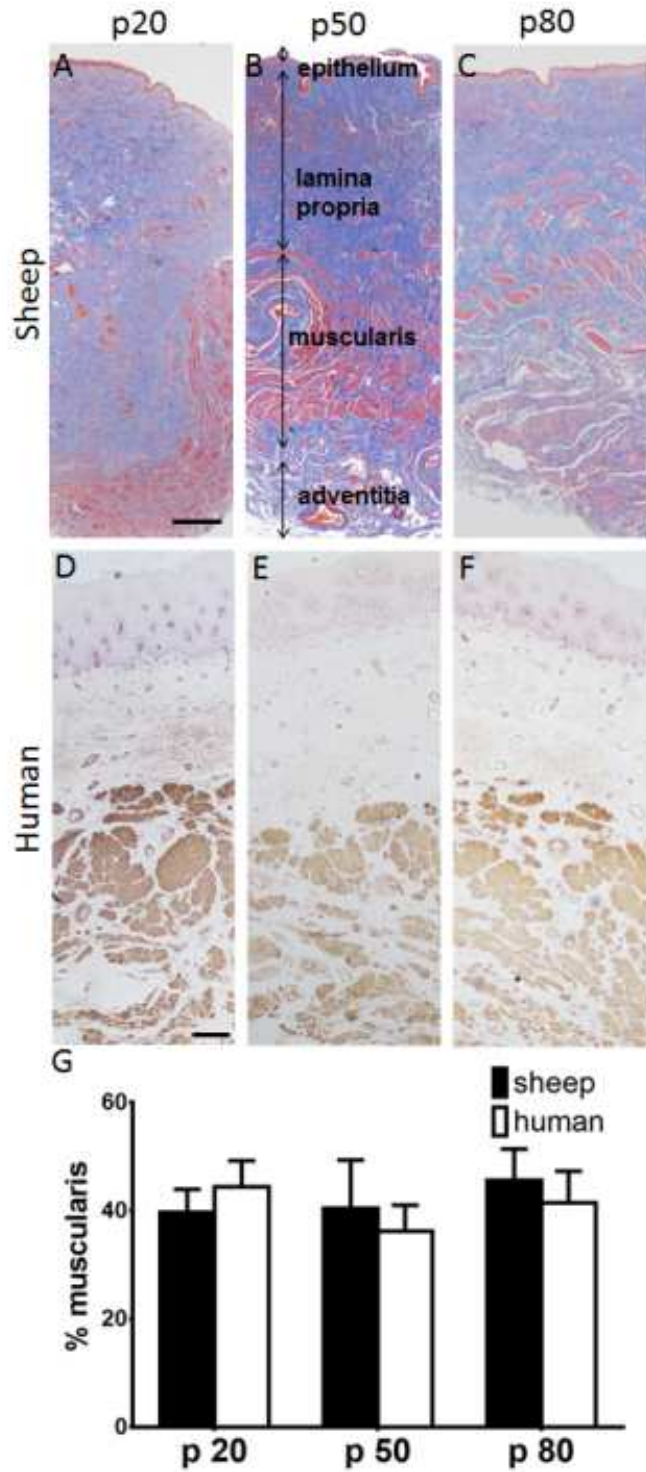


**Figure 4.** Biochemical analysis of the ECM content of postmenopausal ovine and human vaginal wall in relation to p20 (white bars), p50 (grey bars) and -p80 (black bars) location. A and B.. % total collagen per dry weight assessed by hydroxyproline assay in ovine and human vaginal tissue, respectively; C and D. % collagen III/ (I+III) quantified by interrupted SDS-PAGE in ovine and human vaginal tissue, respectively; E and F. % ETAP per dry weight by amino acid analysis in sheep and human vaginal wall, respectively; G and H. % GAG per dry weight assessed by DMMB assay in ovine and human vagina, respectively. Data are presented as mean ( $\pm$ SEM), n=6/ group each for sheep and human.\*\* p< 0.01.

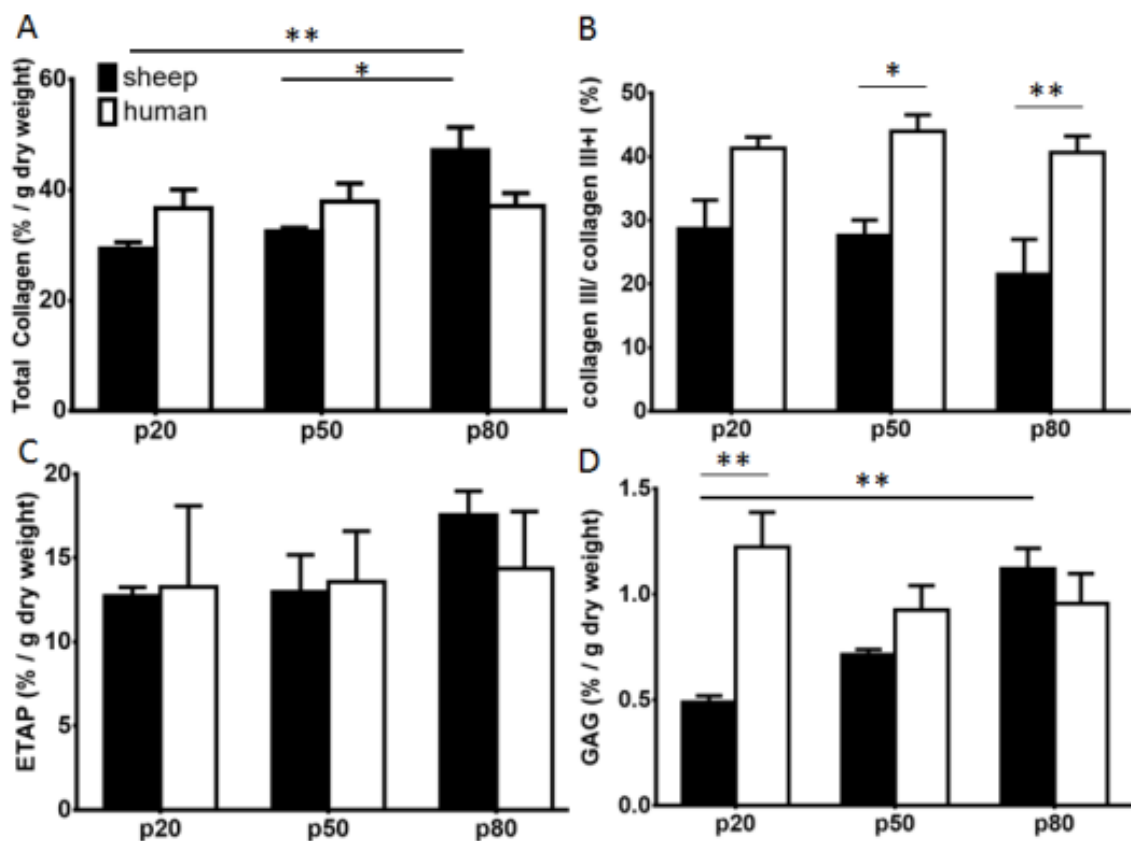
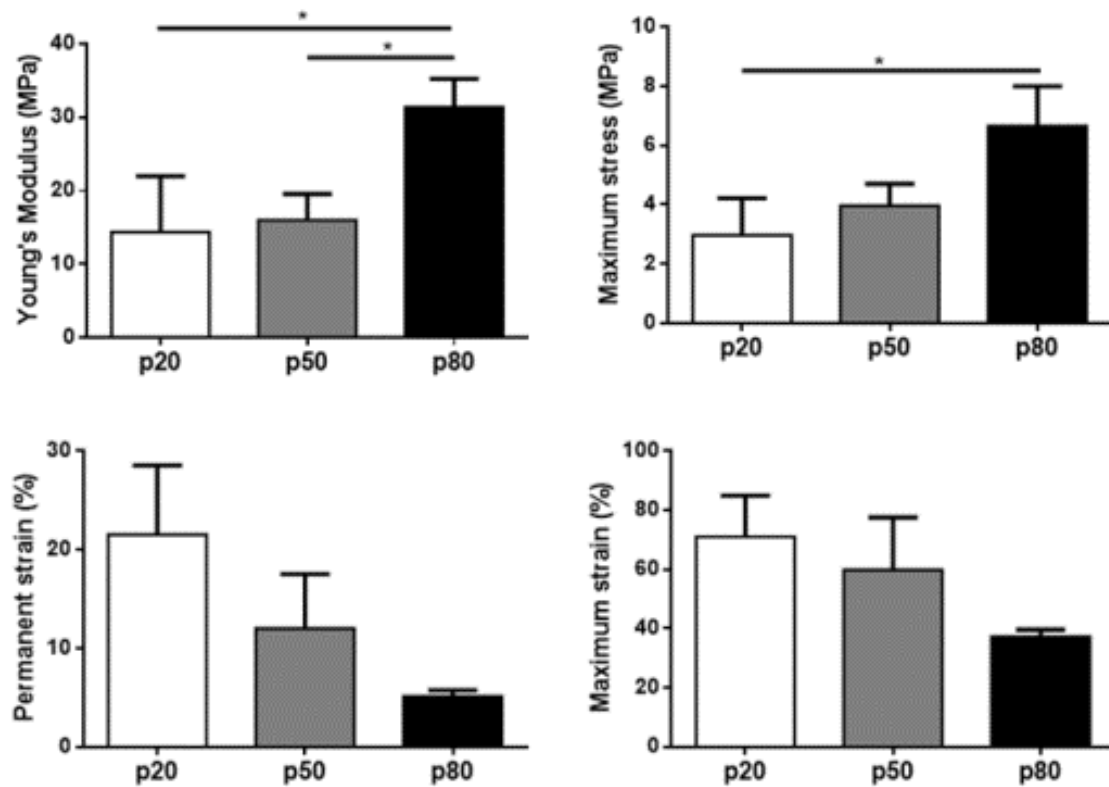


**Figure 5.** Biomechanical evaluation of vaginal tissues from ovariectomised (postmenopausal) parous sheep in relation to p20 (white bars), p50 (grey bars) and p80 (black bars) location. A. Young's modulus (MPa). B. Maximum stress (MPa). C. Permanent strain (%). D. Maximum strain (%). Data is presented as mean ( $\pm$ SEM), n=4-6/group.



## CHAPTER 7

### DISCUSSION

This thesis aimed to develop a cell based therapy for POP repair using a TE approach. The TE constructs comprised new meshes and a novel source of MSC recently identified and characterised in the human endometrium (eMSC) (Gargett et al. 2009). We developed both small and large animal models for the preclinical testing of the newly designed meshes and tissue engineered constructs. Since a single marker had been identified for obtaining the eMSC population (Masuda 2012), magnetic bead-purified eMSC were used to generate the TE constructs. MSC are known to have anti-inflammatory and immunomodulatory properties (Uccelli et al. 2008, Gargett et al. 2012) and these properties are probably greater in a pure population compared to a non-purified stromal cell fraction and therefore more likely to influence the tissue response to the mesh component of the TE construct.

Chapter 2 describes the evaluation of the *in vivo* biocompatibility of the newly designed meshes in a rat abdominal hernia model (Ulrich et al. 2012). PA, PA+G and PEEK meshes showed complex differences compared to the commercially available PP meshes and to the control group. PA and PA+G meshes generated a milder inflammatory response compared to PP, and PA+G stimulated the highest collagen deposition. PA and PEEK meshes induced the most vascularisation. We were able to establish objective measures of tissue inflammation using image analysis whereas previous studies relied on subjective scoring. Therefore we were able to tease out more subtle differences that have not been possible on previous subjective analyses, thus setting new parameters for future studies in the field. Chronic inflammation is a key factor in mesh surgery as many of the side effects result from a strong ongoing foreign body reaction. Vascularisation is also important for good mesh biocompatibility to ensure neo tissue is well supported with oxygen and nutrients. In summary it appeared that the PA+G mesh was superior to the other meshes with respect to inflammation, collagen deposition and vascularisation, which was the reason for choosing the PA+G mesh for assessing the effect of eMSC on mesh biocompatibility in chapter 4.

Many women with POP are postmenopausal and if autologous eMSC are to be used in the TE constructs for POP surgery, it is important that sufficient endometrium is available for biopsy procurement of their eMSC and to confirm that the harvested cells do indeed have MSC properties. Chapter 3 describes the effect of oral estrogen on the endometrium in postmenopausal women using image analysis techniques. Postmenopausal endometrium is thin and atrophic, but has capacity to regenerate under the influence of increased circulating estrogen given as oral estrogen therapy. Both the estrogen-treated and untreated postmenopausal eMSC possessed the key MSC surface phenotype and differentiation capacity similar to premenopausal eMSC. They expressed the W5C5 marker used for prospective isolation and could be obtained in a similar manner as premenopausal MSC. Since endometrium is an easily obtainable source of MSC, the identification of eMSC in postmenopausal women is of great interest. Even though the endometrium is atrophic due to the lack of circulating estrogen during menopause, we showed that eMSC resided in the residual “basalis-like” layer (Nguyen et al. 2012) and can still be collected by a curettage for autologous cell-based therapies. Procurement is facilitated by short term estrogen supplementation if not contraindications This population of eMSC may be responsible for the ability of postmenopausal endometrium to regenerate in response to estrogen only hormone therapy, particularly the stromal vascular components. In a recent gene array study, the human premenopausal eMSC subpopulation highly expressed genes and cell signalling pathways regulating proteolysis, cell motility, haemostasis, vasoconstriction and wound healing suggesting their involvement in tissue repair (Spitzer et al. 2012). It is speculated that these gene pathways are involved in regenerating postmenopausal endometrium. BmMSC are known to drop in numbers and activity during an individual’s lifespan (Haynesworth et al. 1993), however the exact mechanisms that influence adult stem cell aging and cell aging in general are not fully understood (Signer and Morrison 2013). Future studies are needed to compare the properties of young (premenopausal) versus old (postmenopausal) eMSC *in vitro* and *in vivo*. In summary, this study identified that postmenopausal eMSC are a readily available source of MSC for tissue engineering purposes that can be obtained in adequate numbers by a biopsy after short-term oral estrogen therapy. Long term estrogen replacement therapy can be associated with side effects that have not been shown for a short term therapy, however careful consideration regarding patient’s history has to be taken in case of estrogen contraindications.

TE has become popular during the last decade since the discovery of human embryonic stem cells and their potential promise in regenerative medicine applications ranging from tracheal, bladder or vaginal replacement (Dorin et al. 2011, Raya-Rivera et al. 2011, Elliott et al. 2012). Adult stem cells have also been discovered in many tissues and pose a popular cell type for TE applications. Most attempts at using TE for the lower urinary tract are still in the experimental stage and clinical trials are needed before taking untried treatments into the clinic, despite the pressure from patient groups (Sumino and Mimata 2013). It is therefore likely that it might take time for established protocols to be developed for POP repair. At the start of this thesis no attempts using TE for prolapse repair had been published, however rapid progress is being made on all fronts with TE combining all sorts of materials and cells. In this thesis, a proof of principle model for a non-degradable mesh and eMSC tissue engineering construct was developed for use in a preclinical model of POP. The rat fascial wound model is generally well accepted for baseline and proof-of-principle studies although it is not ideal to study the physiology of POP. Mesh implantation in the vagina of nude rats prohibits the use of adequately sized mesh pieces to perform a comprehensive set of informative analyses. While the abdominal hernia model provides pressure from the abdominal organs the aim of chapter 4 was to evaluate the sole effect of eMSC on mesh integration. Therefore the wound repair model was developed. The objective image analysis and biochemical measurements allowed us to obtain comprehensive, more quantitative and reproducible data, setting a benchmark for future studies.

Recently *in vitro* attempts have been made to examine oral fibroblasts and adipose-derived MSC for their tissue engineering potential to treat urogenital disorders when seeded on degradable poly lactic acid (PLA)-based scaffolds (Roman et al. 2013). Both cell types showed similar effects on collagen production and an increase in biomechanical properties. Just recently PLA has been suggested as an alternate option for POP repair models in animal studies. At the start of the thesis, prior to the second FDA warning on the use of synthetic mesh for vaginal surgery, the long term success of non-degradable materials in humans was promising (Maher et al. 2010). In particular we decided to fabricate new non-degradable meshes more closely matching the biomechanical properties of human vaginal tissue to ensure that future TE constructs would continue to support prolapsed tissues and regenerate new tissue or improve the biocompatibility of non-degradable mesh. A key issue with the use of degradable meshes is the large and

unpredictable variation in degradation rate between subjects, making design of such mesh for the general population of women very difficult. In our setting, we performed an *in vivo* experiment and the eMSC improved the biocompatibility of the mesh by increasing early neovascularisation, promoting wound healing, decreasing long term inflammation and changing the mechanical properties to increased compliance (Ulrich et al. 2013). In this setting there was no difference in the amount of collagen produced during the healing phase, and although differences in its quality was shown in the birefringence data, clinical conclusions cannot be fully drawn due to the lack of similar forces experienced on vaginally placed mesh in the dorsum of the rats. The next step will be to test this TE construct in a preclinical large animal model of vaginal surgery to address this issue, i.e. the sheep. Preliminary data from my colleagues show that eMSC are available in sheep uterus and can be used in an autologous setting for a TE construct for analysis in sheep vagina. Since there is increasing evidence that autologous cell use is superior to heterologous the conclusions drawn from this study need to be re-evaluated in an autologous model as a proof of principle, i.e. the sheep. Furthermore the immunomodulatory and anti inflammatory properties and the mechanisms by which eMSC improve mesh biocompatibility need to be investigated.

To develop a reliable animal model for preclinical research it is necessary to define baseline parameters. Chapter 5 provides a comprehensive analysis of ovine vaginal tissue at different reproductive stages to define baseline data for a large animal model of POP vaginal surgery. This study provides the first data that includes several analytical techniques relevant to POP and compares the results between different stages of reproductive life. This data can serve as a basis to plan preclinical studies in this large animal model to test alternative biomaterials and other cell types for their efficacy in POP repair surgery. It may also assist in the development of a model for investigating the aetiology and progression of POP. We found that pregnancy has a major influence on the composition of the ECM and the mechanical properties of vaginal tissue. Interestingly most alterations to the chemical composition and biomechanical behaviour of the ovine vagina normalise to pre-pregnancy values in some but not all parous sheep, which might explain why some individuals develop POP and others with a similar history do not. However, longitudinal, non invasive studies using technologies that do not destroy the tissue are required to confirm this finding.

To link preclinical and clinical studies, in the last chapter a comparison between sheep and human vaginal tissue was attempted in postmenopausal individuals. A postmenopausal ovine model was developed by performing ovariectomy in sheep to establish hormone deprivation. Baseline data was generated along the vaginal wall to further characterise differences between the different regions. We have performed a comprehensive analysis including histological and chemical techniques for both human and sheep tissue from the distal, middle and proximal vaginal regions. It is not ethical to obtain large tissue samples from human, which meant only histological and chemical analyses were conducted on the human tissues. We found significant differences in the sheep between the lower distal and upper proximal vaginal wall whereas these differences were not as pronounced in human tissue. Interestingly the overall ECM content was similar between the two models supporting the hypothesis that sheep are a suitable preclinical model for POP research. To date, there is high level of inconsistency between studies examining vaginal tissue composition (De Landsheere et al. 2013). Reasons could be the inconsistency of the tissue acquisition process; often the precise region from which the tissue was exactly obtained is not known. Furthermore, different authors use different techniques which has hindered comparison between studies. Ethical restrictions in human tissue acquisition also play a role in the paucity of data available.

New treatment strategies for POP are needed since the success rates of native tissue repair are unsatisfying (as low as 40%) (Maher and Baessler 2006, Carey et al. 2009, Guerette et al. 2009) and the side effects resulting from the use of current meshes are relatively high (up to 25%) (Jia et al. 2010). Although POP can be debilitating and significantly affect the quality of life of women, it is not a lethal condition, but this does not justify a high incidence of side effects or risks for treatment options. Additional costs incurred by a tissue engineering approach such as cell isolation and culture expansion, as well as material development have to be considered too. It has been postulated that the first priority for new treatment options for POP is their safety, regardless of success or other factors (Davila 2012). New or alternative materials in combination with different cell sources will have to be evaluated in large preclinical studies to find the optimal treatment option for POP to return to women the quality of life they deserve without inducing any harm. The methodologies, animal models and approaches used in this thesis provide a basis for ongoing development of future innovative treatments for POP.

## REFERENCES

2008. FDA Public Health Notification: Serious Complications Associated with Transvaginal Placement of Surgical Mesh in Repair of Pelvic Organ Prolapse and Stress Urinary Incontinence. Retrieved 06 March, 2014, from <http://www.fda.gov/MedicalDevices/Safety/AlertsandNotices/PublicHealthNotifications/ucm061976.htm>.
2011. FDA Safety Communication: UPDATE on Serious Complications Associated with Transvaginal Placement of Surgical Mesh for Pelvic Organ Prolapse. Retrieved 06 March, 2014, from <http://www.fda.gov/MedicalDevices/Safety/AlertsandNotices/ucm262435.htm>.
- Abberton, K. M., D. L. Healy and P. A. W. Rogers. Smooth muscle alpha actin and myosin heavy chain expression in the vascular smooth muscle cells surrounding human endometrial arterioles. *Hum. Reprod.* 1999; **14**(12): 3095-3100.
- Aboushwareb, T., P. McKenzie, F. Wezel, J. Southgate and G. Badlani. Is Tissue Engineering and Biomaterials the Future for Lower Urinary Tract Dysfunction (LUTD)/Pelvic Organ Prolapse (POP)? *Neurourol. Urodyn.* 2011; **30**(5): 775-782.
- Abramowitch, S. D., A. Feola, Z. Jallah and P. A. Moalli. Tissue mechanics, animal models, and pelvic organ prolapse: A review. *Eur. J. Obstet. Gynecol. Reprod. Biol.* 2009; **144**: S146-S158.
- Alperin, M., A. Feola, R. Duerr, P. Moalli and S. Abramowitch. Pregnancy- and delivery-induced biomechanical changes in rat vagina persist postpartum. *Int Urogynecol J* 2010; **21**(9): 1169-1174.
- Altman, D., T. Vayrynen, M. E. Engh, S. Axelsen, C. Falconer and G. Nordic Transvaginal Mesh. Anterior Colporrhaphy versus Transvaginal Mesh for Pelvic-Organ Prolapse. *N. Engl. J. Med.* 2011; **364**(19): 1826-1836.
- Alvarez, C. V., M. Garcia-Lavandeira, M. E. Garcia-Rendueles, E. Diaz-Rodriguez, A. R. Garcia-Rendueles, S. Perez-Romero, T. V. Vila, J. S. Rodrigues, P. V. Lear and S. B. Bravo. Defining stem cell types: understanding the therapeutic potential of ESCs, ASCs, and iPS cells. *J. Mol. Endocrinol.* 2012; **49**(2): R89-111.
- Ashton-Miller, J. A. and J. O. DeLancey. Functional anatomy of the female pelvic floor. *Ann. N. Y. Acad. Sci.* 2007; **1101**: 266-296.
- Ashton-Miller, J. A. and J. O. Delancey. On the biomechanics of vaginal birth and common sequelae. *Annu. Rev. Biomed. Eng.* 2009; **11**: 163-176.
- Atala, A., S. B. Bauer, S. Soker, J. J. Yoo and A. B. Retik. Tissue-engineered autologous bladders for patients needing cystoplasty. *Lancet* 2006; **367**(9518): 1241-1246.
- Barbalat, Y. and H. S. Tunuguntla. Surgery for pelvic organ prolapse: a historical perspective. *Curr Urol Rep* 2012; **13**(3): 256-261.
- Beltrami, A. R., D. Cesselli, N. Bergamin, P. Marcon, S. Rigo, E. Puppato, F. D'Aurizio, R. Verardo, S. Piazza, A. Pignatelli, A. Poz, U. Bacarani, D. Damiani, R. Fanin, L. Mariuzzi, N. Finato, P. Masolini, S. Burelli, O. Belfuzzi, C. Schneider and C. A. Beltrami.

- Multipotent cells can be generated in vitro from several adult human organs (heart, liver, and bone marrow). *Blood* 2007; **110**(9): 3438-3446.
- Bhatia, N. N. and M. H. Ho. Stem cell therapy for urinary incontinence and pelvic floor disorders: a novel approach. *Curr. Opin. Obstet. Gynecol.* 2004; **16**(5): 397-398.
- Boennelycke, M., L. Christensen, L. F. Nielsen, H. Everland and G. Lose. Tissue response to a new type of biomaterial implanted subcutaneously in rats. *Int Urogynecol J* 2011; **22**(2): 191-196.
- Boennelycke, M., S. Gras and G. Lose. Tissue engineering as a potential alternative or adjunct to surgical reconstruction in treating pelvic organ prolapse. *Int Urogynecol J* 2013; **24**(5): 741-747.
- Boquest, A. C., A. Shahdadfar, K. Fronsdal, O. Sigurjonsson, S. H. Tunheim, P. Collas and J. E. Brinchmann. Isolation and transcription profiling of purified uncultured human stromal stem cells: alteration of gene expression after in vitro cell culture. *Mol. Biol. Cell* 2005; **16**(3): 1131-1141.
- Braekken, I. H., M. Majida, M. E. Engh and K. Bo. Can pelvic floor muscle training reverse pelvic organ prolapse and reduce prolapse symptoms? An assessor-blinded, randomized, controlled trial. *Am. J. Obstet. Gynecol.* 2010; **203**(2).
- Brincat, C. A., K. A. Larson and D. E. Fenner. Anterior Vaginal Wall Prolapse: Assessment and Treatment. *Clin. Obstet. Gynecol.* 2010; **53**(1): 51-58.
- Bringman, S., J. Conze, D. Cuccurullo, J. Deprest, K. Junge, B. Klosterhalfen, E. Parra-Davila, B. Ramshaw and V. Schumpelick. Hernia repair: the search for ideal meshes. *Hernia : the journal of hernias and abdominal wall surgery* 2010; **14**(1): 81-87.
- Brooke, G., T. Rossetti, R. Pelekanos, N. Ilic, P. Murray, S. Hancock, V. Antonenas, G. Huang, D. Gottlieb, K. Bradstock and K. Atkinson. Manufacturing of human placenta-derived mesenchymal stem cells for clinical trials. *Br. J. Haematol.* 2009; **144**(4): 571-579.
- Brostrom, S. and G. Lose. Pelvic floor muscle training in the prevention and treatment of urinary incontinence in women - what is the evidence? A systematic review. *Int Urogynecol J* 2008; **19**: S131-S131.
- Budatha, M., S. Roshanravan, Q. Zheng, C. Weislander, S. L. Chapman, E. C. Davis, B. Starcher, R. A. Word and H. Yanagisawa. Extracellular matrix proteases contribute to progression of pelvic organ prolapse in mice and humans. *J. Clin. Invest.* 2011; **121**(5): 2048-2059.
- Buhring, H. J., V. L. Battula, S. Treml, B. Schewe, L. Kanz and W. Vogel. Novel markers for the prospective isolation of human MSC. *Ann. N. Y. Acad. Sci.* 2007; **1106**: 262-271.
- Bump, R. C., A. Mattiasson, K. Bo, L. P. Brubaker, J. O. DeLancey, P. Klarskov, B. L. Shull and A. R. Smith. The standardization of terminology of female pelvic organ prolapse and pelvic floor dysfunction. *Am. J. Obstet. Gynecol.* 1996; **175**(1): 10-17.
- Caplan, A. I. Adult mesenchymal stem cells for tissue engineering versus regenerative medicine. *J. Cell. Physiol.* 2007; **213**(2): 341-347.
- Caplan, A. I. All MSCs are pericytes? *Cell stem cell* 2008; **3**(3): 229-230.
- Caplan, A. I. Why are MSCs therapeutic? New data: new insight. *J. Pathol.* 2009; **217**(2): 318-324.

- Carey, M., P. Higgs, J. Goh, J. Lim, A. Leong, H. Krause and A. Cornish. Vaginal repair with mesh versus colporrhaphy for prolapse: a randomised controlled trial. *Br. J. Obstet. Gynaecol.* 2009; **116**(10): 1380-1386.
- Carley, M. E. and J. Schaffer. Urinary incontinence and pelvic organ prolapse in women with Marfan or Ehlers Danlos syndrome. *Am. J. Obstet. Gynecol.* 2000; **182**(5): 1021-1023.
- Cervello, I., C. Gil-Sanchis, A. Mas, F. Delgado-Rosas, J. Antonio Martinez-Conejero, A. Galan, A. Martinez-Romero, S. Martinez, I. Navarro, J. Ferro, J. Antonio Horcajadas, F. Jose Esteban, J. Enrique O'Connor, A. Pellicer and C. Simon. Human Endometrial Side Population Cells Exhibit Genotypic, Phenotypic and Functional Features of Somatic Stem Cells. *PLoS One* 2010; **5**(6).
- Cervello, I., C. Gil-Sanchis, A. Mas, A. Faus, J. Sanz, F. Moscardo, G. Higuera, M. Angel Sanz, A. Pellicer and C. Simon. Bone Marrow-Derived Cells from Male Donors Do Not Contribute to the Endometrial Side Population of the Recipient. *PLoS One* 2012; **7**(1).
- Cervello, I., A. Mas, C. Gil-Sanchis, L. Peris, A. Faus, P. T. K. Saunders, H. O. D. Critchley and C. Simon. Reconstruction of Endometrium from Human Endometrial Side Population Cell Lines. *PLoS One* 2011; **6**(6).
- Chan D, C. W. Quantitation of type I and type-III collagens using electrophoresis of alpha chains and cyanogen-bromide peptides. *Anal. Biochem.* 1984; **139**: 322-328.
- Chan, R. W., K. E. Schwab and C. E. Gargett. Clonogenicity of human endometrial epithelial and stromal cells. *Biol. Reprod.* 2004; **70**(6): 1738-1750.
- Chan, R. W. S., T. Kaitu'u-Lino and C. E. Gargett. Role of Label-Retaining Cells in Estrogen-Induced Endometrial Regeneration. *Reprod. Sci.* 2012; **19**(1): 102-114.
- Chandrasekhar, S., M. A. Esterman and H. A. Hoffman. Microdetermination of proteoglycans and glycosaminoglycans in the presence of guanidine-hydrochloride. *Anal. Biochem.* 1987; **161**(1): 103-108.
- Chen, X., M. A. Armstrong and G. Li. Mesenchymal stem cells in immunoregulation. *Immunol. Cell Biol.* 2006; **84**(5): 413-421.
- Choi, H., R. H. Lee, N. Bazhanov, J. Y. Oh and D. J. Prockop. Anti-inflammatory protein TSG-6 secreted by activated MSCs attenuates zymosan-induced mouse peritonitis by decreasing TLR2/NF-kappa B signaling in resident macrophages. *Blood* 2011; **118**(2): 330-338.
- Clarke, R. and G. Smith. Stem cells and tissue homeostasis in mammary glands. *J. Mammary Gland Biol. Neoplasia* 2005; **10**(1): 1-3.
- Cosson, M., E. Lambaudie, M. Boukerrou, P. Lobry, G. Crepin and A. Ego. A biomechanical study of the strength of vaginal tissues - Results on 16 post-menopausal patients presenting with genital prolapse. *Eur. J. Obstet. Gynecol. Reprod. Biol.* 2004; **112**(2): 201-205.
- Couchman, J. R. and C. A. Pataki. An Introduction to Proteoglycans and Their Localization. *J. Histochem. Cytochem.* 2012; **60**(12): 885-897.
- Couri, B. M., A. T. Lenis, A. Borazjani, M. F. Paraiso and M. S. Damaser. Animal models of female pelvic organ prolapse: lessons learned. *Expert Rev. Obstet. Gynecol.* 2012; **7**(3): 249-260.

- Crisan, M., S. Yap, L. Casteilla, C. W. Chen, M. Corselli, T. S. Park, G. Andriolo, B. Sun, B. Zheng, L. Zhang, C. Norotte, P. N. Teng, J. Traas, R. Schugar, B. M. Deasy, S. Badylak, H. J. Buhning, J. P. Giacobino, L. Lazzari, J. Huard and B. Peault. A perivascular origin for mesenchymal stem cells in multiple human organs. *Cell Stem Cell* 2008; **3**(3): 301-313.
- Cui, C.-H., T. Uyama, K. Miyado, M. Terai, S. Kyo, T. Kiyono and A. Umezawa. Menstrual blood-derived cells confer human dystrophin expression in the murine model of Duchenne muscular dystrophy via cell fusion and myogenic transdifferentiation. *Mol. Biol. Cell* 2007; **18**(5): 1586-1594.
- da Silva Meirelles, L., P. C. Chagastelles and N. B. Nardi. Mesenchymal stem cells reside in virtually all post-natal organs and tissues. *J. Cell Sci.* 2006; **119**(Pt 11): 2204-2213.
- Davila, G. W. Optimizing safety and appropriateness of graft use in pelvic reconstructive surgery: introduction to the 2nd IUGA Grafts Roundtable. *Int Urogynecol J* 2012; **23 Suppl 1**: S3-6.
- De Landsheere, L., C. Munaut, B. Nusgens, C. Maillard, C. Rubod, M. Nisolle, M. Cosson and J. M. Foidart. Histology of the vaginal wall in women with pelvic organ prolapse: a literature review. *Int Urogynecol J* 2013; **24**(12): 2011-2020.
- De Filippo, R. E., C. E. Bishop, L. Freitas, J. J. Yoo and A. Atala. Tissue engineering a complete vaginal replacement from a small biopsy of autologous tissue. *Transplantation* 2008; **86**(2): 208-214.
- De Ridder, D. Should we use meshes in the management of vaginal prolapse? *Current Opinion in Urology* 2008; **18**(4): 377-382.
- de Tayrac, R., A. Alves and M. Therin. Collagen-coated vs noncoated low-weight polypropylene meshes in a sheep model for vaginal surgery. A pilot study. *Int Urogynecol J* 2007; **18**(5): 513-520.
- de Tayrac, R., O. Picone, A. Chauveaud-Lambling and H. Fernandez. A 2-year anatomical and functional assessment of transvaginal rectocele repair using a polypropylene mesh. *Int Urogynecol J* 2006; **17**(2): 100-105.
- Delancey, J. O. L. Anatomic aspects of vaginal eversion after hysterectomy. *Am. J. Obstet. Gynecol.* 1992; **166**(6): 1717-1728.
- Deprest, J. and A. Feola. The need for preclinical research on pelvic floor reconstruction. *Br. J. Obstet. Gynaecol.* 2013; **120**(2): 141-143.
- Deprest, J., F. Zheng, M. Konstantinovic, F. Spelzini, F. Claerhout, A. Steensma, Y. Ozog and D. De Ridder. The biology behind fascial defects and the use of implants in pelvic organ prolapse repair. *Int Urogynecol J* 2006; **17 Suppl 1**: S16-25.
- Diani, J., B. Fayolle and P. Gilormini. A review on the Mullins effect. *Eur. Polym. J.* 2009; **45**(3): 601-612.
- Dietz, H. P. Ultrasound imaging of the pelvic floor. Part II: three-dimensional or volume imaging. *Ultrasound Obstet. Gynecol.* 2004; **23**(6): 615-625.
- Dietz, H. P. Prolapse worsens with age, doesn't it? *Aust. N. Z. J. Obstet. Gynaecol.* 2008; **48**(6): 587-591.
- Dietz, H. P. and V. Lanzarone. Levator trauma after vaginal delivery. *Obstet. Gynecol.* 2005; **106**(4): 707-712.

- Dolce, C. J., D. Stefanidis, J. E. Keller, K. C. Walters, W. L. Newcomb, J. J. Heath, H. J. Norton, A. E. Lincourt, K. W. Kercher and B. T. Heniford. Pushing the envelope in biomaterial research: initial results of prosthetic coating with stem cells in a rat model. *Surgical Endoscopy and Other Interventional Techniques* 2010; **24**(11): 2687-2693.
- Dominici, M., K. Le Blanc, I. Mueller, I. Slaper-Cortenbach, F. Marini, D. Krause, R. Deans, A. Keating, D. Prockop and E. Horwitz. Minimal criteria for defining multipotent mesenchymal stromal cells. The International Society for Cellular Therapy position statement. *Cytotherapy* 2006; **8**(4): 315-317.
- Dorin, R. P., A. Atala and R. E. DeFilippo. Bioengineering a Vaginal Replacement Using a Small Biopsy of Autologous Tissue. *Semin. Reprod. Med.* 2011; **29**(1): 38-44.
- Drewes, P. G., H. Yanagisawa, B. Starcher, I. Hornstra, K. Csiszar, S. I. Marinis, P. Keller and R. A. Word. Pelvic organ prolapse in fibulin-5 knockout mice - Pregnancy-induced changes in elastic fiber homeostasis in mouse vagina. *Am. J. Pathol.* 2007; **170**(2): 578-589.
- Drutz, H. P. and M. Alarab. Pelvic organ prolapse: demographics and future growth prospects. *Int Urogynecol J* 2006; **17**: S6-S9.
- Du, H. L. and H. S. Taylor. Contribution of bone marrow-derived stem cells to endometrium and endometriosis. *Stem Cells* 2007; **25**(8): 2082-2086.
- Eckfeldt, C. E., E. M. Mendenhall and C. M. Verfaillie. The molecular repertoire of the 'almighty' stem cell. *Nature Reviews Molecular Cell Biology* 2005; **6**(9): 726-737.
- Edwards, S. L., J. A. Werkmeister, A. Rosamilia, J. A. M. Ramshaw, J. F. White and C. E. Gargett. Characterisation of clinical and newly fabricated meshes for pelvic organ prolapse repair. *J Mech Behav Biomed Mater* 2013; **23**: 53-61.
- Edwards SL, W. J., Rosamilia A, Werkmeister JA, Gargett CE. Scaffolds for the repair of pelvic organ prolapse. *TERMIS-AP Conference Sydney, 15-7 Sept-Abstract 259* 2010.
- Elliott, M. J., P. De Coppi, S. Spegginorin, D. Roebuck, C. R. Butler, E. Samuel, C. Crowley, C. McLaren, A. Fierens, D. Vondrys, L. Cochrane, C. Jephson, S. Janes, N. J. Beaumont, T. Cogan, A. Bader, A. M. Seifalian, J. J. Hsuan, M. W. Lowdell and M. A. Birchall. Stem-cell-based, tissue engineered tracheal replacement in a child: a 2-year follow-up study. *Lancet* 2012; **380**(9846): 994-1000.
- Ennen, S., S. Kloss, G. Scheiner-Bobis, K. Failing and A. Wehrend. Histological, hormonal and biomolecular analysis of the pathogenesis of ovine Prolapsus vaginae antepartum. *Theriogenology* 2011; **75**(2): 212-219.
- Ettinger, B., L. Bainton, D. H. Upmalis, J. T. Citron and A. VanGessel. Comparison of endometrial growth produced by unopposed conjugated estrogens or by micronized estradiol in postmenopausal women. *Am. J. Obstet. Gynecol.* 1997; **176**(1): 112-117.
- Feola, A., S. Abramowitch, K. Jones, S. Stein and P. Moalli. Parity negatively impacts vaginal mechanical properties and collagen structure in rhesus macaques. *Am. J. Obstet. Gynecol.* 2010; **203**(6).
- Fisher, M. B. and R. L. Mauck. Tissue Engineering and Regenerative Medicine: Recent Innovations and the Transition to Translation. *Tissue Engineering Part B-Reviews* 2013; **19**(1): 1-13.
- Foraker, J. E., J. Y. Oh, J. H. Ylostalo, R. H. Lee, J. Watanabe and D. J. Prockop. Cross-talk between human mesenchymal stem/progenitor cells (MSCs) and rat hippocampal

- slices in LPS-stimulated cocultures: the MSCs are activated to secrete prostaglandin E2. *J. Neurochem.* 2011; **119**(5): 1052-1063.
- Friedenstein, A. J., U. F. Gorskaja and N. N. Kulagina. Fibroblast precursors in normal and irradiated mouse hematopoietic organs. *Exp. Hematol.* 1976; **4**(5): 267-274.
- Fuchs, E. and J. A. Segre. Stem cells: a new lease on life. *Cell* 2000; **100**(1): 143-155.
- Fuchs, E., T. Tumber and G. Guasch. Socializing with the neighbors: Stem cells and their niche. *Cell* 2004; **116**(6): 769-778.
- Furness, S., H. Roberts, J. Marjoribanks and A. Lethaby. Hormone therapy in postmenopausal women and risk of endometrial hyperplasia. *Cochrane Database of Systematic Reviews* 2012;(8).
- Gabriel, B., C. Rubod, M. Brieu, B. Dedet, L. de Landsheere, V. Delmas and M. Cosson. Vagina, abdominal skin, and aponeurosis: do they have similar biomechanical properties? *Int Urogynecol J* 2011; **22**(1): 23-27.
- Gargett, B. E. and R. W. S. Chan. Endometrial stem/progenitor cells and proliferative disorders of the endometrium. *Minerva Ginecol.* 2006; **58**(6): 511-526.
- Gargett, C. Stem cells of the human uterus: derivation, characterisation and uses of endometrial stem cells. 2, 2010. *Stem cells: From Bench to Bedside.* A. Bongso and E. Lee.
- Gargett, C. E. Uterine stem cells: What is the evidence? *Hum. Reprod. Update* 2007; **13**(1): 87-101.
- Gargett, C. E., H. P. T. Nguyen and L. Ye. Endometrial regeneration and endometrial stem/progenitor cells. *Rev. Endocr. Metab. Disord.* 2012; **13**(4): 235-251.
- Gargett, C. E., K. E. Schwab, R. M. Zillwood, H. P. Nguyen and D. Wu. Isolation and culture of epithelial progenitors and mesenchymal stem cells from human endometrium. *Biol. Reprod.* 2009; **80**(6): 1136-1145.
- Gelse, K., E. Poschl and T. Aigner. Collagens - structure, function, and biosynthesis. *Adv. Drug Del. Rev.* 2003; **55**(12): 1531-1546.
- Gerhard Meisenberg, W. H. S. P. D., William H. Simmons. Principles of Medical Biochemistry. 2006.
- Gilchrist, A. S., A. Gupta, R. C. Eberhart and P. E. Zimmern. Do Biomechanical Properties of Anterior Vaginal Wall Prolapse Tissue Predict Outcome of Surgical Repair? *J. Urol.* 2010; **183**(3): 1069-1073.
- Glover, J. C., J. L. Boulland, G. Halasi and N. Kasumacic. Chimeric Animal Models in Human Stem Cell Biology. *Ilar Journal* 2010; **51**(1): 62-73.
- Goh, J. T. W. Biomechanical properties of prolapsed vaginal tissue in pre- and postmenopausal women. *Int Urogynecol J* 2002; **13**(2): 76-79.
- Gomes, A. M. N., E. C. Baracat, M. J. Simoes, M. A. Haidar, G. R. A. Focchi, J. EvencioNeto and G. R. deLima. Morphologic and morphometric aspects of the endometrium of postmenopausal women before and after cyclic oestrogen replacement treatment. *European Journal of Obstetrics Gynecology and Reproductive Biology* 1997; **74**(1): 79-82.
- Griffin, M. D., T. Ritter and B. P. Mahon. Immunological aspects of allogeneic mesenchymal stem cell therapies. *Hum. Gene Ther.* 2010; **21**(12): 1641-1655.

- Gronthos, S., M. Mankani, J. Brahim, P. G. Robey and S. Shi. Postnatal human dental pulp stem cells (DPSCs) in vitro and in vivo. *Proc. Natl. Acad. Sci. U. S. A.* 2000; **97**(25): 13625-13630.
- Gronthos, S., A. C. Zannettino, S. J. Hay, S. Shi, S. E. Graves, A. Kortessidis and P. J. Simmons. Molecular and cellular characterisation of highly purified stromal stem cells derived from human bone marrow. *J. Cell Sci.* 2003; **116**(Pt 9): 1827-1835.
- Guerette, N. L., T. V. Peterson, O. A. Aguirre, D. M. VanDrie, D. H. Biller and G. W. Davila. Anterior Repair With or Without Collagen Matrix Reinforcement A Randomized Controlled Trial. *Obstet. Gynecol.* 2009; **114**(1): 59-65.
- Gyhagen, M., M. Bullarbo, T. Nielsen and I. Milsom. The prevalence of urinary incontinence 20years after childbirth: a national cohort study in singleton primiparae after vaginal or caesarean delivery. *Br. J. Obstet. Gynaecol.* 2013; **120**(2): 144-151.
- Gyhagen, M., M. Bullarbo, T. F. Nielsen and I. Milsom. Prevalence and risk factors for pelvic organ prolapse 20 years after childbirth: a national cohort study in singleton primiparae after vaginal or caesarean delivery. *Bjog-an International Journal of Obstetrics and Gynaecology* 2013; **120**(2): 152-160.
- Handa, V. L., E. Garrett, S. Hendrix, E. Gold and J. Robbins. Progression and remission of pelvic organ prolapse: A longitudinal study of menopausal women. *Am. J. Obstet. Gynecol.* 2004; **190**(1): 27-32.
- Haylen, B. T., D. de Ridder, R. M. Freeman, S. E. Swift, B. Berghmans, J. Lee, A. Monga, E. Petri, D. E. Rizk, P. K. Sand and G. N. Schaer. An International Urogynecological Association (IUGA)/International Continence Society (ICS) Joint Report on the Terminology for Female Pelvic Floor Dysfunction. *Neurourol. Urodyn.* 2010; **29**(1): 4-20.
- Haynesworth, S. F., V. M. Goldberg and A. I. Caplan. Diminution of the number of mesenchymal stem-cells as a cause for skeletal aging. 1993. *Musculoskeletal Soft-Tissue Aging: Impact on Mobility.* J. A. Buckwalter, V. M. Goldberg and S. L. Y. Woo: 79-87.
- Hendrix, S. L., A. Clark, I. Nygaard, A. Aragaki, V. Barnabei and A. McTiernan. Pelvic organ prolapse in the Women's Health Initiative: Gravity and gravidity. *Am. J. Obstet. Gynecol.* 2002; **186**(6): 1160-1166.
- Hickey, M., T. M. Lau, P. Russell, I. S. Fraser and P. A. W. Rogers. Microvascular density in conditions of endometrial atrophy. *Hum. Reprod.* 1996; **11**(9): 2009-2013.
- Hida, N., N. Nishiyama, S. Miyoshi, S. Kira, K. Segawa, T. Uyama, T. Mori, K. Miyado, Y. Ikegami, C. Cui, T. Kiyono, S. Kyo, T. Shimizu, T. Okano, M. Sakamoto, S. Ogawa and A. Umezawa. Novel cardiac precursor-like cells from human menstrual blood-derived mesenchymal cells. *Stem Cells* 2008; **26**(7): 1695-1704.
- Higgs, P. J., H. L. Chua and A. R. B. Smith. Long term review of laparoscopic sacrocolpopexy. *Bjog-an International Journal of Obstetrics and Gynaecology* 2005; **112**(8): 1134-1138.
- Hilger, W. S., A. Walter, M. E. Zobitz, K. O. Leslie, P. Magtibay and J. Cornella. Histological and biomechanical evaluation of implanted graft materials in a rabbit vaginal and abdominal model. *Am. J. Obstet. Gynecol.* 2006; **195**(6): 1826-1831.
- Hiltunen, R., K. Nieminen, T. Takala, E. Heiskanen, M. Merikari, K. Niemi and P. K. Heinonen. Low-weight polypropylene mesh for anterior vaginal wall prolapse: a randomized controlled trial. *Obstet. Gynecol.* 2007; **110**(2 Pt 2): 455-462.

- Hinoul, P., W. U. Ombelet, M. P. Burger and J. P. Roovers. A prospective study to evaluate the anatomic and functional outcome of a transobturator mesh kit (Prolift Anterior) for symptomatic cystocele repair. *J. Minim. Invasive Gynecol.* 2008; **15**(5): 615-620.
- Ho, M. H., S. Heydarkhan, D. Vernet, I. Kovanecz, M. G. Ferrini, N. N. Bhatia and N. F. Gonzalez-Cadavid. Stimulating Vaginal Repair in Rats Through Skeletal Muscle-Derived Stem Cells Seeded on Small Intestinal Submucosal Scaffolds. *Obstet. Gynecol.* 2009; **114**(2): 300-309.
- House, M., C. C. Sanchez, W. L. Rice, S. Socrate and D. L. Kaplan. Cervical Tissue Engineering Using Silk Scaffolds and Human Cervical Cells. *Tissue Engineering Part A* 2010; **16**(6): 2101-2112.
- Huebner, M., Y. Hsu and D. E. Fenner. The use of graft materials in vaginal pelvic floor surgery. *International Journal of Gynecology & Obstetrics* 2006; **92**(3): 279-288.
- Hulmes, D. J. S. Building collagen molecules, fibrils, and suprafibrillar structures. *J. Struct. Biol.* 2002; **137**(1-2): 2-10.
- Hunskar, S., K. Burgio, A. Clark, M. C. Lapitan, R. Nelson, U. Sillen and D. Thom. Epidemiology of urinary (UI) and faecal (FI) incontinence and pelvic organ prolapse (POP). 2005. [http://www.icsoffice.org/Publications/ICI\\_3/v1.pdf/chap5.pdf](http://www.icsoffice.org/Publications/ICI_3/v1.pdf/chap5.pdf).
- Hunskar, S. and A. Vinsnes. The quality of life in women with urinary incontinence as measured by the sickness impact profile. *J. Am. Geriatr. Soc.* 1991; **39**(4): 378-382.
- Ikegami, Y., S. Miyoshi, N. Nishiyama, N. Hida, K. Okamoto, K. Miyado, K. Segawa, S. Ogawa and A. Umezawa. Serum-independent Cardiomyogenic Transdifferentiation in Human Endometrium-derived Mesenchymal Cells. *Artif. Organs* 2010; **34**(4): 280-288.
- Ikoma, T., S. Kyo, Y. Maida, S. Ozaki, M. Takakura, S. Nakao and M. Inoue. Bone marrow-derived cells from male donors can compose endometrial glands in female transplant recipients. *Am. J. Obstet. Gynecol.* 2009; **201**(6).
- Jayo, M. J., D. Jain, J. W. Ludlow, R. Payne, B. J. Wagner, G. McLorie and T. A. Bertram. Long-term durability, tissue regeneration and neo-organ growth during skeletal maturation with a neo-bladder augmentation construct. *Regen. Med.* 2008; **3**(5): 671-682.
- Jean-Charles, C., C. Rubod, M. Brieu, M. Boukerrou, J. Fasel and M. Cosson. Biomechanical properties of prolapsed or non-prolapsed vaginal tissue: impact on genital prolapse surgery. *Int Urogynecol J* 2010; **21**(12): 1535-1538.
- Jelovsek, J. E., C. Maher and M. D. Barber. Pelvic organ prolapse. *Lancet* 2007; **369**(9566): 1027-1038.
- Jia, X. L., C. Glazener, G. Mowatt, D. Jenkinson, C. Fraser, C. Bain and J. Burr. Systematic review of the efficacy and safety of using mesh in surgery for uterine or vaginal vault prolapse. *Int Urogynecol J* 2010; **21**(11): 1413-1431.
- Kahn, M. A. and S. L. Stanton. Posterior colporrhaphy: Its effects on bowel and sexual function. *Br. J. Obstet. Gynaecol.* 1997; **104**(1): 82-86.
- Kannan, K., A. McConnell, M. McLeod and A. Rane. Microscopic alterations of vaginal tissue in women with pelvic organ prolapse. *J. Obstet. Gynaecol.* 2011; **31**(3): 250-253.
- Kaplan, J. M., M. E. Youd and T. A. Lodie. Immunomodulatory activity of mesenchymal stem cells. *Curr. Stem Cell Res. Ther.* 2011; **6**(4): 297-316.

- Kapoor, S., A. G. Wilson, B. Sharrack, A. Lobo, M. Akil, L. Sun, C. D. Dalley and J. A. Snowden. Haemopoietic stem cell transplantation - an evolving treatment for severe autoimmune and inflammatory diseases in rheumatology, neurology and gastroenterology. *Hematology* 2007; **12**(3): 179-191.
- Kazemnejad, S., M.-M. Akhondi, M. Soleimani, A. H. Zamani, M. Khanmohammadil, S. Darzi and K. Alimoghadam. Characterization and chondrogenic differentiation of menstrual blood-derived stem cells on a nanofibrous scaffold. *Int. J. Artif. Organs* 2012; **35**(1): 55-66.
- Keating, A. Mesenchymal Stromal Cells: New Directions. *Cell Stem Cell* 2012; **10**(6): 709-716.
- Kim, J. and P. Hematti. Mesenchymal stem cell-educated macrophages: A novel type of alternatively activated macrophages. *Exp. Hematol.* 2009; **37**(12): 1445-1453.
- Klinge, U., K. Junge, M. Stumpf, A. P. Ottinger and B. Klosterhalfen. Functional and morphological evaluation of a low-weight, monofilament polypropylene mesh for hernia repair. *J. Biomed. Mater. Res.* 2002; **63**(2): 129-136.
- Klinge, U., B. Klosterhalfen, V. Birkenhauer, K. Junge, J. Conze and V. Schumpelick. Impact of polymer pore size on the interface scar formation in a rat model. *J. Surg. Res.* 2002; **103**(2): 208-214.
- Klinge, U., V. Schumpelick and B. Klosterhalfen. Functional assessment and tissue response of short- and long-term absorbable surgical meshes. *Biomaterials* 2001; **22**(11): 1415-1424.
- Koc, O. N., S. L. Gerson, B. W. Cooper, S. M. Dyhouse, S. E. Haynesworth, A. I. Caplan and H. M. Lazarus. Rapid hematopoietic recovery after coinfusion of autologous-blood stem cells and culture-expanded marrow mesenchymal stem cells in advanced breast cancer patients receiving high-dose chemotherapy. *J. Clin. Oncol.* 2000; **18**(2): 307-316.
- Kohli, N. Controversies in utilization of transvaginal mesh. *Curr. Opin. Obstet. Gynecol.* 2012; **24**(5): 337-342.
- Konstantinovic, M. L., P. Lagae, F. Zheng, E. K. Verbeken, D. De Ridder and J. A. Deprest. Comparison of host response to polypropylene and non-cross-linked porcine small intestine serosal-derived collagen implants in a rat model. *Br. J. Obstet. Gynaecol.* 2005; **112**(11): 1554-1560.
- Konstantinovic, M. L., Y. Ozog, F. Spelzini, C. Pottier, D. De Ridder and J. Deprest. Biomechanical Findings in Rats Undergoing Fascial Reconstruction With Graft Materials Suggested as an Alternative to Polypropylene. *Neurourol. Urodyn.* 2010; **29**(3): 488-493.
- Konstantinovic, M. L., E. Pille, M. Malinowska, E. Verbeken, D. De Ridder and J. Deprest. Tensile strength and host response towards different polypropylene implant materials used for augmentation of fascial repair in a rat model. *Int Urogynecol J* 2007; **18**(6): 619-626.
- Krampera, M. Mesenchymal stromal cell 'licensing': a multistep process. *Leukemia* 2011; **25**(9): 1408-1414.
- Krause, H. and J. Goh. Sheep and rabbit genital tracts and abdominal wall as an implantation model for the study of surgical mesh. *J. Obstet. Gynaecol. Res.* 2009; **35**(2): 219-224.

- Kudish, B. I., C. B. Iglesia, R. J. Sokol, B. Cochrane, H. E. Richter, J. Larson, S. L. HendriX and B. V. Howard. Effect of Weight Change on Natural History of Pelvic Organ Prolapse. *Obstet. Gynecol.* 2009; **113**(1): 81-88.
- Ladewig, J., P. Koch and O. Brustle. Leveling Waddington: the emergence of direct programming and the loss of cell fate hierarchies. *Nature Reviews Molecular Cell Biology* 2013; **14**(4): 225-236.
- Lalu, M. M., L. McIntyre, C. Pugliese, D. Fergusson, B. W. Winston, J. C. Marshall, J. Granton, D. J. Stewart and G. Canadian Critical Care Trials. Safety of Cell Therapy with Mesenchymal Stromal Cells (SafeCell): A Systematic Review and Meta-Analysis of Clinical Trials. *PLoS One* 2012; **7**(10).
- Langer, R. and J. P. Vacanti. Tissue Engineering. *Science* 1993; **260**(5110): 920-926.
- Lapidot, T., F. Pflumio, M. Doedens, B. Murdoch, D. E. Williams and J. E. Dick. Cytokine stimulation of multilineage hematopoiesis from immature human-cells engrafted in SCID mice. *Science* 1992; **255**(5048): 1137-1141.
- Le Blanc, K., F. Frassoni, L. Ball, F. Locatelli, H. Roelofs, I. Lewis, E. Lanino, B. Sundberg, M. E. Bernardo, M. Remberger, G. Dini, R. M. Egeler, A. Bacigalupo, W. Fibbe and O. Ringden. Mesenchymal stem cells for treatment of steroid-resistant, severe, acute graft-versus-host disease: a phase II study. *Lancet* 2008; **371**(9624): 1579-1586.
- Le Blanc, K. and D. Mougiakakos. Multipotent mesenchymal stromal cells and the innate immune system. *Nat. Rev. Immunol.* 2012; **12**(5): 383-396.
- Le Blanc, K. and O. Ringdén. Immunobiology of Human Mesenchymal Stem Cells and Future Use in Hematopoietic Stem Cell Transplantation. *Biology of blood and marrow transplantation : journal of the American Society for Blood and Marrow Transplantation* 2005; **11**(5): 321-334.
- Lee, R. H., A. A. Pulin, M. J. Seo, D. J. Kota, J. Ylostalo, B. L. Larson, L. Semprun-Prieto, P. Delafontaine and D. J. Prockop. Intravenous hMSCs Improve Myocardial Infarction in Mice because Cells Embolized in Lung Are Activated to Secrete the Anti-inflammatory Protein TSG-6. *Cell stem cell* 2009; **5**(1): 54-63.
- Lei, L., Y. Song and R. Chen. Biomechanical properties of prolapsed vaginal tissue in pre- and postmenopausal women. *Int Urogynecol J* 2007; **18**(6): 603-607.
- Li, Z., C. Liu, Z. Xie, P. Song, R. C. H. Zhao, L. Guo, Z. Liu and Y. Wu. Epigenetic Dysregulation in Mesenchymal Stem Cell Aging and Spontaneous Differentiation. *PLoS One* 2011; **6**(6).
- Li, Z. Y., R. N. Wallace, B. W. Streeten, B. L. Kuntz and A. J. Dark. Elastic fiber components and protease inhibitors in pinguecula. *Invest. Ophthalmol. Vis. Sci.* 1991; **32**(5): 1573-1585.
- Lim, Y. N., R. Muller, A. Corstiaans, S. Hitchins, C. Barry and A. Rane. A long-term review of posterior colporrhaphy with Vypro 2 mesh. *Int Urogynecol J* 2007; **18**(9): 1053-1057.
- Loeffler, M., T. Bratke, U. Paulus, Y. Q. Li and C. S. Potten. Clonality and life cycles of intestinal crypts explained by a state dependent stochastic model of epithelial stem cell organization. *J. Theor. Biol.* 1997; **186**(1): 41-54.

- Lovatsis, D. and H. P. Drutz. Is transabdominal repair of mild to moderate cystocele necessary for correction of prolapse during a modified Burch procedure? *Int Urogynecol J* 2001; **12**(3): 193-198.
- Lowder, J. L., K. M. Debes, D. K. Moon, N. Howden, S. D. Abramowitch and P. A. Moalli. Biomechanical adaptations of the rat vagina and supportive tissues in pregnancy to accommodate delivery. *Obstet. Gynecol.* 2007; **109**(1): 136-143.
- Lu, S. H., H. B. Wang, H. Liu, H. P. Wang, Q. X. Lin, D. X. Li, Y. X. Song, C. M. Duan, L. X. Feng and C. Y. Wang. Reconstruction of Engineered Uterine Tissues Containing Smooth Muscle Layer in Collagen/Matrigel Scaffold In Vitro. *Tissue Engineering Part A* 2009; **15**(7): 1611-1618.
- Lukacz, E. S., J. M. Lawrence, R. Contreras, C. W. Nager and K. M. Luber. Parity, mode of delivery, and pelvic floor disorders. *Obstet. Gynecol.* 2006; **107**(6): 1253-1260.
- Maggini, J., G. Mirkin, I. Bognanni, J. Holmberg, I. M. Piazzon, I. Nepomnaschy, H. Costa, C. Canones, S. Raiden, M. Vermeulen and J. R. Geffner. Mouse bone marrow-derived mesenchymal stromal cells turn activated macrophages into a regulatory-like profile. *PLoS One* 2010; **5**(2): e9252.
- Maher, C. and K. Baessler. Surgical management of anterior vaginal wall prolapse: an evidencebased literature review. *Int Urogynecol J* 2006; **17**(2): 195-201.
- Maher, C., B. Feiner, K. Baessler, E. J. Adams, S. Hagen and C. M. Glazener. Surgical management of pelvic organ prolapse in women. *Cochrane Database of Systematic Reviews* 2010;(4): CD004014.
- Maher, C., B. Feiner, K. Baessler and C. Schmid. Surgical management of pelvic organ prolapse in women. *Cochrane Database of Systematic Reviews* 2013;(4).
- Maher, C. F., A. M. Qataweh, K. Baessler and P. J. Schluter. Midline Rectovaginal fascial plication for repair of rectocele and obstructed defecation. *Obstet. Gynecol.* 2004; **104**(4): 685-689.
- Maher, C. M., B. Feiner, K. Baessler and C. M. A. Glazener. Surgical management of pelvic organ prolapse in women: the updated summary version Cochrane review. *Int Urogynecol J* 2011; **22**(11): 1445-1457.
- Mallipeddi, P. K., A. C. Steele, N. Kohli and M. M. Karram. Anatomic and functional outcome of vaginal paravaginal repair in the correction of anterior vaginal wall prolapse. *Int Urogynecol J* 2001; **12**(2): 83-88.
- Mardon, R. E., S. Halim, L. G. Pawlson and S. C. Haffer. Management of urinary incontinence in Medicare managed care beneficiaries: results from the 2004 Medicare Health Outcomes Survey. *Arch. Intern. Med.* 2006; **166**(10): 1128-1133.
- Masuda, H., S. S. Anwar, H.-J. Buehring, J. R. Rao and C. E. Gargett. A Novel Marker of Human Endometrial Mesenchymal Stem-Like Cells. *Cell Transplant.* 2012; **21**(10): 2201-2214.
- Masuda, H., Y. Matsuzaki, E. Hiratsu, M. Ono, T. Nagashima, T. Kajitani, T. Arase, H. Oda, H. Uchida, H. Asada, M. Ito, Y. Yoshimura, T. Maruyama and H. Okano. Stem Cell-Like Properties of the Endometrial Side Population: Implication in Endometrial Regeneration. *PLoS One* 2010; **5**(4).
- McCracken, G. R. and G. Lefebvre. Mesh-free anterior vaginal wall repair: history or best practice? *The Obstetrician & Gynaecologist* 2007; **9**(4): 233-242.

- Meisel, R., A. Zibert, M. Laryea, U. Gobel, W. Daubener and D. Dilloo. Human bone marrow stromal cells inhibit allogeneic T-cell responses by indoleamine 2,3-dioxygenase-mediated tryptophan degradation. *Blood* 2004; **103**(12): 4619-4621.
- Meng, X., T. E. Ichim, J. Zhong, A. Rogers, Z. Yin, J. Jackson, H. Wang, W. Ge, V. Bogin, K. W. Chan, B. Thebaud and N. H. Riordan. Endometrial regenerative cells: A novel stem cell population. *J. Transl. Med.* 2007; **5**.
- Milani, A. L., P. Hinoul, J. M. Gauld, V. Sikirica, D. van Drie, M. Cosson and M. I. Prolift. Trocar-guided mesh repair of vaginal prolapse using partially absorbable mesh: 1 year outcomes. *Am. J. Obstet. Gynecol.* 2011; **204**(1).
- Miyahara, Y., N. Nagaya, M. Kataoka, B. Yanagawa, K. Tanaka, H. Hao, K. Ishino, H. Ishida, T. Shimizu, K. Kangawa, S. Sano, T. Okano, S. Kitamura and H. Mori. Monolayered mesenchymal stem cells repair scarred myocardium after myocardial infarction. *Nat. Med.* 2006; **12**(4): 459-465.
- Moalli, P. A., K. M. Debes, L. A. Meyn, N. S. Howden and S. D. Abramowitch. Hormones restore biomechanical properties of the vagina and supportive tissues after surgical menopause in young rats. *Am. J. Obstet. Gynecol.* 2008; **199**(2).
- Moalli, P. A., N. S. Howden, J. L. Lowder, J. M. Navarro, K. M. Debes, S. D. Abramowitch and S. L. Y. Woo. A rat model to study the structural properties of the vagina and its supportive tissues. *Am. J. Obstet. Gynecol.* 2005; **192**(1): 80-88.
- Moalli, P. A., S. J. Ivy, L. A. Meyn and H. M. Zyczynski. Risk factors associated with pelvic floor disorders in women undergoing surgical repair. *Obstet. Gynecol.* 2003; **101**(5): 869-874.
- Moalli, P. A., S. H. Shand, H. M. Zyczynski, S. C. Gordy and L. A. Meyn. Remodeling of vaginal connective tissue in patients with prolapse. *Obstet. Gynecol.* 2005; **106**(5 Pt 1): 953-963.
- Moalli, P. A., L. C. Talarico, V. W. Sung, W. L. Klingensmith, S. H. Shand, L. A. Meyn and S. C. Watkins. Impact of menopause on collagen subtypes in the arcus tendineous fasciae pelvis. *Am. J. Obstet. Gynecol.* 2004; **190**(3): 620-627.
- Mobarakeh, Z. T., J. Ai, F. Yazdani, S. M. R. Sorkhabadi, Z. Ghanbari, A. N. Javidan, S. A. Mortazavi-Tabatabaei, M. Massumi and S. E. Barough. Human endometrial stem cells as a new source for programming to neural cells. *Cell Biol. Int. Rep.* 2012; **19**(1): e00015-e00015.
- Morikawa, S., Y. Mabuchi, Y. Kubota, Y. Nagai, K. Niibe, E. Hiratsu, S. Suzuki, C. Miyauchi-Hara, N. Nagoshi, T. Sunabori, S. Shimmura, A. Miyawaki, T. Nakagawa, T. Suda, H. Okano and Y. Matsuzaki. Prospective identification, isolation, and systemic transplantation of multipotent mesenchymal stem cells in murine bone marrow. *J. Exp. Med.* 2009; **206**(11): 2483-2496.
- Morrison, S. J., N. M. Shah and D. J. Anderson. Regulatory mechanisms in stem cell biology. *Cell* 1997; **88**(3): 287-298.
- Murphy, M. B., K. Moncivais and A. I. Caplan. Mesenchymal stem cells: environmentally responsive therapeutics for regenerative medicine. *Exp. Mol. Med.* 2013; **45**: e54.
- Musina, R. A., A. V. Belyavski, O. V. Tarusova, E. V. Solovyova and G. T. Sukhikh. Endometrial Mesenchymal Stem Cells Isolated from the Menstrual Blood. *Bull. Exp. Biol. Med.* 2008; **145**(4): 539-543.

- Nakamura, T., T. Sato, M. Araki, S. Ichihara, A. Nakada, M. Yoshitani, S. Itoi, M. Yamashita, S. Kanemaru, K. Omori, Y. Horii, K. Endo, Y. Inada and K. Hayakawa. In situ tissue engineering for tracheal reconstruction using a luminal remodeling type of artificial trachea. *J. Thorac. Cardiovasc. Surg.* 2009; **138**(4): 811-819.
- Nemeth, K., A. Leelahavanichkul, P. S. T. Yuen, B. Mayer, A. Parmelee, K. Doi, P. G. Robey, K. Leelahavanichkul, B. H. Koller, J. M. Brown, X. Hu, I. Jelinek, R. A. Star and E. Mezey. Bone marrow stromal cells attenuate sepsis via prostaglandin E-2-dependent reprogramming of host macrophages to increase their interleukin-10 production. *Nat. Med.* 2009; **15**(1): 42-49.
- Nguyen, H. P., C. N. Sprung and C. E. Gargett. Differential expression of Wnt signaling molecules between pre- and postmenopausal endometrial epithelial cells suggests a population of putative epithelial stem/progenitor cells reside in the basalis layer. *Endocrinology* 2012; **153**(6): 2870-2883.
- Nygaard, I., M. D. Barber, K. L. Burgio, K. Kenton, S. Meikle, J. Schaffer, C. Spino, W. E. Whitehead, J. Wu and D. J. Brody. Prevalence of symptomatic pelvic floor disorders in US women. *JAMA* 2008; **300**(11): 1311-1316.
- Ochoa, I., E. Pena, E. J. Andreu, M. Perez-Illarbe, J. E. Robles, C. Alcaine, T. Lopez, F. Prosper and M. Doblare. Mechanical properties of cross-linked collagen meshes after human adipose derived stromal cells seeding. *Journal of Biomedical Materials Research Part A* 2011; **96A**(2): 341-348.
- Olsen, A. L., V. J. Smith, J. O. Bergstrom, J. C. Colling and A. L. Clark. Epidemiology of surgically managed pelvic organ prolapse and urinary incontinence. *Obstet. Gynecol.* 1997; **89**(4): 501-506.
- Ozog, Y., M. L. Konstantinovic, E. Werbrouck, D. De Ridder, M. Edoardo and J. Deprest. Shrinkage and biomechanical evaluation of lightweight synthetics in a rabbit model for primary fascial repair. *Int Urogynecol J* 2011; **22**(9): 1099-1108.
- Ozog, Y., E. Mazza, D. De Ridder and J. Deprest. Biomechanical effects of polyglycaprone fibers in a polypropylene mesh after abdominal and rectovaginal implantation in a rabbit. *Int Urogynecol J* 2012; **23**(10): 1397-1402.
- Paraiso, M. F. R., M. D. Barber, T. W. Muir and M. D. Walters. Rectocele repair: A randomized trial of three surgical techniques including graft augmentation. *Am. J. Obstet. Gynecol.* 2006; **195**(6): 1762-1771.
- Pascual, G., M. Rodriguez, V. Gomez-Gil, N. Garcia-Honduvilla, J. Bujan and J. M. Bellon. Early tissue incorporation and collagen deposition in lightweight polypropylene meshes: bioassay in an experimental model of ventral hernia. *Surgery* 2008; **144**(3): 427-435.
- Patel, A. N., E. Park, M. Kuzman, F. Benetti, F. J. Silva and J. G. Allickson. Multipotent menstrual blood stromal stem cells: Isolation, characterization, and differentiation. *Cell Transplant.* 2008; **17**(3): 303-311.
- Patel, A. N. and F. Silva. Menstrual blood stromal cells: the potential for regenerative medicine. *Regen. Med.* 2008; **3**(4): 443-444.
- Paulson, R. J., R. Boostanfar, P. Saadat, E. Mor, D. E. Tourgeman, C. C. Slater, M. M. Francis and J. K. Jain. Pregnancy in the sixth decade of life - Obstetric outcomes in women of advanced reproductive age. *Jama-Journal of the American Medical Association* 2002; **288**(18): 2320-2323.

- Pellegrini, G., R. Ranno, G. Stracuzzi, S. Bondanza, L. Guerra, G. Zambruno, G. Micali and M. De Luca. The control of epidermal stem cells (holoclonal) in the treatment of massive full-thickness burns with autologous keratinocytes cultured on fibrin. *Transplantation* 1999; **68**(6): 868-879.
- Pereira-Lucena, C. G., R. Artigiani-Neto, G. J. Lopes, C. V. G. Frazao, A. Goldenberg, D. Matos and M. M. Linhares. Experimental study comparing meshes made of polypropylene, polypropylene plus polyglactin and polypropylene plus titanium: inflammatory cytokines, histological changes and morphometric analysis of collagen. *Hernia : the journal of hernias and abdominal wall surgery* 2010; **14**(3): 299-304.
- Peron, J. P. S., T. Jazedje, W. N. Brandao, P. M. Perin, M. Maluf, L. P. Evangelista, S. Halpern, M. G. Nisenbaum, C. E. Czeresnia, M. Zatz, N. O. S. Camara and L. V. Rizzo. Human Endometrial-Derived Mesenchymal Stem Cells Suppress Inflammation in the Central Nervous System of EAE Mice. *Stem Cell Reviews and Reports* 2012; **8**(3): 940-952.
- Pierce, L. M., M. A. Grunlan, Y. Hou, S. S. Baumann, T. J. Kuehl and T. W. Muir. Biomechanical properties of synthetic and biologic graft materials following long-term implantation in the rabbit abdomen and vagina. *Am. J. Obstet. Gynecol.* 2009; **200**(5): 549.e541-548.
- Pines, A., D. W. Sturdee and A. H. MacLennan. Quality of life and the role of menopausal hormone therapy. *Climacteric* 2012; **15**(3): 213-216.
- Pittenger, M. F., A. M. Mackay, S. C. Beck, R. K. Jaiswal, R. Douglas, J. D. Mosca, M. A. Moorman, D. W. Simonetti, S. Craig and D. R. Marshak. Multilineage potential of adult human mesenchymal stem cells. *Science* 1999; **284**(5411): 143-147.
- Prockop, D. J. Marrow stromal cells as stem cells for nonhematopoietic tissues. *Science* 1997; **276**(5309): 71-74.
- Prockop, D. J. Repair of Tissues by Adult Stem/Progenitor Cells (MSCs): Controversies, Myths, and Changing Paradigms. *Mol. Ther.* 2009; **17**(6): 939-946.
- Prockop, D. J. and K. I. Kivirikko. Collagens- Molecular-Biology, Diseases, and potentials for therapy. *Annu. Rev. Biochem.* 1995; **64**: 403-434.
- Prockop, D. J. and J. Youn Oh. Mesenchymal Stem/Stromal Cells (MSCs): Role as Guardians of Inflammation. *Mol. Ther.* 2012; **20**(1): 14-20.
- Prokhorova, T. A., L. M. Harkness, U. Frandsen, N. Ditzel, H. D. Schroder, J. S. Burns and M. Kassem. Teratoma Formation by Human Embryonic Stem Cells Is Site Dependent and Enhanced by the Presence of Matrigel. *Stem cells and development* 2009; **18**(1): 47-54.
- Rahn, D. D., M. D. Ruff, S. A. Brown, H. F. Tibbals and R. A. Word. Biomechanical properties of the vaginal wall: effect of pregnancy, elastic fiber deficiency, and pelvic organ prolapse. *Am. J. Obstet. Gynecol.* 2008; **198**(5): 590.e591-596.
- Rajaraman, G., J. White, K. S. Tan, D. Ulrich, A. Rosamilia, J. A. Werkmeister and C. E. Gargett. Optimisation and scale up culture of human endometrial multipotent mesenchymal stromal cells: potential for clinical application. *Tissue Eng Part C Methods* 2013; **19**(1): 80-92.
- Ramshaw, J. A., Y. Y. Peng, V. Glattauer and J. A. Werkmeister. Collagens as biomaterials. *J. Mater. Sci. Mater. Med.* 2009; **20 Suppl 1**: S3-8.

- Raya-Rivera, A., D. R. Esquiliano, J. J. Yoo, E. Lopez-Bayghen, S. Soker and A. Atala. Tissue-engineered autologous urethras for patients who need reconstruction: an observational study. *Lancet* 2011; **377**(9772): 1175-1182.
- Reilly, E. T. C., R. M. Freeman, M. R. Waterfield, A. E. Waterfield, P. Steggles and F. Pedlar. Prevention of postpartum stress incontinence in primigravidae with increased bladder neck mobility: a randomised controlled trial of antenatal pelvic floor exercises. *Bjog-an International Journal of Obstetrics and Gynaecology* 2002; **109**(1): 68-76.
- Ren, G., L. Zhang, X. Zhao, G. Xu, Y. Zhang, A. I. Roberts, R. C. Zhao and Y. Shi. Mesenchymal stem cell-mediated immunosuppression occurs via concerted action of chemokines and nitric oxide. *Cell stem cell* 2008; **2**(2): 141-150.
- Ringden, O., T. Erkers, S. Nava, M. Uzunel, E. Iwarsson, R. Conrad, M. Westgren, J. Mattsson and H. Kaipe. Fetal Membrane Cells for Treatment of Steroid-Refractory Acute Graft-Versus-Host Disease. *Stem Cells* 2013; **31**(3): 592-601.
- Ritz-Timme, S., I. Laumeier and M. Collins. Age estimation based on aspartic acid racemization in elastin from the yellow ligaments. *Int. J. Legal Med.* 2003; **117**(2): 96-101.
- Roddy, G. W., J. Y. Oh, R. H. Lee, T. J. Bartosh, J. Ylostalo, K. Coble, R. H. Rosa, Jr. and D. J. Prockop. Action at a Distance: Systemically Administered Adult Stem/Progenitor Cells (MSCs) Reduce Inflammatory Damage to the Cornea Without Engraftment and Primarily by Secretion of TNF-alpha Stimulated Gene/Protein 6. *Stem Cells* 2011; **29**(10): 1572-1579.
- Roman, S., A. Mangera, N. I. Osman, A. J. Bullock, C. R. Chapple and S. Macneil. Developing a tissue engineered repair material for treatment of stress urinary incontinence and pelvic organ prolapse-which cell source? *Neurourol. Urodyn.* 2013: doi: 10.1002/nau.22443.
- Rubod, C., M. Boukerrou, M. Brieu, P. Dubois and M. Cosson. Biomechanical properties of vaginal tissue. Part 1: New experimental protocol. *J. Urol.* 2007; **178**(1): 320-325.
- Rubod, C., M. Boukerrou, M. Brieu, C. Jean-Charles, P. Dubois and M. Cosson. Biomechanical properties of vaginal tissue: preliminary results. *Int Urogynecol J* 2008; **19**(6): 811-816.
- Rubod, C., M. Brieu, M. Cosson, G. Rivaux, J.-C. Clay, L. de Landsheere and B. Gabriel. Biomechanical properties of human pelvic organs. *J. Urol.* 2012; **79**(4): 968.e917-922.
- Salem, H. K. and C. Thiemermann. Mesenchymal stromal cells: current understanding and clinical status. *Stem Cells* 2010; **28**(3): 585-596.
- Santamaria, X., E. E. Massasa, Y. Feng, E. Wolff and H. S. Taylor. Derivation of insulin producing cells from human endometrial stromal stem cells and use in the treatment of murine diabetes. *Mol. Ther.* 2011; **19**(11): 2065-2071.
- Schaffer, J. I., C. Y. Wai and M. K. Boreham. Etiology of pelvic organ prolapse. *Clin. Obstet. Gynecol.* 2005; **48**(3): 639-647.
- Schofield, R. Relationship between spleen colony-forming cell and hematopoietic stem-cell- hypothesis. *Blood Cells* 1978; **4**(1-2): 7-25.
- Schwab, K. E., R. W. S. Chan and C. E. Gargett. Putative stem cell activity of human endometrial epithelial and stromal cells during the menstrual cycle. *Fertil. Steril.* 2005; **84**: 1124-1130.

- Schwab, K. E. and C. E. Gargett. Co-expression of two perivascular cell markers isolates mesenchymal stem-like cells from human endometrium. *Hum. Reprod.* 2007; **22**(11): 2903-2911.
- Schwab, K. E., P. Hutchinson and C. E. Gargett. Identification of surface markers for prospective isolation of human endometrial stromal colony-forming cells. *Hum. Reprod.* 2008; **23**(4): 934-943.
- Scott, N., K. McCormack, P. Graham, P. Go, S. Ross and A. Grant. Open mesh versus non-mesh for repair of femoral and inguinal hernia. *Cochrane Database Syst Rev.* 2002; **4**: CD002197.
- Shackleton, M., F. Vaillant, K. J. Simpson, J. Stingl, G. K. Smyth, M. L. Asselin-Labat, L. Wu, G. J. Lindeman and J. E. Visvader. Generation of a functional mammary gland from a single stem cell. *Nature* 2006; **439**(7072): 84-88.
- Shepherd, P. R. Vaginal Prolapse in Ewes. *Vet. Rec.* 1992; **130**(25): 564-564.
- Shi, S. and S. Gronthos. Perivascular niche of postnatal mesenchymal stem cells in human bone marrow and dental pulp. *J. Bone Miner. Res.* 2003; **18**(4): 696-704.
- Signer, R. A. J. and S. J. Morrison. Mechanisms that regulate stem cell aging and life span. *Cell stem cell* 2013; **12**(2): 152-165.
- Simmons, P. J. and B. Torok-Storb. Identification of stromal cell precursors in human bone marrow by a novel monoclonal antibody, STRO-1. *Blood* 1991; **78**(1): 55-62.
- Sivasubramanian, K., A. Harichandan, S. Schumann, M. Sobiesiak, C. Lengerke, A. Maurer, H. Kalbacher and H. J. Buehring. Prospective Isolation of Mesenchymal Stem Cells from Human Bone Marrow Using Novel Antibodies Directed Against Sushi Domain Containing 2. *Stem cells and development* 2013; **22**(13): 1944-1954.
- Skoczylas, L. C., Z. Jallah, Y. Sugino, S. E. Stein, A. Feola, N. Yoshimura and P. Moalli. Regional Differences in Rat Vaginal Smooth Muscle Contractility and Morphology. *Reprod. Sci.* 2013; **20**(4): 382-390.
- Smith, F. J., C. D. Holman, R. E. Moorin and N. Tsokos. Lifetime risk of undergoing surgery for pelvic organ prolapse. *Obstet. Gynecol.* 2010; **116**(5): 1096-1100.
- Sobiesiak, M., K. Sivasubramanian, C. Hermann, C. Tan, M. Oergel, S. Treml, F. Cerabona, P. de Zwart, U. Ochs, C. A. Mueller, C. E. Gargett, H. Kalbacher and H.-J. Buehring. The Mesenchymal Stem Cell Antigen MSCA-1 is Identical to Tissue Non-specific Alkaline Phosphatase. *Stem cells and development* 2010; **19**(5): 669-677.
- Soderberg, M. W., C. Falconer, B. Bystrom, A. Malmstrom and G. Ekman. Young women with genital prolapse have a low collagen concentration. *Acta Obstet. Gynecol. Scand.* 2004; **83**(12): 1193-1198.
- Spelzini, F., M. L. Konstantinovic, I. Guelinckx, G. Verbist, E. Verbeken, D. De Ridder and J. Deprest. Tensile strength and host response towards silk and type i polypropylene implants used for augmentation of fascial repair in a rat model. *Gynecol. Obstet. Invest.* 2007; **63**(3): 155-162.
- Spitzer, T. L. B., A. Rojas, Z. Zelenko, L. Aghajanova, D. W. Erikson, F. Barragan, M. Meyer, J. S. Tamesis, A. E. Hamilton, J. C. Irwin and L. C. Giudice. Perivascular Human Endometrial Mesenchymal Stem Cells Express Pathways Relevant to Self-Renewal, Lineage Specification, and Functional Phenotype. *Biol. Reprod.* 2012; **86**(2).

- Stanford, E. J., A. Cassidenti and M. D. Moen. Traditional native tissue versus mesh-augmented pelvic organ prolapse repairs: providing an accurate interpretation of current literature. *Int Urogynecol J* 2012; **23**(1): 19-28.
- Stanford, E. J., T. F. Mattox and C. J. Pugh. Outcomes and Complications of Transvaginal and Abdominal Custom-shaped Light-weight Polypropylene Mesh Used in Repair of Pelvic Organ Prolapse. *J. Minim. Invasive Gynecol.* 2011; **18**(1): 64-67.
- Sumino, Y. and H. Mimata. Regenerative medicine as a new therapeutic strategy for lower urinary tract dysfunction. *Int. J. Urol.* 2013; **20**(7): 670-675.
- Sykes, B., B. Puddle, M. Francis and R. Smith. Estimation of 2 collagens from human dermis by interrupted gel- electrophoresis. *Biochem. Biophys. Res. Commun.* 1976; **72**(4): 1472-1480.
- Takahashi, K., K. Tanabe, M. Ohnuki, M. Narita, T. Ichisaka, K. Tomoda and S. Yamanaka. Induction of pluripotent stem cells from adult human fibroblasts by defined factors. *Cell* 2007; **131**(5): 861-872.
- Tanaka, S. T., R. Thangappan, J. A. Eandi, K. N. Leung and E. A. Kurzrock. Bladder Wall Transplantation-Long-Term Survival of Cells: Implications for Bioengineering and Clinical Application. *Tissue Engineering Part A* 2010; **16**(6): 2121-2127.
- Tang, Q. O., C. F. Carasco, Z. Gamie, N. Korres, A. Mantalaris and E. Tsiroidis. Preclinical and clinical data for the use of mesenchymal stem cells in articular cartilage tissue engineering. *Expert Opin. Biol. Ther.* 2012; **12**(10): 1361-1382.
- Taylor, H. S. Endometrial cells derived from donor stem cells in bone marrow transplant recipients. *JAMA* 2004; **292**(1): 81-85.
- Till, J. E. and C. E. Mc. A direct measurement of the radiation sensitivity of normal mouse bone marrow cells. *Radiat. Res.* 1961; **14**: 213-222.
- Torrente, Y. and E. Polli. Mesenchymal Stem Cell Transplantation for Neurodegenerative Diseases. *Cell Transplant.* 2008; **17**(10-11): 1103-1113.
- Uccelli, A., L. Moretta and V. Pistoia. Mesenchymal stem cells in health and disease. *Nature Reviews Immunology* 2008; **8**(9): 726-736.
- Ulrich, D., P. Dwyer, A. Rosamilia, Y. Lim and J. Lee. The effect of vaginal pelvic organ prolapse surgery on sexual function. *Neurourol. Urodyn.* 2014: doi: 10.1002/nau.22569.
- Ulrich, D., S. Edwards, K. Su, J. F. White, J. Ramshaw, G. Jenkin, J. Deprest, A. Rosamilia, J. Werkmeister and C. Gargett. Influence of reproductive status on tissue composition and biomechanical properties of ovine vagina. *PLoS One* 2014: in press.
- Ulrich, D., S. L. Edwards, K. Su, K. S. Tan, J. F. White, J. A. Ramshaw, C. Lo, A. Rosamilia, J. A. Werkmeister and C. E. Gargett. Human Endometrial Mesenchymal Stem Cells Modulate the Tissue Response and Mechanical Behaviour of Polyamide Mesh Implants for Pelvic Organ Prolapse Repair. *Tissue Eng.* 2013; **20**(3-4): 785-798.
- Ulrich, D., S. L. Edwards, J. F. White, T. Supit, J. A. M. Ramshaw, C. Lo, A. Rosamilia, J. A. Werkmeister and C. E. Gargett. A Preclinical Evaluation of Alternative Synthetic Biomaterials for Fascial Defect Repair Using a Rat Abdominal Hernia Model. *PLoS One* 2012; **7**(11).
- Ulrich, D., R. Muralitharan and C. Gargett. Toward the use of endometrial and menstrual blood mesenchymal stem cells for cell-based therapies. *Expert Opin. Biol. Ther.* 2013; **13**(10).

- Vaananen, H. K. Mesenchymal stem cells. *Ann. Med.* 2005; **37**(7): 469-479.
- Varmus, H. NIH funds support more than a researcher's own lab. *Nature* 2008; **452**(7189): 811.
- Vulic, M., T. Strinic, S. Tomic, V. Capkun, I. A. Jakus and S. Ivica. Difference in expression of collagen type I and matrix metalloproteinase-1 in uterosacral ligaments of women with and without pelvic organ prolapse. *European Journal of Obstetrics & Gynecology and Reproductive Biology* 2011; **155**(2): 225-228.
- Walker, G. J. A. and P. Gunasekera. Pelvic organ prolapse and incontinence in developing countries: review of prevalence and risk factors. *Int Urogynecol J* 2011; **22**(2): 127-135.
- Wang, H., P. Jin, M. Sabatino, J. Ren, S. Civini, V. Bogin, T. E. Ichim and D. F. Stroncek. Comparison of endometrial regenerative cells and bone marrow stromal cells. *J. Transl. Med.* 2012; **10**.
- Wang, J., S. Chen, C. Zhang, S. Stegeman, T. Pfaff-Amesse, Y. Zhang, W. Zhang, L. Amesse and Y. Chen. Human Endometrial Stromal Stem Cells Differentiate into Megakaryocytes with the Ability to Produce Functional Platelets. *PLoS One* 2012; **7**(8).
- Waterman, R. S., S. L. Tomchuck, S. L. Henkle and A. M. Betancourt. A new mesenchymal stem cell (MSC) paradigm: polarization into a pro-inflammatory MSC1 or an immunosuppressive MSC2 phenotype. *PLoS One* 2010; **5**(4): e10088.
- Wilson, A. and A. Trumpp. Bone-marrow haematopoietic-stem-cell niches. *Nature Reviews Immunology* 2006; **6**(2): 93-106.
- Woessner, J. F. Determination of hydroxyproline in tissue and protein samples containing small proportions of this imino acid. *Arch. Biochem. Biophys.* 1961; **93**(2): 440-&.
- Woessner, J. F. Matrix metalloproteinases and their inhibitors in connective-tissue remodelling. *FASEB J.* 1991; **5**(8): 2145-2154.
- Woessner, J. F. and T. H. Brewer. Formation and breakdown of collagen and elastin in human uterus during pregnancy and post-partum involution. *Biochem. J.* 1963; **89**(1): 75-&.
- Wolff, E. F., X. B. Gao, K. V. Yao, Z. B. Andrews, H. L. Du, J. D. Elsworth and H. S. Taylor. Endometrial stem cell transplantation restores dopamine production in a Parkinson's disease model. *J. Cell. Mol. Med.* 2011; **15**(4): 747-755.
- Ylostalo, J. H., T. J. Bartosh, K. Coble and D. J. Prockop. Human mesenchymal stem/stromal cells cultured as spheroids are self-activated to produce prostaglandin E2 that directs stimulated macrophages into an anti-inflammatory phenotype. *Stem Cells* 2012; **30**(10): 2283-2296.
- Young, S. B. Vaginal Surgery for Pelvic Organ Prolapse. *Obstet. Gynecol. Clin. North Am.* 2009; **36**(3): 565-+.
- Young, S. B., J. J. Daman and L. G. Bony. Vaginal paravaginal repair: One-year outcomes. *Am. J. Obstet. Gynecol.* 2001; **185**(6): 1360-1366.
- Yurteri-Kaplan, L. A. and R. E. Gutman. The Use of Biological Materials in Urogynecologic Reconstruction: A Systematic Review. *Plast. Reconstr. Surg.* 2012; **130**(5): 242S-253S.
- Zhang, J. W., C. Niu, L. Ye, H. Y. Huang, X. He, W. G. Tong, J. Ross, J. Haug, T. Johnson, J. Q. Feng, S. Harris, L. M. Wiedemann, Y. Mishina and L. H. Li. Identification

of the haematopoietic stem cell niche and control of the niche size. *Nature* 2003; **425**(6960): 836-841.

Zheng, F., Y. Lin, E. Verbeken, F. Claerhout, M. Fastrez, D. De Ridder and J. Deprest. Host response after reconstruction of abdominal wall defects with porcine dermal collagen in a rat model. *Am. J. Obstet. Gynecol.* 2004; **191**(6): 1961-1970.

Zhou, L., J. H. Lee, Y. Wen, C. Constantinou, M. Yoshinobu, S. Omata and B. Chen. Biomechanical Properties and Associated Collagen Composition in Vaginal Tissue of Women with Pelvic Organ Prolapse. *J. Urol.* 2012; **188**(3): 875-880.

Zimmern, P. E., R. C. Eberhart and A. Bhatt. Methodology for Biomechanical Testing of Fresh Anterior Wall Vaginal Samples From Postmenopausal Women Undergoing Cystocele Repair. *Neurourol. Urodyn.* 2009; **28**(4): 325-329.

Zong, W., S. E. Stein, B. Starcher, L. A. Meyn and P. A. Moalli. Alteration of Vaginal Elastin Metabolism in Women With Pelvic Organ Prolapse. *Obstet. Gynecol.* 2010; **115**(5): 953-961.

## **APPENDICES**

### **Appendix 1**

**Ulrich D**, Muralitharan R, Gargett CE. Toward the use of endometrial and menstrual blood MSC for cell based therapies. Expert Opinion on Biological Therapy. 2013 Oct;13(10):1387-400.

### **Appendix 2**

Rajaraman, G; White, J; Werkmeister, J; Tan, KS; **Ulrich, D**; Rosamilia, A; Gargett, C. Optimisation and scale up culture of human endometrial mesenchymal stem cells: potential for clinical application. Tissue Engineering C 2013 Jan; 19(1):80-92.

### **Appendix 3**

Front cover of the Journal of Tissue Engineering using Figure 6 out of my published manuscript: **Ulrich D**, Edwards SE, Su C, Tan KS, White J, Ramshaw JAM, Lo C, Rosamilia A, Werkmeister JA, Gargett CE. Human Endometrial Mesenchymal Stem Cells Modulate the Tissue Response and Mechanical Behaviour of Polyamide Mesh Implants for Pelvic Organ Prolapse Repair. Tissue Engineering A 2014 Feb;20(3-4):785-98.

## EXPERT OPINION

1. Introduction
2. Mesenchymal stem cells
3. Endometrial MSCs
4. Endometrial regenerative cells from menstrual blood
5. Preclinical 'Proof of Principle' animal studies with eMSCs
6. Preclinical 'Proof of Principle' animal studies with ERCs
7. Clinical trials using ERCs
8. Future clinical trials using ERCs
9. Conclusion
10. Expert opinion

**informa**  
healthcare

# Toward the use of endometrial and menstrual blood mesenchymal stem cells for cell-based therapies

Daniela Ulrich, Rikeish Muralitharan & Caroline E Gargett<sup>†</sup>

Monash University, Monash Institute of Medical Research, The Ritchie Centre, Melbourne, Australia

**Introduction:** Bone marrow is a widely used source of mesenchymal stem cells (MSCs) for cell-based therapies. Recently, endometrium – the highly regenerative lining of the uterus – and menstrual blood have been identified as more accessible sources of MSCs. These uterine MSCs include two related cell types: endometrial MSCs (eMSCs) and endometrial regenerative cells (ERCs).

**Areas covered:** The properties of eMSCs and ERCs and their application in preclinical *in vitro* and *in vivo* studies for pelvic organ prolapse, heart disorders and ischemic conditions are reviewed. Details of the first clinical Phase I and Phase II studies will be provided.

**Expert opinion:** The authors report that eMSCs and ERCs are a readily available source of adult stem cells. Both eMSCs and ERCs fulfill the key MSC criteria and have been successfully used in preclinical models to treat various diseases. Data on clinical trials are sparse. More research is needed to determine the mechanism of action of eMSCs and ERCs in these regenerative medicine models and to determine the long-term benefits and any adverse effects after their administration.

**Keywords:** endometrial mesenchymal stem cells, endometrial regenerative cells, glioma, hind limb ischemia, menstrual blood, mesenchymal stem cells, muscular dystrophy, myocardial infarct, pelvic organ prolapse, stroke

*Expert Opin. Biol. Ther.* (2013) **13**(10):1387-1400

## 1. Introduction

The unique properties of stem cells are self-renewal, differentiation into one or more lineages and high proliferative potential [1]. There are two main types of stem cells: embryonic stem cells and adult stem cells. Embryonic stem cells are derived from the inner cell mass of the blastocyst embryo and as pluripotent cells they can differentiate into all cell types derived from the three embryonic germ layers, namely, ectoderm, endoderm and mesoderm [2]. In contrast, adult stem cells are rare, long-lived cells found in most adult tissues. Adult stem cells also self-renew but are more restricted in differentiation repertoire (i.e., multipotent) and are less proliferative. Problems associated with embryonic stem cells are their unpredictable differentiation, tendency to generate teratomas [3], ethical issues and difficulty of access, therefore making adult stem cells an attractive option for cell-based therapies.

## 2. Mesenchymal stem cells

Mesenchymal stem cells or mesenchymal stromal cells (MSC) are defined as plastic adherent cells with a characteristic surface phenotype, with a capacity to proliferate

**Article highlights.**

- There are two methods for harvesting MSCs from the endometrium: an endometrial biopsy from the uterine cavity via the cervix or collection of menstrual blood.
- The eMSCs can be extracted from the stromal fraction using FACS sorting (CD146<sup>+</sup> CD140b<sup>+</sup> cells) or magnetic bead sorting (W5C5/SUSD2<sup>+</sup> cells).
- ERCs are cultured from menstrual blood similar to bmMSCs and includes fibroblasts. Some purify cultured menstrual blood cells by CD117 magnetic bead sorting.
- Few animal studies exist that test the *in vivo* effect of eMSCs or ERCs.
- To date, several clinical studies have used ERCs for non-uterine problems without adverse effects in any of the patients (n = 4).
- Several clinical studies are currently being developed using ERCs for uterine and non-uterine diseases.

This box summarizes key points contained in the article.

extensively and with a clonogenic activity [4]. MSC were first discovered in bone marrow in 1966 and later described by Friedenstein *et al.* as adherent fibroblast-like cells [5]. According to the International Society for Cellular Therapy (ISCT), MSCs must fulfill three main criteria: plastic adherence, multilineage differentiation into osteoblasts, adipocytes and chondrocytes, myocytes and other connective tissue cells *in vitro* and possession of key surface markers, including CD29, CD44, CD73, CD105 and CD146 but not the following hematopoietic cell markers CD34, CD45, CD14, CD11b, CD79 $\alpha$ , CD19 and HLA-DR [6,7]. MSCs from different sources may possess unique markers that can be used for their prospective isolation. CD271 and STRO-1 have been used in identifying and isolating bone marrow MSCs (bmMSCs) [8,9].

MSCs have been identified in most tissues including bone marrow, dental pulp, umbilical cord, corneal stroma, cord blood, amniotic fluid, skeletal muscle, periosteum, scalp tissue, pancreas, placenta, synovial membrane and endometrium [10-13]. MSCs appear to transdifferentiate into several cell lineages other than their mesodermal germ layer of origin, making them an attractive source for cell-based therapies for future treatment options [14]. Furthermore, substantial evidence indicates that MSCs are a subset of pericytes that line blood vessels [10,12,15,16] and promote tissue repair. MSCs are a heterogeneous population, especially when obtained by the plastic adherence method. A more pure population can be obtained when MSCs are extracted using specific markers.

MSCs were originally thought to aid tissue repair by transdifferentiation [17,18] into the cell types required. However, there is an increasing recognition that MSCs act in a paracrine manner by homing to damaged tissues and secreting copious quantities of bioactive molecules. These molecules promote angiogenesis, limit fibrosis and scarring, inhibit apoptosis and promote tissue-specific progenitor cells to proliferate [19].

MSCs also dampen the inflammatory response and modulate both the innate and adaptive immune system.

The precise mechanisms by which MSCs operate are still unclear and these functions are yet to be fully elucidated [17,20-23]. However, in an inflammatory milieu, cytokines such as tumor necrosis factor  $\alpha$  (TNF- $\alpha$ ) and interferon (IFN- $\gamma$ ) license MSCs [24] to produce anti-inflammatory mediators including prostaglandin E2 (PGE2) [25], indoleamine 2,3-dioxygenase (IDO) [26] and nitric oxide [27], which in turn modulate the function of natural killer cells and macrophages, which are key cells involved in the innate immune response. When macrophages are cocultured with MSCs, their production of proinflammatory cytokines such as TNF- $\alpha$  and IL-6 are diminished and anti-inflammatory cytokines such as IL-10 are increased [28,29]. MSC production of PGE2 drives a phenotypic change in macrophages from proinflammatory (M1) to anti-inflammatory (M2) phenotypes [29] through interaction with macrophage prostanoid receptors. MSCs also modulate the inflammatory response through toll-like receptor (TLR) signaling. Viral dsRNA activation of TLR-3 on MSC initiates an anti-inflammatory response in macrophages, while a proinflammatory macrophage response results from lipopolysaccharide (Gram-negative bacterial cell wall component) activation of TLR-4 on MSCs. This suggests that there are two different MSC phenotypes: MSC1 (proinflammatory) and MSC2 (anti-inflammatory) [30]. These phenotypes were speculated to result from stimulation by low concentrations of agonists, as expected *in vivo*. Further studies are needed to confirm the differential effects of TLR-3 and TLR-4 stimulation on these MSC phenotypes, as others have also shown that lipopolysaccharide-stimulated MSCs exert an anti-inflammatory response [28,31].

The immunosuppressive effects of MSCs on the adaptive immune system predominantly affect T-cell proliferative responses to foreign, non-self major histocompatibility complex molecules on antigen-presenting cells. These immunomodulatory properties of MSC have been exploited for treating acute graft-versus-host disease and indeed bmMSCs have been used in a successful clinical trial for this purpose [32]. More recently, placental stromal cells were also successfully used for the treatment for acute graft-versus-host disease with a response rate of 75% in a trial of eight patients [33]. Still much remains to be learned about the normal role of MSC in tissue repair and how this can be manipulated to create new therapeutics.

MSC are rare and few are available for harvest from adult tissues, requiring their substantial expansion *ex vivo*. As with most adult stem cells, prolonged culture of MSC results in their spontaneous differentiation to fibroblasts. The number of bmMSCs decrease with ageing, with a tenfold loss occurring within the first 10 years of life, and a similar rate of loss that continues until adulthood [34]. Furthermore, MSC defining surface markers are also expressed on fibroblasts and other cells, making it difficult to identify and purify MSCs from adjacent tissue cells [2]. They are predominantly

identified by key stem cell properties in cell culture, but flow cytometry phenotyping and fluorescence-activated cell sorting (FACS) using recently identified markers have also been used by some [9,35]. Furthermore, MSCs change their surface marker expression in culture, making it more difficult to obtain pure MSCs [36]. Identification of specific markers for MSC purification is a priority of current research, together with optimization of culture conditions to prevent spontaneous differentiation and loss of MSC activity and to achieve the desired cell type for transplantation [37].

### 2.1 Survival of transplanted MSC

Many animal and human studies have demonstrated a beneficial effect of MSC infusion or implantation on tissue and organ repair. MSCs home to sites of tissue damage when infused intravenously, where they secrete bioactive molecules that promote tissue repair, with little evidence of engraftment [38]. When infused cells are tracked *in vivo* after administration, few are found as they are rapidly trapped in the lungs and cleared from tissues. For example, intravenous injection of bmMSC in a mouse model of coronary artery disease (coronary vessel ligation) significantly improved myocardial parameters after 3 weeks; however, the cells were not detected after 48 h [39]. Large numbers of MSCs were found in the lungs where they induced upregulation of 50 genes including TNF- $\alpha$  [39]. Similarly, the inflammatory response in a rat model of corneal injury was reduced after intraperitoneal infusion of bmMSC. After 10 million cells were injected, < 10 were detected on day 3 suggesting that the cells do not engraft but rather release anti-inflammatory cytokines and proteins, including TNF- $\alpha$ -stimulated gene/protein 6 [40]. Similar results were observed in models of peritonitis and sepsis [41,42].

It has been suggested that MSCs act through a 'touch and go' mechanism. MSCs rapidly migrate to the damaged site and are cleared after release of their immunomodulatory payload [43]. Culture-expanded bmMSCs do not express human leukocyte antigen (HLA) class II cell surface molecules indicating their lack of involvement in the specific immune response [44]. MSCs can, therefore, be used in an allogeneic setting and there are several companies developing 'off-the-shelf' allogeneic products (e.g., Mesoblast, Medistem Inc.) with the advantage that a single donor can produce thousands of doses. It is currently unclear if immune rejection will be provoked if repeated doses from different individuals are administered. A recent review did not find an increased rate of toxicity events after unmatched heterologous MSC administration suggesting that MSCs are 'immune-privileged' [45]. In most of these studies, multiple doses of MSCs have not been administered and therefore it is still uncertain whether allogeneic MSC just might initiate an immune response in these circumstances. Multiple treatments are not an issue for autologous MSC and regulatory requirements are simpler.

### 3. Endometrial MSCs

Recently, a small population of clonogenic endometrial stromal cells with typical adult stem cell properties of self-renewal, high proliferative potential and multilineage mesodermal differentiation capacity was identified in human endometrium [46-48]. These were defined as endometrial MSCs (eMSCs). Cells with eMSC properties have also been identified as a component of the side population (SP) cells [49-51]. The eMSCs can be easily obtained by uterine biopsy with access via the cervix (Figure 1). In contrast, the procurement of bmMSCs and adipose MSCs requires at least local anesthesia, while the endometrium is one source of human MSCs that does not require an anesthetic [52]. While this may be considered a trivial issue by some, it can be an important consideration for other patients. Some researchers, therefore, prefer cord blood MSCs as they can be obtained from a waste product and are therefore easily accessible. The endometrium undergoes regular cycles of shedding and regeneration for up to 500 times during a woman's reproductive years [48]. Epithelial progenitor cells have also been found in endometrium; however, this review will focus on the MSC population. The eMSCs were found in both reproductive age and postmenopausal women and in the endometrium of women on oral contraceptive therapy [53] (unpublished observations by the authors), indicating that eMSCs can be harvested from women of all ages irrespective of hormonal status or treatments. The eMSCs are clonogenic and self-renew as demonstrated by serial cloning in culture [46]. They are also highly proliferative, undergoing 30 population doublings with a total cellular output of several billion cells from a single cell [46], indicating their capacity for *ex vivo* expansion and potential utility in cell-based therapies. On average,  $1 \times 10^6$  W5C5<sup>+</sup> cells can be obtained from either a curette or from a pipelle biopsy (unpublished observation).

#### 3.1 eMSC differentiation

Large endometrial stromal colony-forming units (CFU) undergo multilineage differentiation into four mesodermal lineages when cultured under appropriate conditions, including smooth muscle, fat, cartilage and bone [46]. Typical markers used in phenotyping bmMSCs and adipose tissue MSCs [7] were observed in endometrial stromal CFU-derived cells. Some of the colonies expressed  $\alpha$ -smooth muscle actin suggesting myofibroblastic differentiation [47]. Cultured endometrial stromal cells containing eMSCs differentiate down typical mesodermal lineages. eMSCs also differentiate into other non-endometrial cells, including platelet-releasing megakaryocytes *in vitro* [54], possibly by a direct transdifferentiation mechanism that does not involve de-differentiation or transition through distinct hierarchies of hematopoietic stem cells [55]. The eMSCs also differentiate into ectodermal and endodermal lineages, including neural cells *in vitro* and *in vivo* [56,57] and insulin-producing cells *in vitro* [58], thus

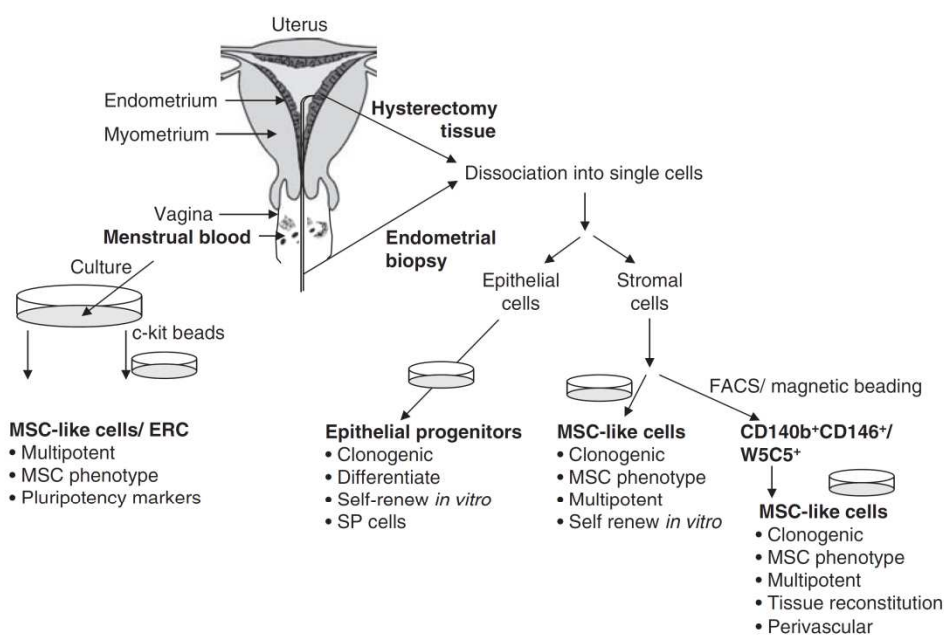


**Figure 1. Schematic representation showing isolation procedures for obtaining endometrial stem/progenitor cells from human uterus and menstrual blood.** Endometrial stem/progenitor cells are sourced from hysterectomy, endometrial biopsy and menstrual blood. Culture dishes indicate when culture occurs in the isolation or characterization procedures. Adult stem cell features conducted on the various cell populations are shown as dot points.

Adapted and reproduced with kind permission from World Scientific Publishers, Singapore [96].

making them a possible source for use in neurodegenerative diseases, such as stroke, Parkinson’s disease, Alzheimer’s disease, amyotrophic lateral sclerosis, epilepsy, trauma and intoxications, and for treatment of diabetes.

### 3.2 Source of eMSCs

The source of eMSCs is not yet clear. An endogenous source derived from residual fetal stem cells has been proposed [59], while there is some evidence that bone marrow cells may incorporate into human and mouse endometrium and contribute to the generation of endometrial cells [60,61]. Currently, it is not known if these incorporating bone marrow-derived cells are hematopoietic stem cells, MSCs, myeloid cells or endothelial progenitor cells, but they do not contribute to the SP [62]. In single antigen HLA mismatched bone marrow transplanted women, significant chimerism ranging from 0.2 to 52% of the endometrial glands and stroma was observed in four patients [63]. Most glands consisted entirely of host- or donor-derived cells indicating monoclonal derivation, although chimeric endometrial glands have also been reported in three women who had received gender mismatched bone marrow transplants [63]. It seems, therefore, more likely that eMSCs originate from resident stem/progenitor cells than bone marrow-derived cells; however, more research is needed.

### 3.3 Prospective isolation and scale-up culture of eMSCs

MSCs from bone marrow and adipose tissue are frequently obtained from simple culture of adherent cells and contain a mixture of fibroblasts and MSCs. STRO 1 has been used to purify bmMSCs, but this marker is not expressed on eMSCs [64]. Specific markers for eMSCs have been identified which can be used to prospectively isolate eMSCs from human endometrium as the co-expressing CD146<sup>+</sup>CD140b<sup>+</sup>-cell population (Figure 1) [12]. This CD146<sup>+</sup>CD140b<sup>+</sup> population fulfils the minimal criteria for MSCs, including surface phenotype (CD29, CD44, CD73, CD90 and CD105 expression). A recent gene profiling study of the three populations sorted from endometrial stromal cells immunostained with CD140b and CD146 antibodies confirmed that eMSCs are found in the double-positive population and expressed genes involved in angiogenesis, inflammation, immunomodulation, cell communication and proteolysis [65].

A recent innovation was the identification of a single marker, W5C5 for eMSCs [16]. The W5C5 antibody detects the SUSD2 transmembrane protein expressed on the cell surface [66]. Extracting eMSCs via magnetic beading is possible with a single marker and preferable to FACS sorting, as it is rapid and less traumatic for the cells [16]. On average, 4.2% of endometrial stromal cells are positive for W5C5 [16]. The

W5C5<sup>+</sup> eMSCs fulfill the minimal criteria for MSC [7] making them preferable for use as a cell-based therapy in proof-of-principle animal models [67].

### 3.4 *ex vivo* culture of eMSCs for cell-based therapies

The niche regulates stem cells by providing a specific physiological environment. Niche cells produce growth factors and other cytokines that together with extracellular matrix molecules regulate their functional state. Certain growth factors support the growth of eMSCs in serum-free medium, including epidermal growth factor, transforming growth factor- $\alpha$  (TGF- $\alpha$ ) and platelet-derived growth factor-BB (PDGF-BB) [53]. Owing to their rarity, freshly isolated eMSCs are only available in small numbers which makes *in vitro* expansion necessary (Figure 1). In preparation for clinical use, protocols have been developed for serum-free culture expansion of eMSCs [68]. In our first steps to achieve clinical grade production, we have shown that eMSCs can be cultured in serum-free medium without changing surface marker expression, differentiation capacity or proliferative potential [68].

### 3.5 W5C5<sup>+</sup> eMSCs regenerate stromal tissue *in vivo*

One of the most important functions of stem cell populations is their ability to reconstruct the appropriate tissue *in vivo*. W5C5<sup>+</sup> eMSCs reconstituted endometrial stromal tissue after transplantation under the kidney capsule in nonobese diabetic/severe combined immunodeficient IL-2 receptor  $\gamma$ -deficient (NOD/SCID  $\gamma$  or NSG) mice [16]. Similarly endometrial stromal tissue was also reconstituted when human endometrial SP cells were transplanted under the kidney capsule of immunocompromised mice [50,51]. These findings indicate that prospectively isolated, culture expanded eMSCs have the capacity to regenerate tissue and therefore have utility as a cell-based therapy.

## 4. Endometrial regenerative cells from menstrual blood

The endometrium is partially shed during menstruation every month, leaving behind the basal regenerative layer from which the new functional layer grows [52,69]. The markers used to purify eMSCs, co-expression of CD140b and CD146 or the single marker, W5C5/SUSD2, reveal their perivascular location in both the basal and functional layers, thus indicating they will be shed each month during menstruation. It is, therefore, not surprising that viable MSCs have been identified in menstrual blood. These have been isolated and characterized in a similar manner as bmMSCs using plastic adherence (Figure 1). These cultures include both MSCs and fibroblasts. These adherent cells were described as endometrial regenerative cells (ERCs) [70] and in this article, we will use this term. ERCs express key MSC markers (CD9, CD29, CD41a, CD44, CD59, CD73, CD90 and CD105) and lack the negative markers CD14, CD34 and CD45. Similar to eMSCs, they do not express STRO-1. The ERCs retained a stable karyotype for up to 68 passages and doubled every 19 h showing a higher proliferation rate than cord blood

MSCs [70]. ERCs have also been extracted from cultured menstrual blood mononuclear cells by c-kit selection [71]. Matrix metalloproteinases were highly expressed in ERCs; they produced high levels of MMP3, MMP10 and growth factors including granulocyte-macrophage colony-stimulating factor, angiopoietin-2 and PDGF-BB [70]. ERCs differentiated into nine different cell lineages from the three germ layers, including cardiomyocyte, neuronal, hepatic and pancreatic lineages [70,71]. ERCs express the pluripotent markers OCT-4 and SSEA-4 [72]. An independent group showed that ERCs were clonogenic, expressed typical MSC surface markers and differentiated into mesodermal lineages [73]. Myogenic differentiation of ERCs was demonstrated by coculture with rat cardiomyocytes. Some cultured cells started to beat spontaneously, formed sheets of heart muscle and incorporated into cardiac muscle when transplanted as a patch *in vivo* [74]. Similarly, cardiomyogenic transdifferentiation was observed when ERCs were cultured in serum-free medium, showing greater physiological similarity to cardiomyocytes compared to those cultured in serum-containing medium, likely due to unknown quantities of inhibitory factors present in some batches of serum [75].

### 4.1 ERCs and bmMSCs have similar properties

A recent, comprehensive comparative profiling of ERCs and bmMSCs for gene expression, miRNAs and cytokine production showed similar but not identical profiles [76]. The bmMSCs express higher levels of vascular endothelial growth factor (VEGF), IL-6, TGF $\beta$ 1 or TGF $\beta$ 2, whereas ERCs express higher levels of IL-8 and ICAM-1, thus suggesting that ERCs may have a role in acute inflammation and may be more suitable for different tissue engineering purposes. Other angiogenic cytokines, PDGF-BB and angiopoietin, were 27-fold and 14-fold higher in ERCs compared to bmMSCs, respectively, thus suggesting that alternative angiogenesis pathways may be activated by ERCs. Further studies are needed to determine if ERCs stimulate more angiogenesis *in vivo* than bmMSCs. ERCs seeded onto nanofibrous polycaprolactone scaffolds produced proteoglycans and collagen type II, indicating their potential for differentiating into cartilaginous tissue [77]. ERCs proliferate faster than bmMSCs and express the pluripotency marker, OCT-4, but like eMSCs [64] lack the MSC marker, STRO1 [77]. ERCs have been isolated by three independent groups [70,71,73] and appear similar to endometrial MSCs. Although comparative studies have not been reported for eMSCs and ERCs, it is expected that purified eMSC populations (CD140b<sup>+</sup>CD146<sup>+</sup> or W5C5<sup>+</sup>/SUSD2<sup>+</sup>) would be more potent than unfractionated plastic-adherent stromal cells cultured from menstrual blood. Further studies are also needed to compare eMSCs directly with bmMSCs.

## 5. Preclinical 'Proof of Principle' animal studies with eMSCs

Given that both eMSCs and ERCs were only recently discovered, only a few studies exist on their clinical suitability. These

have been summarized in Table 1. We are developing an autologous tissue engineering construct using synthetic meshes [78,79] and eMSCs to treat pelvic organ prolapse and have tested this in a small animal skin wound repair model [67]. Compared to mesh alone, the meshes implanted with W5C5<sup>+</sup> eMSCs showed better tissue integration by increasing initial neovascularization, reducing chronic inflammation, promoting deposition of better organized non-scarring collagen fibers and by increasing distensibility and reducing stiffness of the mesh–tissue complex after 3 months. Collectively, eMSCs diminished the foreign body reaction and improved mesh integration in the long term even though they only remained around the implanted mesh for ~ 14 days. Thus, eMSCs may have clinical application in favorably modulating tissue response to implanted foreign materials.

The potential clinical utility of intraperitoneal administration of eMSCs in a mouse model of encephalomyelitis [80] was demonstrated by fewer infiltrating mononuclear cells in the lesions, reduced recruitment of both Th1 and Th17 cells into the central nervous system and upregulation of cytokines IL-10 and IL-27 in the spleen, suggesting that eMSCs exerted a systemic anti-inflammatory effect. It has to be noted that the control group in this study was not properly described, so further studies evaluating the immunomodulatory properties of eMSCs are necessary.

## 6. Preclinical 'Proof of Principle' animal studies with ERCs

ERCs have also been examined in preclinical small animal models for a range of clinical applications, as summarized in Table 2.

Neural differentiation of ERCs was tested *in vitro* and *in vivo*. In an *in vitro* rat model of stroke, oxygen-deprived primary neuronal cell cultures exposed to human culture-expanded CD117-purified ERC exhibited significantly reduced cell death compared to the untreated neurons [81]. The soluble neuroprotective trophic factors released by ERCs included VEGF, brain-derived neurotrophic factor (BDNF) and neurotrophin-3 (NT-3). In an *in vivo* model of ischemic stroke, rats transplanted or injected with ERCs showed significantly lower behavioral and histological impairments compared to vehicle-only treated rats [81]. After 14 days, few of the inoculated ERCs were found, suggesting that ERCs had a trophic effect, secreting factors that promoted survival of the neural cells. It is unclear whether the ERCs developed into new tissue.

In another preclinical model of hind limb ischemia,  $1 \times 10^6$  ERCs were administered intramuscularly in rats 0, 2 and 4 days after ligating the femoral artery. The ERCs promoted angiogenesis thereby preventing limb necrosis [82]. A similar angiogenic effect of the ERCs was observed in a mouse model of muscular dystrophy which resulted in improved muscle repair [83]. In this study,  $2 \times 10^7$  ERCs were injected into the thigh muscle of dystrophic mice and were compared to

saline-injected controls. Mice treated with cells showed increased dystrophin expression in the affected muscles and improved muscle regeneration determined by quantitative immunohistochemistry.

ERCs have also been used to treat myocardial infarction in a rat coronary artery ligation model. Rats received  $1 - 2 \times 10^6$  ERCs or bmMSCs into the infarct lesion, 2 weeks after artery ligation. The size of the myocardial infarction zone was reduced in ERC-treated rats compared to the control or bmMSC group [74], suggesting that ERCs have a stronger reparative effect than bmMSCs. The safety profile of ERCs was investigated by comparing their tumorigenicity in immunocompromised mice with a positive control fibrosarcoma cell line at low, medium and high doses of ERCs ( $3 \times 10^4$ ,  $1 \times 10^5$  and  $2 \times 10^5$ ) to a negative control group administered saline. After 90 days, no adverse effects were observed in the ERCs and control groups, whereas the fibrosarcoma cell group developed tumors at the site of injection [84]. Histomorphological analysis of many organs showed no abnormalities in the ERCs and control groups. It was important to note that endometriosis did not develop in any mice treated with ERCs for any of the doses. However, larger studies are needed at higher doses to draw conclusions on the safety profile of ERCs.

In a rat model of intracranial glioma, unselected cultured ERCs were intravenously infused ( $3 \times 10^6$ ) or intratumorally administered ( $1 \times 10^6$ ). In both modes of delivery, the blood vessel density as determined by quantitative immunohistochemistry was reduced causing tumor shrinkage of almost 50%, indicating the ERCs had an anti-angiogenic effect. However the data are preliminary, since ERCs from only one patient were administered 2 days after C6/LacZ7 tumor cell injection into eight rats, while controls received no treatment, not even a saline injection. As a result, it is difficult to determine the robustness of the outcome measures [85]. These preliminary data suggest that ERCs inhibited tumor angiogenesis in contrast to their proangiogenic effect in ischemic tissues.

## 7. Clinical trials using ERCs

More than 600 trials using bmMSCs are currently registered and > 2000 patients have received MSCs therapy for a wide range of conditions (www.clinicaltrials.gov), but none have revealed adverse effects [32,52,86,87].

The first clinical report describing the use of ERCs was published in 2009 [88]. The safety of allogeneic ERC administration was assessed in a clinical setting by treating four women with multiple sclerosis. Between  $1.6 - 3.0 \times 10^7$  ERCs were infused three to six times within 10 days intravenously and/or intrathecally. No adverse side effects or immunological reactions were reported 12 months after the infusion. As the patients received various other specific treatments for concomitant disease and because a different ERC administration protocol was followed, a clinical effect could

Table 1. Preclinical animal trials using eMSCs.

Study	Method	Measurements	Results	Conclusions
A novel tissue engineering construct using human eMSCs and polyamide mesh for pelvic organ prolapse (POP) repair Ulrich <i>et al.</i> 2012 [67]	Warp-knitted polyamide scaffolds coated with gelatin were seeded with and without 250,000 DIO-labeled P6 W5C5 eMSCs/mesh (combined from two donors and used for the whole experiment). Tissue engineering constructs implanted into the dorsum of female CBH-rnu nude rats. Explantation was on days 7, 30, 60 and 90 Limitations: late passage eMSCs used. Rat is a poor model for human POP	FACS to determine phenotype of P6 cells and detect DIO-labeled cells Immunohistochemical staining for αSMA, CD45, CD68, CCR7, CD163, SDS-PAGE for collagen III(I+III) ratio Uniaxial testing to determine mechanical properties of explanted mesh	eMSCs survived ~ 14 days in the xenograft model Rats treated with cells showed higher neovascularization, reduced chronic inflammation, non-scarring collagen deposition, less foreign body reaction, increased mesh distensibility and less mesh stiffness at 90 days; long after the eMSCs had disappeared	eMSCs exerted multiple actions on the tissue response to the implanted mesh early on that had long-lasting effects which improved its biocompatibility
Human endometrial-derived MSCs suppress inflammation in the central nervous system of EAE mice Peron <i>et al.</i> 2012 [80]	Endometrial stromal cells from one donor were intraperitoneally injected (1.10 <sup>6</sup> cells) 1 day before experimental autoimmune encephalomyelitis (EAE) induction in C57B/6 female mice Limitations: cells from one donor used, time points examined were not stated and ERCs were given before rather than after disease induction	Real-time PCR for IL-10, IL-27, IDO, Foxp3 expression FACS for CD14, CD29, CD31, CD44, CD45, CD73, CD90 HLA-ABC, HLA-DR, SH4, Th1-(CD4 <sup>+</sup> IFN-γ), Th17 (CD4 <sup>+</sup> IL-17) H&E staining to determine mononuclear inflammatory cells	eMSC-treated mice showed significantly reduced EAE and reduced absolute numbers of CNS infiltrating mononuclear cells, lower percentage and absolute numbers of both Th1- and Th17 and upregulated transcription of IL-10 and IL-27 No difference in the percentage of CD4 <sup>+</sup> TNF-α <sup>+</sup> cells	eMSCs suppressed the development of neuroinflammation in a murine model of multiple sclerosis by reducing Th1- and Th17-biased cells

P: passage.

Table 2. Preclinical animal trials using ERCs.

Study	Method	Measurements	Results	Conclusions
Menstrual blood cells display stem cell-like phenotypic markers and exert neuroprotection following transplantation in experimental stroke Borlongan et al. 2010 [81]	<i>In vitro</i> : Primary rat neurons were cocultured for 2 days with P6-9 CD117 <sup>+</sup> ERCs or exposed to conditioned media (CM) from ERC cultures or control media <i>In vivo</i> : P6 or P9 ERC were transplanted into the striatum (IC) ( $4 \times 10^5$ ) or injected i.v. ( $4 \times 10^6$ ) in male SD stroke rats for 14 days ERCs were from Cryo-Cell International, Inc. Limitations: late passage number	<i>In vitro</i> : MTT assay for cell viability Immunocytochemistry for Oct4, SSEA, Nanog, CXCR4, Nestin, MAP2, GFAP, NeuN ELISA for VEGF, BDNF, NT-3, GDNF <i>In vivo</i> : Elevated body swing test for motor asymmetry Immunohistochemistry for MAP2, HuNu, Oct4 Morphology for endogenous cells in penumbra	ERC positive for Oct4, SSEA, Nanog at P9 ERCs differentiate into neural cells Neurons cocultured with ERCs or ERC CM increased cell viability ERCs produce VEGF, BDNF, NT-3 Rats showed reduced motor and neurological impairments, higher host cell survival in i.c. and i.v. dosed animals Better motor coordination in i.c. animals 15 and 1% graft survival rates for i.c. and i.v., respectively	ERCs protect cocultured neurons from experimental <i>in vitro</i> stroke ERCs improved stroke-related outcomes <i>in vivo</i>
Inhibition of intracranial glioma growth by endometrial regenerative cells Han et al. 2009 [85]	Male SD rats implanted intracranially (i.c.) with C6 tumor cells on day 0, day 2: three groups received either no treatment, (i.v.) $3 \times 10^6$ or $1 \times 10^6$ ERCs from one donor (i.c.) Limitation: passage number not stated, and cells were from only one donor. Controls did not receive any treatment	Day 14: X-gal stain for tumor size Immunohistochemistry for CD34, CD133	Reduced tumor volume of 49% in i.v. and i.c. group compared to control Reduced neovascularization	ERC have an anti-angiogenic effect in the tumor setting
Menstrual blood-derived cells confer human dystrophin expression in the murine model of Duchenne muscular dystrophy via cell fusion and myogenic transdifferentiation Cui et al. 2007 [83]	$2 \times 10^7$ ERCs (P2-3) injected into the thigh muscle in mice and compared to a control (saline injection) ERCs were collected from 21 patients Mice were examined 3 weeks later	RT-PCR for Myf5, MyoD, desmin, myogenin, myosin heavy chain- $\beta$ /d, dystrophin Immunohistochemistry for vimentin, dystrophin, anti-human Immunocytochemistry for skeletal myosin, MF20, $\alpha$ -sarcomeric actin, desmin Western Blotting for desmin, muogenin, dystrophin	No endometriosis formation at injection site Mice treated with ERCs showed positive staining for vimentin ERCs increased dystrophin-positive myofibers compared to control	ERCs differentiated into myoblasts/myotubes <i>in vivo</i>

P: passage.

Table 2. Preclinical animal trials using ERCs (continued).

Study	Method	Measurements	Results	Conclusions
Novel cardiac precursor-like cells from human menstrual blood-derived mesenchymal cells Hida <i>et al.</i> 2008 [74]	F344 nude rats received $1 - 2 \times 10^6$ ERCs or bmMSCs 2 weeks after coronary artery ligation into the main infarct lesion, and controls received fibroblasts from 6 donors BmMSC were obtained from a 41-year-old male Limitations: only one sample for bmMSC treatment group	Immunocytochemistry for cardiac troponin-I, sarcomeric $\alpha$ -actinin, connexin 43 Fluorescence inverted microscope to determine action potential of cells 5-azacytidine to differentiate cells into cardiomyogenic cells FISH chromosome painting RT-PCR for cardiac transcription factors and cardiac hormones Flow cytometry for phenotyping Histology for Masson's trichrome to determine infarcted area	ERCs transdifferentiated into cardiomyocytes, which beat in synchronized manner and expressed cardiac troponin-I, sarcomeric $\alpha$ -actinin and connexin-43 ERCs expressed human-cardiomyocyte-specific genes The rats treated with ERCs had reduced size of the myocardial infarction compared to the control or bmMSCs group	ERCs are incorporated into cardiac muscle and express cardiomyocyte specific markers ERCs are able to restore impaired cardiac function in a rat model

P: passage.

not be measured. This study also did not include control patients. The latest follow up in 2012 did not reveal any further complications [84]; however, more studies are required by treating more patients to determine the long-term safety of ERC administration.

The second case report was from a young man suffering from Duchenne muscular dystrophy who received 7 intramuscular doses of ERCs ( $8 - 28 \times 10^6$  cells/dose) over 11 days followed by a second cycle 4 months later including 4 doses over 4 days [89]. No adverse effects were noted for the first 3 years of follow up and the patient was in a stable healthy condition at the latest follow up. Increased muscle strength occurred in all muscle groups after both administration cycles. Confirmatory histology showed normal levels of muscular dystrophin. Furthermore, a decrease of respiratory infections was noted.

The third case report showed that intravenous ERC administration ( $3 \times 10^6$  cells on days 1, 2, 3, 4 and 7) to a patient with congestive heart failure improved the ejection fraction from 30 to 40%, decreased the 'Minnesota Living with Heart Failure Questionnaire' score and reduced basic natriuretic peptide values (Pro-BNP), a marker for heart failure, at one year follow up. No clinical or laboratory abnormalities could be detected [90].

## 8. Future clinical trials using ERCs

The preliminary results of the first clinical trial of ERCs were recently published. In the RECOVER-ERC trial launched by Medistem, 17 patients with congestive heart failure were administered ERCs using a minimally invasive retrograde coronary sinus delivery system ( $50 - 100 \times 10^6$  cells). Study end points were major cardiac adverse events, any other adverse events, and specific cardiac, blood and other diagnostic results. To date, none of the enrolled patients have shown any side effects, but the clinical data has not yet been published [84].

There has been recent notification of the imminent commencement of several Phase I and Phase II clinical trials involving ERCs. One Phase I/II trial aims to treat critical limb ischemia in a dose-escalating manner in patients who are not eligible for surgical or catheter-based interventions [91]. This trial was approved by the FDA but recruitment has not yet started. Patients will receive 25, 50 or  $100 \times 10^6$  ERCs in 10 separate injections on day 0 with 2 cm spacing between injection sites. The main outcome will be the safety of ERC administration. Secondary outcomes will be improvement in rest pain, toe pressure, transcutaneous oximetry and ulcer status.

Another trial aims to administer ERCs to improve the liver function in patients with liver cirrhosis [92]. There will be two treatment arms, one group will receive 2 weeks of conventional liver cirrhosis therapy plus ERC treatment ( $1 \times 10^6$  ERCs twice per week over a period of 2 weeks); the other group will receive 2 weeks of conventional therapy plus

placebo treatment. The main outcome will be overall survival. The secondary outcomes will be liver function improvement, complications, improvement of ascites and improved scores specific to liver disease.

To test the effect of ERCs in patients suffering from type 1 diabetes, another trial has been launched [93]. ERCs will be infused through the pancreatic artery or intravenously once a week for four consecutive ERC administrations ( $1 \times 10^6$ /kg/administration). The main outcome measure will be changes in glycosylated hemoglobin (HbA1c). Secondary outcomes measures will be side effects associated with the administered cells, number of severe and documented hypoglycemic events, reduction in fasting blood glucose, increase in basal C-peptide, postprandial blood glucose and random glucose levels.

In the reproductive setting, the effect of ERCs on embryo implantation following embryo transfer will be evaluated [94]. Undifferentiated ERCs and ERCs differentiated into endometrial stromal cells will be deposited into the uterine cavity just prior to embryo transfer during *in vitro* fertilisation (IVF) procedures to determine whether ERCs improve the implantation rate compared to a control group (no cells). The main outcome will be the implantation rate. Secondary outcomes include endometrial volume and vascularity measured by ultrasound.

## 9. Conclusion

MSCs can be obtained from the endometrium either by biopsy or by collecting menstrual blood. The eMSCs obtained by biopsy can be prospectively isolated using FACS or magnetic bead sorting, although some investigators simply culture the stromal fraction from tissue digests without MSC selection procedures. ERCs can be collected noninvasively and isolated using magnetic bead sorting; however, most studies simply culture the menstrual blood. Both eMSCs and ERCs possess key MSC properties including high proliferative potential, differentiation into several lineages and characteristic surface phenotype. The eMSCs and ERCs appear to have immunomodulatory, neuroprotective, anti-tumorigenic and angiogenic properties – the latter in an ischemic setting. The few clinical studies that have been published to date indicate that ERC administration is not associated with any severe side effects. Clinical Phase I and Phase II trials are currently underway and will reveal whether ERCs are of benefit in various clinical settings. In conclusion, eMSCs and ERCs provide an alternative, readily available source of MSCs for cell-based therapies.

## 10. Expert opinion

Both eMSCs and ERCs are an attractive source of adult MSCs as they are easy to obtain with minimal morbidity and are readily expandable in culture. Methods for the prospective isolation of eMSCs are quite advanced. At this stage, the advantage of using eMSCs is that purified eMSCs can be

easily extracted by magnetic bead sorting using the W5C5/SUSD2 marker [16]. Furthermore, protocols for culture expansion of eMSCs under clinical grade good manufacturing practice (cGMP) conditions are being developed [68] and the effects of these cells have been evaluated in an animal model [67]. There is a lack of information for cGMP production of ERCs. Most investigators do not use specific MSC markers to extract the ERCs but rather rely on MSCs' adherence to plastic. The purity of ERCs is therefore not guaranteed and these cultures include fibroblasts.

ERC collection from menstrual blood utilizes body waste and requires no invasive procedures, whereas a pipelle biopsy is needed to collect eMSCs. ERCs are collected in a menstrual cup over several hours on days 2 – 3 of the menstrual period, providing sufficient cell numbers. This source might increase the risk of infections through vaginal contact; however, after treatment with antibiotics and antimycotics, investigators have not reported any issues.

The eMSCs and ERCs possess stem cell properties; however, comparative studies are lacking to determine the exact profile of these cell types. While it is likely that they are from the same population, to date it has not been shown whether eMSCs and ERCs are the same or different populations. It is also likely that a purified eMSC population isolated from endometrial tissue using specific markers will be a more concentrated population of MSCs than plastic-adherent stromal cells cultured from menstrual blood.

The ability of eMSCs to reconstitute tissue *in vivo* has been shown [16,50]. However, there is concern that endometriosis could develop from the use of eMSCs or ERCs. To date, none of the preclinical animal models have shown endometriosis-like lesions [84], although this should be more thoroughly investigated. It seems that eMSCs and ERCs can be used outside of the uterine setting as has been shown in several studies examining their reparative effect in neurodegenerative or cardiac applications [74,81,83,89,95]. However, bmMSCs may be the best source for bone repair as they readily differentiate into osteocytes *in vitro* and *in vivo*. MSCs from the uterus may have a greater clinical potential in muscular and soft tissue repair and might be more suitable for endometrial regeneration and gynecologic surgery.

ERCs were rapidly introduced into clinical trials without preclinical evaluation in large animal models. It has not been established which large animal models are ideal to mimic the clinical setting and provide enough data in terms of adverse events. Furthermore, the mechanism of action of eMSCs or ERCs is not yet fully understood. Mechanistic studies providing more data on the fate of injected or implanted cells is necessary in both short and long term. It is unclear whether there is a potential risk of tumor formation since little data is available, although bmMSCs appear safe in this respect and it is likely that eMSCs and ERCs will behave similarly.

As with MSC therapies, there is debate on whether autologous or allogeneic cell-based therapies are preferable. The

advantage of autologous treatment is that there is no risk of infection or immune reaction, provided xeno-free culture conditions are applied. However, autologous treatment options are expensive in their development and unattractive for commercialization, whereas allogeneic therapies are more cost effective and commercially attractive. The current literature does not provide enough evidence on whether allogeneic cell-based therapies eventually lead to an immune response, particularly after repeated dosages, and this should be investigated.

Autologous therapies lend themselves to eMSC or ERC banking as a mechanism of guaranteeing a life-long supply of a woman's own cells. However, autologous therapies with eMSCs or ERCs exclude 50% of the population. The reproductive age of women ends in their early 50s with no further possibility of ERC collection. We are evaluating the potential of postmenopausal eMSCs (unpublished data). If they prove potent, eMSC collection could occur after menopause. However, many women undergo hysterectomy for various reasons, sometimes before menopause. Should the endometrium be collected from these women and the eMSCs banked for potential future use? Or should they be banked for allogeneic use? There is a private cord blood banking company in the United States that offers collection and storage of menstrual blood ERCs for future use (<http://www.cryo-cell.com/menstrual/stem-cells>). Personal storage of ERCs can be purchased in the United States for US\$4075 for a 25-year storage plan including collection and processing. Additional costs need to be considered depending on the future indication.

In summary, the endometrium has been a previously overlooked regenerative tissue that provides a novel source of

MSCs readily collected by biopsy or in menstrual blood. Their potential as an alternative source of MSCs for use in cell-based therapies has only just commenced. More animal studies are needed to determine their suitability for clinical therapies as well as their possible side effects. This new field of research is likely to rapidly expand in the coming years as these cells and their mechanism of action are further characterized. Their application will not only be for reproductive problems and infertility but also be for many other conditions where MSC-based therapies have shown promise.

## Acknowledgment

The assistance of R Gualano in manuscript preparation is gratefully acknowledged. We also acknowledge our collaborators for helpful discussions: J Werkmeister, J Ramshaw and S Edwards (CSIRO) as well as A Rosamilia (Monash University, Department of Obstetrics and Gynaecology).

## Declaration of interest

The authors acknowledge support from the Australian National Health and Medical Research Council grants (1021126) and Senior Research Fellowship 1042298 (CE Gargett), the CASS Foundation (CEG) and SMART (South East Melbourne Alliance for Regenerative Therapies) grant (CEG) and the Victorian Government's Operational Infrastructure Support Program. DU received scholarships from Monash University and the Australian Stem Cell Centre.

## Bibliography

Papers of special note have been highlighted as either of interest (●) or of considerable interest (●●) to readers.

- Eckfeldt CE, Mendenhall EM, Verfaillie CM. The molecular repertoire of the 'almighty' stem cell. *Nat Rev Mol Cell Biol* 2005;6(9):726-37
- Alvarez CV, Garcia-Lavandera M, Garcia-Rendueles ME, et al. Defining stem cell types: understanding the therapeutic potential of ESCs, ASCs, and iPS cells. *J Mol Endocrinol* 2012;49(2):R89-111
- Prokhorova TA, Harkness LM, Frandsen U, et al. Teratoma Formation by Human Embryonic Stem Cells Is Site Dependent and Enhanced by the Presence of Matrigel. *Stem Cells Dev* 2009;18(1):47-54
- Vaananen HK. Mesenchymal stem cells. *Ann Med* 2005;37(7):469-79
- Friedenstein AJ, Gorskaja UF, Kulagina NN. Fibroblast precursors in normal and irradiated mouse hematopoietic organs. *Exp Hematol* 1976;4(5):267-74
- Caplan AL. Adult mesenchymal stem cells for tissue engineering versus regenerative medicine. *J Cell Physiol* 2007;213(2):341-7
- Dominici M, Le Blanc K, Mueller I, et al. Minimal criteria for defining multipotent mesenchymal stromal cells. The International Society for Cellular Therapy position statement. *Cytotherapy* 2006;8(4):315-17
- Simmons PJ, Torok-Storb B. Identification of stromal cell precursors in human bone marrow by a novel monoclonal antibody. STRO-1. *Blood* 1991;78(1):55-62
- Buhring HJ, Battula VL, Trembl S, et al. Novel markers for the prospective isolation of human MSC. *Ann N Y Acad Sci* 2007;1106:262-71
- Crisan M, Yap S, Casteilla L, et al. A perivascular origin for mesenchymal stem cells in multiple human organs. *Cell Stem Cell* 2008;3(3):301-13
- Gronthos S, Mankani M, Brahimi J, et al. Postnatal human dental pulp stem cells (DPSCs) in vitro and in vivo. *Proc Natl Acad Sci USA* 2000;97(25):13625-30
- Schwab KE, Gargett CE. Co-expression of two perivascular cell markers isolates mesenchymal stem-like cells from human endometrium. *Human Reproduction* 2007;22(11):2903-11
- Brooke G, Rossetti T, Pelekanos R, et al. Manufacturing of human placenta-derived mesenchymal stem cells for clinical trials. *Br J Haematology* 2009;144(4):571-9

#### D. Ulrich et al.

14. Pittenger MF, Mackay AM, Beck SC, et al. Multilineage potential of adult human mesenchymal stem cells. *Science* 1999;284(5411):143-7
15. Caplan AI. All MSCs are pericytes? *Cell Stem Cell* 2008;3(3):229-30
16. Masuda H, Anwar SS, Buehring H-J, et al. A novel marker of human endometrial mesenchymal stem-like cells. *Cell Transplant* 21(10):2201-14
17. Prockop DJ, Youn Oh J. Mesenchymal Stem/Stromal Cells (MSCs): role as Guardians of Inflammation. *Mol Ther* 2012;20(1):14-20
18. Griffin MD, Ritter T, Mahon BP. Immunological aspects of allogeneic mesenchymal stem cell therapies. *Human Gene Ther* 2010;21(12):1641-55
19. Caplan A. Why are MSCs therapeutic? New data: new insight. *J Pathol* 2009;217(2):318-24
20. Le Blanc K, Mougiakakos D. Multipotent mesenchymal stromal cells and the innate immune system. *Nat Rev Immunol* 2012;12(5):383-96
21. Le Blanc K, Ringdén O. Immunobiology of Human Mesenchymal Stem Cells and Future Use in Hematopoietic Stem Cell Transplantation. *Biol Blood Marrow Transplant* 2005;11(5):321-34
22. Kaplan JM, Youd ME, Lodie TA. Immunomodulatory activity of mesenchymal stem cells. *Curr Stem Cell Res Ther* 2011;6(4):297-316
23. Chen X, Armstrong MA, Li G. Mesenchymal stem cells in immunoregulation. *Immunol Cell Biol* 2006;84(5):413-21
24. Krampera M. Mesenchymal stromal cell 'licensing': a multistep process. *Leukemia* 2011;25(9):1408-14
25. Ylostalo JH, Bartosh TJ, Coble K, Prockop DJ. Human mesenchymal stem/stromal cells cultured as spheroids are self-activated to produce prostaglandin E2 that directs stimulated macrophages into an anti-inflammatory phenotype. *Stem Cells* 2012;30(10):2283-96
26. Meisel R, Zibert A, Laryea M, et al. Human bone marrow stromal cells inhibit allogeneic T-cell responses by indoleamine 2,3-dioxygenase-mediated tryptophan degradation. *Blood* 2004;103(12):4619-21
27. Ren G, Zhang L, Zhao X, et al. Mesenchymal stem cell-mediated immunosuppression occurs via concerted action of chemokines and nitric oxide. *Cell Stem Cell* 2008;2(2):141-50
28. Maggini J, Mirkin G, Bognanni I, et al. Mouse bone marrow-derived mesenchymal stromal cells turn activated macrophages into a regulatory-like profile. *PLoS ONE* 2010;5(2):e9252
29. Kim J, Hematti P. Mesenchymal stem cell-educated macrophages: a novel type of alternatively activated macrophages. *Exp Hematol* 2009;37(12):1445-53
30. Waterman RS, Tomchuck SL, Henkle SL. A new mesenchymal stem cell (MSC) paradigm: polarization into a pro-inflammatory MSC1 or an immunosuppressive MSC2 phenotype. *PLoS ONE* 2010;5(4):e10088
31. Foraker JE, Oh JY, Ylostalo JH, et al. Cross-talk between human mesenchymal stem/progenitor cells (MSCs) and rat hippocampal slices in LPS-stimulated cocultures: the MSCs are activated to secrete prostaglandin E2. *J Neurochem* 2011;119(5):1052-63
32. Le Blanc K, Frassoni F, Ball L, et al. Mesenchymal stem cells for treatment of steroid-resistant, severe, acute graft-versus-host disease: a phase II study. *Lancet* 2008;371(9624):1579-86
33. Ringden O, Erkers T, Nava S, et al. Fetal membrane cells for treatment of steroid-refractory acute graft-versus-host disease. *Stem Cells* 2013;31(3):592-601
34. Haynesworth SF, Goldberg VM, Caplan AI. Diminution of the number of mesenchymal stem-cells as a cause for skeletal aging. In: Buckwalter JA, Goldberg VM, Woo SLY, editors. *Musculoskeletal soft-tissue aging: impact on mobility*. Amer Acad Orthopaedic Surgeons, Rosemont, IL; 1993. p. 79-87
35. Shi S, Gronthos S. Perivascular niche of postnatal mesenchymal stem cells in human bone marrow and dental pulp. *J Bone Mineral Res* 2003;18(4):696-704
36. Boquest AC, Shahdadfar A, Fronsdal K, et al. Isolation and transcription profiling of purified uncultured human stromal stem cells: alteration of gene expression after in vitro cell culture. *Mol Biol Cell* 2005;16(3):1131-41
37. Tang QO, Carasco CF, Gamie Z, et al. Preclinical and clinical data for the use of mesenchymal stem cells in articular cartilage tissue engineering. *Expert Opin Biol Ther* 2012;12(10):1361-82
38. Prockop DJ. Repair of tissues by adult stem/progenitor cells (MSCs): controversies, myths, and changing paradigms. *Mol Ther* 2009;17(6):939-46
39. Lee RH, Pulin AA, Seo MJ, et al. Intravenous hMSCs improve myocardial infarction in mice because cells embolized in lung are activated to secrete the anti-inflammatory protein TSG-6. *Cell Stem Cell* 2009;5(1):54-63
40. Roddy GW, Oh JY, Lee RH, et al. Action at a distance: systemically administered adult stem/progenitor cells (MSCs) reduce inflammatory damage to the cornea without engraftment and primarily by secretion of TNF-alpha stimulated gene/protein 6. *Stem Cells* 2011;29(10):1572-9
41. Nemeth K, Leelahavanichkul A, Yuen PST, et al. Bone marrow stromal cells attenuate sepsis via prostaglandin E-2-dependent reprogramming of host macrophages to increase their interleukin-10 production. *Nat Med* 2009;15(1):42-9
42. Choi H, Lee RH, Bazhanov N, et al. Anti-inflammatory protein TSG-6 secreted by activated MSCs attenuates zymosan-induced mouse peritonitis by decreasing TLR2/NF-kappa B signaling in resident macrophages. *Blood* 2011;118(2):330-8
43. Uccelli A, Moretta L, Pistoia V. Mesenchymal stem cells in health and disease. *Nat Rev Immunol* 2008;8(9):726-36
44. Koc ON, Gerson SL, Cooper BW, et al. Rapid hematopoietic recovery after coinfusion of autologous-blood stem cells and culture-expanded marrow mesenchymal stem cells in advanced breast cancer patients receiving high-dose chemotherapy. *J Clin Oncol* 2000;18(2):307-16
45. Lalu MM, McIntyre L, Pugliese C, et al. Safety of Cell Therapy with Mesenchymal Stromal Cells (SafeCell): a systematic review and meta-analysis of clinical trials. *PLoS ONE* 2012;7(10):e47559
46. Gargett CE, Schwab KE, Zillwood RM, et al. Isolation and culture of epithelial progenitors and mesenchymal stem cells from human endometrium. *Biol Reprod* 2009;80(6):1136-45
47. Chan RW, Schwab KE, Gargett CE. Clonogenicity of human endometrial

- epithelial and stromal cells. *Biol Reprod* 2004;70(6):1738-50
48. Gargett CE, Masuda H. Adult stem cells in the endometrium. *Mol Hum Reprod* 2010;16(11):818-34
  49. Cervello I, Gil-Sanchis C, Mas A, et al. Human endometrial side population cells exhibit genotypic, phenotypic and functional features of somatic stem cells. *PLoS ONE* 2010;5(6):e10964
  50. Cervello I, Mas A, Gil-Sanchis C, et al. Reconstruction of Endometrium from Human Endometrial Side Population Cell Lines. *PLoS One* 2011;6(6):e21221
  51. Masuda H, Matsuzaki Y, Hiratsu E, et al. Stem Cell-Like Properties of the Endometrial Side Population: implication in Endometrial Regeneration. *PLoS One* 2010;5(4):e10387
  - **A comprehensive study describing a simple prospective isolation protocol for eMSCs using a single novel single marker (W5C5). The W5C5<sup>+</sup> eMSCs fulfilled the ISCT criteria for MSCs and reconstituted endometrial stromal tissue *in vivo*.**
  52. Gargett CE, Nguyen HP, Ye L. Endometrial regeneration and endometrial stem/progenitor cells. *Rev Endocr Metab Disord* 2012;13(4):235-51
  53. Schwab KE, Chan RWS, Gargett CE. Putative stem cell activity of human endometrial epithelial and stromal cells during the menstrual cycle. *Fertil Steril* 2005;84:1124-30
  54. Wang J, Chen S, Zhang C, et al. Human endometrial stromal stem cells differentiate into megakaryocytes with the ability to produce functional platelets. *PLoS ONE* 2012;7(8):e44300
  55. Ladewig J, Koch P, Brustle O. Leveling Waddington: the emergence of direct programming and the loss of cell fate hierarchies. *Nat Rev Mol Cell Biol* 2013;14(4):225-36
  56. Mobarakeh ZT, Ai J, Yazdani F, et al. Human endometrial stem cells as a new source for programming to neural cells. *Cell Biol Intern Rep* (2010) 2012;19(1):e00015-e15
  57. Wolff EF, Gao XB, Yao KV, et al. Endometrial stem cell transplantation restores dopamine production in a Parkinson's disease model. *J Cell Mol Med* 2011;15(4):747-55
  58. Santamaria X, Massasa EE, Feng Y, et al. Derivation of insulin producing cells from human endometrial stromal stem cells and use in the treatment of murine diabetes. *Mol Ther* 2011;19(11):2065-71
  59. Gargett CE. Uterine stem cells: what is the evidence? *Human Reprod Update* 2007;13(1):87-101
  60. Du HL, Taylor HS. Contribution of bone marrow-derived stem cells to endometrium and endometriosis. *Stem Cells* 2007;25(8):2082-6
  61. Taylor HS. Endometrial cells derived from donor stem cells in bone marrow transplant recipients. *JAMA* 2004;292(1):81-5
  62. Cervello I, Gil-Sanchis C, Mas A, et al. Bone Marrow-Derived Cells from Male Donors Do Not Contribute to the Endometrial Side Population of the Recipient. *PLoS ONE* 2012;7(1):e30260
  63. Ikoma T, Kyo S, Maida Y, et al. Bone marrow-derived cells from male donors can compose endometrial glands in female transplant recipients. *Am J Obstet Gynecol* 2009;201(6):e1-8
  64. Schwab KE, Hutchinson P, Gargett CE. Identification of surface markers for prospective isolation of human endometrial stromal colony-forming cells. *Hum Reprod* 2008;23(4):934-43
  65. Spitzer TLB, Rojas A, Zelenko Z, et al. Perivascular human endometrial mesenchymal stem cells express pathways relevant to self-renewal, lineage specification, and functional phenotype. *Biol Reprod* 2012;86(2):58
  66. Sivasubramanian K, Harichandan A, Schumann S, et al. Prospective isolation of mesenchymal stem cells from human bone marrow using novel antibodies directed against sushi domain containing 2. *Stem Cells Dev* 2013;22(13):1944-54
  67. Ulrich D, Edwards S, White J, et al. A novel tissue engineering construct using human endometrial mesenchymal stem cells and polyamide mesh for pelvic organ prolapse (POP) repair. *J Tissue Eng Regen Med* 2012;6(Suppl 1):130
  68. Rajaraman G, White J, Tan KS, et al. Optimisation and scale up culture of human endometrial multipotent mesenchymal stromal cells: potential for clinical application. *Tissue Eng Part C Methods* 2013;19(1):80-92
  69. Gargett CE, Chan RW, Schwab KE. Hormone and growth factor signaling in endometrial renewal: role of stem/progenitor cells. *Mol Cell Endocrinol* 2008;288(1-2):22-9
  70. Meng X, Ichim TE, Zhong J, et al. Endometrial regenerative cells: a novel stem cell population. *J Transl Med* 2007;5:57
  71. Patel AN, Park E, Kuzman M, et al. Multipotent menstrual blood stromal stem cells: isolation, characterization, and differentiation. *Cell Transplant* 17(3):303-11
  72. Patel AN, Silva F. Menstrual blood stromal cells: the potential for regenerative medicine. *Regen Med* 2008;3(4):443-4
  73. Musina RA, Belyavski AV, Tarusova OV, et al. Endometrial mesenchymal stem cells isolated from the menstrual blood. *Bull Exp Biol Medicine* 2008;145(4):539-43
  74. Hida N, Nishiyama N, Miyoshi S, et al. Novel cardiac precursor-like cells from human menstrual blood-derived mesenchymal cells. *Stem Cells* 2008;26(7):1695-704
  - **A well-designed study evaluating the potential of ERCs *in vitro* and *in vivo* for cardiac tissue repair, showing cardiac transdifferentiation of ERCs and improved cardiac function after ERC administration.**
  75. Ikegami Y, Miyoshi S, Nishiyama N, et al. Serum-independent Cardiomyogenic Transdifferentiation in Human Endometrium-derived Mesenchymal Cells. *Artif Organs* 2010;34(4):280-8
  76. Wang H, Jin P, Sabatino M, et al. Comparison of endometrial regenerative cells and bone marrow stromal cells. *J Transl Med* 2012;10:207
  77. Kazemnejad S, Akhondi M-M, Soleimani M, et al. Characterization and chondrogenic differentiation of menstrual blood-derived stem cells on a nanofibrous scaffold. *Int J Artif Organs* 2012;35(1):55-66
  78. Ulrich D, Edwards SL, White JF, et al. A Preclinical evaluation of alternative synthetic biomaterials for fascial defect repair using a rat abdominal hernia model. *PLoS ONE* 2012;7(11):e50044
  79. Edwards SE, Werkmeister JA, Rosamilia A, et al. Characterisation of clinical and newly fabricated meshes for

- pelvic organ prolapse repair. *J Mech Behav Biomed Mater* 2013;23:53-61
80. Peron JPS, Jazedje T, Brandao WN, et al. Human endometrial-derived mesenchymal stem cells suppress inflammation in the central nervous system of EAE mice. *Stem Cell Rev Rep* 2012;8(3):940-52
  81. Borlongan CV, Kaneko Y, Maki M, et al. Menstrual blood cells display stem cell-like phenotypic markers and exert neuroprotection following transplantation in experimental stroke. *Stem Cells Dev* 2010;19(4):439-51
  - **An interesting study investigating the *in vitro* and *in vivo* effect of ERCs in a stroke model, showing that ERCs are neuroprotective in both settings.**
  82. Murphy MP, Wang H, Patel AN, et al. Allogeneic endometrial regenerative cells: an "Off the shelf solution" for critical limb ischemia? *J Transl Med* 2008;6:45
  83. Cui C-H, Uyama T, Miyado K, et al. Menstrual blood-derived cells confer human dystrophin expression in the murine model of Duchenne muscular dystrophy via cell fusion and myogenic transdifferentiation. *Mol Biol Cell* 2007;18(5):1586-94
  84. Bockeria L, Bogin V, Bockeria O, et al. Endometrial regenerative cells for treatment of heart failure: a new stem cell enters the clinic. *J Transl Med* 2013;11:56
  85. Han X, Meng X, Yin Z, et al. Inhibition of intracranial glioma growth endometrial regenerative cells. *Cell Cycle* 2009;8(4):606-10
  86. Horwitz EM, Gordon PL, Koo WK, et al. Isolated allogeneic bone marrow-derived mesenchymal cells engraft and stimulate growth in children with osteogenesis imperfecta: implications for cell therapy of bone. *Proc Natl Acad Sci USA* 2002;99(13):8932-7
  87. Lazarus HM, Koc ON, Devine SM, et al. Cotransplantation of HLA-identical sibling culture-expanded mesenchymal stem cells and hematopoietic stem cells in hematologic malignancy patients. *Biol Blood Marrow Transplant* 2005;11(5):389-98
  88. Zhong Z, Patel AN, Ichim TE, et al. Feasibility investigation of allogeneic endometrial regenerative cells. *J Transl Med* 2009;7:15
  89. Ichim TE, Alexandrescu DT, Solano F, et al. Mesenchymal stem cells as anti-inflammatories: implications for treatment of Duchenne muscular dystrophy. *Cell Immunol* 2010;260(2):75-82
  90. Ichim TE, Solano F, Lara F, et al. Combination stem cell therapy for heart failure. *Int Arch Med* 2010;3(1):5-5
  91. Phase I/II Trial of Endometrial Regenerative Cells (ERC) in patients with critical limb ischemia. 2013. Available from: <http://clinicaltrials.gov/ct2/show/NCT01558908?term=NCT01558908&rank=1> [Cited 1 April 2013]
  92. Human menstrual blood-derived mesenchymal stem cells for patients with liver cirrhosis. 2013. Available from: <http://clinicaltrials.gov/ct2/show/NCT01483248?term=menstrual+blood+cells&rank=1> [Cited 21 April 2013]
  93. Human menstrual blood-derived mesenchymal stem cells transplantation in treating Type 1 Diabetic Patients. 2013. Available from: <http://clinicaltrials.gov/ct2/show/NCT01496339?term=menstrual+blood+cells&rank=2> [Cited 21 April 2013]
  94. Role of stem cells in improving implantation rates in ICSI Patients. 2013. Available from: <http://clinicaltrials.gov/ct2/show/NCT01649752?term=endometrial+regenerative+cells&rank=2> [Cited 21 April 2013]
  95. Ichim TE, Solano F, Brenes R, et al. Placental mesenchymal and cord blood stem cell therapy for dilated cardiomyopathy. *Reprod Biomed Online* 2008;16(6):898-905
  96. Gargett CE. Stem cells of the human uterus: derivation, characterisation and uses of endometrial stem cells. In: Bongso A, Lee EH, editors. *Stem cells: from bench to bedside*. 2nd edition. World Scientific Publishing, New Jersey, London, Singapore; 2010. p. 583-609

#### Affiliation

Daniela Ulrich<sup>1,2</sup>, Rikeish Muralitharan<sup>1</sup> & Caroline E Gargett<sup>†1</sup>

<sup>†</sup>Author for correspondence

<sup>1</sup>Monash University, Monash Institute of Medical Research, The Ritchie Centre, 27-31 Wright Street, PO Box 5418, Clayton, Melbourne, 3168, Australia  
E-mail: caroline.gargett@monash.edu

<sup>2</sup>Medical University Graz, Department of Obstetrics and Gynecology, Auenbruggerplatz 14, 8036 Graz, Austria

## Appendix 2

TISSUE ENGINEERING: Part C  
Volume 19, Number 1, 2013  
© Mary Ann Liebert, Inc.  
DOI: 10.1089/ten.tec.2011.0718

# Optimization and Scale-up Culture of Human Endometrial Multipotent Mesenchymal Stromal Cells: Potential for Clinical Application

Gayathri Rajaraman, Ph.D.,<sup>1,2</sup> Jacinta White, B.App.Sci.,<sup>3</sup> Ker Sin Tan, M.Sc.,<sup>1,2</sup> Daniela Ulrich, M.D.,<sup>1,2,4</sup> Anna Rosamilia, MBBS, Ph.D., FRANZCOG,<sup>2</sup> Jerome Werkmeister, Ph.D.,<sup>3</sup> and Caroline E. Gargett, Ph.D.<sup>1,2</sup>

We have previously identified and purified multipotent mesenchymal stromal cell (MSC)-like cells in the highly regenerative endometrial lining of the human uterus (eMSC) as CD140b<sup>+</sup>CD146<sup>+</sup> cells. Due to ease of accessibility with minimal morbidity via biopsy, we are proposing to use eMSC in cell-based therapies; however, culture conditions compliant with Good Manufacturing Practice have not been established for eMSC. The aim of this study was to optimize serum-free and xeno-free culture conditions for expansion of eMSC for potential clinical use. Real-time cell assessment (Xcelligence) and MTS viability assays were used to measure attachment and proliferation of freshly isolated, flow cytometry-sorted CD140b<sup>+</sup>CD146<sup>+</sup> eMSC cultured in several commercially available and in-house serum-free and xeno-free media in combination with five attachment matrices (fibronectin, collagen, gelatin, laminin, and Cell Start-XF<sup>®</sup>). Comparisons were made with a standard serum-containing medium, DMEM/F-12/10% fetal bovine serum. Under all conditions examined, eMSC attachment and proliferation was greatest using a fibronectin matrix, with Lonza TP-SF<sup>®</sup> and our in-house DMEM/SF/FGF2/EGF serum-free xeno-product-containing medium similar to serum-containing medium. Hypoxia increased eMSC proliferation in the DMEM/SF/FGF2/EGF serum-free medium. Culture of eMSC for 7 days on a fibronectin matrix in DMEM/SF/FGF2/EGF serum-free media in 5% O<sub>2</sub> maintained greater numbers of undifferentiated eMSC expressing CD140b, CD146, and W5C5 compared to culture under similar conditions in Lonza TP-SF medium. However, the percentage of cells expressing typical MSC phenotypic markers, CD29, CD44, CD73, and CD105, were similar for both media. eMSC showed greater expansion in 2D compared to 3D culture on fibronectin-coated microbeads using the optimized DMEM/SF/FGF2/EGF medium in 5% O<sub>2</sub>. In the optimized 2D culture conditions, eMSC retained CFU activity, multipotency, and MSC surface phenotype, representing the first steps in their preparation for potential clinical use.

### Introduction

MESENCHYMAL STEM CELLS, also known as multipotent stromal cells or mesenchymal stromal cells (MSC),<sup>1</sup> were first discovered in the bone marrow as an adherent, clonogenic, nonhemopoietic cell population with capacity to undergo extensive proliferation in culture and differentiate into multiple mesodermal lineages.<sup>2</sup> MSC have since been identified in adipose tissue and multiple human organs, including the pancreas, skeletal muscle, endometrium,<sup>3,4</sup> and placenta,<sup>5-7</sup> where they are postulated to generate connective tissue over the lifespan. Substantial evidence indicates that MSC are a subset of pericytes that line the blood vessels<sup>7,8</sup> and secrete trophic and immunomodulatory factors in response to injury.<sup>9</sup>

MSC home to sites of tissue damage when infused intravenously, and secrete bioactive molecules that promote tissue repair, with little evidence of engraftment.<sup>10</sup> Transplanted MSC act in a paracrine manner secreting large quantities of angiogenic, antifibrotic, antiapoptotic, immunosuppressive factors and other molecules inducing endogenous tissue-specific progenitor cell mitosis to promote cellular replacement, angiogenesis, and limit scarring, cell death, immunosurveillance, and chronic inflammation—processes that collectively repair damaged tissue.<sup>9</sup> These important characteristics warrant MSC as a highly attractive cell source for regenerative medicine. Indeed, clinical trials using allogeneic bone marrow MSC for treatment of spinal cord injury, heart disease, stroke, and cartilage repair have already commenced.<sup>11,12</sup>

<sup>1</sup>The Ritchie Centre, Monash Institute of Medical Research, Clayton, Australia.

<sup>2</sup>Department of Obstetrics and Gynaecology, Monash University, Clayton, Australia.

<sup>3</sup>CSIRO, Division of Materials Science and Engineering, Clayton, Australia.

<sup>4</sup>Department of Obstetrics and Gynaecology, Medical University Graz, Graz, Austria.

We have previously identified MSC-like cells in human endometrium,<sup>4,8</sup> a highly regenerative tissue undergoing >400 cycles of growth, differentiation and shedding during a woman's reproductive years. We have demonstrated that a large, single human endometrial stromal colony forming unit (CFU) undergoes ~30 population doublings yielding ~ $6.1 \times 10^{12}$  cells, can be subcloned or replated at clonal level at least three times, and differentiates into mesodermal lineages, smooth muscle, osteocytes, adipocytes, and chondrocytes *in vitro*<sup>4</sup>, indicating that endometrial stromal CFU possess key adult stem cell properties of self-renewal, differentiation, and high proliferative capacity. Endometrial MSC (eMSC) can be prospectively isolated from hysterectomy<sup>8</sup> and endometrial biopsy<sup>13</sup> tissues as CD140b<sup>+</sup>CD146<sup>+</sup> cells, which have similar phenotype, proliferative capacity, and differentiation potential as other MSC. eMSC are enriched 10-fold in the CD140b<sup>+</sup>CD146<sup>+</sup> subpopulation over freshly isolated endometrial stromal cells.<sup>8</sup> These eMSC are found in a perivascular location, suggesting their role in endometrial repair and angiogenesis each menstrual cycle. Cultured stromal cells derived from endometrial biopsies also expressed CD140b and CD146 and differentiated into functional dopaminergic neurons<sup>14</sup> and insulin-producing pancreatic cells,<sup>15</sup> demonstrating the broad potential of eMSC for cell-based therapies.

Key advantages of using endometrial tissue as a source of MSC for cell-based therapies are the ease of accessibility via biopsy without the need for anesthetic, the lack of scarring, and the minimal pain incurred during their harvest. Therefore, we hypothesize that human eMSC are a readily available source of autologous cells that may provide a novel cell-based therapy for potential clinical applications. As eMSC comprise approximately 1% of endometrial stromal cells,<sup>4</sup> it will be necessary to first expand these cells in culture to obtain sufficient numbers for clinical use. This requires serum-free and xeno-free (animal product-free) culture conditions compliant with Good Manufacturing Practice (GMP).<sup>16,17</sup>

A potential autologous application for eMSC is pelvic organ prolapse (POP), a major hidden disease burden affecting millions of women.<sup>18</sup> POP is the herniation of the uterus, bladder, and/or bowel into the vagina, which can result in externalization of one or more these organs.<sup>19</sup> The symptoms of POP include urinary and bowel incontinence and sexual dysfunction; 25% of all women have one or more symptoms of POP.<sup>20</sup> The major risk factor for POP is vaginal delivery due to pelvic floor tissue damage after childbirth; however, aging, chronic constipation, chronic asthma, and obesity increase the risk of POP development.<sup>19</sup> Current treatment for POP is reconstructive surgery, frequently involving augmentation with synthetic mesh.<sup>21</sup> Nineteen percent of women have POP surgery, and of these, 15% will have further operations due to surgical failure or complications associated with mesh usage.<sup>22</sup> We are currently designing tissue engineering constructs incorporating human eMSC into novel scaffolds as an autologous cell-based therapy to regenerate the lost and damaged fascia of the vaginal wall and provide support for the pelvic organs.<sup>23</sup> In this study, we aim to optimize eMSC culture under serum-free or xeno-free conditions and scale up eMSC in 3D culture in preparation for potential clinical use in POP surgery.

## Materials and Methods

### Patient samples

Human endometrial tissue was collected from 38 premenopausal women aged 23–47 ( $35.9 \pm 1.2$ ) years undergoing Pipelle biopsy ( $n=29$ ) or hysterectomy ( $n=9$ ) for non-endometrial pathologies and who had not taken exogenous hormones for 3 months before surgery. eMSC have been purified and characterized in both hysterectomy<sup>8</sup> and biopsy<sup>13</sup> tissues. Written informed consent was obtained from each patient and human ethics approval was obtained from the Southern Health and Monash University Human Research Ethics committees. Tissues were collected via our departmental tissue bank.

### Endometrial stromal cell isolation

Endometrial tissue from hysterectomy tissue was scraped off from the underlying myometrial layer and dissociated to single cells using enzymatic and mechanical digestion as previously described.<sup>3,4</sup> Biopsy tissue was similarly dissociated. Briefly, endometrium was finely minced and dissociated in Ca<sup>2+</sup>- and Mg<sup>2+</sup>-free DMEM/F-12/10% fetal bovine serum (FBS) medium (Invitrogen) containing 0.5% (wt/vol) collagenase type 1 (Worthington Biochemical Corporation) and 40 µg/mL deoxyribonuclease type 1 (Roche Diagnostics) in a rotating MacsMix (Miltenyi Biotech) at 37°C for 90 min. The cell suspension was then filtered using a 40-µm sterile sieve (Becton-Dickinson Labware) to separate stromal cells from epithelial gland fragments and undigested tissue. The stromal cells in the filtrate were resuspended in HEPES-buffered DMEM/F-12/5% newborn calf serum (Bench medium), erythrocytes removed by Ficoll-Paque (Pharmacia Biotechnology) density gradient centrifugation, and then washed to produce single cell suspensions of endometrial stromal cells.

### Multicolor flow cytometry sorting to obtain eMSC

eMSC were obtained as previously described.<sup>8</sup> Briefly, purified endometrial stromal cell suspensions ( $>5 \times 10^6$  cells/mL) were labeled with CD146 antibody (CC9 clone, IgG2a) supernatant<sup>24</sup> (gift from P. Simmons; previously Peter MacCallum Cancer Centre), CD140b (PDGFR-β, 20 µg/mL, clone PR72 112, IgG<sub>1</sub>, R&D Systems), or isotype-matched negative control IgG<sub>2a</sub> and IgG<sub>1</sub> for 30 min, followed by washing and then fluorescein isothiocyanate (FITC)-conjugated anti-mouse IgG2a (50 µg/mL) and phycoerythrin (PE)-conjugated anti-mouse IgG<sub>1</sub> (10 µg/mL) (Becton Dickinson). Cells were then incubated with allophycocyanin (APC)-conjugated anti-CD45 (10 µg/mL; Caltag Laboratories), washed, and resuspended in 2% fetal calf serum/phosphate buffered saline (FCS/PBS) containing 5 µM SytoBlue cell viability marker (Invitrogen).

Flow cytometry cell sorting (FACS) was then performed to isolate CD140b<sup>+</sup>CD146<sup>+</sup> eMSC on a MoFlo<sup>®</sup> XDP cell sorter (Beckman Coulter) using established protocols for setting gates<sup>8</sup> and Summit software (version 5.2; Cytomation, Inc.). Flow cytometry-sorted eMSC cells were cultured in DMEM/F-12/10%FBS medium containing 10 ng/mL human fibroblast growth factor-2 (FGF2) (Millipore) in fibronectin-coated flasks (10 µg/mL; Becton Dickinson Biosciences) for 2 passages to generate sufficient numbers for use in subsequent

experiments as done previously.<sup>25</sup> Cells subject to serum-free and xeno-free conditions were weaned off serum by transfer from 10%FBS to 5%FBS to 1%FBS-supplemented DMEM/F-12 media for 24–48 h each, and then serum-starved in DMEM/0.5% bovine serum albumin, AlbuMAX I (derived from BSE-free animals, Invitrogen) medium for 24 h before experimental use.

#### *Xcelligence real-time cell assessment*

The Xcelligence Real-time Cell Assessment System (Roche Diagnostics) dynamically monitors cell activity by measuring changes in impedance, detected by the electrode sensor surface of the wells.<sup>26</sup> 96-well Xcelligence E-plates (ACEA Biosciences, Roche Diagnostics) were coated with various attachment matrices; 10 µg/mL fibronectin (Becton Dickinson Biosciences), 0.05% gelatin in PBS (Sigma Aldrich), collagen type-IV (1:100 dilution; Roche, gift from Dr. Ursula Manuelpillai, Monash Institute of Medical Research, Melbourne, Australia), Cell Start-XF<sup>®</sup> (1:50 dilution; xeno-free matrix; Invitrogen), and laminin (1:50 dilution; Invitrogen gift from Dr. Terry Johns, Monash Institute of Medical Research, Melbourne, Australia) for 1 h at 37°C. Serum- and xeno-free media were added in 50-µL volumes to appropriate wells and equilibrated at room temperature for 15 min before a background reading was taken on the Xcelligence Real-Time Cell Assessment System. Media examined were Lonza Therapeak chemically defined serum-free medium containing human serum albumin (Lonza TP-SF<sup>®</sup>), DMEM/SF/FGF2/EGF in-house serum-free xeno product-containing medium with 10 ng/mL FGF2, 10 ng/mL epidermal growth factor (EGF), 0.5% BSA (AlbuMAX I, Invitrogen), ITS (10 µg/mL insulin, 5.5 µg/mL transferrin, 6.7 ng/mL sodium selenite, 11 µg/mL sodium pyruvate; Invitrogen), 50 µM 2-mercaptoethanol (Sigma-Aldrich), 100 µM L-ascorbic acid-2-phosphate (Sigma-Aldrich), 100 µg/mL heparin (Sigma-Aldrich), 10 nM linoleic acid (Sigma-Aldrich), 2 mM glutamine, and antibiotic-antimycotic solution as previously described,<sup>3</sup> StemPro-XF<sup>®</sup> (xeno-free, Invitrogen), Mesencult-XF<sup>®</sup> (Stem-Cell Technologies), and DMEM/F-12/10%FBS (Gibco Invitrogen) (standard serum medium containing 1% glutamine and antibiotics). Endometrial stromal cells or eMSC cell suspensions were seeded in triplicate for each condition into E-plate wells at 1000 cells/well in a final volume of 100 µL. Initial attachment and spreading was monitored continuously by measuring real-time cell index (CI) every 5 min for the first 2 h. Thereafter, CI was measured every 30 min for 7–10 days, with medium changes every 2–3 days. Rate of attachment (CI/h) and CI doubling time for proliferating cells (between second and third media change) were calculated using Xcelligence RTCA software (version 1.2; ACEA Biosciences, Inc.).

#### *MTS proliferation assay*

The MTS-based colorimetric assay measuring cell viability was used to assess cell proliferation as described previously.<sup>27</sup> Endometrial stromal cells or eMSC cell suspensions were seeded into wells of a 96-well culture plate at 1000 cells/well in 100-µL volumes in triplicate for each condition and incubated in normoxia (20% O<sub>2</sub>, 5% CO<sub>2</sub>, 37°C) or hypoxia (5% O<sub>2</sub>, 5% CO<sub>2</sub>, 37°C) (Thermo Scientific Australia, Trigas incubator), MTS reagent (Cell Titer 96 Aqueous One

Solution; Promega) was added 2 h after seeding (time 0) and then after 4, 7, and 10 days of culture, and incubated for 2 h. Absorbance (490 nm) was measured on a microplate reader (SpectraMax Plus384; Molecular Devices) using SoftMax Pro software (version 4.8; Molecular Devices). Regular medium changes were every 2–3 days.

#### *Evaluation of eMSC phenotype cultured in optimized serum-free medium*

Paired cultures of passage 3 eMSC were cultured in Lonza-TP-SF and our in-house DMEM/SF/FGF2/EGF serum-free xeno-product containing medium for 7 days until 80% confluency and lifted with TrypLE<sup>™</sup> Express. The surface phenotype for typical MSC markers was examined by flow cytometry as described previously.<sup>8</sup> Briefly, cells were incubated with antibodies against CD29 (1 µg/mL, clone mAb 13, rat IgG2a; Becton Dickinson), CD44 (1 µg/mL, clone G44-26, mouse IgG2b; Becton Dickinson), CD73 (20 µg/mL, clone AD2, mouse IgG1; Becton Dickinson), CD105 (10 µg/mL, clone 266, mouse IgG1; Becton Dickinson), CD146 (CC9 supernatant), and their respective isotype IgGs at the same concentration and followed by either Alexa Fluor 488-conjugated anti-rat IgG (10 µg/mL; Molecular Probes), anti-mouse FITC conjugated IgG<sub>2b</sub> (Dako), or PE-conjugated anti-mouse Ig F(ab')<sub>2</sub> fragment (10 µL/mL; Chemicon Australia). Some cells were incubated directly with PE-Cy5.5-conjugated anti-CD34 (50 µL/mL, clone 581, mouse IgG1; Southern Biotech), APC-conjugated anti-CD45 (as above), FITC-conjugated anti-CD90 (1 µg/mL, clone 5E10, mouse IgG1; Becton Dickinson), PE-CD140b (20 µg/mL, clone PR72112, IgG<sub>1</sub>, R&D Systems), or PE-anti-human W5C5 (BioLegend). Conjugated isotype-matched controls were included for each antibody. Cells were then incubated with 5 µM Flow SYTOX Blue and viable cells were analyzed on a MoFlo cytometer as described above.<sup>8</sup>

#### *Evaluation of eMSC properties in optimized DMEM/SF/FGF2/EGF serum-free medium*

To assess CFU activity, passage 3 eMSC were cultured in DMEM/SF/FGF2/EGF serum-free xeno-product containing medium for 7 days until 80% confluency and were lifted with TrypLE Express. About 2000 cells were seeded at 100 cells/cm<sup>2</sup> in fibronectin-coated 6-cm culture dishes for 15 days, and cloning efficiency was calculated from formalin-fixed, hematoxylin-stained plates as reported previously.<sup>3</sup> To assess differentiation capacity, the remaining cells were cultured in standard adipogenic, myogenic, and osteogenic induction media and control medium (1% serum) on 13-mm coverslips for 3 weeks as described previously<sup>8</sup> and were assessed by Oil Red O or 1% Alizarin Red (pH 4.1) staining or immunostained using an alkaline phosphatase kit (Sigma-Aldrich) or  $\alpha$  smooth muscle actin ( $\alpha$  SMA; 3.6 µg/mL, clone 1A4; Dako) for adipogenic, osteogenic, and myogenic differentiation, respectively. Stained cells were examined under an Olympus microscope (Olympus Corporation) and images were captured using a digital video camera (Fujix; Fuji).

#### *3D culture of human eMSC*

Human eMSC were cultured on CultiSpher-S gelatin beads (Percell Biolytica, Sweden)<sup>28</sup> with and without

fibronectin (50 µg/mL) coating in DMEM/SF/FGF2/EGF serum-free xeno product-containing medium and DMEM/F-12/10%FBS media. Cells were seeded at 500,000 cells/0.45 mL hydrated settled CultiSpher-S beads (75 mg dry) as described previously<sup>29,30</sup> in 125-mL spinner flasks with a fluid level of 50 mL with intermittent stirring, 25 rpm for 2 min every 30 min for the first 21 h, and then stirred continuously at 25 rpm thereafter. Cell viability was assessed at various time points from 2 to 21 days using the Live/Dead<sup>®</sup> cell viability assay (Molecular Probes). Bead/cell suspensions were washed in warm PBS and incubated in the Live/Dead stain (2 µM calcein and 4 µM ethidium homodimer-1) for 15 min at 37°C. Live cells were stained green by Calcein-AM and dead cells red by ethidium homodimer-1. Viability was assessed using Nikon TE-2000U inverted fluorescence microscope. Cell production was determined by counting eMSC cultured for 6 and 12 days and harvested by Pronase (5 mg/mL, 6 min) (Calbiochem; EMD Biosciences) and counted by hemocytometer. For phenotyping, cells were harvested using xeno-free TrypLE Express (Gibco, Life Technologies) and then examined by flow cytometry.

#### Statistical analysis

Rate of stromal cell and eMSC attachment and CI doubling time (real-time Xcelligence data obtained using RTCA software) and MTS cell proliferation data were analyzed using GraphPad Prism software (version 5; GraphPad Software, Inc.). As data were not normally distributed by D'Agostino-Pearson test, nonparametric Friedman analysis and Dunn's *post-hoc* test were used to determine significant differences ( $p < 0.05$ ). Data are reported as means  $\pm$  SEM of  $n = 3$  experiments from three different patients' stromal cells or eMSC.

## Results

### Optimal serum-free and xeno-free culture conditions for human endometrial stromal cells

Unsorted endometrial stromal cells were initially cultured on five different matrices and uncoated plastic in six different culture media in a checkerboard manner using the Xcelligence system in order to identify key culture conditions for subsequent testing on eMSC. Our initial experiments focused on testing in-house serum-free medium previously used for eMSC clonal culture<sup>31</sup> and several commercially available serum-free and xeno-free media produced under GMP conditions and designed for bone marrow MSC culture. The serum-containing medium<sup>3</sup> was used as a comparator. Given that serum contains factors promoting cell attachment, it was necessary to identify the optimal matrix for cell attachment for use with serum-free and xeno-free media. Initial Xcelligence real-time experiments revealed that endometrial stromal cell attachment was most rapid for fibronectin-coated surfaces when cultured in each of the media examined, although this was only significant between the other surfaces for Lonza TP-SF and serum-containing medium (Supplementary Fig. S1A-a, b; Supplementary Data are available online at [www.liebertpub.com/tec](http://www.liebertpub.com/tec)). Similar rates of stromal cell attachment and spreading on fibronectin were observed between

StemPro-XF, Lonza TP-SF, and our in-house DMEM/SF/FGF2/EGF (Supplementary Fig. S1A-f). Stromal cells cultured in the xeno-free medium StemPro-XF showed a similar rapid attachment on the xeno-free matrix Cell Start XF as on fibronectin and gelatin (Supplementary Fig. S1A-c). Stromal cells showed poor rates of attachment to all matrices in Mesencult-XF medium (Supplementary Fig. S1A-d), and in general attached more rapidly on collagen than gelatin or laminin matrices and least on uncoated plastic in the various media, although these were not significantly different (Supplementary Fig. S1A).

We next investigated stromal cell proliferation in the various media. Xcelligence real-time cell assessment was used to measure proliferation as the CI doubling time, where the shortest doubling times indicate the most rapid cell proliferation, observed as the lowest positive value. In conditions where cells survived but did not proliferate or eventually detached and died, the CI doubling time was reported as zero.<sup>32</sup> As expected, endometrial stromal CI doubling times were lowest ( $\sim 25$  h) in serum-containing DMEM/F-12/10%FBS irrespective of matrix, indicating that rapid proliferation was promoted by the serum content of the medium (Supplementary Fig. S1B-a). Similar short CI doubling times were also observed on fibronectin coating for Lonza TP-SF ( $16.3 \pm 6.8$  h) and in-house DMEM/SF/FGF2/EGF ( $28.4 \pm 12.4$  h) media (Supplementary Fig. S1B-b, d), superior to all other matrix/media combinations (Supplementary Fig. S1B-e). In Lonza TP-SF medium, doubling times were considerably longer for collagen ( $119 \pm 11.2$  h), gelatin ( $106 \pm 13.2$ ), and laminin ( $109 \pm 1.4$  h), but only significantly different from uncoated surfaces for gelatin ( $p < 0.05$ ). StemPro-XF only supported stromal cell proliferation on gelatin-coated ( $62.1 \pm 5.0$  h) and collagen-coated ( $52.5 \pm 16.2$  h) surfaces, but not on its partner matrix Cell Start-XF (Supplementary Fig. S1B-c). The CI doubling times for Mesencult XF were zero for all matrices (data not shown), indicating cell death and its failure to support longterm growth of endometrial stromal cells.

The MTS viability (endpoint) assay was used to verify the proliferation rates of freshly isolated human endometrial stromal cells in the same media and matrix combinations as for Xcelligence over a similar 7-day period. As shown in Supplementary Figure S1C, cells cultured in-house DMEM/SF/FGF2/EGF medium (Fig. 1C-e) and commercially available Lonza TP-SF medium (Fig. 1C-b) showed similar proliferation rates as serum-containing medium (DMEM/F-12/10%FBS) (Fig. 1C-a) on fibronectin coating ( $p > 0.05$ ). However, cells showed greater proliferation in the in-house DMEM/SF/FGF2/EGF medium on fibronectin ( $A_{490nm}$  day 7,  $2.9 \pm 0.6$ ) compared with the uncoated surface ( $1.93 \pm 0.3$ ) ( $p < 0.05$ ) (Supplementary Fig. S1C-e). Similar proliferation rates were also observed for endometrial stromal cells cultured in the Lonza TP-SF medium on Cell Start-XF, collagen, gelatin, and laminin matrices ( $p > 0.05$ ), and slightly lower on an uncoated surface, although this was not significant (Supplementary Fig. S1C-b). Low proliferation rates were observed for xeno-free StemPro-XF ( $p < 0.05$ ) (Supplementary Fig. S1C-c) and Mesencult-XF ( $p < 0.05$ ) (Supplementary Fig. S1C-d) on all matrices compared with serum-containing and serum-free Lonza TP-SF and in house DMEM/SF/FGF2/EGF media on their respective matrices.

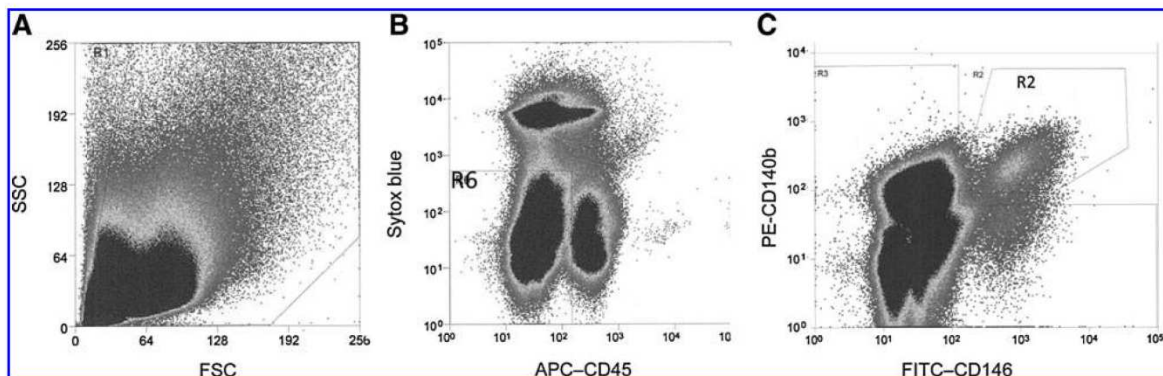


**FIG. 1.** Flow cytometry sorting of human endometrial mesenchymal stromal cells (MSC). **(A)** Scatterplot of human endometrial cells. **(B)** Electronic gating used to obtain viable (Sytox Blue<sup>neg</sup>) and exclude CD45<sup>+</sup> leukocytes. Region R6 was then analyzed for **(C)** coexpression of CD140 and CD146. Double-stained CD140b<sup>+</sup>CD146<sup>+</sup> cells in R2 gate were then sorted.

#### Human eMSC attachment and spreading on various matrices

Having identified key culture conditions on unsorted stromal cells that contain a small population of eMSC, we then examined flow cytometry-sorted endometrial cells to obtain purified eMSC as previously published.<sup>8</sup> Isolated stromal cells were first gated on size on the scatterplot (Fig. 1A), dead cells and CD45<sup>+</sup> leukocytes then were excluded (Fig. 1B), and the CD140b<sup>+</sup>CD146<sup>+</sup> double-positive eMSC (1%–1.5%) were sorted from each patient ( $n=12$ ) (Fig. 1C) and expanded in culture. eMSC attachment and spreading was determined by Xcelligence real-time cell assessment. Figure 2A shows a representative real-time CI curve for the initial 2 h of culturing CD140b<sup>+</sup>CD146<sup>+</sup> eMSC in the serum-containing medium (DMEM/10% FBS). The rate of eMSC attachment (CI/h) was significantly increased on fibronectin matrix (black bars) compared with culture on uncoated surfaces for in-house serum-free DMEM/SF/FGF2/EGF (fibronectin  $0.23 \pm 0.07$  vs. uncoated  $0.042 \pm 0.006$ ,  $p < 0.05$ ,  $n=3$ ) and Lonza TP-SF serum-free media (fibronectin  $0.19 \pm 0.07$  vs. uncoated  $0.036 \pm 0.003$ ,  $p < 0.05$ ,  $n=3$ ), and for StemPro-XF xeno-free medium (fibronectin  $0.26 \pm 0.02$  vs. uncoated  $0.063 \pm 0.003$ ,  $p < 0.05$ ,  $n=3$ ) (Fig. 2B). There was a trend for a higher rate of eMSC attachment in the serum medium on uncoated surfaces (white bars) compared to serum-free and xeno-free media, likely due to fibronectin present in serum, but this was not significant ( $p > 0.05$ ) (Fig. 2B). Although eMSC consistently showed an apparent lower rate of attachment on gelatin-coated wells compared to fibronectin and appeared greater than uncoated surfaces, these differences were not significant ( $p > 0.05$ ) (Fig. 2B). However, eMSC attachment to fibronectin was significantly greater than to the xeno-free matrix, Cell Start-XF in all culture media examined ( $p < 0.05$ ) except for xeno-free medium, StemPro-XF. In fact, eMSC cultured in StemPro-XF showed similar rates of attachment on Cell start-XF as on fibronectin, and was significantly increased compared with no coating (Cell Start-XF  $0.19 \pm 0.12$  vs. uncoated  $0.06 \pm 0.003$ ) ( $p < 0.05$ ,  $n=3$  separate isolates) (Fig. 2B).

#### Human eMSC proliferation on several matrixes in various media

Having established that fibronectin was the best attachment factor for CD140b<sup>+</sup>CD146<sup>+</sup> eMSC, we then

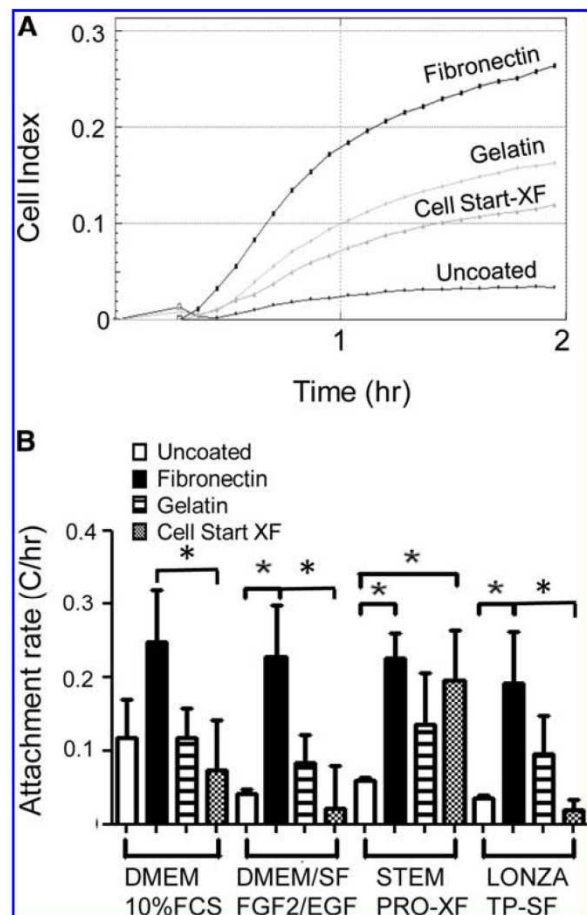


**FIG. 2.** Attachment of human endometrial MSC to various matrices when cultured in serum-containing, and serum- and xeno-free media measured using Xcelligence. **(A)** Representative real-time traces of CI in DMEM/10% FCS on four different matrices. **(B)** Rate of endometrial MSC (eMSC) attachment (CI/h). Data are mean  $\pm$  SEM ( $n=3$  samples from three different patients). \* $p < 0.05$ . CI, cell index; FCS, fetal calf serum; SF, serum-free, XF, xeno-free; FGF2, fibroblast growth factor 2; EGF, epidermal growth factor.

investigated eMSC proliferation by determining the CI doubling times using Xcelligence real-time cell assessment. Figure 3A shows representative real-time CI traces over 7 days with repeated measurements every 30 min. Figure 3B shows that eMSC cultured in in-house DMEM/SF/FGF2/EGF (fibronectin  $32.5 \pm 6.7$  h vs. uncoated 0 h) and in Lonza TP-SF serum-free media (fibronectin  $51.4 \pm 17.1$  h vs. uncoated 0 h) proliferated significantly more on fibronectin compared with no coating ( $p < 0.05$ ,  $n = 3$ ) as indicated by the lowest positive CI doubling times. However, on gelatin and Cell Start-XF matrices, neither medium supported eMSC proliferation, nor did the StemPro-XF medium as indicated the zero CI doubling times, suggesting that under these

conditions, there was a loss of cell viability as cells lifted off the surfaces (Fig. 3B). This was prevented in serum-containing medium (DMEM/F-12/10%FBS), which showed positive CI doubling times for eMSC on uncoated plastic, gelatin, and Cell Start-XF (Fig. 3B), suggesting that fibronectin in the serum contributed to this growth-enhancing effect.

#### eMSC proliferation in SF medium is enhanced under hypoxic culture conditions

Xcelligence CI doubling time data for eMSC were next verified using MTS proliferation assays. The effect of hypoxia (5%  $O_2$ ) was also examined. Figure 4B shows that when  $CD140b^+CD146^+$  eMSC were cultured in in-house DMEM/SF/FGF2/EGF serum-free medium in hypoxia, they grew more rapidly compared to typical normoxic (atmospheric) conditions (Fig. 4A).  $CD140b^+CD146^+$  eMSC cultured for 7 days in the four media on three different matrices and uncoated surfaces showed significantly increased proliferation in the in-house DMEM/SF/FGF2/EGF SF medium on fibronectin in hypoxia compared with normoxia (hypoxia  $2.72 \pm 0.19$  vs. normoxia  $2.17 \pm 0.26$ ) ( $p < 0.05$ ,  $n = 3$  separate isolates) (Fig. 4C). eMSC proliferation also increased significantly in Lonza TP-SF and StemPro-XF media when cultured on fibronectin compared with uncoated surfaces in normoxia ( $p < 0.05$ ,  $n = 3$ ), although significance for these media was not observed when cultured under hypoxic conditions (Fig. 4C).

#### eMSC retain MSC properties and phenotype after culture expansion in optimized serum-free medium

Having identified optimal conditions for serum-free culture of eMSC, we next investigated the phenotype of passage 3 eMSC following 7 days culture in both Lonza TP-SF and our in house serum-free xeno-containing DMEM/SF/FGF2/EGF media on fibronectin-coated flasks in 5%  $O_2$ . Figure 5A shows that the percentage of cells expressing the surface markers used for isolating eMSC from endometrial tissues,  $CD140b$ ,  $CD146^8$ , or  $W5C5^{25}$ , was consistently higher in the DMEM/SF/FGF2/EGF medium than in the Lonza TP-SF medium, indicating less spontaneous differentiation in the former. However, the MSC phenotype ( $CD29^+$ ,  $CD44^+$ ,  $CD73^+$ ,  $CD105^+$ ,  $CD34^-$ , and  $CD45^-$ ) was similar for both serum-free media (Fig. 5A). Further evaluation of eMSC function was undertaken on eMSC cultured in the DMEM/SF/FGF2/EGF medium. The cloning efficiency of passage 3 eMSC was  $1.32\% \pm 0.65\%$  ( $n = 5$ ), which is similar to our previously published 1.25% for freshly isolated endometrial stromal cells cultured in serum-containing medium.<sup>3</sup> Passage 3 eMSC previously cultured in serum-free DMEM/SF/FGF2/EGF medium for 7 days before differentiation induction media, retained capacity to differentiate into (Fig. 5B-a) adipocytes stained with the fat soluble dye, Oil Red O, (Fig. 5B-b)  $\alpha$ SMA-expressing smooth muscle cells, and (Fig. 5B-c) alkaline phosphatase-expressing osteocytes, which generated mineral calcium as detected by Alizarin Red (Fig. 5B-d).

#### eMSC 3D culture for scale-up cell production

Culture expansion of cells in a 3D environment promotes cell-cell interactions resulting in rapid proliferation and cell

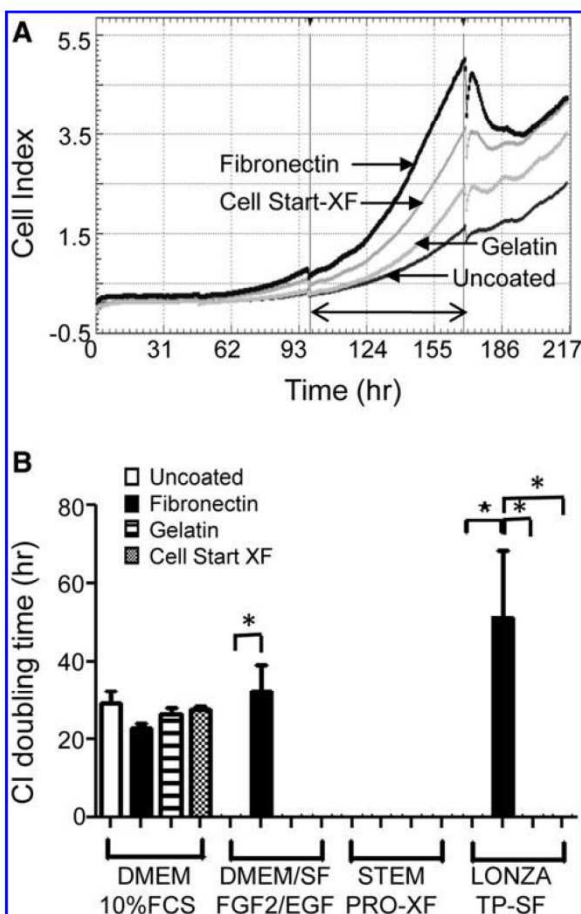


**FIG. 3.** Growth rate of human endometrial MSC cultured on various matrices in serum-containing, and serum- and xeno-free media measured using Xcelligence. (A) Real-time CI traces of a single representative sample of eMSC cultured in DMEM/10%FCS for over 200 h. Second and third media changes are observed by the interruption in the traces. (B) CI doubling time was calculated for the period between the second and third media change as shown by the arrow for DMEM/10%FCS, DMEM/SF/FGF2/EGF/Stem Pro-XF<sup>®</sup>, and Lonza TP-SF<sup>®</sup>. Lowest positive value is the most rapid doubling time. Zeros indicate loss of cell viability. Data are mean  $\pm$  SEM ( $n = 3$  samples from three different patients). \* $p < 0.05$ .

**FIG. 4.** Effect of hypoxia on endometrial MSC proliferation in serum-free media. Endometrial MSC cultured in DMEM/SF/FGF2/EGF on fibronectin in (A) normoxia (20% O<sub>2</sub>) and (B) hypoxia (5% O<sub>2</sub>). (C) Proliferation of endometrial MSC cultured in serum-containing, serum-free, and xeno-free media on various matrices in hypoxia (gray bars) or normoxia (black bars) as measured by MTS viability assay on day 7. Data are mean ± SEM (*n* = 3 samples from three different patients). Values for each condition for each patient sample were means of triplicate wells. \**p* < 0.05.

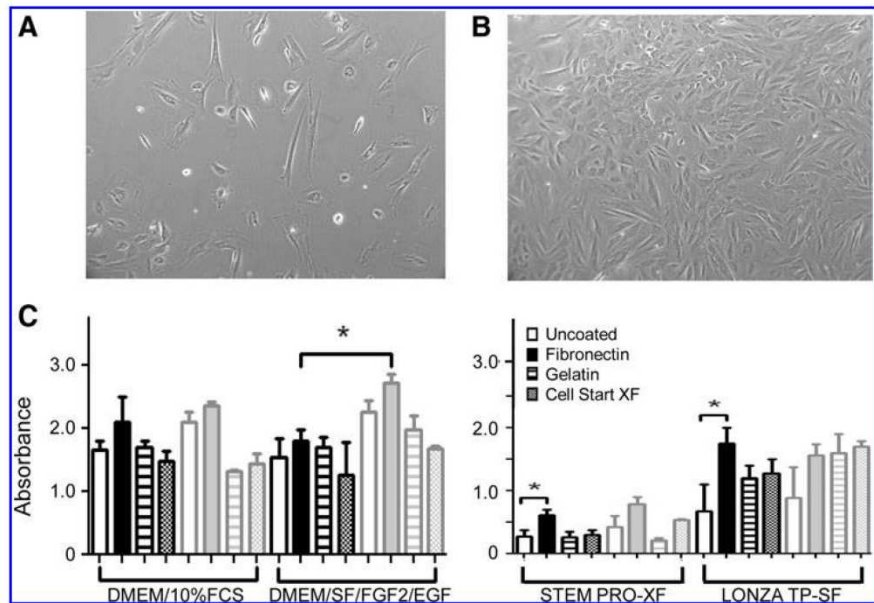
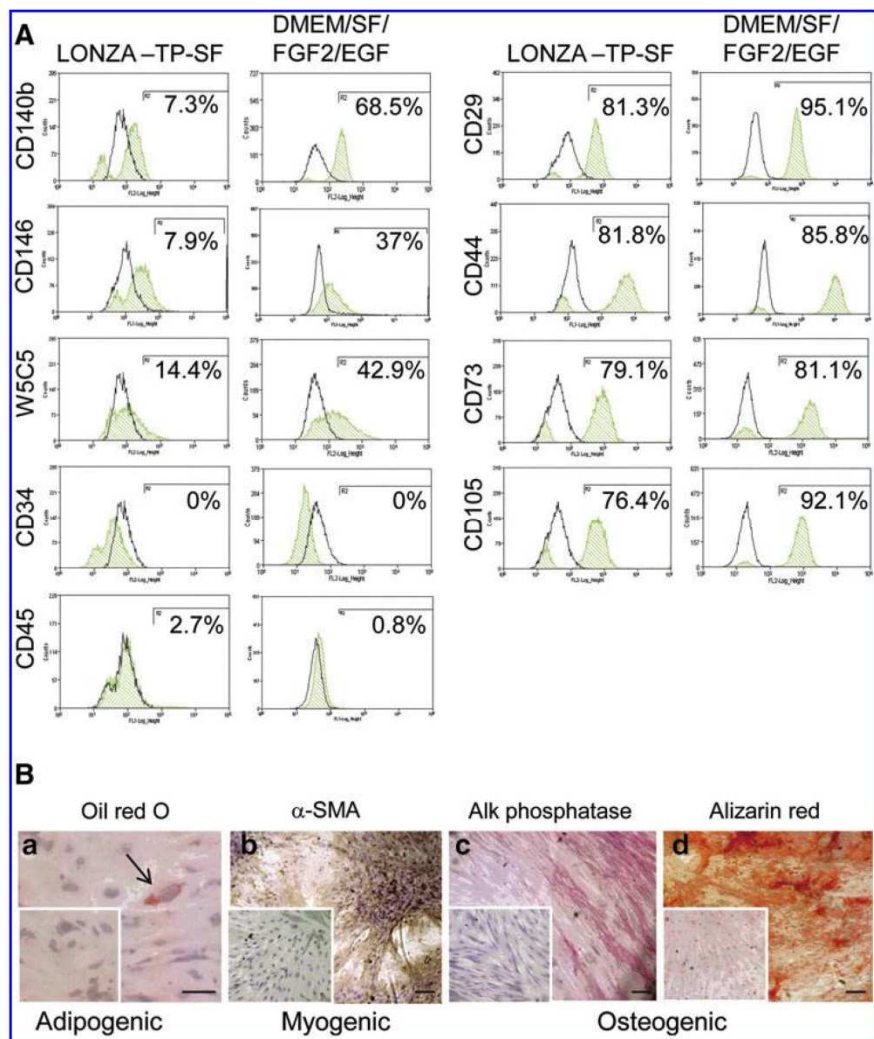


**FIG. 5.** Phenotype and differentiation of eMSC cultured in serum-free medium. Passage 3 eMSC (*n* = 2 separate samples) were each cultured in Lonza TP-SF and DMEM/SF/FGF2/EGF media on fibronectin-coated flasks in 5% O<sub>2</sub> for 7 days and then (A) examined for surface phenotype by single-color flow cytometry for multiple MSC markers (green histograms are positive cells; black histograms are isotype controls), and (B) for differentiation potential by culture in (a) adipogenic, (b) myogenic, and (c) osteogenic media (controls were in 1% serum-containing medium) for 3 weeks. (a) Oil Red O was used to visualize fat droplets after adipogenic induction, ↑, adipocyte (b) αSMA immunohistochemistry for myogenic induction and (c) alkaline phosphatase and (d) Alizarin Red for osteogenic induction. Controls cultures shown as insets were similarly treated. Results are from a single-experiment representative of two independent experiments on two separate patient eMSC samples. Scale bars 100 μm. Color images available online at [www.liebertpub.com/tec](http://www.liebertpub.com/tec)



production of a more physiological extracellular matrix (ECM).<sup>28</sup> We therefore assessed the 3D culture of eMSC on matrix-coated microbeads. Given that eMSC culture was superior on fibronectin-coated surfaces, CD140b<sup>+</sup>CD146<sup>+</sup> eMSC were attached onto Cultispher-S gelatin beads with and without fibronectin coating and cultured in serum-containing DMEM/F-12/10%FBS (Fig. 6A-a, c, e, g) and serum-free DMEM/SF/FGF2/EGF media (Fig. 6A-b, d, f, h). Fibronectin coating was confirmed by antifibronectin immunohistochemistry (Fig. 6B-i, j). Live/Dead staining 2 days after seeding showed increased eMSC attachment and spreading on fibronectin-coated beads in both serum and serum-free media (Fig. 6A-c, d) compared with gelatin beads (Fig. 6A-a, b). Live/Dead stain on day 15 showed that eMSC underwent greater proliferation on fibronectin-coated than gelatin beads in DMEM/SF/FGF2/EGF medium (Fig. 6A-f, h). In DMEM/F-12/10%FBS, there was even greater eMSC proliferation on fibronectin (Fig. 6A-e, g).

We next compared 2D and 3D culture of eMSC in our in-house DMEM/SF/FGF2/EGF medium using passage 3 eMSC seeded onto fibronectin-coated flasks and Cultispher microbeads at similar seeding densities (2000 cells/cm<sup>2</sup>) and cultured for 12 days under hypoxic conditions (5% O<sub>2</sub>). Cells in the culture flasks were passaged once on day 6 when 80% confluent. The eMSC cultured in 2D underwent 6.4 PD (mean, *n*=2 samples) generating 27.3×10<sup>6</sup> (mean, *n*=2 samples) from an initial 0.32×10<sup>6</sup> cells. In comparison, paired cultures of eMSC cultured for the same time at the same initial seeding density (2000 cells/cm<sup>2</sup>) underwent of 2.2 PD (mean, *n*=2 samples) on fibronectin coated microbeads generating 3.53×10<sup>6</sup> (mean, *n*=2 samples) from an initial 0.5×10<sup>6</sup> cells, indicating a trend to greater expansion on 2D compared to 3D surfaces. While the phenotype of the eMSC cultured on the microbeads retained typical MSC markers, there was a reduction in the percentages of CD146<sup>+</sup> cells (Fig. 6C) compared with 2D culture (Fig. 5A center left panels), suggesting that 3D culture promoted fibroblast differentiation.

## Discussion

Published guidelines<sup>33</sup> recommend that stem cells for regenerative medicine applications should meet the following criteria: (1) harvested by minimally invasive procedures, (2) differentiated along multiple cell lineage pathways in a regulatable and reproducible manner, and (3) manufactured in accordance with current GMP guidelines (using serum-free and xeno-free (animal product-free) reagents). In compliance with these guidelines, eMSC are an attractive candidate for regenerative medicine applications. In this study we investigated the scale-up culture of eMSC in serum-free and xeno-free culture conditions on various matrices using high-throughput real-time Xcelligence screening of cellular function as a first step in defining GMP conditions for this novel and readily available source of MSC. We identified two serum-free conditions that promoted the most rapid adhesion and proliferation of eMSC, notably our in-house DMEM/SF/FGF2/EGF and commercially available Lonza TP-SF media when using a fibronectin matrix. Culture expansion of eMSC in serum-free media in physiological oxygen concentration was also identified as an important

condition for optimal eMSC growth in the DMEM/SF/FGF2/EGF medium. Our studies identified fibronectin as the superior matrix and highly important for eMSC attachment and growth in both 2D and 3D culture expansion protocols. The commercially available Cell Start-XF matrix is unlikely to contain fibronectin as it failed to support eMSC attachment or growth in the range of media and matrices tested. Enhanced cell attachment through the use of attachment factors is particularly important in tissue engineering applications using biological or synthetic scaffolds aiming to incorporate and grow MSC for cell delivery to damaged tissues.

Importantly, we demonstrated that culture of CD140<sup>+</sup>CD146<sup>+</sup> eMSC<sup>8</sup> in our optimized serum-free xeno-product containing DMEM/SF/FGF2/EGF medium on fibronectin matrix in relative hypoxia (5% O<sub>2</sub>) retained their relative numbers, phenotype, cloning efficiency, and multilineage differentiation capacity. Expansion of eMSC was superior on 2D surfaces in culture flasks compared to 3D on microbeads, which appeared to promote eMSC fibroblast differentiation. Thus, we have now identified the first set of serum-free conditions enabling the culture expansion of human eMSC for use in tissue engineering applications.

Fibronectin is an important ECM protein that interacts with MSC integrins in their microenvironmental niche to regulate attachment, migration, proliferation, and differentiation.<sup>34</sup> Fibronectin has key roles during development and in mediating wound repair. Interestingly, fibronectin and its major ligand  $\alpha_5\beta_1$  integrin are upregulated during monthly endometrial remodeling and repair,<sup>35</sup> a process likely mediated by PDGFR- $\beta$  activation.<sup>36</sup> eMSC express high levels of PDGFR- $\beta$ <sup>8</sup> (this study) and are likely key cells mediating endometrial repair. It was therefore not surprising that fibronectin was identified as a critical factor in promoting eMSC attachment and proliferation in our *in vitro* culture protocols. Our data are consistent with a recent report on enhanced growth of human endometrial stromal cells encapsulated in alginate microbeads functionalized with multimeric fibronectin.<sup>37</sup>

As for all MSC, establishment of optimal *ex vivo* growth conditions for eMSC is an important prerequisite for their potential use in cell-based therapies, since low numbers retrieved from endometrium necessitates substantial *ex vivo* expansion. We have previously identified four growth factors, FGF2, EGF, TGF $\alpha$ , and PDGF-BB, that individually supported CFU activity of freshly isolated human endometrial stromal cells in serum-free media.<sup>31</sup> However, CFU activity in these single growth factor media formulations was less than in the serum medium. In this study we therefore combined both EGF and FGF2 in our in-house DMEM/SF/FGF2/EGF serum-free medium and showed similar proliferative activity of endometrial stromal cells and flow cytometry sorted CD140b<sup>+</sup>CD146<sup>+</sup> eMSC populations. However, endometrial stromal cells and eMSC proliferated poorly if at all in the two commercially available xeno-free media formulated for bone marrow MSC. Similarly umbilical cord MSC only proliferated in the Stem Pro XF<sup>®</sup> medium when 2% human serum was included, although the Mesencult-XF medium supported their growth.<sup>38</sup> This indicates the importance in defining optimal media/matrix combinations compliant with GMP for *ex vivo* culture expansion of each MSC source.

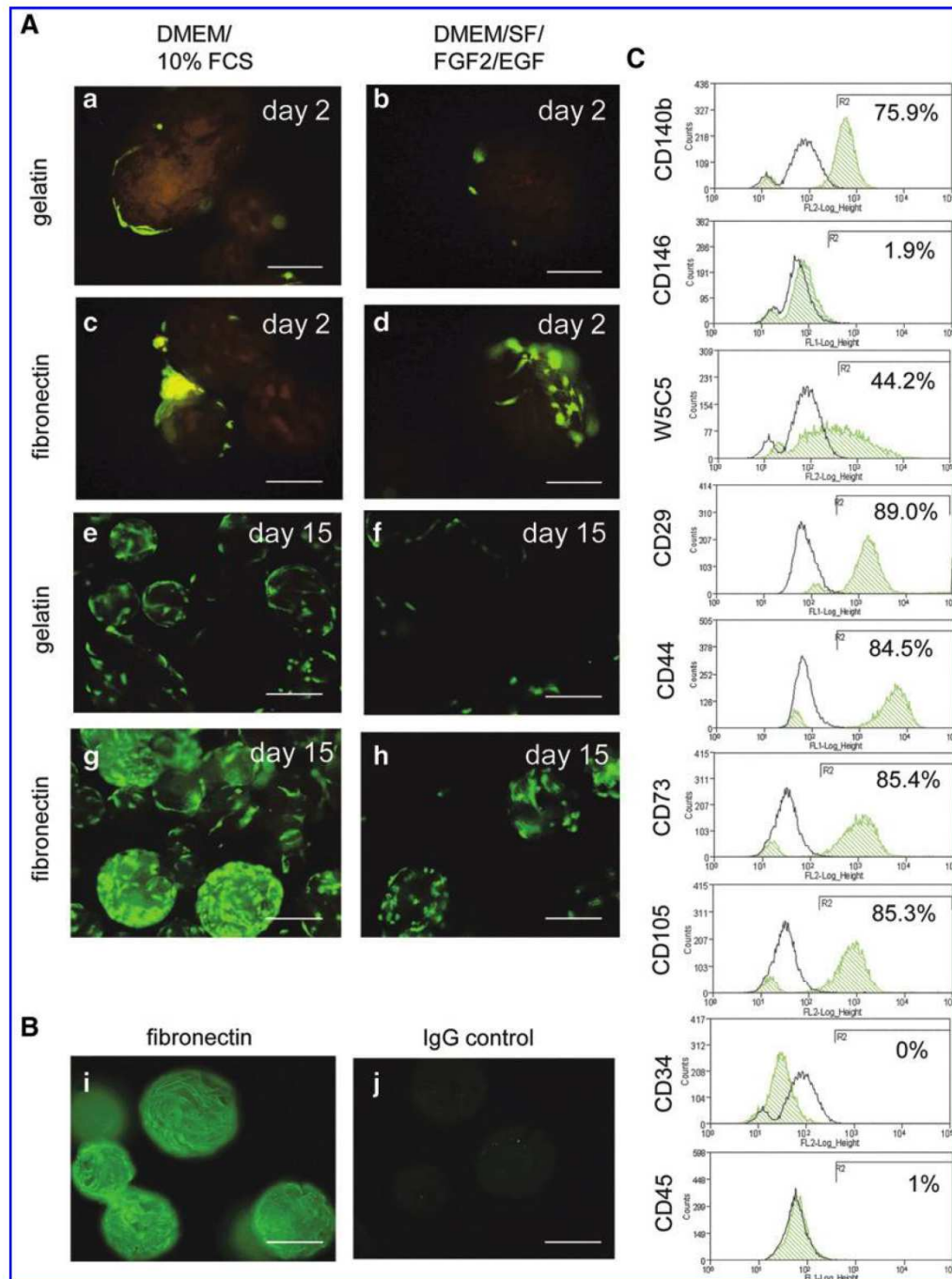


**FIG. 6.** 3D culture of endometrial MSC on (A) gelatin- and fibronectin-coated microbeads in serum-containing (DMEM/10%FCS) (left panel) or serum-free (DMEM/SF/FGF2/EGF) (right panel) media. Endometrial MSC cultured for (a–d) 2 days on (a, b) gelatin or (c, d) fibronectin-coated microbeads, (e–h) 15 days on (e, f) gelatin or (g, h) fibronectin-coated microbeads. Cells are stained with Live/Dead<sup>®</sup> stain (2  $\mu$ M calcein and 4  $\mu$ M ethidium homodimer-1) to detect viable (green) and dead (red) cells. (B) Immunostained fibronectin-coated microbeads (i) with anti-fibronectin antibody (FITC) and (j) negative control IgG. Scale bars 100  $\mu$ m. (C) After 12 days in culture, cells were recovered from the microbeads and examined for surface phenotype by single color flow cytometry for multiple markers (green histograms are positive cells, black histograms are isotype controls). Color images available online at [www.liebertpub.com/tec](http://www.liebertpub.com/tec)

Hypoxia is another important condition influencing *ex vivo* expansion of bone marrow-derived MSC. Similarly, we showed that in serum-free conditions (DMEM/SF/FGF2/EGF on fibronectin) eMSC proliferation and long-term viability *in vitro* was significantly enhanced under low oxygen (5% O<sub>2</sub>) compared with normoxia (20% O<sub>2</sub>). Similar findings were observed for human endometrial stromal side population cells, likely closely related to the eMSC population, which showed greater proliferation when cultured in hypoxia compared to normoxia.<sup>39</sup> These findings are consistent with previous studies showing increased efficiency in bone marrow MSC expansion in hypoxic compared with normoxic conditions.<sup>40–42</sup> Culture expansion of bone marrow MSC under hypoxic conditions mimicking *in vivo* tissue O<sub>2</sub> tension promotes proliferation through alteration of cellular metabolism, maintaining CFU activity, self-renewal, and undifferentiated phenotypes, and prolonging MSC lifespan.<sup>40,41,43</sup> The effect of hypoxia in preserving the progenitor phenotype and function of MSC is more pronounced in serum-free conditions compared to serum medium<sup>40</sup> (this study). In conditions of low O<sub>2</sub> tension, bone marrow MSC synthesize more fibronectin in both 2D and 3D culture<sup>42</sup> as well as angiogenic and growth promoting growth factors (VEGF, FGF2, HGF, and IGF-1). It is possible that hypoxia induces similar beneficial effects on eMSC. Thus, culture of eMSC in hypoxia will be an important consideration for minimizing *ex vivo* expansion times and generating sufficient numbers of cells for clinical use.

This study also showed that eMSC can be scaled up in 3D culture in serum-free medium on fibronectin-coated beads consistent with 2D culture results. Culture expansion of MSC in 3D using matrix-coated beads is a well-established method for tissue engineering applications as it provides a biochemical and physiological microenvironment more similar to *in vivo* conditions than 2D monolayer culture.<sup>42,44,45</sup> In particular, 3D culturing allows MSC to adopt their native morphology by facilitating cell–cell and cell–ECM interactions. Cell size decreases,<sup>45</sup> cell signaling changes,<sup>44</sup> and MSC surface antigen expression alters in a reversible manner<sup>45</sup> and subsequent differentiation capacity of MSC is enhanced.<sup>44–46</sup> Collectively, our data suggest that 2D culture expansion protocols in serum-free medium on fibronectin matrix under hypoxic conditions promotes eMSC viability, proliferation, and maintains the eMSC phenotype to a greater extent than 3D culture, pointing to some differences in MSC growth characteristics between bone marrow and eMSC *in vitro*.

MSC are increasingly being used as a cell-based therapy in a number of clinical applications for treating a range of degenerative and inflammatory diseases.<sup>11,12,16,47</sup> MSC have been reported in preclinical studies to improve disease outcomes, including enhanced myocardial function after infarction, in repairing liver damage and lung damage.<sup>48–50</sup> Bone marrow MSC are currently the most common source for clinical use.<sup>11,51</sup> Extensive studies of bone marrow-derived MSC have proven their multipotent differentiation potential and powerful immunosuppressive qualities. However, the collection of bone marrow is an invasive procedure requiring anesthesia. It involves significant discomfort to the donor and often results in low MSC yields, although bone marrow may also be harvested during orthopedic surgery.<sup>52</sup> The quality of these cells is also variable with respect to both

expansion, differentiation potential, and age of donor.<sup>53,54</sup> Similarly, adipose tissue MSC are obtained from an invasive liposuction procedure also requiring anaesthesia.<sup>55</sup> In contrast eMSC can be obtained from endometrial biopsy, a minimally invasive office-based procedure without anesthetic.<sup>56</sup> Others have obtained eMSC from menstrual blood<sup>57–59</sup> and demonstrated their potential in tissue engineering applications in repairing ischemic heart and skeletal muscle in animal models.<sup>57,58</sup> eMSC have been purified and characterized in both hysterectomy<sup>8,25</sup> and biopsy<sup>13,39,60,61</sup> tissues. CD140b<sup>+</sup> CD146<sup>+</sup> cells purified from both hysterectomy<sup>25</sup> and biopsy<sup>13</sup> have similar MSC properties and their perivascular location spans both functionalis and basalis layers; these indicate that eMSC derived from these sources are indeed the same subpopulation. Thus, the highly regenerative human endometrium provides a novel, readily available source of MSC, obtainable with minimal morbidity for future cell-based therapies.<sup>56</sup>

The poor ability of eMSC to grow in several commercially available xeno-free media designed for bone marrow MSC culture (Mesencult-XF and Stem Pro-XF) suggests some differences between these two sources of MSC, possibly related to key nutritional requirements. However, these may be relatively minor because eMSC grew well in the Lonza Therapeak SF<sup>®</sup> medium also formulated for bone marrow MSC, perhaps indicating eMSC may be more sensitive to xeno-free conditions. Nevertheless, eMSC show similar features to bone marrow-derived MSC for the minimal defining characteristics of MSC.<sup>62</sup> It is possible that eMSC originate from bone-marrow derived MSC as these cells circulate in low numbers and there is some evidence that bone marrow MSC incorporate into damaged human endometrium.<sup>63</sup> Bone marrow MSC can partially differentiate into endometrial decidual cells *in vitro*.<sup>64</sup> Thus, differences in culture requirements between bone marrow and eMSC may be related to their respective microenvironments and their relative turnover *in vivo*. eMSC are recruited to replace 5–10 mm of endometrial stroma each month, while bone marrow MSC would be a relatively stable population.

Findings from this study indicate that our in-house DMEM/SF/FGF2/EGF serum-free xeno product-containing medium provided optimal conditions for expansion of eMSC in culture, although the commercially available, GMP-compliant Lonza TP-SF serum-free medium also supported expansion of eMSC. Interestingly, several of the commercially available xeno-free GMP-compliant MSC media used to expand bone marrow-derived MSC, failed to support eMSC attachment and growth. Therefore, one of the next steps is to develop our DMEM/SF/FGF2/EGF medium under GMP-compliant conditions in preparation for clinical use. To this end we will modify our isolation procedure by replacing reagents containing animal products with GMP-compliant reagents. We also plan to simplify the purification of eMSC using our recently discovered single marker, W5C5<sup>25</sup>, and magnetic beads rather than flow cytometry sorting. We will then expand our selected eMSC population in our in house serum-free xeno-product containing DMEM/SF/FGF2/EGF medium in 2D on fibronectin-coated culture flasks in 5% O<sub>2</sub> for at least four passages. In conclusion, this study represents the first steps in preparing eMSC for potential clinical use. Collectively, the findings warrant further investigation of eMSC and substantiate the potential clinical

use of these cells in regenerative medicine applications for clinical unmet needs. In particular, autologous or allogeneic eMSC may be a novel cell source for tissue engineering applications for the treatment of common conditions affecting large numbers of women such as pelvic organ prolapse.<sup>23,56</sup>

#### Acknowledgments

The authors acknowledge Frances Walker and Pamela Marners for collection of the tissue, and Dr. Mark Lawrence and Dr. Tony Lawrence from Waverley Private Hospital for the provision of hysterectomy tissue. This study was supported by the Australian Stem Cell Centre (SDF-05) (CEG, JW, AR), NHMRC Project grant (1021126) (CEG, JW, AR), NHMRC RD Wright Career Development Award 465121 (CEG), and Victorian Government's Operational Infrastructure Support Program.

#### Disclosure Statement

The authors indicate no potential conflicts of interest.

#### References

- Nombela-Arrieta, C., Ritz, J., and Silberstein, L.E. The elusive nature and function of mesenchymal stem cells. *Nat Rev Mol Cell Biol* **12**, 126, 2011.
- Friedenstein, A.J., Chailakhyan, R.K., Latsinik, N.V., Panasyuk, A.F., and Keiliss-Borok, I.V. Stromal cells responsible for transferring the microenvironment of the hemopoietic tissues. Cloning *in vitro* and retransplantation *in vivo*. *Transplantation* **17**, 331, 1974.
- Chan, R.W.S., Schwab, K.E., and Gargett, C.E. Clonogenicity of human endometrial epithelial and stromal cells. *Biol Reprod* **70**, 1738, 2004.
- Gargett, C.E., Schwab, K.E., Zillwood, R.M., Nguyen, H.P.T., and Wu, D. Isolation and culture of epithelial progenitors and mesenchymal stem cells from human endometrium. *Biol Reprod* **80**, 1136, 2009.
- Pittenger, M.F., Mackay, A.M., Beck, S.C., Jaiswal, R.K., Douglas, R., Mosca, J.D., Moorman, M.A., Simonetti, D.W., Craig, S., and Marshak, D.R. Multilineage potential of adult human mesenchymal stem cells. *Science* **284**, 143, 1999.
- Zuk, P.A., Zhu, M., Ashjian, P., De Ugarte, D.A., Huang, J.I., Mizuno, H., Alfonso, Z.C., Fraser, J.K., Benhaim, P., and Hedrick, M.H. Human adipose tissue is a source of multipotent stem cells. *Mol Biol Cell* **13**, 4279, 2002.
- Crisan, M., Yap, S., Casteilla, L., Chen, C.W., Corselli, M., Park, T.S., Andriolo, G., Sun, B., Zheng, B., Zhang, L., Norotte, C., Teng, P.N., Traas, J., Schugar, R., Deasy, B.M., Badyrak, S., Buhning, H.J., Jacobino, J.P., Lazzari, L., Huard, J., and Peault, B. A perivascular origin for mesenchymal stem cells in multiple human organs. *Cell Stem Cell* **3**, 301, 2008.
- Schwab, K.E., and Gargett, C.E. Co-expression of two perivascular cell markers isolates mesenchymal stem-like cells from human endometrium. *Hum Reprod* **22**, 2903, 2007.
- Caplan, A.I. Why are MSCs therapeutic? New data: new insight. *J Pathol* **217**, 318, 2009.
- Prockop, D.J. Repair of tissues by adult stem/progenitor cells (MSCs): controversies, myths, and changing paradigms. *Mol Ther* **17**, 939, 2009.
- Parekkadan, B., and Milwid, J.M. Mesenchymal stem cells as therapeutics. *Annu Rev Biomed Eng* **12**, 87, 2010.
- Martin, I., Baldomero, H., Bocelli-Tyndall, C., Slaper-Cortenbach, I., Passweg, J., and Tyndall, A. The survey on cellular and engineered tissue therapies in Europe in 2009. *Tissue Eng Part A* **17**, 2221, 2011.
- Spitzer, T.L., Rojas, A., Zelenko, Z., Aghajanova, L., Erikson, D.W., Barragan, F., Meyer, M., Tamareisis, J.S., Hamilton, A.E., Irwin, J.C., and Giudice, L.C. Perivascular human endometrial mesenchymal stem cells express pathways relevant to self-renewal, lineage specification, and functional phenotype. *Biol Reprod* **86**, 58, 2012.
- Wolff, E.F., Gao, X.B., Yao, K.V., Andrews, Z.B., Du, H., Elsworth, J.D., and Taylor, H.S. Endometrial stem cell transplantation restores dopamine production in a parkinson's disease model. *J Cell Mol Med* **15**, 747, 2010.
- Santamaria, X., Massasa, E.E., Feng, Y., Wolff, E., and Taylor, H.S. Derivation of insulin producing cells from human endometrial stromal stem cells and use in the treatment of murine diabetes. *Mol Ther* **19**, 2065, 2011.
- Bieback, K., Kinzebach, S., and Karagianni, M. Translating research into clinical scale manufacturing of mesenchymal stromal cells. *Stem Cells Int* **2010**, 193519, 2011.
- Sensebe, L., and Bourin, P. Mesenchymal stem cells for therapeutic purposes. *Transplantation* **87**, S49, 2009.
- Delancey, J.O. The hidden epidemic of pelvic floor dysfunction: achievable goals for improved prevention and treatment. *Am J Obstet Gynecol* **192**, 1488, 2005.
- Jelovsek, J.E., Maher, C., and Barber, M.D. Pelvic organ prolapse. *Lancet* **369**, 1027, 2007.
- Nygaard, I., Barber, M.D., Burgio, K.L., Kenton, K., Meikle, S., Schaffer, J., Spino, C., Whitehead, W.E., Wu, J., and Brody, D.J. Prevalence of symptomatic pelvic floor disorders in US women. *JAMA* **300**, 1311, 2008.
- Deprest, J., Zheng, F., Konstantinovic, M., Spelzini, F., Claerhout, F., Steensma, A., Ozog, Y., and De, R.D. The biology behind fascial defects and the use of implants in pelvic organ prolapse repair. *Int Urogynecol J Pelvic Floor Dysfunct* **17 Suppl 1**, S16, 2006.
- Smith, F.J., Holman, C.D., Moorin, R.E., and Tsokos, N. Lifetime risk of undergoing surgery for pelvic organ prolapse. *Obstet Gynecol* **116**, 1096, 2010.
- Gargett, C.E., and Ye, L. Endometrial reconstruction from stem cells. *Fertil Steril* **98**, 11, 2012.
- Filshie, R.J.A., Zannettino, A.W.C., Makrynika, V., Gronthos, S., Henniker, A.J., Bendall, L.J., Gottlieb, D.J., Simmons, P.J., and Bradstock, K.F. MUC18, a member of the immunoglobulin superfamily, is expressed on bone marrow fibroblasts and a subset of hematological malignancies. *Leukemia* **12**, 414, 1998.
- Masuda, H., Anwar, S.S., Buhning, H.J., Rao, J.R., and Gargett, C.E. A novel marker of human endometrial mesenchymal stem-like cells. *Cell Transplant*. [Epub ahead of print]; DOI:10.3727/096368911X637362, 2012.
- Atienza, J.M., Zhu, J., Wang, X., Xu, X., and Abassi, Y. Dynamic monitoring of cell adhesion and spreading on microelectronic sensor arrays. *J Biomol Screen* **10**, 795, 2005.
- Gargett, C.E., Bucak, K., and Rogers, P.A.W. Isolation, characterization and long-term culture of human myometrial microvascular endothelial cells. *Hum Reprod* **15**, 293, 2000.
- Werkmeister, J.A., Adhikari, R., White, J.F., Tebb, T.A., Le, T.P., Taing, H.C., Mayadunne, R., Gunatillake, P.A., Danon, S.J., and Ramshaw, J.A. Biodegradable and injectable cure-on-demand polyurethane scaffolds for regeneration of articular cartilage. *Acta Biomater* **6**, 3471, 2010.

29. Glattauer, V., White, J.F., Tsai, W.B., Tsai, C.C., Tebb, T.A., Danon, S.J., Werkmeister, J.A., and Ramshaw, J.A. Preparation of resorbable collagen-based beads for direct use in tissue engineering and cell therapy applications. *J Biomed Mater Res A* **92**, 1301, 2010.
30. Tebb, T.A., Tsai, S.W., Glattauer, V., White, J.F., Ramshaw, J.A., and Werkmeister, J.A. Development of porous collagen beads for chondrocyte culture. *Cytotechnol* **52**, 99, 2006.
31. Schwab, K.E., Chan, R.W., and Gargett, C.E. Putative stem cell activity of human endometrial epithelial and stromal cells during the menstrual cycle. *Fertil Steril* **84** (Suppl 2), 1124, 2005.
32. Diemert, S., Dolga, A.M., Tobaben, S., Grohm, J., Pfeifer, S., Oexler, E., and Culmsee, C. Impedance measurement for real time detection of neuronal cell death. *J Neurosci Methods* **203**, 69, 2012.
33. Gimble, J.M., Katz, A.J., and Bunnell, B.A. Adipose-derived stem cells for regenerative medicine. *Circ Res* **100**, 1249, 2007.
34. Lindner, U., Kramer, J., Behrends, J., Driller, B., Wendler, N.O., Boehrsen, F., Rohwedel, J., and Schlenke, P. Improved proliferation and differentiation capacity of human mesenchymal stromal cells cultured with basement-membrane extracellular matrix proteins. *Cytotherapy* **12**, 992, 2010.
35. Cao, W., Mah, K., Carroll, R.S., Slayden, O.D., and Brenner, R.M. Progesterone withdrawal up-regulates fibronectin and integrins during menstruation and repair in the rhesus macaque endometrium. *Hum Reprod* **22**, 3223, 2007.
36. Veevers-Lowe, J., Ball, S.G., Shuttleworth, A., and Kielty, C.M. Mesenchymal stem cell migration is regulated by fibronectin through  $\alpha_5\beta_1$ -integrin-mediated activation of PDGFR- $\beta$  and potentiation of growth factor signals. *J Cell Sci* **124**, 1288, 2011.
37. Li, Z., Kreiner, M., Edrada-Ebel, R., Cui, Z., van der Walle, C.F., and Mardon, H.J. Perfusion culture enhanced human endometrial stromal cell growth in alginate-multivalent integrin  $\alpha_5\beta_1$  ligand scaffolds. *J Biomed Mater Res A* **99A**, 211, 2011.
38. Hartmann, I., Hollweck, T., Haffner, S., Krebs, M., Meiser, B., Reichart, B., and Eißner, G. Umbilical cord tissue-derived mesenchymal stem cells grow best under GMP-compliant culture conditions and maintain their phenotypic and functional properties. *J Immunol Methods* **363**, 80, 2010.
39. Cervello, I., Gil-Sanchis, C., Mas, A., gado-Rosas, F., Martinez-Conejero, J.A., Galan, A., Martinez-Romero, A., Martinez, S., Navarro, I., Ferro, J., Horcajadas, J.A., Esteban, F.J., O'Connor, J.E., Pellicer, A., and Simon, C. Human endometrial side population cells exhibit genotypic, phenotypic and functional features of somatic stem cells. *PLoS One* **5**, e10964, 2010.
40. dos Santos F., Andrade, P.Z., Boura, J.S., Abecasis, M.M., da Silva, C.L., and Cabral, J.M. *Ex vivo* expansion of human mesenchymal stem cells: a more effective cell proliferation kinetics and metabolism under hypoxia. *J Cell Physiol* **223**, 27, 2010.
41. Fehrer, C., Brunauer, R., Laschober, G., Unterluggauer, H., Reitinger, S., Kloss, F., Gully, C., Gassner, R., and Lepperdinger, G. Reduced oxygen tension attenuates differentiation capacity of human mesenchymal stem cells and prolongs their lifespan. *Aging Cell* **6**, 745, 2007.
42. Grayson, W.L., Zhao, F., Izadpanah, R., Bunnell, B., and Ma, T. Effects of hypoxia on human mesenchymal stem cell expansion and plasticity in 3D constructs. *J Cell Physiol* **207**, 331, 2006.
43. Tamama, K., Kawasaki, H., Kerpedjieva, S.S., Guan, J., Ganju, R.K., and Sen, C.K. Differential roles of hypoxia inducible factor subunits in multipotential stromal cells under hypoxic condition. *J Cell Biochem* **112**, 804, 2011.
44. Cukierman, E., Pankov, R., Stevens, D.R., and Yamada, K.M. Taking cell-matrix adhesions to the third dimension. *Science* **294**, 1708, 2001.
45. Frith, J.E., Thomson, B., and Genever, P.G. Dynamic three-dimensional culture methods enhance mesenchymal stem cell properties and increase therapeutic potential. *Tissue Eng Part C Methods* **16**, 735, 2010.
46. Karlsen, T.A., Mirtaheeri, P., Shahdadfar, A., Floisand, Y., and Brinchmann, J.E. Effect of three-dimensional culture and incubator gas concentration on phenotype and differentiation capability of human mesenchymal stem cells. *J Cell Biochem* **112**, 684, 2011.
47. Brooke, G., Cook, M., Blair, C., Han, R., Heazlewood, C., Jones, B., Kambouris, M., Kollar, K., McTaggart, S., Pelekanos, R., Rice, A., Rossetti, T., and Atkinson, K. Therapeutic applications of mesenchymal stromal cells. *Semin Cell Dev Biol* **18**, 846, 2007.
48. Silva, G.V., Litovsky, S., Assad, J.A., Sousa, A.L., Martin, B.J., Vela, D., Coulter, S.C., Lin, J., Ober, J., Vaughn, W.K., Branco, R.V., Oliveira, E.M., He, R., Geng, Y. J., Willerson, J.T., and Perin, E.C. Mesenchymal stem cells differentiate into an endothelial phenotype, enhance vascular density, and improve heart function in a canine chronic ischemia model. *Circulation* **111**, 150, 2005.
49. Lee, K.D., Kuo, T.K., Whang-Peng, J., Chung, Y.F., Lin, C.T., Chou, S.H., Chen, J.R., Chen, Y.P., and Lee, O.K. *In vitro* hepatic differentiation of human mesenchymal stem cells. *Hepatology* **40**, 1275, 2004.
50. Ortiz, L.A., Gambelli, F., McBride, C., Gaupp, D., Baddoo, M., Kaminski, N., and Phinney, D.G. Mesenchymal stem cell engraftment in lung is enhanced in response to bleomycin exposure and ameliorates its fibrotic effects. *Proc Natl Acad Sci U S A* **100**, 8407, 2003.
51. Le, B.K., Frassoni, F., Ball, L., Locatelli, F., Roelofs, H., Lewis, I., Lanino, E., Sundberg, B., Bernardo, M.E., Remberger, M., Dini, G., Egeler, R.M., Bacigalupo, A., Fibbe, W., and Ringden, O. Mesenchymal stem cells for treatment of steroid-resistant, severe, acute graft-versus-host disease: a phase II study. *Lancet* **371**, 1579, 2008.
52. Suva, D., Garavaglia, G., Menetrey, J., Chapuis, B., Hoffmeyer, P., Bernheim, L., and Kindler, V. Non-hematopoietic human bone marrow contains long-lasting, pluripotential mesenchymal stem cells. *J Cell Physiol* **198**, 110, 2004.
53. Mareddy, S., Crawford, R., Brooke, G., and Xiao, Y. Clonal isolation and characterization of bone marrow stromal cells from patients with osteoarthritis. *Tissue Eng* **13**, 819, 2007.
54. Bonab, M.M., Alimoghaddam, K., Talebian, F., Ghaffari, S.H., Ghavamzadeh, A., and Nikbin, B. Aging of mesenchymal stem cell *in vitro*. *BMC Cell Biol* **7**, 14, 2006.
55. Yoshimura, K., Shigeura, T., Matsumoto, D., Sato, T., Takaki, Y., Iba-Kojima, E., Sato, K., Inoue, K., Nagase, T., Koshima, I., and Gonda, K. Characterization of freshly isolated and cultured cells derived from the fatty and fluid portions of liposuction aspirates. *J Cell Physiol* **208**, 64, 2006.
56. Gargett, C.E., and Masuda, H. Adult stem cells in the endometrium. *Mol Hum Reprod* **16**, 818, 2010.
57. Cui, C.H., Uyama, T., Miyado, K., Terai, M., Kyo, S., Kiyono, T., and Umezawa, A. Menstrual blood-derived cells confer

- human dystrophin expression in the murine model of duchenne muscular dystrophy via cell fusion and myogenic transdifferentiation. *Mol Biol Cell* **18**, 1586, 2007.
58. Hida, N., Nishiyama, N., Miyoshi, S., Kira, S., Segawa, K., Uyama, T., Mori, T., Miyado, K., Ikegami, Y., Cui, C.H., Kiyono, T., Kyo, S., Shimizu, T., Okano, T., Sakamoto, M., Ogawa, S., and Umezawa, A. Novel cardiac precursor-like cells from human menstrual blood-derived mesenchymal cells. *Stem Cells* **26**, 1695, 2008.
  59. Patel, A.N., Park, E., Kuzman, M., Benetti, F., Silva, F.J., and Allickson, J.G. Multipotent menstrual blood stromal stem cells: isolation, characterization, and differentiation. *Cell Transplant* **17**, 303, 2008.
  60. Wolff, E.F., Wolff, A.B., Du, H., and Taylor, H.S. Demonstration of multipotent stem cells in the adult human endometrium by *in vitro* chondrogenesis. *Reprod Sci* **14**, 524, 2007.
  61. Schuring, A.N., Schulte, N., Kelsch, R., Ropke, A., Kiesel, L., and Gotte, M. Characterization of endometrial mesenchymal stem-like cells obtained by endometrial biopsy during routine diagnostics. *Fertil Steril* **95**, 423, 2011.
  62. Dominici, M., Le, B.K., Mueller, I., Slaper-Cortenbach, I., Marini, F., Krause, D., Deans, R., Keating, A., Prockop, D., and Horwitz, E. Minimal criteria for defining multipotent mesenchymal stromal cells. The international society for cellular therapy position statement. *Cytotherapy* **8**, 315, 2006.
  63. Taylor, H.S. Endometrial cells derived from donor stem cells in bone marrow transplant recipients. *JAMA* **292**, 81, 2004.
  64. Aghajanova, L., Horcajadas, J.A., Esteban, F.J., and Giudice, L.C. The bone marrow-derived human mesenchymal stem cell: potential progenitor of the endometrial stromal fibroblast. *Biol Reprod* **82**, 1076, 2010.

Address correspondence to:

Caroline Gargett, Ph.D.

The Ritchie Centre

Monash Institute of Medical Research

27-31 Wright Street,

Clayton, Victoria, 3168

Australia

E-mail: caroline.gargett@monash.edu

Received: December 19, 2011

Accepted: June 25, 2012

Online Publication Date: August 2, 2012

## Appendix 3

